PROTEOMICS AND METABOLOMICS ANALYSIS OF CELLULAR RESPONSE TO ANTI-COAGULATING DRUG WARFARIN

BAI JING

School of Chemical and Biomedical Engineering

A thesis submitted to the Nanyang Technological University
in partial fulfillment of the requirement for the degree of
Doctor of Philosophy

2011

Dedicated to my family, especially my mother and my father

Acknowledgement

First of all, I would like to express my deepest gratitude to my supervisor A/Prof. CHEN Wei Ning William, for all his valuable instructions made this work possible. I am deeply grateful of his help in the completion of this thesis. His effective advice, shrewd comments have kept the thesis in the right direction. I am also greatly indebted to him who gave me the chances to improve on English language. My deep thanks also go to my co-supervisor A/P Balram Chowbay in National Cancer Center, Singapore for his kindly providing me the clinical patients' serum samples and helpful discussion.

Secondly, I would like to express my thanks to Nanyang Technological University for providing me the opportunity for Ph.D. programme with full research scholarship in these years. And thanks also go to School of Chemical and Biomedical Engineering, for providing of the experiment facilities.

Thirdly, I would like to express my heartful thanks to my lab colleagues and alumni: Dr. TAN Tuanlin, Dr. SUI Jianjun, Dr. FENG Huixing, Dr. NIU Dandan, Mr. ZHANG Jianhua, Miss. REN Yudan, Miss ZHOU Yusi, Mr. WANG Mingxuan, Miss. Bahareh Haji RASOULIHA, Miss. Laleh SADROLODABAEE, and Miss TAN Yilin Jane for their constructive suggestions and friendship, they constantly encouraged me when I felt frustrated with some drawbacks.

Finally, I would like to express my utmost thanks to my family, my beloved father and mother, for their helping out of the difficulties and supporting without a single word of complaint.

Publications

1. **Bai J**, Sadrolodabaee L, Ching C, Chowbay B, Chen W (2010). A comparative proteomic analysis of HepG2 cells incubated by S(-) and R(+) enantiomers of anti-coagulating drug warfarin. *Proteomics, 10(7):1463-1473*
2. **Bai J**, Sadrolodabaee L, Chowbay B, Chen W (2010). Secreted Protein Profile Analysis on HepG2 cells Incubated by S(-) and R(+) Enantiomers of Chiral Drug Warfarin. *Proteomics-Clinical Applications, 4(10-11):808-815*
3. Saminathan R[1], **Bai J[1]**, Sadrolodabaee L[1], Karthik G, Singh O, Subramaniyan K, Ching C, Chowbay B, Chen W (2010). *VKORC1* Pharmacogenetics and Pharmacoproteomics In Patients On Warfarin Anticoagulant Therapy: Transthyretin precursor as a potential biomarker. *PloS ONE, 5(12):e15064*
4. **Bai J**, Wang M, Chowbay B, Ching C, Chen W (2010). Metabolic Profiling of HepG2 cells Incubated by S(-) and R(+) Enantiomers of Chiral Drug Warfarin. *Metabolomics, in press*
5. Ren YD, Lu YW, **Bai J**, Chen W (2008). The BH3-containing HBSP, a spliced variant apoptotic hepatitis B viral protein, interacts with cellular anti-apoptotic proteins. *IUBMB Life, 60(10): 700-702*
6. Wang M, **Bai J**, Ching C, Chen W (2010). Metabolomic Profiling of Cellular Responses to Carvedilol Enantiomers in Vascular Smooth Muscle Cells. *PloS ONE, 5(11):e15441*

[1] These authors contributed equally to this work.

Table of Contents

List of Tables

List of Figures

List of Abbreviations

iTRAQ	isobaric tag for relative and absolute quantitation
2D	two-dimensional
LC	liquid chromatography
MS	mass spectrometry
DNA	deoxynucleic acid
PCR	polymerase chain reaction
ROS	reactive oxygen species
2-DE	two-dimensional gel electrophoresis
SDS–PAGE	sodium dodecyl sulphate–polyacrylamide gel electrophoresis
MALDI	matrix-assisted laser desorption/ionization
ESI	electrospray ionization
PTMs	post-translational modifications
TOF	time-of-flight
FTICR	Fourier transform ion cyclotron resonance
SILAC	Stable isotope labelling with amino acids in cell culture
CID	collision-induced dissociation
HPLC	high-performance liquid chromatography
SCX	strong cation exchange
RP	reversed-phase
MEM	minimum essential medium
MTT	3-(4, 5-dimethylthiazol-2-yl)-2, 5-diphenyltetrazolium bromide

ECL	enhanced chemiluminescence
EF	error factor
PDIA3	protein disulfide isomerase A3
GCMS	gas chromatography mass spectrometry
TTR	transthyretin
QTOF	quadrupole with time of flight mass analysers
VKOR	vitamin K epoxide reductase
PCA	principle components analysis
MGP	matrix Gla protein
GGCX	γ-glutamyl carboxylase
Gla	γ-carboxyglutamic acid
Glu	glutamic acid
NQO1	NAD(P)H quinone dehydrogenase 1
NAD(P)H	nicotinamide adenine dinucleotide phosphate plus hydrogen
APOE	apolipoprotein E
GPIb	glycoprotein Ib
GPIX	glycoprotein IX
GPV	glycoprotein V
PK	prekallikrein
vWF	von Willebrand factor
HK/HMWK	high-molecular-wieght kininogen

TFPI	tissue factor pathway inhibitor
ICAT	isotope-coded affinity tag
ICPL	isotope-coded protein labeling
NHS	N-hydroxysuccinimide
GIST	global internal standard technology
TrkA	tyrosine kinase receptor
GFP	green fluorescent protein
EGF	epidermal growth factor
NMR	nuclear magnetic resonance
BSTFA	N, O-bis(trimethylsilyl) trifluoroacetamide
MSTFA	N-methyl-N-(trimethylsilyl) trifluoroacetamide
TMCS	trimethylchlorosilane
PLS	partial least squares
INR	international normalized ratio
DMSO	dimethylsulfoxide
CHAPS	3-[(3-Cholanidopropyl)dimethylammonio]-1-propanesulfonate
BSA	bovine serum albumin
TCEP	tris-(2-carboxyethyl)phosphine
TEMED	N, N, N', N'- tetramethyl-ethylenediamine
APS	ammonium persulfate
PBS	phosphate buffered saline

HRP	Horseradish peroxidase
TBHP	*tert*-butyl hydroperoxide
carboxy-H2DCFDA	5-(and-6)-carboxy-2′,7′-dichlorodihydrofluorescein diacetate
AART	automatic adjustment of retention time
EI	electron impact ionization
NIST	national institute of standards and technology
GSH	glutathione
RBP	retinol binding protein
CYP450	cytochrome P450
IG	immunoglobulin
DIC	disseminated intravascular coagulation
HDL	high density lipoprotein
GST	Glutathione S transferase

Summary

Warfarin is considered as one of the most common anticoagulation drugs worldwide. It is a racemic of S(-) and R(+) enantiomer drug, with S(-) warfarin being more biologically active than the optical congener. However, narrow therapeutic index in different patients and risk of bleeding complications remains a challenge, thus treatment with this drug must be done carefully. Recognition of high and low dose requirement for patients is of high importance in this regard. Although the existing high-throughput genotyping can facilitate pharmacogenetic prognosis, pharmacoproteomic studies can complement the analysis on the prediction of warfarin dose requirements in patients, as well as understanding the mechanism of drug actions.

To identify a potential warfarin dosage marker, a combined pharmacogenetics and iTRAQ-coupled LC-MS/MS pharmacoproteomics approach was used in this project to analyze plasma protein profiles in 53 Asian patients on warfarin therapy. Significant upregulated level of transthyretin precursor was found in patients receiving low dose of warfarin but not in those on high dose of warfarin. Transthyretin precursor, a multi-functional protein, was associated with specific dosing regimens of warfarin, vitamin K epoxide reductase subunit 1(VKORC1) genetic polymorphism and affected warfarin dosage. Our further validation experiments such as protein immunoblot analysis have confirmed that the level of transthyretin precursor in patients receiving low-dose of warfarin was significantly higher than that in those on high-dose warfarin. Our *in vitro*

Western blotting analysis has shown that transthyretin precursor expressed differentially in HepG2 cells with low- and high- dose of warfarin. This protein might therefore be as a potential biomarker for better prognosis of warfarin therapy.

To validate the clinical results, we expanded the study to an *in vitro* cell-line system to identify specific proteins which might interact with transthyretin precursor and be involved in mechanism of drug action. Intracellular protein profile in HepG2 cells incubated with S(-) and R(+) warfarin, using iTRAQ-coupled 2D LC-MS/MS, was investigated because cell-based systems offer an environment with high-level of homogeneicity and high reproducibility in the understanding of drug intrinsic mechanism. Our results indicated that around 600 unique proteins were identified and protein disulfide-isomerase A3 may be part of enzymes complex providing electrons to the VKOR enzyme's active center. The down-regulation of this protein appeared more in S(-) warfarin rather than in R(+) warfarin, which indicated a higher level of vitamin K cycle inhibition in S(-) warfarin than in R(+) warfarin. Another protein, Protein DJ-1 on both S(-) and R(+) warfarin treated samples was down-regulated. This protein is a sensor for intracellular oxidative stress. Vitamin K is a redox cycling reaction. The down-regulation of the protein indicated that the S(-) and R(+) warfarin incubated cells have lower level of oxidative cytoplasmic environment compared to untreated group. Interestingly, another function of protein DJ-1 is to act as a protease. Transthyretin precursor was identified as a substrate for DJ-1 protease[1]. It is possible

to postulate that protein DJ-1 may be associated with and reflect the intracellular interaction of transthyretin precursor, thus provide more information on the discovery of unknown mechanism of varied warfarin dosage. Another down-regulated protein 14-3-3 protein σ might interact with coagulation factors which influence the coagulation process[2].

Moreover, secreted protein profile were identified in culture medium of HepG2 cells incubated with S(-) and R(+) warfarin by application of iTRAQ-coupled 2D LC-MS/MS proteomics. A total of 76 unique proteins in which 49 secreted proteins were identified in cell-line system, with 5 proteins showed changes in their level. The results indicated that 1) the up-regulation of inter-α-trypsin inhibitor may interact with coagulating factors thus inhibit their normal functions. 2) up-regulation of α-2-macroglobulin acts as an inhibitor of coagulation by inhibiting thrombin formation[3], and protected from thrombosis. 3) down-regulation of α-2-HS-glycoprotein upon warfarin incubation may associate with reduced MGP expression and related to warfarin's side-effects. 4) down-regulated protein, apolipoprotein A-I may associate with procoagulant effect from plasma lipids. 5) down-regulated Fibrinogen gamma chain indicated a lower level of blood clots formation.

Clinical findings for the 5 proteins showed the same trends of changes, which indicated that the cell-line based systems can be validated by clinical data. The

findings also indicated that in S(-) and R(+) warfarin incubated HepG2 cells, transthyretin precursor slightly varied compared to HepG2 without incubation, but no differences was observed in between the enantiomer drugs. This observation suggests an iTRAQ-coupled 2D LC-MS/MS with warfarin dose-varied cell-line system is to be built in future for reveal underlying mechanism of action of transthyretin precursor on warfarin specific dosing regimens.

To complement our proteomics analysis, the metabolomic analysis was carried out to establish the changes in metabolite which are truly reflective of the physiological state of cells. In this project, the intracellular metabolic profile in HepG2 cells incubated with S(-) and R(+) warfarin by GCMS analysis was analyzed. A total of 80 metabolites belong to different categories were identified. Among these, glucuronic acid showed significant decrease in cells incubated with R(+) warfarin but not in those incubated with S(-) warfarin. R(+) warfarin may be more tended to be glucuronidated. Glucuronidation could abolish the binding between warfarin and its targeting enzyme, VKOR, due to introduction of a bulky acidic sugar. It may partially explain the lower bio-activity of R(+) warfarin. And arachidonic acid showed increased in cells incubated with S(-) warfarin but not in those incubated with R(+) warfarin. In addition, a number of small molecules involved in γ-glutamyl cycle thus influence Vitamin K Epoxide Reductase (VKOR) activity displayed ratio variations. These molecules with the expressions were: elevated level of glycine, L-glutamine, 5-oxoproline and

decreased level of L-glutamate. In addition, intracellular glutathione detection was further validated the results.

Taken together, our clinical proteomics analysis has successfully identified transthyretin precursor at higher level in patients on low dose of warfarin therapy. This finding has the potential to make transthyretin precursor a useful biomarker for effective warfarin therapy in Asian patients. Our findings from the combined analysis of pharmacoproteomics and metabolomics have provided molecular evidence on a comprehensive proteomic and metabolic profile on warfarin-cell interaction which may shed new lights on future improvement of warfarin therapy.

1. Introduction

1.1 Chiral Drugs

Chirality is formally defined as the geometric property of a rigid object of not being superimposable with the mirror image[4]. This property can be found in all biological systems, from the basic life building substances like amino acids, fatty acids, to the structures of all the organisms. The two chiral objects are called enantiomers. Enantiomer always comes in pair. The two enantiomers have structure similarity but can behave very differently in the biological functions due to their differences in 3-D shapes[5].

There are three nomenclatures generally accepted for enantiomers: (i) enantiomer is named based on the direction of optical rotations in the plane, as designated as (+) and (−). If it rotates the light clockwise, the enantiomer is labeled (+). The other one is labeled as (−). (ii) Enantiomer is named by relating the molecule to glyceraldehyde, the smallest commonly used chiral molecule, which forms the D/L system. (iii) The *R/S* system, which is the most widely accepted, describes absolute stereochemical configuration. Each of the four groups attached to chiral center is given a priority. The priority is assigned by the atomic number. We view the molecule which has the lowest priority away from us. In the other three groups, if the atomic numbers decrease in

clockwise the enantiomer is labeled *R.* If the atomic numbers decrease counterclockwise, it is designated as *S*-enantiomer[4]. A chiral molecule may have more than one chiral center. Chiral center most often arises from a carbon atom to which four various groups attached.

In pharmacology, many drugs currently in use are mixture of enantiomers. Two enantiomers of a given drug are classified as different drugs, as they are different in their rate of metabolism, metabolites, selectivity for receptors and toxicity[6]. In a particular drug, the number of enantiomers depends on the number of chiral centers in the molecule. The molecular base for a particular drug to be biologically active is spatial interaction between drug molecules and receptors. From recognition, approaching, anchoring to binding, the whole process is molecular interaction with effect groups on the drug binding to affinity binding sites on the receptors. The more and stronger the bindings, the more active the drug is. Most receptor bindings are chiral and asymmetric.

Since 1980, new technologies for synthesis and separation of chiral drug have been developed. It has been reported that single-enantiomer drugs starts to be available commercially in the new drug in an increasing manner, from 20% ten years ago to 75% in present[7]. To date, existing racemic mixtures separated into single

enantiomers[8] is now a dominant part in the drug development portfolios. The use of enantiomer drugs may lead to more selective pharmacological profiles.

The chiral drugs can be classified into three groups according to the bioactivities of single enantiomers. In group 1, one enantiomer is response for therapeutic effect while the others are inactive or very less active or undesirable effects. In group 2, both enantiomers are bio-active with one enantiomer being more effective than the other. In group 3, racemic drugs have identically bioactive enantiomers [5, 9]. For example, the anti-coagulating drug warfarin belongs to the second group. It is a racemic drug with S(-) enantiomer being more effective than R(+) enantiomer for 3-5 times[10], and the enantiomers of this drug are under stereoselective metabolism. Understanding the chiral mechanism of drugs will provide clinician with more safety and efficacious medication for the treatment of patients.

1.2 Warfarin, vitamin K cycle and coagulation process

Warfarin enantiomers

Warfarin is a commonly used oral anticoagulant for patients with prosthetic valve disease, venous thromboembolism and stroke[11]. It decreases blood coagulation indirectly by inhibiting vitamin K cycle, a necessary process for the maturation of several blood coagulating factors, namely prothrombin and factor VII, IX, X.

Warfarin is a racemic drug consists of S(-) and R(+) enantiomers, with S(-) form being more effective in vitro (3-5 times)[12-15]. Figure 1.1 demonstrates the structures of the 2 enantiomers.

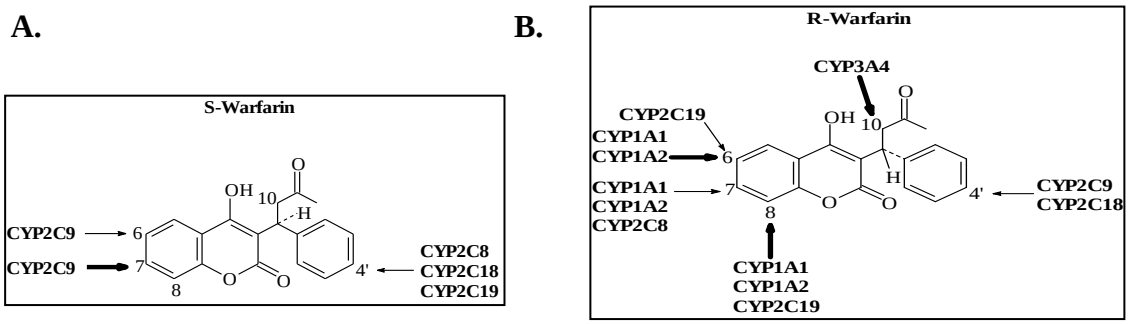

Figure 1.1 Structures of warfarin Enantiomers. A. S(-) warfarin; B. R(+) warfarin[16](permission from ref.16 was obtained from publisher to use this figure).

Clinically, racemic warfarin is normally used to treat patients without enantiomeric separation, as warfarin enantiomers have activities that qualitatively similar but quantitatively different[15]. In vivo situation indicated that 60% to 70% anticoagulation effects in racemic warfarin were contributed from S(-) enantiomer[13]. There are reported that steady-state doses required to maintain the same anticoagulation effect, for S(-), racemic and R(+) warfarin were around 6.5, 9.5 and 18(mg/70kg/day), respectively[17]. Racemic warfarin was in between of S(-) and R(+) warfarin while more similar with the S(-) enantiomer. The biological half life for racemic warfarin is also in between of S(-) and R(+) warfarin[14]. In racemic warfarin, the effect of one enantiomer is not altered by the presence of the other.

Vitamin K cycle

Vitamin K is a group of naphthoquinone derivatives synthesized only in eubacterial and plants, and functions as a free radical scavenger to maintain intracellular redox homeostasis[18]. In animals, vitamin K can only be obtained from food or metabolism of intestinal bacteria. In vitamin K cycle in the liver, vitamin K is first reduced by vitamin K reductase to its hydroquinone form, which acts as a mediator to activate the enzyme γ-glutamyl carboxylase (GGCX). Several coagulating factors undergo vitamin K-dependent posttranslational modification by GGCX. The Glutamic acid (Glu) residues on those coagulating factors are modified into γ-carboxyglutamic acid (Gla), resulting in the maturation of those coagulating factors. Gla residue will mediate those coagulating factors to bind to Ca^{2+} in the blood stream. The binding is needed for activation of platelets as well as other downstream coagulation factors and pathways [11, 19]. Once completed the γ-carboxylation process, vitamin K hydroquinone is then oxidized to vitamin K epoxide form. Another enzyme, integrated in the rough endoplasmic reticulum[19], vitamin K 2,3 epoxide reductase (VKOR), reduces vitamin K epoxide to its reduced form, and the cycle repeats. Figure 1.2 illustrates the process of vitamin K cycle(page 6).

In liver, two pathways have been described for reduction of vitamin K to vitamin K hydroquinone. The first, performed by VKORC1, is highly inhibited by warfarin, uses

vitamin K-epoxide as well as vitamin K as substrate; the second is via the microsomal enzyme NAD(P)H quinone dehydrogenase 1 (NQO1)[20].

VKOR uses two sulfhydryl groups for the catalytic reaction and they are oxidized back to a disulfide bond during each catalytic cycle[18, 21-23]. Warfarin inhibits vitamin K cycle through interfering with VKOR activity by binding to the enzyme's disulfide motif, thus prevents the formation of free sulfhydryls leading to the inactivation of the enzyme [24-25]. It showed that warfarin binds to the oxidized form of VKOR and prevents the formation of the free sulfhydryls requisite for vitamin K cycle activity [18, 26-27].

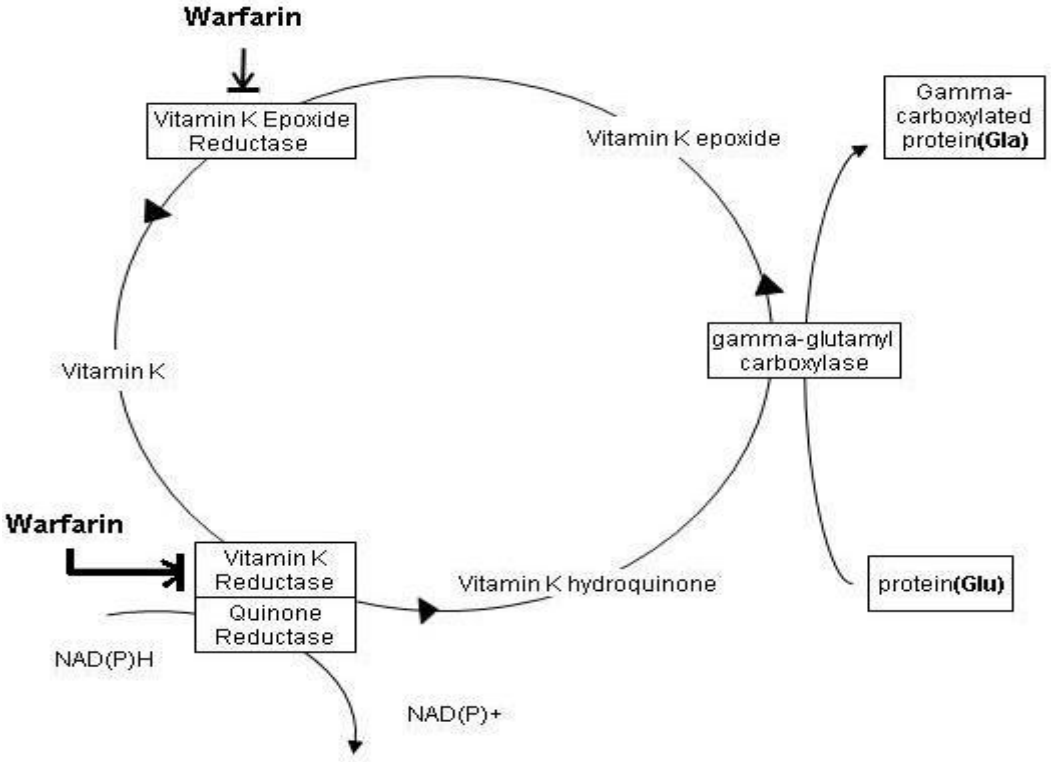

Figure 1.2 The Vitamin K Cycle. (Detailed description in page 5)

However, either from vitamin K epoxide form to vitamin K, or from vitamin K to hydroquinone, the overall cellular redox system for this enzyme is still unknown. It remains possible that one or more unknown physiological reductant could associate with VKOR to form enzyme complex[28].

Warfarin Dosage

Dosing and biological response needs to be further investigated for better clinical usage, as warfarin is a drug with narrow therapeutic index and large inter-individual variability in patient response. Pharmacogenetic study has reported that around 30 genes might be involved in warfarin actions[29]. Systematic searches of references show that more than 100 genetic variants are able to alternate the behavior of proteins. Well known examples are cytochrome P450 (CYP 450) enzyme, apolipoprotein E (APOE), as well as vitamin K 2,3 epoxide reductase (VKOR) gene polymorphism with different response to warfarin[16, 18, 22, 27, 29-30]. Optimizing warfarin dosage has remained a challenge in the clinical setting. Routine monitoring parameters such as INR (International Normalization Ratio) has limited value in the optimization of warfarin doses in individual patients. Target genes of warfarin therapy include Vitamin K 2, 3-epoxide reductase (*VKORC1*) and apolipoprotein E (*APOE*)[31]. Recently, functional genetic variants in the *VKORC1* gene were found to affect the pharmacodynamics of warfarin and influence patients' dosing requirements [32].

Other vitamin K-dependent Proteins

Warfarin inhibits maturation of vitamin K dependent coagulating factors II, VII, IX and X, and vitamin K-dependent protein C, protein S, and protein Z, which play regulatory roles in blood coagulating process. Other vitamin K dependent proteins such as osteocalcin and matrix Gla protein which are not involved in coagulating may also be influenced by vitamin K dose variation[33-35].

1.3 Coagulation process

Coagulation is a process of blood clots formation. The process involves platelet and fibrin covering of blood clotting then dissolution and repairing of the injury. It is termed hemostasis[36]. Coagulation is an important process for regulating hemostasis. It starts from immediate blood vessel injury in endothelium. There are two stages of hemostasis which occur simultaneously. Firstly, primary hemostasis involves platelets adhere to exposed collagen from blood vessel wall and hemostatic plug formation. Secondary hemostasis is related to coagulation factors in the blood plasma responding to a complex blood coagulation cascade, and to generate fibrin cross-linked polymer and to strengthen the platelet plug[37].

Platelet Activation and von Willebrand Factor (vWF)

Circulating platelets bind to collagen. The binding is strengthened by von Willebrand factor, a multimeric circulating protein. It forms links between the platelet GPIb-

GPIX-GPV and collagen fibrils[36]. The platelet is then activated and releases the contents of their granules into plasma and this process will further activate other platelets. The activated platelets undergo a conformation change and expose phospholipid surface for the coagulation factors binding.

Coagulation cascade

In secondary hemostasis, there are two pathways: intrinsic (contact activation) and extrinsic (tissue factor) pathway, combining with final common pathway leads to fibrin cross-linked polymer formation. Physiologically, the intrinsic cascade has less in vivo significance than the extrinsic cascade.

Tissue factor pathway

Tissue factor pathway aims to form thrombin, which is necessary to convert fibrinogen to fibrin. And the generated "thrombin burst" has feedback activation roles to regulate the clotting cascades.

Contact activation pathway

The contact activation pathway is activated by the contact which is made between blood and exposed surface factors. Several blood coagulating factors are involved in the process, such as factor VIII, IX, X, XI and XII. In addition, other proteins including prekallikrein (PK) and high molecular weight kininogen (HK/HMWK) are also involved.

Final common pathway

In this pathway, thrombin converts fibrinogen into fibrin. It activates factors VIII and V with their inhibitor protein C and factor XIII, to form cross-linked fibrin polymers. Figure1.3 describes the coagulating cascade and pathways(page 10).

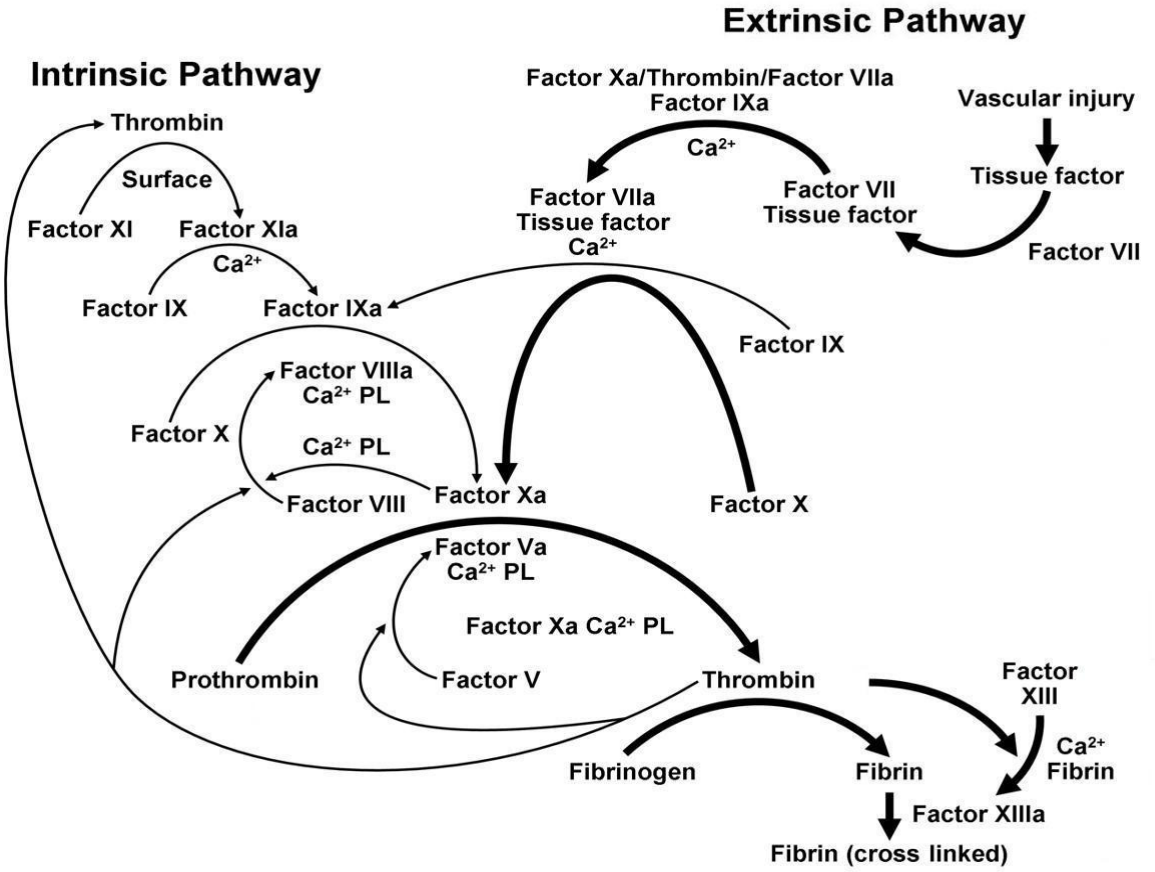

Figure 1.3 Intrinsic and Extrinsic Pathways in Coagulation Process[38](page 9) (permission from ref.38 was obtained from publisher to use this figure).

Cofactors and Inhibitors

There are various cofactors and inhibitors involved in the coagulation cascade. Calcium and phospholipid are required for the formation of prothrombinase complex and calcium is needed in binding to activated coagulation factors[39]. Vitamin K is an necessary factor for maturation of various liver-generated coagulation factors, as well as protein S, protein C and protein Z. Inhibitors such as protein C and protein S are

major physiological anticoagulant[40], while antithrombin and tissue factor pathway inhibitor(TFPI) also keep the coagulation cascade in check[41].

1.4 Proteomics

Technology development for large-scale protein analysis blooms in the post-genomic era. Instead of study one particular gene or protein in an organism, a comprehensive understanding of genomics, proteomics and metabolomics makes the systematic analysis of all cellular components become possible[42]. Proteomics, termed in 1994, is used to describe "the complete set of proteins that is expressed, and modified following expression, by the entire genome in the lifetime of a cell"[43]. It acts as a "bridge" between the genomic function and complex cellular structure or behavior. The analysis involves large-scale identification and characterization of proteins, including post-translational modifications, phosphorylation and glycosylation.

Commonly, the platform to study proteomics is built on the following steps:

1. Sample preparation – 1 D or 2 D gels, liquid chromatography;
2. Protein information- mass spectrometer or Edman degradation;
3. Protein identification – bioinformatics;
4. Cell mapping – protein-protein interactions, 3D structure, cellular localization, post-translational modifications.[43]

Gel-based Proteomics

Several separation tools are available for analysis of protein profile. These tools can be applied either individually or in combined. Analysis of protein profiles is based on the nature of proteins, e.g. physical or chemical properties, localization, mass-to-charge

ratio, solubility and affinity to substrates[44]. 2-dimentional Gel is one technology for protein separation, by which thousands of proteins can be separated in a single run. Combined with mass spectrometry (MS), the technology identify proteins automatically by analyzing the sequence of the peptides generated by digesting of gel spots [45]. In 2-D gel electrophoresis with mass spectrometry (2DE/MS), a mixture of proteins is separated by an immobilized pH gradient strip in the first dimension. In second dimension, proteins are separated by sodium dodecyl sulphate polyacrylamide gel electrophoresis(SDS-PAGE)[46]. Separated protein patterns can be observed by staining with Commassie Brilliant Blue or silver. Staining protein patterns from two or more different mixtures of proteins are compared. Different proteins are defined and interesting protein spots are subsequently undergone in-gel digestion by using proteolytic enzyme *e.g.* trypsin. MS analysis of the peptide sequences is conducted. Particularly, the matrix-assisted laser desorption/ionization (MALDI), which is a soft ionization technique, consists of a laser beam for molecule ionization and a dry crystalline matrix which is applied to reduce the level of sample damage by direct laser beam and act to facilitate sample vaporization and ionization process[47]. This ionization method is suitable for fragile large organic molecules. However, proteins which are in low abundance may be missed in gel-based identification.

Chromatography-based Proteomics

Alternatively, other separation tools like chromatography have taken steps to substitute the gel-based technology as they are much quicker and more sensitive. Recent developments of mass spectrometry (MS) and chromatography provide useful tools in proteomic analysis, especially the combination of liquid (LC) or gas chromatography (GC) and mass spectrometry [48-49]. Liquid or gas chromatography acts as separation

tools while mass spectrometry is used for protein identification. In most cases, LC coupled with tandem MS is needed for a more accurate detection, also refers to as LC-MS/MS. Tandem MS allows a single charged peptide to be selected, separated, sequenced and detected. In the other aspect, LC with downscaled nano-flow rates proves to be more sensitive in proteomics analysis[50].

LC-MS systems normally consist of: 1) one or more chromatography columns, which separate the mixed peptides by their physical or chemical properties (e.g. hydrophobicity, charges). Each separation is according to a physicochemical property forms a dimension in LC. Peptides are eluted with different concentrations of organic solvent in a stepwise manner before reaching MS. The most commonly used method for separation of mixed peptides is reverse-phase liquid chromatography. It separates and elutes the peptides according to their hydrophobicity. A second dimensional chromatography usually is strong cation-exchange (SCX) liquid chromatography, which separate the peptides by the nature of charges. SCX can be applied off-line, and followed by reverse-phase liquid chromatography then MS[48]. 2) An ionization source (e.g. MALDI or electrospray ionization (ESI)), which is used to build charges on eluted peptides. In ESI, high voltages forms small droplets in their gas phase, and the droplets evaporate and leave the charges on the peptides [51-52]. The advantages to use ESI than MALDI is the ions created in ESI are from solution. The fine droplets encompass the molecules. Before passing through the mass analyzers, ions must be condensed into a stream and enter a high-vacuum entrance. 3) Mass analyzers, separate ions based on *m/z* ratios; and 4) a detector, which detects the relative abundance of ions at discrete *m/z*[43, 49-50, 53]. Figure1.4 has demonstrated the generate flow of LC-MS/MS system.

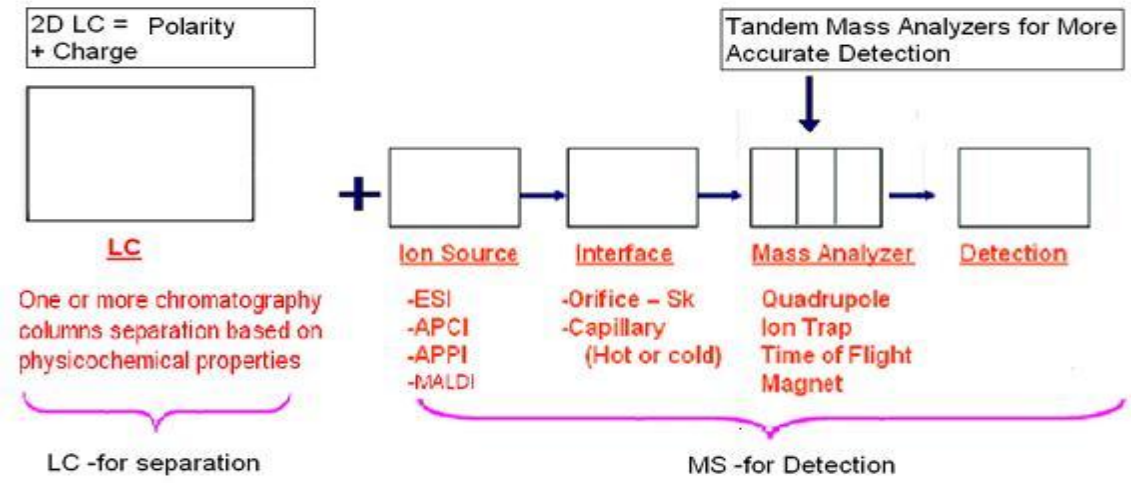

Figure 1.4 The General Flow Chart of LC-MS.

Mass analyzers are the most important parts in MS. There are mainly four types of mass analyzer used in proteomics research including 1) quadrupole, 2) reflector time-of-flight (TOF), 3) quadrupole ion trap and 4) Fourier transform ion cyclotron resonance (FTICR) analyzers. One example is, two or more quadrupole mass analyzers are combined in series. Quadrupole mass analyzer consists of four cylindrical quartz rods incorporated in ceramic collars[54]. A dc and an oscillating RP signal are applied on the cylindrical rods. The changing in the dc/RF signals will allow ions with specific m/z to pass through. The second quadrupole introduces collision gas which fragments the selected ions. Ion trap mass analyzer has similar mechanism with quadrupole while the difference is: ions are trapped into a three-dimensional chamber with a radio frequency field. In addition, the sensitivity has been reported that ion trap is up to 100 times more sensitive than a quadrupole[54]. Fourier transform ion cyclotron resonance (FTICR), a relatively new development, traps the ions by strong magnetic fields which significantly improves the sensitivities[55]. Time-of-flight mass analyzer accelerates ions by high voltage pulse to a high kinetic energy state and the flight time of each fragment is dependent on its m/z ratio, the lighter the ion, the faster it reaches the

detector. To detect a particular m/z ion, a diode-array detector is activated only for a given time-slice window. Figure1.5 has described the working principles of the two ionization methods and four mass analyzers(page 17).

Tandem MS

Another example, the design of Hybrid TOF mass analyzer has overcome the limitation of ambiguous results. The design of in series quadrupole and TOF mass analyzer gives out accurate mass measurement both qualitatively and quantitatively. Figure1.6 illustrates the structure of QTOF mass analyzer (page 18). Q1, Q2 are individual quadrupole mass analyzers.

In the first MS step, the intact peptide which is named precursor ion, its mass is obtained. In the second MS step, the particular precursor ions are isolated from others and fragmented into product ions. Collision-induced dissociation (CID) is needed to create product ions. The masses of which are determined in the second MS step yield MS/MS spectra [49, 56]. The fragmented peptide ions' spectra will then be analyzed by bioinformatic software and compared with proteins databases. Identification of particular protein in a mixture is demonstrated in Figure 1.7(page 19). Basically, protein A, B, C is digested before LC-MS/MS analysis. In MS, the peptides are firstly detected by survey scan (MS scan). After MS scan, co-eluted peptides (e.g. A1, B2, C4) is ready for sequence analysis by MS/MS. Random selection of one peptide ions(with different charged states) are sequenced. Bioinformatic software matches the generated MS/MS spectra for peptide sequencing. Automatically, one survey scan is followed by multiple MS/MS scans.

Sequence analysis by MS/MS is done by a single MS/MS scan. Computer software is used to match database spectra because the location of fragmented peptide along the sequence can be predicted. In Figure 1.8 (page 20) panel A compares the N-terminal sequencing and MS/MS sequencing. MS/MS shows more advantages on much faster detection. Panel B is the nomenclatures of fragment ions. Fragment peptides with the original N-terminus are named a-, b- and c-type. Fragment peptides with the original C-terminus are named x-, y- and z-type ions. Commonly abundant ions are b- and y-type. The numbers for b- and y- represent the resident number in the original peptide.

Protein identification by LC-MS was performed by bioinformatic software (e.g. ProteinPilot^{TM} from Applied Biosystems) and databases, including SWISS-PROT, TrEMBL PIR, NCBInr, ESTdb.

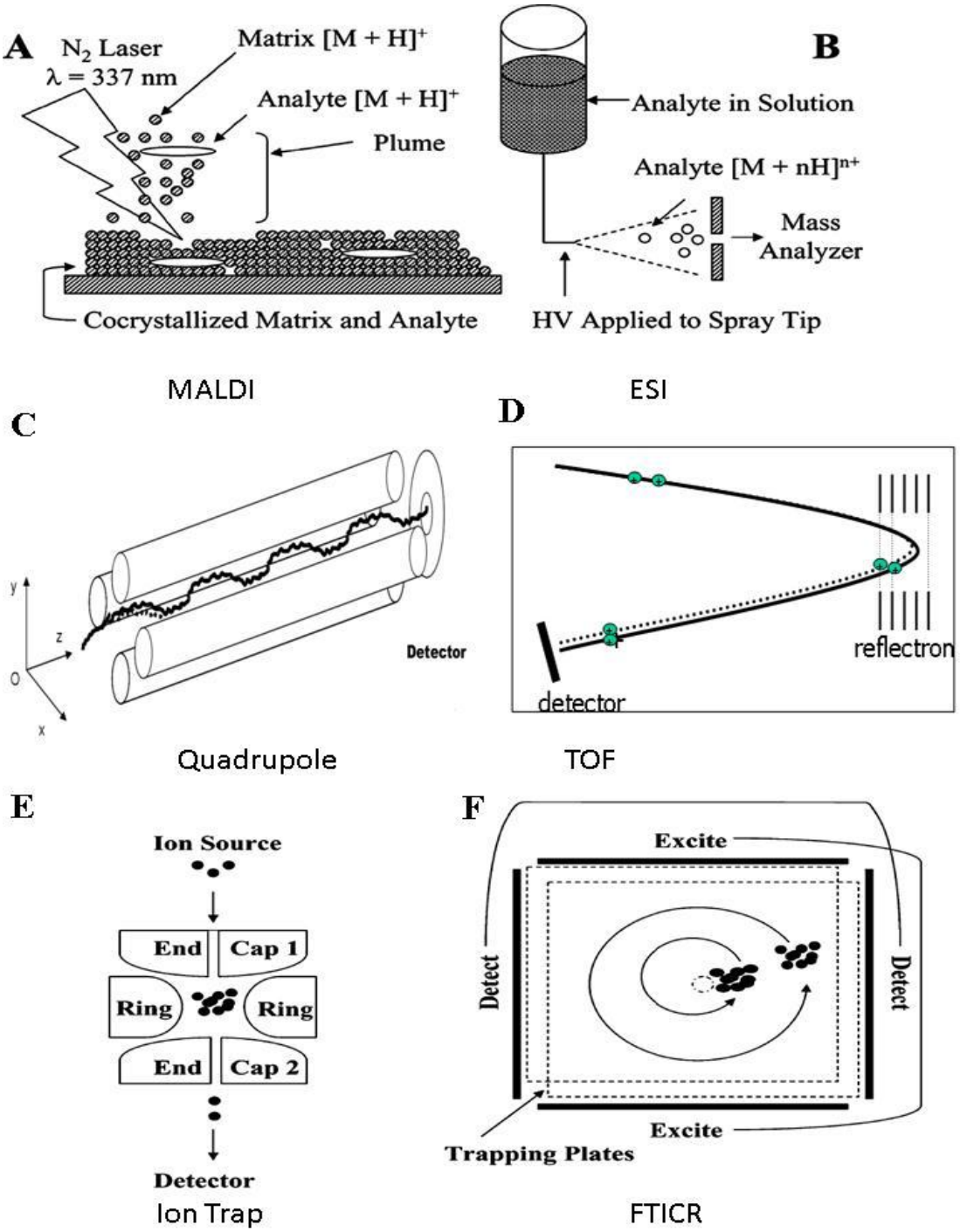

Figure 1.5 Working Principles of Two Ionization Methods and Four Mass Analyzers (permission from ref.51 was obtained from publisher to use this figure)[51]. A. MALDI; B. ESI; C. Quadrupole; D. TOF; E. Ion Trap; F. FTICR[51].(Detailed description in page 14)

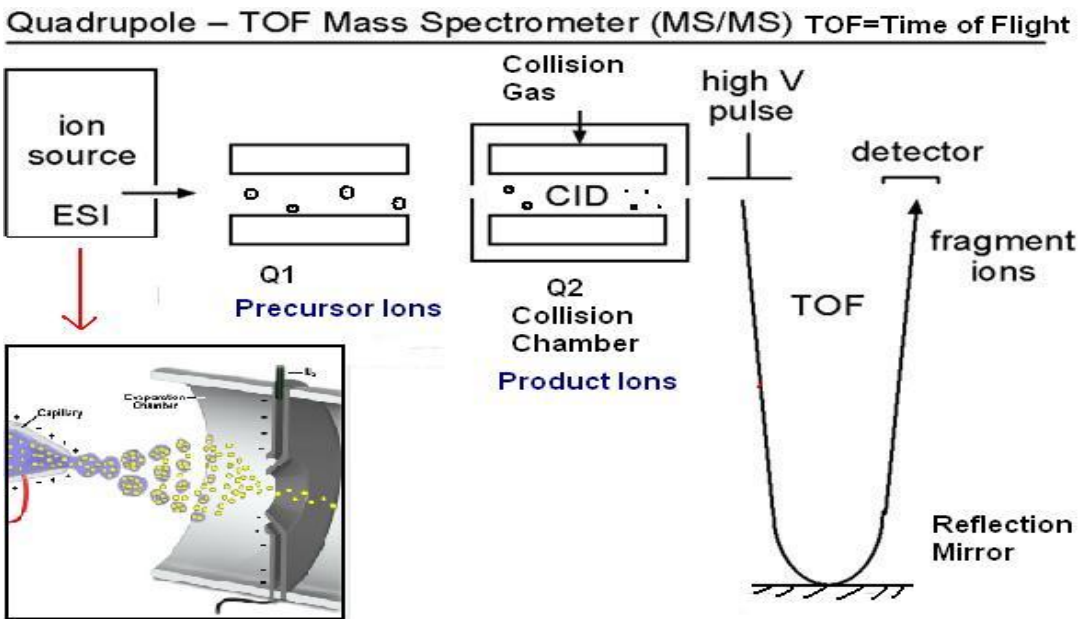

Figure 1.6 Structure of Q-TOF Mass Analyzer(Detailed description in page 14-15)

1.5 Quantitative Proteomics

Quantitative proteomics reveals the different biological states such as normal and pathological states. Abundant ratios of individual proteins in various biological states, although do not include the information on absolute amount of proteins, the data obtained still uncover the underlining pathological trends. For proteomic quantification, either label or label-free technique is applied. Non-gel-based LC/MS-based shotgun proteomic technology is widely in use for the label-free proteomics. Basically, two or more samples were compared and quantified by chromatographic peak alignment[57].

Comparison of MS signals only between several runs are not reliable since a small amount of sample differences will lead to the variation of ionization rates of particular peptides and retention time[49]. Then labeling the samples with chemical reagents prior to analysis is adopted. The strategy of labeling is to label the samples with chemical reagents which have variations on the isotopic composition thus on their

molecular weights. Relative quantification is conducted by comparing obtained signal intensities. Basically, there are three major types of labeling: 1) metabolic labeling; 2) labeling on the protein level; 3) labeling on the peptide level.

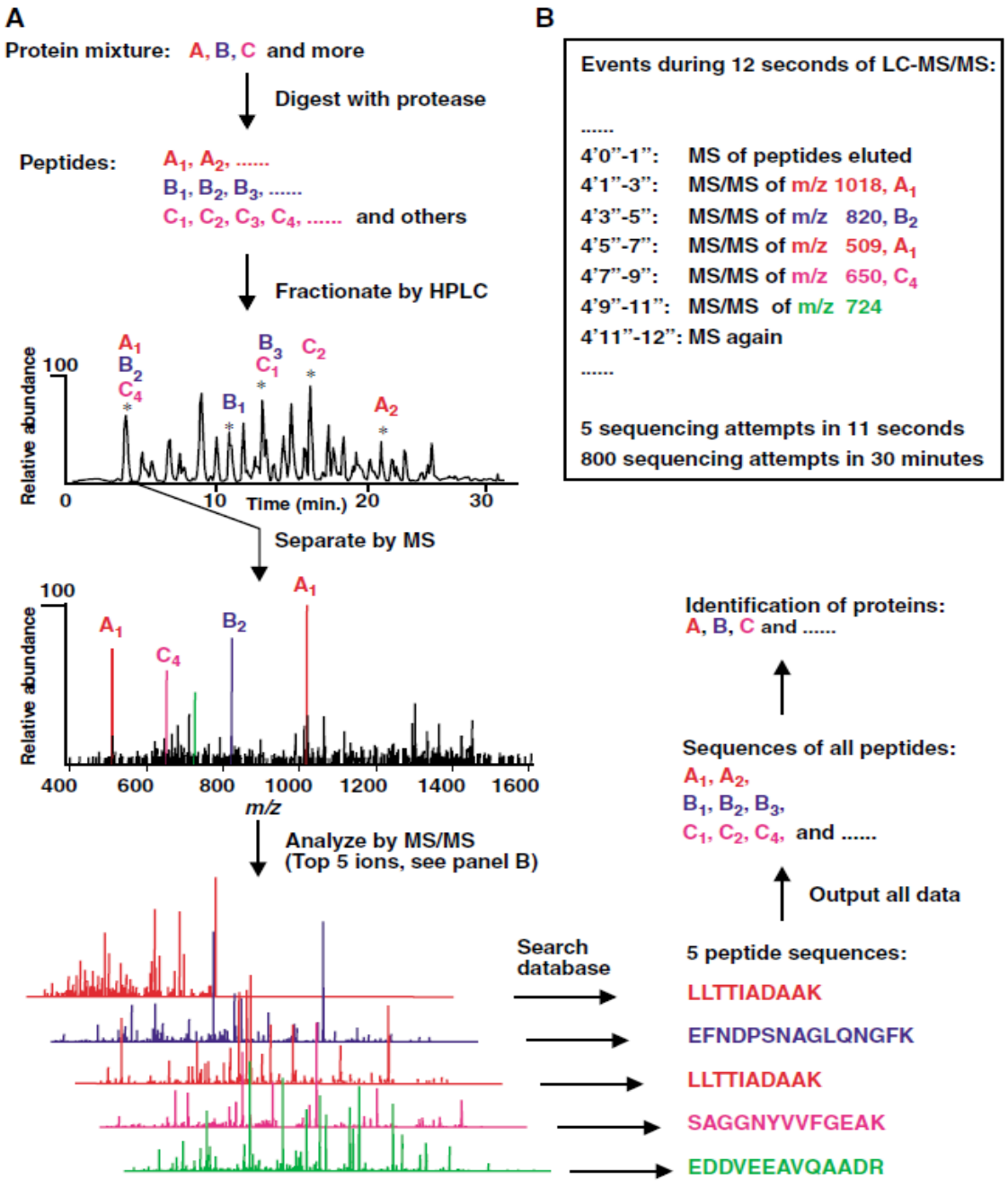

Figure 1.7 On-line LC-MS/MS Analysis Procedure of Complex Peptide Mixture[42] (permission from ref.42 was obtained from publisher to use this figure), (Detailed description in page 15)

Isotope (usually stable and non-radioactive isotopes such as $^{12}C/^{13}C$, $^{14}N/^{15}N$, $^{1}H/^{2}H$, $^{16}O/^{18}O$) labeled amino acids are introduced into the culture media of metabolic active organism. This technique is termed SILAC (Stable-Isotope-Labeling by Amino acids in Cell culture), usually isotope coded leucine, arginine or lysine are in use[58-61]. SILAC has advantages on accurate quantification at level of living cells instead of post-lysis. However, the application is only restricted to cell culture related experiments.

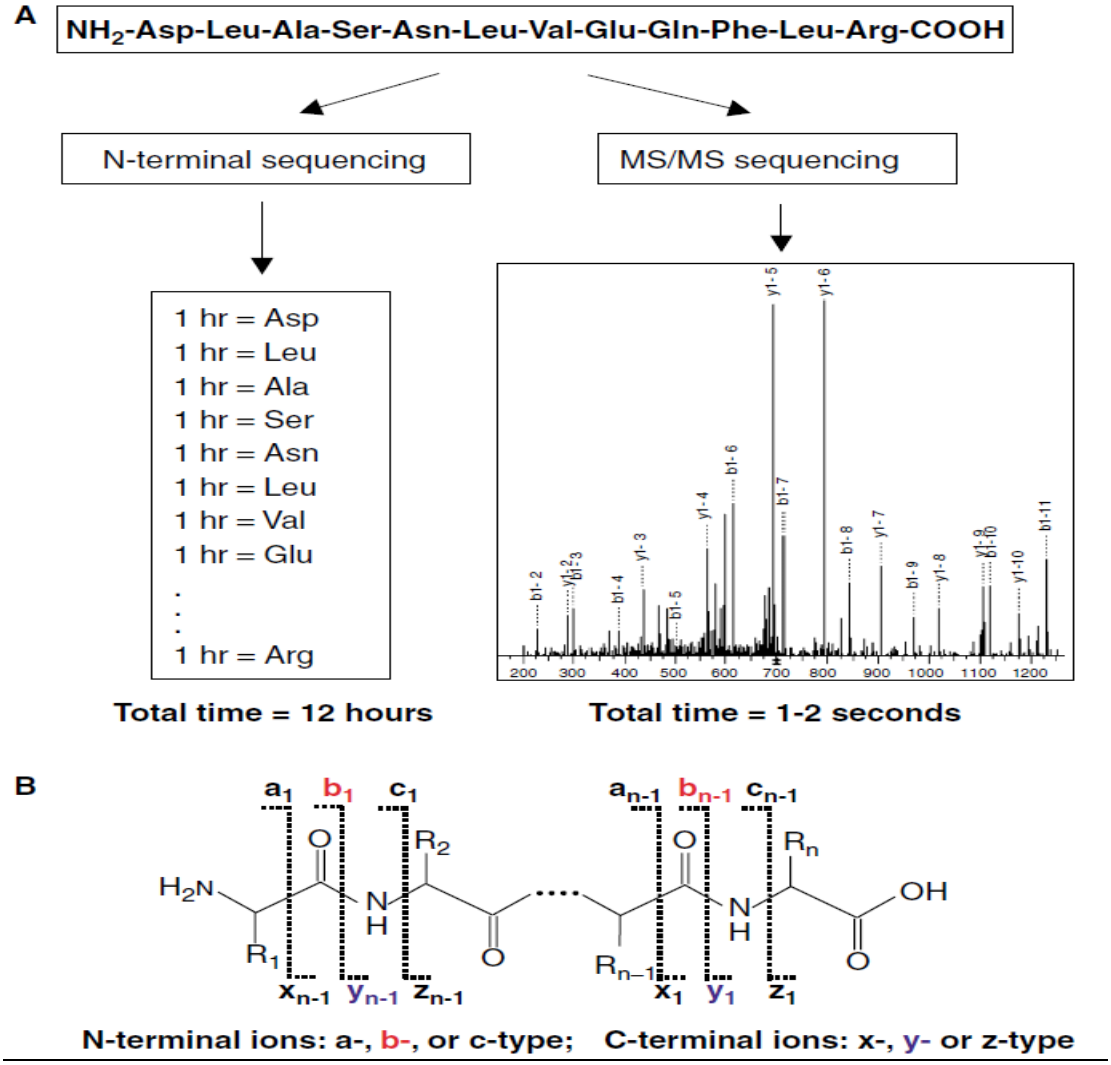

Figure1.8 A. Comparison of N-terminal Sequencing and MS/MS Sequencing B. The Nomenclatures of Fragment Ions[42] (permission from ref.42 was obtained from publisher to use this figure), (Detailed description in page 15)

Labeling at protein level has overcome the disadvantages of SILAC. Several techniques including Isotope-coded affinity tag (ICAT), whose functional group is a thiol reactive group which has affinity to cysteines on proteins. The tag linked by a biotinyl group is able to separate the labeled proteins through an avidin affinity chromatography[62]. There are other technologies such as Cleavable ICAT, which is using $^{12}C/^{13}C$ instead of $^{1}H/^{2}H$ for removing biotinyl group before LC-MS analysis[63], and Isotope-coded protein labeling (ICPL), which is using isotope coded nicotinoyl group with an amino reactive N-hydroxysuccinimide (NHS), targeting lysine and amino group of N-terminus[64].

Labeling on the peptide level has the advantage on improving the number of labeled peptides, thus increase the accuracy of quantitative measurement. Global internal standard technology (GIST) labels the amino-group at N-terminus and lysine with N-acetoxysuccinimid which is isotope tagged. This technique is to acetyl modified the amino groups followed by enzymatic cleavage[65]. However, the most widely applied technique for labeling on peptide level is iTRAQ.

Isobaric tag for relative and absolute quantification (iTRAQ) is based on analyzing the MS/MS spectra rather than precursor ions spectra. The reagents are composed of an amino reactive NHS group coupled to a balancer and reporter group. The most commonly used is iTRAQ 4-plex. It is up to four samples which can be done in a single experiment, with four different reporter groups (MW: 114Da, 115Da, 116Da, 117Da). Accordingly, the molecular weights of the balancers are: 31Da, 30Da, 29Da, 28Da. Each reporter group will connect to a balancer, contributing to the total molecular weight of 145. The NHS group can label all the digested peptides at the

lysine side chain. At the first MS, all the same labeled peptides which are from different samples will elute at the same retention time as they have the same molecular weight. At the second MS (MS/MS), lost of balancer occurs. The label dissociates and releases the reporter group as a single charged ion of masses 114Da, 115Da, 116Da, or 117Da, respectively. Relative peak area of the reporter groups indicate the contribution of each sample to total peptide present, providing a measure of relative abundance[66]. Now there are iTRAQ 8-plex commercially available, allowed eight samples being analyzed in a single run.

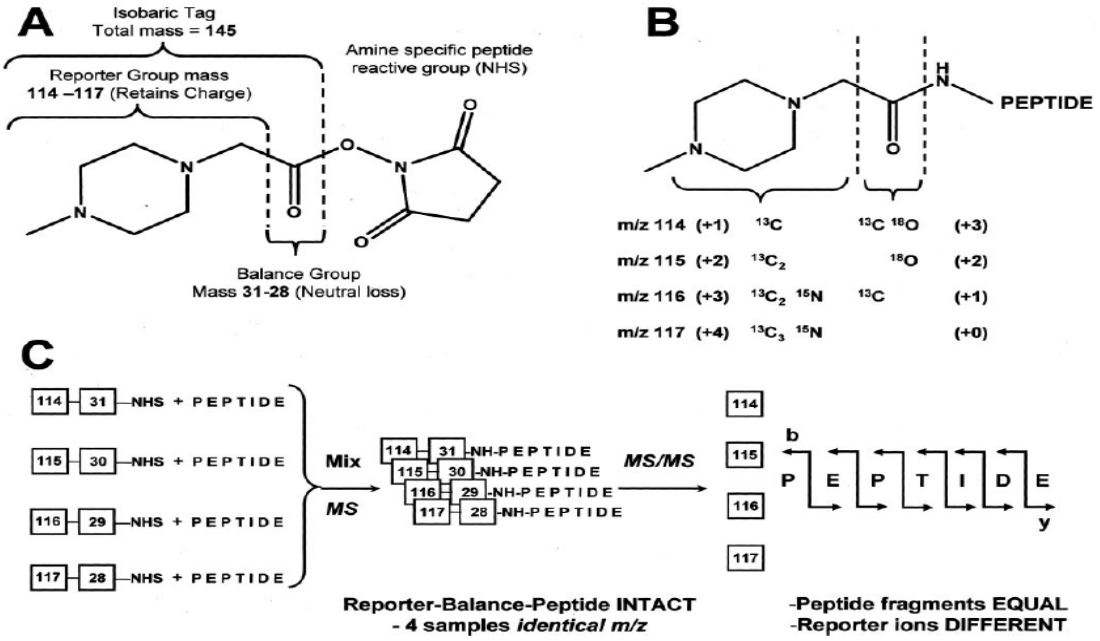

Figure 1.9 Working Mechanism of iTRAQ Reagents [66]. (Permission from ref.66 was obtained from publisher to use this figure)

1.6 Application on Proteomics

Protein-protein interactions

Besides large-scale identification of individual proteins, cell mapping is necessary to achieve a complete understanding of cellular complexity or pathological mechanisms. An integrated view of how the protein complements changes is required to understand particular role of a defined protein in a protein network and how the environment influences cellular states. In diseased conditions, a group of proteins may vary in the expression ratio compared to normal condition. Identification of these protein functions and relocates them in defined cellular signal pathways will draw up necessary information on biomolecular mechanism of the diseases. Cell mapping involves understanding of protein-protein interactions, protein 3-D structures, cellular locations and protein post-translational modifications.

Protein-protein interactions are crucial for understanding of cellular mechanism. Most of proteins carry out their functions by interacting with other proteins in cellular process. Yeast two-hybrid assays[67-69] and direct affinity capture methods[70-71] have been applied to reveal many protein-protein interactions. Compared to these physical methods, LC-MS/MS based method is able to exclude most of non-specific interactions. In addition, it has the advantages that the modified protein can served as the affinity tags to isolate the binding partners. Multi-component complexes can be isolated and examined in a single operation[72]. This analytical method preserves particular protein interaction states which physical methods are not possible to distinguish for a given protein. The interaction states including: post-translational

modification (e.g. phosphorylation, glycosylation, acetylation, ubiquitination), cellular localization, presence of ligands, alternate splicing, proteolytic cleavage, oligomeric state and protein conformation[50]. An example of using LC-MS/MS to study the protein-protein interactions is to identify binding proteins involved in tyrosine kinase receptor (TrkA) signaling in breast cancer cells. In the study, wild type and modified tyrosine kinase receptor chimeric constructs with green fluorescent protein(GFP) were transfected in MCF-7 cells, co-immunoprecipitated proteins were resolved by SDS-PAGE then analyzed by LC-MS/MS. Several TrkA signaling proteins were identified, e.g. Ku70, a DNA repair protein, play important role in carcinogenesis[73].

Challenges in study protein-protein interactions by LC-MS/MS remains, mainly at a defined time, only one or several states of particular proteins can be revealed. However, systematical study of protein-protein interactions aims to describe all states in a given organism, either permanent or temporal, to draw an overall picture of cellular networking[74-75].

Analysis of protein Post-translational modification

Post-translational modification (PTM) is to change the functions of proteins by excising specific groups proteolytically or by a modifying group being added at particular sites of proteins. PTM can determine proteins' active states, localization and interaction with other proteins. A few important PTMs are addressed: phosphorylation,

acetylation, methylation, glycosylation, disulfide bond formation and ubiquitination. MS based technology has allowed large-scale study of PTMs. As modification to protein at molecular weight level thus leading to variation on m/z will be detected by the nature of mass spectrometry. Several recently developed approaches, especially in protein phosphorylation identification, are beginning to yield results for proteome-wide PTM analysis[76]. The general method of PTM mapping for a particular protein is to digest it by enzyme into a group of peptides. The peptides are separated by LC followed by MS and MS/MS detection. PTMs are determined by peptide masses differences compared to the expected peptide masses from protein sequencing. Examples of acetylation (+42 Da) and arginine methylation (+14 Da)[76]. Phosphorylation can be either stable or liable. For stable phosphorylation, +80 Da masses can be applied to localize the modified sites by MS. For liable phosphorylation, an alternative approach named affinity-based enrichment of modified protein is in use. This method uses biochemical, genetic and immunological methods to enrich the defined modified proteins for detection[77]. An example of cells stimulated with EGF, and tyrosine- phosphorylated proteins were immunoprecipitated by anti-phosphotyrosine antibodies[78]. Other PTMs were also reported to be analyzed by this strategy. Another example is histidine-tag allowed purifying and identifying ubiquitinated proteome[79].

Challenges remains for LC-MS based PTM analysis, including high coverage of proteins in complex mixtures, as well as digestion efficacies. Algorithms of optimization for PTM specific databases are still needed. In addition, more affinity tags for labeling PTM sites of proteins requires to be developed.

Membrane Proteomics

Plasma membrane proteins interacts with both intracellular and extracellular molecules, receptors and signaling partner and plays critical roles in cellular functions. In addition, understanding of membrane proteins help scientists to reveal more drug and hormone-targeted proteins as many drug and hormone-targeted proteins are on plasma membrane. MS based techniques are powerful to profile the membrane proteins. However, extraction and separation of membrane proteins remains a challenge for membrane proteins' hydrophobicity and microheterogeneity. There are several methods for isolation of membrane and its components, including zonal centrifugation using a density gradient[80], or partitioning in an aqueous two-phase polymer system[81]. The latter method can be further improved by addition of affinity ligands, e.g. antibodies or receptor agonists and antagonists[82-85].

MS-based Protein Sequencing

Protein sequencing involves *De novo* sequencing and sequence confirmation. *De novo* sequencing is different from sequence confirmation that a peptide's amino acid

sequence is gained without prior known of the protein sequence, while sequence confirmation is the protein sequence already known and only correctness is needed to be compared.

De Novo protein sequencing and sequence confirmation can be performed by MS/MS[86]. peptides are randomly fragmented within a mass spectrometer, and then structural information from the fragment ions was obtained for characterization of proteins. This sequencing is particularly useful for biopharmaceutical products and detection of unknown proteins. In the other aspect, MS-based technology gives another option for protein sequencing confirmation.

Proteomics, especially MS-based proteomic analysis, is rapidly becoming a mature technology to provide a platform for large-scaled protein profile analysis. It is now possible to identify hundreds to thousands of proteins in a single sample. This technology even allowed researchers to study on comparative proteomics quantitatively, with analysis of protein-protein interactions to identify new targets in cellular signal pathways, therefore facilities a better biological understanding of environment-generated stimulations in a particular organism. However challenges for proteomics still remain, e.g. improvement of quantity of proteins detected; separation on a particular group of proteins; removal of abundant proteins and *deja vu.* proteins

while searching for low-abundant but high important ones; as well, methods developed for isolation of plasma membrane-anchored proteins.

1.7 Metabolomics

Metabolome has been defined as "the qualitative and quantitative collection of all low molecular weight molecules present in a cell that are participants in general metabolic reactions and required for the maintenance, growth and normal function of a cell"[87]. These molecules consist of metabolic intermediates, hormones, other signaling molecules, and secondary metabolites [88]. Small biological molecules present in organism are usually the basic units for the formation of biological macromolecules. The small molecules are categorized as metabolites by two criteria: 1) molecular weights are less than 1000Da; 2) involved in metabolism or generated in metabolic pathways. Although comprehensive profiling of metabolites in an organism is not feasible, large scale quantitatively and qualitatively measuring cellular metabolites by employing multiple technologies are at the pioneer stage[47, 55, 89-92].

Metabolomics has played an important role on biomarker identification for diagnosis of particular disease, as the metabolite biomarkers are more towards the endpoint of biological effects. Currently, two approaches are applied for metabolomics. The first one is metabolic profiling. Physiological interactions can be identified in a particular biochemical pathway, reflecting enzymatic activity. Quantitative information is generated among normal and diseased samples. The second approach is named metabolic fingerprinting. Instead of identifying all compounds in metabolic profiling, this approach compares different patterns that induced by environment changes.

Identification of the two metabolomic approaches is usually conducted by NMR-based[93-95] or MS-based technologies[47, 96]. Compared to NMR-based technology, MS-based one has higher sensitivities that leads to low-abundance metabolites being detected. It provides coverage for metabolites in a lower concentration range and steady results[97]. MS is the most widely applied technology in metabolomics, in addition, it provides a better way to identify metabolites effectively, both quantitative and qualitative. Figure1.10 schemes the general flow chart of metabolomic analysis.

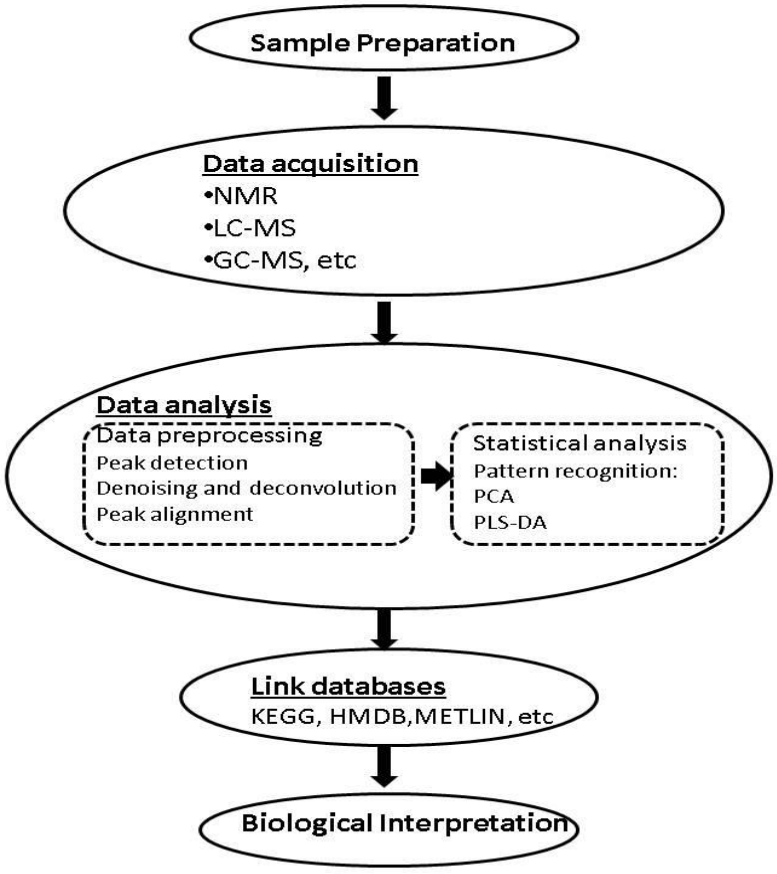

Figure 1.10 Flowchart for Metabolomic Analysis (detailed description in page 28).

Currently, LC-MS and GC-MS have been applied on metabolomic investigation. LC-MS provides data on more dynamic range with combined to multivariate statistical methods. However, in various metabolites identification, in contrast to the well-established gene and protein databases, currently there is no such complete tool for metabolomics[98-99]. At present, only starting point is offered for metabolites structure characterization. There are several databases for metabolite detections, e.g. DB Spectra Database, ChemBioFinder, Metabolite toolbox, chEBI, mass bank, KEGG ligand database, METLIN, etc. One example is MarkerView^{TM} software (Applied Biosystems) which is developed for metabolites analysis on LC-MS. This software analyses the mass spectra generated by LC-MS and provides m/z ratio for detected compounds. Although the mass spectra obtained offers valuable hints to determine the structures of the molecules of interest, the number of candidate molecules isolated from free online chemicals database based on the molecular weight and fragmentation ion peaks may be varied. In that case it is time consuming and costly to test every one of them to see if any one of the candidates is well matched with the molecule of interest. Furthermore, it is unsurprised that none of the candidate chemicals were proved to be the molecule of interest due to incomplete chemicals database.

GC-MS

In contrast, at present, mass spectrometry (MS) interfaced with gas chromatography (GC) with relative complete databases is more liable in study of metabolomics. However, robust analytes and hydrophobic molecules are ideally suitable for GC-MS.

For non-volatile molecules have to be chemical derivatised to suit the needs for GC-MS.

The ionization mechanism between GC-MS and LC-MS is different. There are mainly two methods in GC-MS sample ionization: Electron Impact Ionization (EI) and Chemical Ionization (CI)[100-101]. Samples collide with an electron beam to create ions in EI, while a reagent gas is used to create ions in CI. In MS, mass analyzers are: single quadrupole, TOF, FT-ICR and Orbitrap[53].

Sample preparation and derivatization

Metabolites are extracted by different methods according to the nature of the organisms. Generic methods involves: enzymatic digestion, chemical (water-methanol-chloroform, boiling ethanol) and physical (freeze/thawing, heating) extractions[101]. Obtained metabolites are needed to be derivatised before GC-MS analysis. To detect as many metabolites as possible, the most widely used for derivatization is silylation. In this process, a silyl group [$-Si(CH_3)_3$] replaces an active hydrogen within a molecule thus to make the molecule less polar and more volatile[102]. Active hydrogens can be found in hydroxyls, thiols, amines, amides, imines, and carboxylic acids. For enol forms of aldehydes and ketones, methoxymation is needed before silylation, aims to convert the functional groups to oximes and alkyloximes. The most widely used reagent for methoxymation is O-methoxylamine hydrochloride in pyridine solution. For silylation, BSTFA [N, O-bis(trimethylsilyl) trifluoroacetamide] and MSTFA [N-methyl-N-(trimethylsilyl) trifluoroacetamide] are usually in use with a small amount (1%) of TMCS (trimethylchlorosilane) is applied as catalyst for silylation reactions.

Data processing and statistical identification

After raw mass spectra are obtained, peak enumeration is needed, followed by spectral deconvolution, adjustment of retention time and normalization by the built-in software in GC-MS, e.g. GC-MS Solution (Shimadzu), MassFrontier (ThermoFisher). In biology, normally there is a tendency to use multi-variables to characterize the observations. The data generated can be arranged into an array, where each row represents a specific observation and column indicates the factors we want to measure. In metabolomic analysis, chemometrics, as defined, is modeling variables with statistic methods and is an essential part in data analysis. Multivariate statistical analysis is necessary to recruit the hidden information in various peaks generated from GC-MS. In metabolomic analysis, objects are firstly characterized by specific criteria, and then the corresponding observations are determined. In GC-MS based metabolite profiling, the objects and observations are usually the name of metabolites and their relative peak intensities, respectively. As well, other information such as incubation conditions are needed for the building of the model in various case studies.

The most commonly used chemometric method is principle component analysis (PCA) which determines linear combinations (PC's) of the original variables that explain the variance in the data. It uses several PCs, e.g.: PC1, PC2, PC3… to represent the original variables and each PC can be represented by loadings and defined variables, e.g.:PC1 = p1x1 + p2x2+ p3x3…, where p's are called the loading and represent the importance of the variables (x) to the PC. The larger the loading is, the more important the variable to the PC's value. It indicates the directions of variance. Along the maximum direction, each sample can be assigned a value which is called the score. The difference of the scores for each sample explains the variances between the

samples. This method is an unsupervised clustering method, which looks for linear combinations of variables that explain those biggest differences between individual samples[103]. Besides PCA, other statistical methods, such as partial least squares (PLS)[104] and hierarchical clustering are applied as well whenever needed[105].

1.8 Application of metabolomics

Metabolomic analysis, besides looking for particular biomarkers induced by environment changes, is also critical for drug development. Small molecules present might interfere with drugs and influence both biological response and drug metabolism[52, 106-108] This Omic-study can potentially generate data based on the drug efficacy, biomarkers, toxicity for characterization of new compounds, gives more supporting for the pre-clinical and even clinical assessment. One example is analysis of a chemokine receptor 5 antagonist which is hepatotoxic. Metabolomic analysis revealed that abnormally induced drug of fatty acid metabolism was detected, by identification of medium chain dicarboxylic acids which are not commonly found in urine[109]. In disease diagnosis, metabolomic analysis has also started to have impact. This junior member of "Omics" family also has application on cancer diagnosis and treatment. Comparison of cancerous and healthy tissue or body fluids metabolic pattern give more evidences on molecular pathology and on those effects by particular medicine. The profiling reveals the alterations on key metabolic pathways including glycolysis, pentose phosphate pathway, tricarboxylic acid cycle and biosynthetic

pathways of fatty acids and amino acids[110]. Metabolomic analysis is also applied to identification of new biomarkers of cardiovascular disease[111].

In addition, identifying inborn errors of metabolism through body fluids by metabolomic approach has also been reported[112]. As well, metabolic profiling also has been used in plant science. One example is to detect the metabolic response to salt stress of barley[113].

However, compared to other "-omics" study, metabolomics is still in early developing stage. The diverse chemical properties of metabolites and large dynamic range of metabolite concentrations restrict the analysis using current technologies. As well, development of new algorithms and bioinformatics software packages is still in need.

2. Objectives

Warfarin, a synthetic derivative of coumarin, is a commonly used oral anticoagulant drug. It prevents the formation of blood clots, thereby reducing the risk of stroke, a result of rapid loss of brain functions caused by thrombosis and a leading cause of adult disability and death all over the world. Clinical studies have indicated that patients display different dosing requirement for warfarin, for its best beneficial effects over the undesirable side-effects. Patients have been categorized in low- and high-dose groups. Pharmacogenetic analysis of patients on low- and high-dose has provided helpful information on DNA polymorphism differences between the groups of patients. However, other factors including differentially expressed proteins may affect warfarin dosage. Identification of serum markers by comparative proteomics and/or metabolomics may complement the genotyping analysis for better prognosis of the dosing requirement of new patients on warfarin therapy.

Proteomics analysis allows the identification of large scale cellular proteins, which provides a platform to screen for particular biomarkers induced by environment changes. Application of proteomics on studying underlying pharmaceutical mechanisms, and identifying particular biomarkers are usually referred to as pharmacoproteomics[114]. Our project offers a two-pronged approach. First, specific potential dosage related proteins were identified in clinical serum of a group of Asian patients receiving warfarin by application of iTRAQ-coupled 2D LC-MS/MS-based

quantitative proteomics. However, intrinsic differences amongst patients have limitation on the identification of such markers in patients' serum samples, which affect the statistical consistency of clinical analysis.

Therefore, cell-based systems offer an environment with high-level of homogeneicity and high reproducibility in the understanding of drug intrinsic mechanism. As complementary to clinical results, protein profiles generated by chiral drug warfarin incubated liver cells HepG2 were analyzed by iTRAQ-coupled 2D LC-MS/MS-based proteomics. Warfarin is a racemic mixture with two enantiomers, name S(-) and R(+), with each of them displays unique properties and therapeutic effects. Intracellular protein profiles revealed the mechanism of drug actions, while extracellular protein profiles give more evidence on the discovery of potential biomarker. The findings in clinical can be validated by cell-line system and vice versa.

Metabolomics analysis allows the detection of a whole set of biological small molecules which participates in metabolic reactions. This technology has been applied to investigate drug behavior and toxicity. In addition to proteomics, metabolomics can be applied to explore the physiological relevance of our proteomics data. We therefore analyzed the intracellular metabolite profiles in HepG2 cells incubated by individual enantiomers of warfarin, with a GC-MS system.

Our findings (extracellularly and intracellularly) may also provide molecular insights on the enantiomer-based drug side effects. The combined proteomics and metabolomics information on the status of drug treatment and drug functions should provide a comprehensive understanding on overall warfarin-cell interaction and the dynamics of cellular responses. It is to be hoped that our interactive cell-based coupled with clinical analysis platform can be expanded to other new drugs for their preclinical drug toxicity testing.

3. Materials and Methods

Proteomics

3.1 Cell Cultures

HepG2 cells from the American Type Culture Collection were cultured in minimum essential medium (MEM, supplemented with 10% FBS, penicillin (100 U/mL), and streptomycin (100 U/mL)). Cells were maintained at 37 °C in an atmosphere of 5% CO2. Subcultures of cells were carried out from a 1:4 split of 80%-90% confluent monolayer using 0.125% Trypsin-EDTA solution. All culture media and media supplements were purchased from Life Technologies. For the first set of experiment, cells were incubated only by either S(-) or R(+) warfarin(commercially available in Sigma Aldrich, Product Number:UC213 and UC214, purities ≥ 97% (HPLC)). After cell seeding and reaching 80% confluence (10cm tissue culture dish), the cells were incubated with either S (-) or R (+) warfarin at 20μM each, for 24 hours without serum. For the second set, cells were supplied with physiological concentration of vitamin K (Sigma Aldrich) (0.5μM) for 12 hours, then again 20μM of either S(-) or R(+) enantiomer of warfarin was used to incubate the cells separately for another 24 hours, in the absence of serum. Cell pellets were then harvested by low-speed centrifugation and kept in -80ºC before lysis.

3.2 Patient Selection

Local patients were recruited for this pilot study. The study population consisted of patients receiving long-term warfarin anticoagulant therapy at the Singapore General Hospital Anticoagulant Clinic. These patients were part of a larger cohort of patients that participated in a previously reported study[31]. All patients were required to be on a stable maintenance dose of warfarin for at least one month with their international normalized ratio (INR) maintained between 2.0 and 3.0, and had no bleeding episodes. Patients with severe congestive heart failure (NYHA class 3 or greater), liver cirrhosis and thyroid disease were excluded from the study. Eligible patients were required to have a stable maintenance dose of warfarin for at least 1 month (defined as no fluctuation in warfarin requirement for 1 month) and INR value variations ≤ 15% over 1 month, and had no bleeding episodes. Patients on medication known to interact with warfarin (NSAIDs, antiepileptics, sulphonamides, rifampicin and amiodarone) were excluded. The selection of patients was approved by the Institutional Review Board (i.e., Helsinki Declaration) to assure protection of subjects. Serum from a healthy volunteer was collected as the control sample for clinical group. All patients' serum samples were compared with the control sample.

3.3 MTT Assay

MTT reduction test were used to determine cytotoxic concentrations. MTT [3-(4, 5-dimethylthiazol-2-yl)-2, 5-diphenyltetrazolium bromide] assay, first described by

Mosmann in 1983 [115]. The working mechanism of this assay is: the mitochondrial dehydrogenase enzymes in living cells can excise the tetrazolium ring in the MTT and purple formazan are created. The crystals are then solubilized by DMSO. The number of living cells is linear proportional to the amount of the dark blue formazan crystals formed, which can then be quantified by colorimetric assay. Firstly, warfarin enantiomers' cytotoxic concentration was determined. In this experiment, HepG2 cells were seeded onto 96-well plate, with cell density 60,000 – 70,000 /ml. S(-) and R(+) warfarin were each dissolved in DMSO, and concentration range was from 5μM to 500μM, 6 points. Treatment was taken for 24 hours, and media was removed and cells were incubated by 5mg/ml MTT solution (dissolved in PBS) for 4 hours, then MTT was removed, and the formazan salts were dissolved in DMSO. Finally, MTT reduction data were expressed as absorbance at 570 nm on a microplate reader (Benchmark Plus). The experiment was done for three times. Secondly, vitamin K's cytotoxic concentration was also determined following the same method above, except the concentration range was 0.5μM to 50μM, and vitamin K incubation time was 12 hours. MTT results were obtained by light absorption values, in terms of survival ratio compared with untreated group.

3.4 Cell Lysis, Protein Digestion, and Labeling with iTRAQ Reagents.

Cells were obtained and cell lysis was carried out on ice for 20 minutes, in 150μL lysis buffer consisting of 8 M urea, 4% (w/v) CHAPS, and 0.05% SDS (w/v), then vortex

for a minute for evenly mixing. The mixture was centrifuged at 4 °C at 15 000*g* for 60 min, supernatant (proteins) was removed, and the concentration was measured by 2-D Quant Kit (Ge Healthcare). Bovine Serum Albumin was used to build a standard for quantification. For each sample, 100μg proteins were separated and precipitation with 4 volumes of acetone (Fisher Scientific) was done at -20ºC for 2 hours. After that, acetone was removed by centrifugation and proteins were suspended in dissolution buffer(0.5M triethyammonium bicarbonate). Then proteins were denatured by denaturant(2% SDS), followed by cleavage of disulfide bonds(50mM tris-(2-carboxyethyl)phosphine(TCEP)). All of these reagents came from iTRAQ 4-plex Reagent Kit (Applied Biosystems). Those steps were to make sure that all the proteins were maintained in their denatured forms. Every sample was digested by 20 μl solution of sequence grade modified trypsin (Promega) whose concentration was 0.25μg/ μl. The incubation was subjected at 37 °C overnight. After that, the peptides were labeled with the iTRAQ reagents and incubated as the followings: For the first set (w/o vitamin K), HepG2 without treatment iTRAQ =114; HepG2 incubated with S (-) warfarin = iTRAQ 116; HepG2 incubated with R(+) warfarin = iTRAQ 117. Then the three labeled samples were mixed in one plastic tube. For the second set (w/vitamin K), HepG2 without treatment iTRAQ =114; HepG2 incubated with vitamin K only = iTRAQ 115; HepG2 incubated with vitamin K then S(-) enantiomer = iTRAQ 116; HepG2 incubated with vitamin K then R(+) enantiomer = iTRAQ 117.

Then the four labeled samples were mixed and ready for LC-MS/MS analysis. Figure 3.1 is the layout for the experiment design.

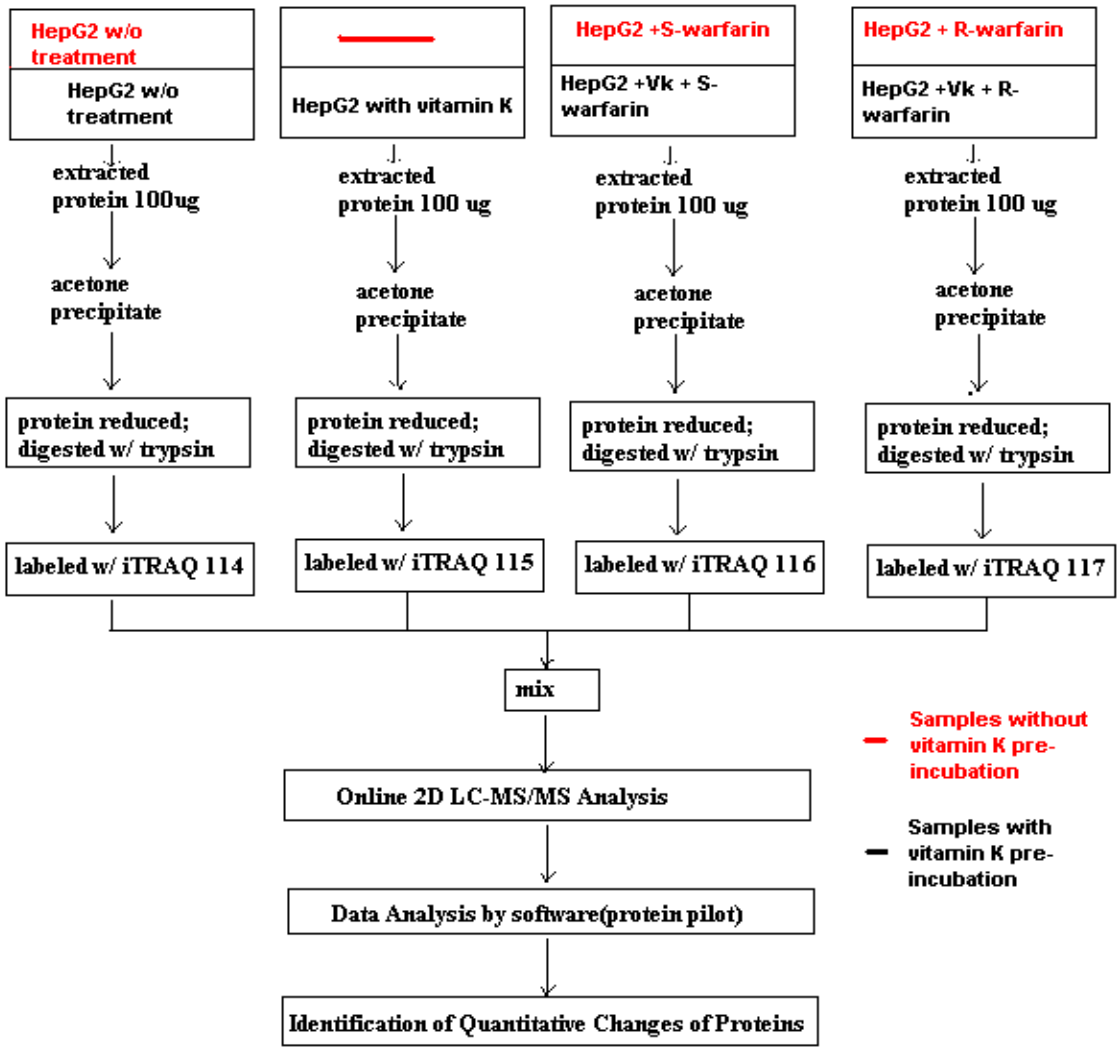

Figure 3.1 Layout for the Experiment Design

3.5 2D Nano-LC/MS/MS Procedure

The following protocol was performed on three individual iTRAQ experiments for each of the two sets. The separation and detection was performed by Agilent 1200 nanoflow LC coupled with mass spectrometer (QSTAR XL) (Applied Biosystems/MDS Sciex) system. In the LC separation, firstly, 3µl of peptide mixtures

were injected onto a PolySulfoethyl A strong cation exchange column (0.32 x 50mm, 5μm). Buffer D consisting of a group of KCl solution from 10mM to 1M (10,20,30,40,50,60,80,100,300,500,1000 mM) used to wash the remaining peptides off from the SCX column in a stepwise manner by sequential injections[116-117]. Each KCl elution of peptides took up 100 minutes. Totally 11 runs made up a whole program. In the first run (Position 1, Figure 3.2, page44) , some of the peptides bound to the SCX column during the flow, while those did not bind were retained in the ZORBAX 300SB-C18 enrichment column(trap column) (0.3x5 mm, 5μm) and washed by buffer A (5% acetonitrile, 0.1% formic acid) at 0.5 ml/min to remove the extra reagent. There were two enrichment columns in total, which was alternatively turned onto the solvent path of the nano pump between the 11 runs by a 10-port valve. In the second run with an increased of KCL solution(Position 2, Figure 3.2, page 44), the 10-port switching valve switched to another position. The previous enrichment column which trapped the unbound peptides in the first run was turned onto the solvent path in the nanopump. Peptides were eluted using the buffer B (0.1% formic acid) and the buffer C (95% acetonitrile, 0.1% formic acid). The concentration started with 5% buffer C and increased to 80% of the same buffer C in a 100 minutes interval at 500 nl/min. This gradient wash was to make sure that most of the peptides could be eluted out. Separation on the next dimension was conducted in analytical Zorbax 300SB C-18 reversed-phase column (analytical column, 75 μm x 50 mm, 3.5 μm), which separated peptides according to their hydrophobic-hydrophilic properties.

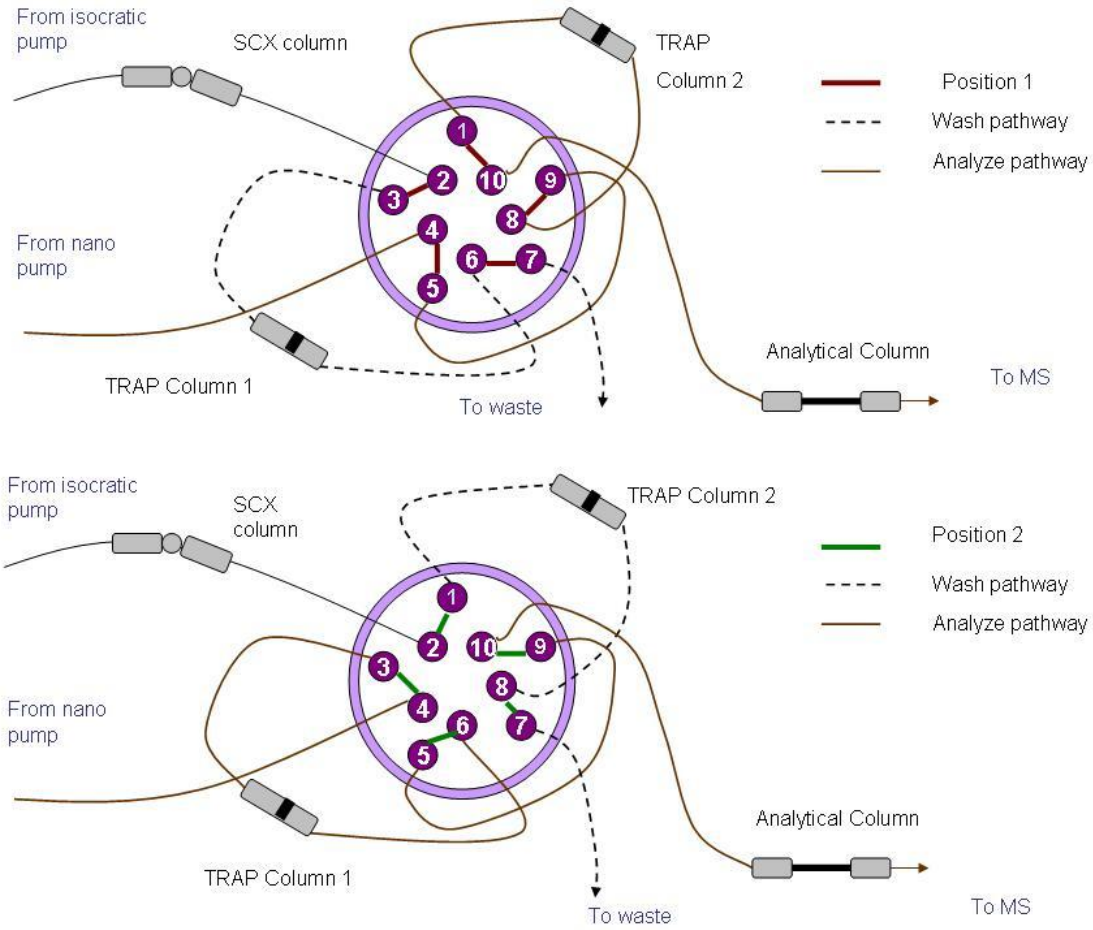

Figure 3.2 Flow Diagram for Nano-2D LC [133](permission from ref.133 was obtained from publisher to use this figure), (detailed description in page 43)

In the MS detection, the ionization method was electrospray ionization. Survey scans were selected from *m*/*z* 300 to m/z 1500. Up to two precursors whose intensity > 15 were selected for MS/MS analysis. In addition, the same peptide could not be selected within 60s. The MS/MS scan was carried out from *m*/*z* 100 to m/z 2000 using dynamic exclusions. Collision energy was applied to accelerate fragmentations. Finally, detection was performed on the AnalystQS (Applied Biosystems) software for every 100-mins run coming from LC.

3.6 Protein Identification and Data Analysis

The analysis of iTRAQ experiments was performed on ProteinPilot™ 2.0(Applied Biosystems, Software Revision 50861). Each MS/MS spectrum was identified using MS/MS data interpretation algorithms in the software and then searched against the Swiss-Prot protein database for the species of Homo sapiens (UniProt_sprot_20070123). The searches were conducted under the following parameter: modifications of methylmethanethiosulfate-labeled cysteine were fixed. iTRAQ modifications of free amine in the amino terminus and lysine was fixed. iTRAQ modification of tyrosine was variable. And serine and threonine residues were allowed to undergo side reaction with iTRAQ reagents. Other parameters such as allowance for number of missed cleavage, parent ion and fragment ion mass accuracy are built-in function in ProteinPilot software. Relative protein quantifications of iTRAQ were the ratios of area under the peaks of 114, 115, 116, and 117 Da. 114, 115, 116 and 117 were the masses of iTRAQ tags reagents, respectively. The relative amount of a peptide within every sample was measured by dividing the peak area at m/z 116 and 117 by 114 (without vitamin K); and m/z 114, 116, 117 by 115 (with vitamin K). To further analyze the statistical values, the following criteria were set up: unused protein score was more than 1.3 (95% confidence) per experiment, at least two unique peptides whose confidence was more than 95% needed to be detected; p value had to be less than 0.05; and protein quantitative ratio of expression of >1.1 or <0.9 was chosen. As for certain proteins, 10% changes may result in significant changes in

protein functions. The error factor (EF), which is a statistic value describing a peptide's 95% confidence interval, for the detected proteins must be less than 2. The proteins detected were examined by Protein ID in the ProteinPilot software. The peptides whose free amino acids were not modified in the sequence terminus or were not modified by iTRAQ were not selected for protein ratio calculations. To correct the small differences in protein loading, the generated ratios of all detected proteins were normalized by bias correction and other built-in function tools in the software.

3.7 Western Blot Analysis

Western blot was performed on Bio-Rad mini-protein electrophoresis system. Sodium dodecyl sulphate-poly acrylamide gel electrophoresis (SDS-PAGE) separates proteins by the molecular weights. SDS-protein complex eliminates the original charges on the protein thus the movement of proteins in the electrophoresis is not influenced by the charges on the proteins or the structures of the proteins. The gel consists of stacking gel(top) and separation gel(bottom). The separating gel was prepared first, which consisting of: for 10% gel , 5 mL mixture of 1)1.3ml separating gel buffer (1.5 M Tris-HCl, pH 8.8), 2)1.67 ml of monomer solution (29 % acrylamide : 1 % bisacrylamide) (Bio-Rad), 3) 0.05 ml of 10% SDS, 4) 0.05 ml of 10% ammonium persulfate (APS), 5) 1.93 ml of distilled water and 6) 5 μl of N, N, N', N'- tetramethyl-ethylenediamine (TEMED). For 12% gel, 2.0ml monomer solution (29 % acrylamide : 1 %

bisacrylamide) and 1.6ml of distilled water was applied, while the rest were the same with 10% gel.

After loading of the separating gel, distilled water was used to make a flat surface. 20 to 30 minutes were needed for polymerization. The distilled water was removed and casting stacking gel was carried out. Basically, 3 ml mixture of 1) 0.5ml 29 % acrylamide: 1 % bisacrylamide), 2) 0.38 ml of stacking gel buffer (0.5 M Tris-HCl, pH 6.8), 3)30 μl of 10 % SDS, 4)30 μl of 10 % APS, 5) 2.1 ml of distilled water and 6) 3 µl of TEMED and loaded onto the top of separation gel. 1mm thickness comb was used to create wells on the stacking gel. 15 min at room temperature was required for polymerization of stacking gels.

The gel run was carried out in a chamber which was filled with 1 X SDS running buffer (0.025 M Tris, 0.192 M glycine, pH 8.3, 0.1 % SDS). Protein samples were mixed with 2 X loading buffer and boiled for 5 min. Molecular weight rainbow markers RPN 756 (GE Healthcare) was used as protein ladder (up to 200 kDa molecular weight). Constant current was applied to run the gels. For the stacking run, the current was set to 12mA and was changed to 18mA for the subsequent phase when the samples reached the separating gel. After electrophoresis, the gel was carefully removed and transferring proteins onto the membrane were taken place.

SDS-PAGE gel was transferred onto 0.45 μm nitrocellulose membrane (GE Hybond) via Bio-Rad's semi-dry transfer system. Figure3.3 was the layout setup for the semi-dry system. Nitrocellulose membranes were pre-rinsed with transfer buffer (25 mM Tris, 192 mM glycine, 20 % (v/v) methanol). In this study the settings for the transfer is fixed at constant voltage (21 V) for 50 minutes. The loaded rainbow marker could indicate the transfer efficacy instead of Ponceau S staining.

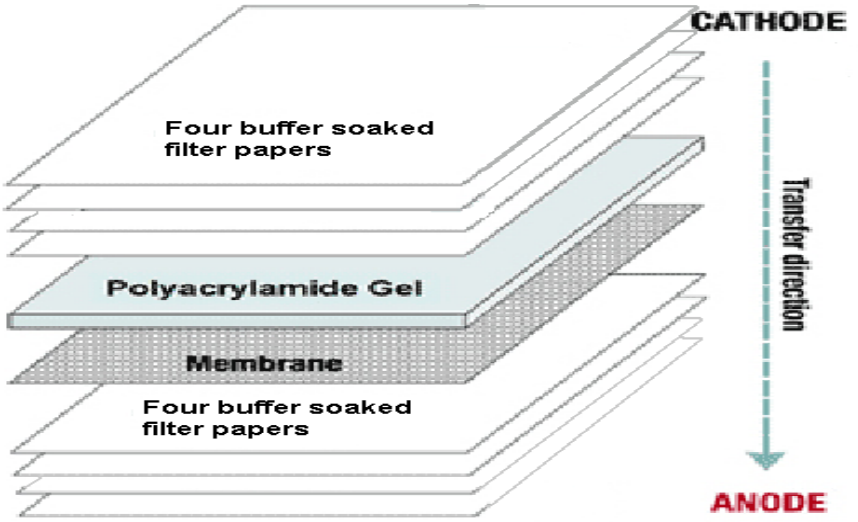

Figure 3.3 Layout Setup for the Western Blot Transfer Semi-dry System (Detailed description in page 47)

Transferred membranes were then subjected to blocking in 5 % non-fat milk dissolved in 1 X PBST for 1 h at room temperature. After blocking, specific primary antibodies, dissolved in 5 % non-fat milk / 1 X PBST solution, was reacted with the proteins on the membrane at 4° C overnight. Unbounded antibodies were removed by washing for three times. Each washing took up at least 15 min, with cold 0.005 % Tween-20 / 1X PBS solution. Secondary antibody tagged with Horseradish Peroxidase (HRP) was dissolved in 5 % nonfat milk / 1 X PBST solution, and reacted with primary antibody

for 1 h at room temperature. Again, unbounded antibodies were removed by washing three times. Each washing took up at least 15 min, with cold 0.005 % Tween-20 / 1X PBS solution. Enhanced chemiluminescence (ECL) using SuperSignal West Pico chemiluminescent substrate (Pierce) was applied on the transferred membrane. 0.5 ml stable peroxide solution and luminol /enhancer solution each were mixed and incubated for 2 to 3 minutes in dark at room temperature. The signals on the membrane were measured on CLxposure X-ray film (Pierce) or ECL hyperfilm (GE healthcare). Both developing and fixing reagents (Kodak) were diluted 5 times by distilled water before use. The exposure time was from several minutes to overnight depending on the nature of primary antibodies.

In intracellular experiment, Part 5, the proteins obtained from cell lysis used in LC-MS /MS analysis were applied on Western blot analysis. Three of the proteins detected in LC-MS/MS were analyzed by Western blot, namely, Protein DJ-1, 14-3-3 protein σ, and PDIA3 (ERp57). The separation was performed by 12% SDS-PAGE for the two proteins, Protein DJ-1 (23kDa) and 14-3-3 protein σ (30Da), while ERp57 (61kDa) separation was done by running a 10% SDS-PAGE. The expression of three proteins was examined on two individual sets (set 1 and set 2): set 1, R (+) enantiomer, and S (-) enantiomer-incubated cells without the presence of vitamin K; set 2, R (+) enantiomer, and the S (-) enantiomer-incubated cells with the presence of vitamin K. Then proteins detection was carried out by individual antibodies: Protein DJ-1: sc-55572, dilution

1:100, 14-3-3 protein σ: sc-100638, dilution 1:200 and PDIA3 (ERp57): sc-23886, dilution 1:100,000 (Santa Cruz). The developed films were scanned by Densitometer (Bio-Rad). And quantitaion of proteins was analyzed by QualityOne software (Bio-Rad).

In extracellular experiment, Part 6, the proteins secreted from HepG2 culture media used in LC-MS /MS analysis were used in Western blot analysis. Apolipoprotien A-I (30kDa) detected in LC-MS/MS were analyzed by Western blot. The separation was performed by 12% SDS-PAGE. This protein expression was examined on two individual sets: set 1, R (+) enantiomer, and S (-) enantiomer-incubated cells without the presence of vitamin K; set 2, R (+) enantiomer, and the S (-) enantiomer-incubated cells in the presence of vitamin K. Then protein was transferred to nitrocellulose membrane, and detections of apolipoprotein A-I were carried out by using antibody Santa Cruz sc-69755. Again, the results were visible using Supersignal West solutions (1856136, Pierce). The developed films were scanned by Densitometer (Bio-Rad). And quantitation of proteins was analyzed by QualityOne software (Bio-Rad).

3.8 Commassie Blue Staining

For validation on Western blot analysis of secreted protein, Commassie blue staining of gel was used to roughly quantify the total protein. For each sample, 15 µg protein was used. Firstly, a fresh 0.75 mm 12% acrylamide gel was prepared and

electrophoresis was carried out. The electrophoresis procedures were the same with Western blotting in part 3.7. After electrophoresis, the gel was washed with the gel-fixing solution (50% (v/v) ethanol in water with 10% (v/v) acetic acid) and soaked in fix solution for 1 hour. Then the gel was washed by gel-washing solution (50% (v/v) methanol in water with 10% (v/v) acetic acid). After that, the gel was covered with 200ml of the Commassie stain (0.1% (w/v) Commassie blue R350, 20% (v/v) methanol, and 10% (v/v) acetic acid). In room temperature, staining the gel at room temperature was taken for 3 to 4 hours with gentle shaking. Then the gel was soaked in destaining solution (50% (v/v) methanol in water with 10% (v/v) acetic acid) and undergoes gently shaking. The destaining solution should be continuously changed for several times until the protein bands can be viewed without background.

3.9 Cellular ROS Level Assay

The ROS (Reactive oxygen species) level of HepG2 cells on incubation of S(-) and R(+) warfarin with and without the presence of vitamin K was measured by Image-IT^{TM} LIVE Green Reactive Oxygen Species Detection Kit (Invitrogen). The assay was performed to verify the cellular level of oxidative condition upon S(-) and R(+) warfarin incubation. It is based on 5-(and-6)-carboxy-2′,7′-dichlorodihydrofluorescein diacetate (carboxy-H2DCFDA), a reliable fluorogenic marker for ROS in live cells[118]. The kit consists of three components: carboxy-H2DCFDA; *tert*-butyl hydroperoxide (TBHP) solution (inducer of ROS production, positive control), DMSO.

On the presence of ROS, the carboxy-H2DCFDA is oxidized and emits bright green and is reliably distinguished by fluorescence Microscopy. The more cells with green fluorescence are, the higher the intracellular ROS level is. Briefly, 2 x 10^4 HepG2 cells were seeded to each well of 24-well plates. We still designed two sets of experiment (without and with vitamin K) as described above. When the cell reached 70% confluence, for the first set, 20μM of S(-) enantiomer, R(+)enantiomer of warfarin were added, respectively, and incubated for 24 h. For the second set, each well was incubated with 0.5μM vitamin K for 12 hour, then again 20μM of S(-) enantiomer, R(+) enantiomer of warfarin were added and incubated for another 24 hours. For positive control, prior to measuring ROS level, *tert*-butyl hydroperoxide (TBHP) dissolved in 0.5 ml culture medium at concentration of 100 mM was used to incubate the cells for 1 hour; 0.5 ml 25 mM carboxy-H2DCFDA was used to incubate the cells for 30 minutes at 37ºC in each well in the plate. The cells were washed for two times by PBS. Then the cells were viewed under a fluorescent microscope (Olympus). The oxidized product of carboxy-H2DCFDA has excitation/emission of 495/529 nm and could be viewed by standard fluorescent filtering set[119].

Metabolomics

3.10 Cell lysis, Metabolite Extraction and Derivatization

To minimize the factors which may contribute to metabolites' instability and to maintain the integrity of metabolite profiles, the cells were immediately stored in

liquid nitrogen before lysis. Metabolites were extracted using mono-phasic mixture of chloroform/methanol/water, according to the generic protocols described in previous articles [120-121], with minor modification. Basically, 1ml of chloroform /methanol /water mixture in the ratio of 20:50:20 was added to each sample, in a chemical fume hood since chloroform is a carcinogen. Then every sample was transferred to separate 2ml glass tubes, as chloroform may react with plastic. Next, cells with extraction reagents were undergone ultra-sonication at room temperature in a water bath sonicator for 100 minutes and votexed for 2 minutes. Subsequently, the samples were transferred to 1.5ml centrifugation tubes and centrifuged at 4ºC at 18000g for 20 minutes. Then for each sample, 0.8ml supernatant was collected. The supernatant was dried completely by centrifugal evaporator (Jouan) overnight.

For GC-MS analysis, two-stage chemical derivatizations were carried out on the obtained metabolites. Firstly, methoxymation was conducted to convert enol forms of aldehydes and ketones in the metabolites to oximes or alkyloximes[102]. The dry samples were each dissolved in 100µl of methoxylamine hydrochloride (20mg/mL in pyridine, Sigma Aldrich), and votexed for 1 minute, and incubated at room temperature for 1 hour. Secondly, silylation was performed by MSTFA (N-methyl-N-(trimethylsilyl) trifluoroacetamide, Sigma Aldrich) to make the metabolites less polar and more volatile. Basically, 100µl MSTFA with 1% TMCS (Trimethylchlorosilane,

Sigma Aldrich) was applied to each sample. Samples were incubated at 70ºC for 30 minutes, and then transferred to vials for GC-MS analysis.

3.11 GC-MS Analysis

The separation and detection of metabolites was performed by a Shimadzu QP2010plus GC-MS system (Shimadzu, Kyoto, Japan), with a 30m x 0.25mm i.d. DB5 capillary column (122-5033 Agilent Technologies), in the splitless mode. Each 1.0µl aliquot of the derivatized sample was injected by Shimadzu AOC-20i+s auto-sampler (Shimadzu, Kyoto, Japan) and rinsed the needle with acetone each 5 times for both pre- and post-run to avoid sample cross-contamination. The solvent cutoff time was set to 3.5 minutes. Helium was used as carrier gas and the column flow was 1.1 ml/min. the injection temperature was set to 280ºC and ion source temperature was set to 200ºC. The initial oven temperature was kept at 100ºC for 4 minutes, increased at 4ºC/min to 320ºC. At 320ºC, it held for 1.56 minutes. The mode for mass spectrometry was electron impact (EI) ionization (70eV) and data acquisition was carried out in full scan mode (m/z from 35 to 600). Between each sample, acetone was run as blank with the same method to avoid further cross-contamination. Before analysis, standard alkane series mixture which contains C-10 to C-40 was used to correct the retention time before analysis. This correction was performed by AART (automatic adjustment of Retention time) from Shimadzu GCMSsolution (version 2.5) software package.

3.12 Metabolites Detection and Quantification

The total ion chromatogram and deconvolution was acquired by Shimadzu GCMSsolution software package. The chromatogram of every sample analyzed was under noise reduction and baseline correction before peak integration. Interesting peaks, whose width at half-height must be more than 2 seconds, were selected and subjected to library search. It is the standard to distinguish between noises and peaks. Other parameters, such as automatic assignments of unique fragment ions for all metabolites, and sensitivity of peak detection, were built-in functions in the software. In this study we used two libraries, National Institute of Standards and Technology (NIST) Mass Spectra Library and Shimadzu's GC-MS Metabolite Mass Spectra Database to search for candidate compounds. Peaks with similarity index more than 70% were selected and named for the compounds. If more than one compounds fulfilled the requirement, then Shimadzu's GC-MS Metabolite Organic Acids Mass Spectra Library equipped with retention indices was used to give a more specific and reliable identification of candidate compounds. After normalization of data, the large amount of metabolite information was analyzed with PCA by software SIMCA-P (version 12.0; Umetrics, Umeå, Sweden). This method is an unsupervised clustering method, which looks for linear combinations of variables that explain those biggest differences between individual samples. Relative quantification of selected compounds was performed by normalizing and comparing the relative chromatograph peak areas.

3.13 Intracellular Glutathione (GSH) Detection

Glutathione (GSH) plays a central role in protecting cells from free radical damages. It exists in two forms: reduced form GSH and oxidized form GSSG. The GSH/GSSG ratio decrease reflects cellular ROS (Reactive Oxygen Species) increasing. To determine the intracellular GSH level and verify warfarin's effect on γ-glutamyl cycle, ThiolTracker^{TM} Violet dye (Invitrogen) was applied. This dye is a thiol reactive dye to label cells, and can be efficiently excited for imaging with fluorescence microscopes. Basically, 2 x 10^4 HepG2 cells were seeded to each well of 24-well plates. We still designed two sets of experiment (without and with vitamin K) as described above. When the cell reached 70% confluence, for the first set, 20μM of S(-) enantiomer, R(+)enantiomer of warfarin were added, respectively, and incubated for 24 h. For the second set, each well was incubated with 0.5μM vitamin K for 12 hour, then again 20μM of S(-) enantiomer, R(+) enantiomer of warfarin were added and incubated for another 24 hours. Then media were removed and cells were rinsed twice by PBS. 0.5 ml PBS with final concentration 20 μM ThiolTracker Violet dye was applied to incubate the cells in each vial at 37°C for 30 minutes. Then the dye was removed and replaced by PBS. Cells were viewed under a fluorescent microscope (Olympus). The ThiolTracker Violet has excitation/emission maxima of 404/526 nm and can be observed using standard fluorescence filter set.

3.14 Statistical Analysis

For clinical part, the non-parametric Mann-Whitney U test and Kruskal-Wallis test were used to assess differences in *VKORC1* diplotype classes and warfarin dose levels association with different parameters TTR and IL-6 and for cell-line part, T-test was carried out, respectively. The level of significance was set as $P<0.05$ for all comparisons.

4. Warfarin Pharmacoproteomics in Asian Patients Receiving Warfarin Treatment: Potential in Effective Warfarin Dosing

4.1 Introduction

Recognition of specific protein changes in response to drug treatment has the potential to facilitate personalized medicine. These changes can be identified by pharmacoproteomics approach based on proteomic technologies, to characterize particular drugs for molecular diagnosis in addition to the profiling of genetic polymorphism. Warfarin therapy needs to be improved because this drug has narrow therapeutic index and large inter-individual variability in patient response. There are wide inter-individual variations in therapeutic responses, and warfarin is a leading cause of serious medication-related adverse events [122].

Optimizing warfarin dosage has remained a challenge in the clinical setting. Recently, functional genetic variants in the *VKORC1* gene were found to affect the pharmacodynamics of warfarin and influence dosage requirements in patients [32]. Although the availability of high-throughput genotyping capabilities can facilitate pharmacogenetic diagnosis, pharmacoproteomic studies may provide additional information on warfarin dose requirements in patients. Phenotypic traits are often the result of various proteins functioning in a concerted manner and may be important in

influencing interindividual variations to warfarin treatment. The field of pharmacoproteomics may be as important as the pharmacogenetics of individual patients as it connects genotypes to phenotypes and represents the effects of functional proteins which may also serve as diagnostic biomarkers for patients. The objective of this pilot study was to investigate the proteomic profile of patients receiving low- and high-dose warfarin and to perform correlative studies between genotypic and proteomic markers in the two groups of patients.

4.2 Experiment Procedures

In this study, 58 patients were selected for the pilot study. The selection criteria were described in Section 3.2. All human participants selected in this study have been approved by Singapore General Hospital Ethics Committee. Written informed consent has been obtained and all clinical investigations have been conducted according to the principles expressed in the Declaration of Helsinki. The serum was collected. Briefly, blood samples were centrifuged, supernatant stored at -80ºC until use. And serum protein was quantified using 2-D Quant Kit. For each patient sample, 100µg proteins were separated, precipitated, digested and labeled by the method described in Section 3.4. All samples were analyzed in three independent analyses by the method described in Section 3.5 and 3.6.

In addition, Healthy, non-cancerous liver tissues certified to be of malignancy free by pathologic examinations (n=36) (from Chinese cancer patients undergoing hepatectomy for metastasis from a colonic primary malignancy) were available for the present genotyping and gene expression studies. All patients provided approved informed consent for participating in the study, and permission was also obtained from the institution's Ethics Committee.

Genotype testing was carried out though: PCR to amplify a specific fragment of the gene of interest; then followed by Agarose Gel electrophoresis to check for the presence of the PCR product. Next, purify the PCR product to remove residual PCR components. Then direct DNA sequencing was conducted to determine the nucleotide sequence of the PCR product. To determine the genotype of the sample, SNP reading via sequence analysis was used. And the haplotypes were constructed in sequential order from the different genotypes using expectation-maximazation algorithm from HelixTree software. The diplotypes were ranked according to specifically setting of probability values.

Total protein from warfarin exposed HepG2 cells were extracted, 200 µg protein was loaded per well to 12% SDS-PAGE gel. Rabbit polyclonal Prealbumin antibody from abcam® (ab16006) diluted in PBS/T (1:3000) was used. This is an *in vitro* model to see whether the differential expression levels of TTR were due to warfarin treatment effect, under serum-minus as well as serum-plus conditions.

4.3 Results

4.3.1 Patient demographics

Approximately 70% of the patients were males and the median age of the patients were 63 years (range: 46 to 75 years) and 50 years (range: 29 to 81 years) in the low- and high-dose warfarin groups, respectively. The median warfarin dose in patients receiving low-dose warfarin was 2.5-fold lower compared to patients receiving high-dose warfarin [low-dose versus high dose: 2.5 mg (range: 1 mg to 3.5 mg) vs. 6.25 mg (range: 4.5 mg to 10.5 mg)] Indications for warfarin therapy included deep vein thrombosis (44%) and cardiovascular conditions (atrial fibrillation, mitral valve regurgitation, transient ischaemic attack and stroke), (56%).

4.3.2 Pharmacogenetics of VKORC1, CYP2C9 and CYP2C19

25 and 28 local Chinese patients requiring low- and high-dose of warfarin treatment respectively were randomly selected in this pilot study. The majority of the patients in the low dose warfarin group carried the *VKORC1* H1H1 genotype (N=23; 92%) while H1H7 haplotype was the predominant haplotype in the high dose group (N=14; 50%). *VKORC1* haplotype data were not available in two patients. The samples of genotypes were shown in Figure 4.1 (page62). This pharmacogenetic related analysis was carried out in National Cancer Center, Singapore.

4.3.3 Protein identified by iTRAQ-coupled 2D LC-MS/MS

The iTRAQ (Isobaric tags for relative and absolute quantitation)-coupled 2D LC-MS/MS, recently applied in the analysis of cellular protein profile in response to incubation with various chiral drugs, such as propranolol[116], ibuprofen[119] and atenolol[117], was used to investigate the proteomic profile in patients receiving low- and high-dose warfarin therapy. A total of 163 proteins were identified by iTRAQ-coupled LCMS/MS analysis.

CYP2C9	*1/*1	*1/*2	*1/*3	*2/*2	*2/*3	*3/*3	TOTAL
Low Dose	21	0	2	0	0	2	25
High Dose	27	1	0	0	0	0	28
CYP2C19	***1/*1**	***1/*2**	***1/*3**	***2/*2**	***2/*3**	***3/*3**	**TOTAL**
Low Dose	9	9	2	2	3	0	25
High Dose	16	11	1	0	0	0	28
VKORC1	**H1H1**	**H1H7**	**H1H9**	**H7H7**	**H7H8H9**	**Missing**	**TOTAL**
Low Dose	23	2	0	0	0	0	25
High Dose	1	14	2	6	3	2	28

Figure 4.1 the distribution of VKORC1 haplotypes as well as CYP2C9 and CYP2C19 genotype frequencies in patients receiving low-dose (N=25) and high-dose (N=28) warfarin. (This work is done in collaboration with my co-supervisor's group) (Detailed description in page 61)

Identification of protein with significant expression level was based on the ProtScore with the cut-off at 2.0 and a confidence value of 99%. A total of 13 proteins satisfied these criteria and the results were reproducible when repeated in triplicates (Table 4.1, page 66). As shown in Figure 4.2 (page64) and Figure 4.3(page 65) of the differential proteins that were detected, the expression levels of transthyretin precursor was found

to be significantly different between the patients requiring low- and high warfarin dose ($P < 0.001$).

4.3.4 Influence of VKORC1 diplotypes on transthyretin levels

Figure 4.4 A&B (page 67) is a box and whisker plot representation of the influence of *VKORC1* diplotypes on transthyretin precursor levels. Patients with the H1H1 diplotype had significantly higher levels of the transthyretin precursor compared with patients harboring the

H7H7 or H7/H8/H9 diplotype which is associated with high warfarin dose requirement (H1H1 vs. H7H7 or H7/H8/H9, $P < 0.0001$).

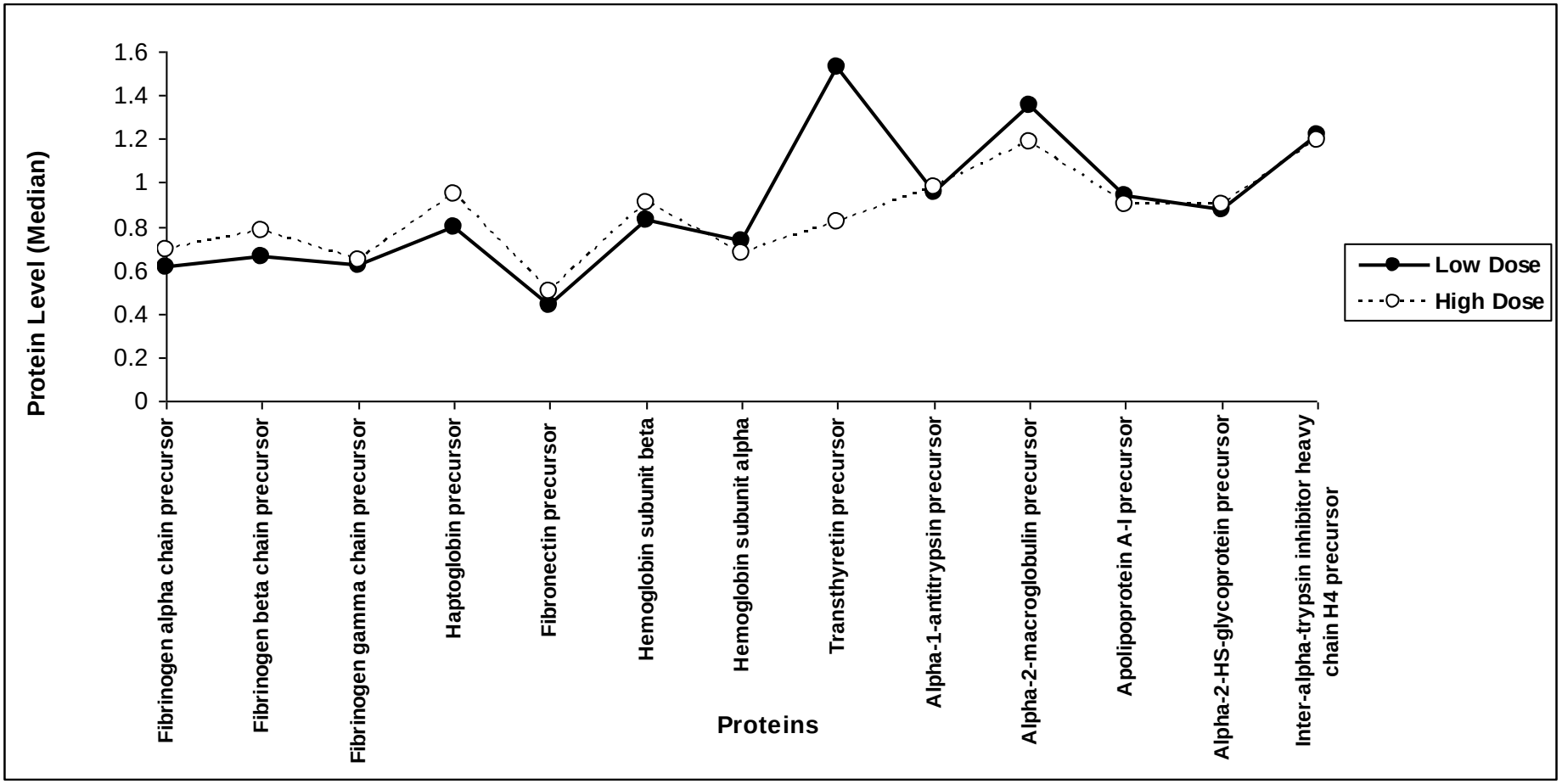

Figure 4.2 Differential Expression of Protein Levels in Patients Requiring Low- and High Warfarin Dose. (Detailed description in page 62)

4.3.5 TTR protein expression in HepG2 cells (done byA/P Chowbay's Lab)

In order to explain the reverse correlation between TTR expression and the dose dependent warfarin treatment, we carried out an *in vitro* experiment using HepG2 cells exposed to low (1µg/ml) and high (10µg/ml) dose warfarin treatment for 24 hrs (with or without serum). Compared with control, a 2.3 fold difference in the TTR protein expression was observed in cells exposed to low and high dose warfarin at 24 hours. Figure 4.5 (page 68)showed the results of western blotting, indicated higher levels of TTR expression in cell culture system exposed to low concentrations of warfarin compared with those exposed to high concentrations of warfarin.

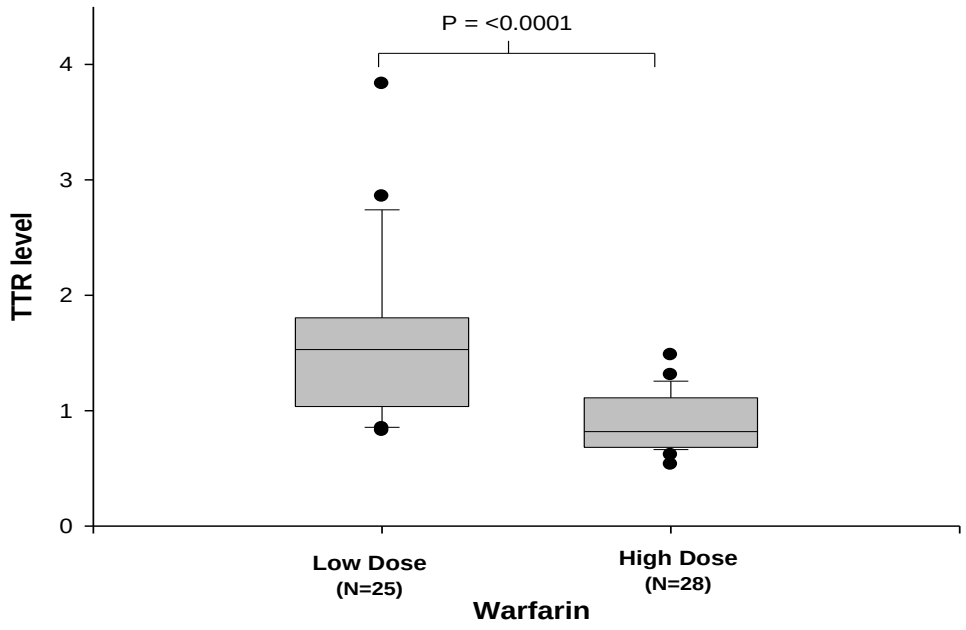

Figure 4.3 Expression Level of transthyretin precursor (P<0.05)
(This work is done in collaboration with my co-supervisor's group) (Detailed description in page 62)

Table 4.1: ProtScore List of Protein with Significant Expression Level with the Cut-off at 2.0 and a Confidence Value of 99% (Detailed description in page62)

S.No.	*Protein code*	*Protein Name*	Low Dose (N=25) Median (min-max)	High Dose (N=28) Median (min-max)	P-value (LD vs. HD)
1	P02671	Fibrinogen alpha chain precursor	0.613 (0.49 - 1.578)	0.69 (0.497 - 1.549)	0.258
2	P02675	Fibrinogen beta chain precursor	0.662 (0.42 - 1.555)	0.7825 (0.555 - 1.471)	0.094
3	P02679	Fibrinogen gamma chain precursor	0.618 (0.341 - 1.291)	0.645 (0.486 - 1.555)	0.065
4	P00738	Haptoglobin precursor	0.793 (0.074 - 1.468)	0.948 (0.173 - 1.899)	0.444
5	P02751	Fibronectin precursor	0.437 (0.324 - 1.352)	0.5045 (0.263 - 1.492)	0.139
6	P68871	Hemoglobin subunit beta	0.828 (0.523 - 2.159)	0.9055 (0.52 - 4.588)	0.382
7	P69905	Hemoglobin subunit alpha	0.729 (0.471 - 1.601)	0.674 (0.504 - 1.518)	0.306
8	P02766	Transthyretin precursor	1.53 (0.828 - 3.833)	0.818 (0.534 - 1.483)	3.94E-06
9	P01009	Alpha-1-antitrypsin precursor	0.956 (0.775 - 1.252)	0.979 (0.799 - 1.267)	0.392
10	P01023	Alpha-2-macroglobulin precursor	1.351 (0.891 - 1.727)	1.189 (0.822 - 1.719)	0.014
11	P02647	Apolipoprotein A-I precursor	0.936 (0.758 - 1.218)	0.8995 (0.633 - 1.207)	0.286
12	P02765	Alpha-2-HS-glycoprotein precursor	0.874 (0.593 - 1.125)	0.902 (0.454 - 1.058)	0.055
13	Q14624	Inter-alpha-trypsin inhibitor heavy chain H4 precursor	1.215 (1.045 - 1.759)	1.194 (0.928 - 1.697)	0.096

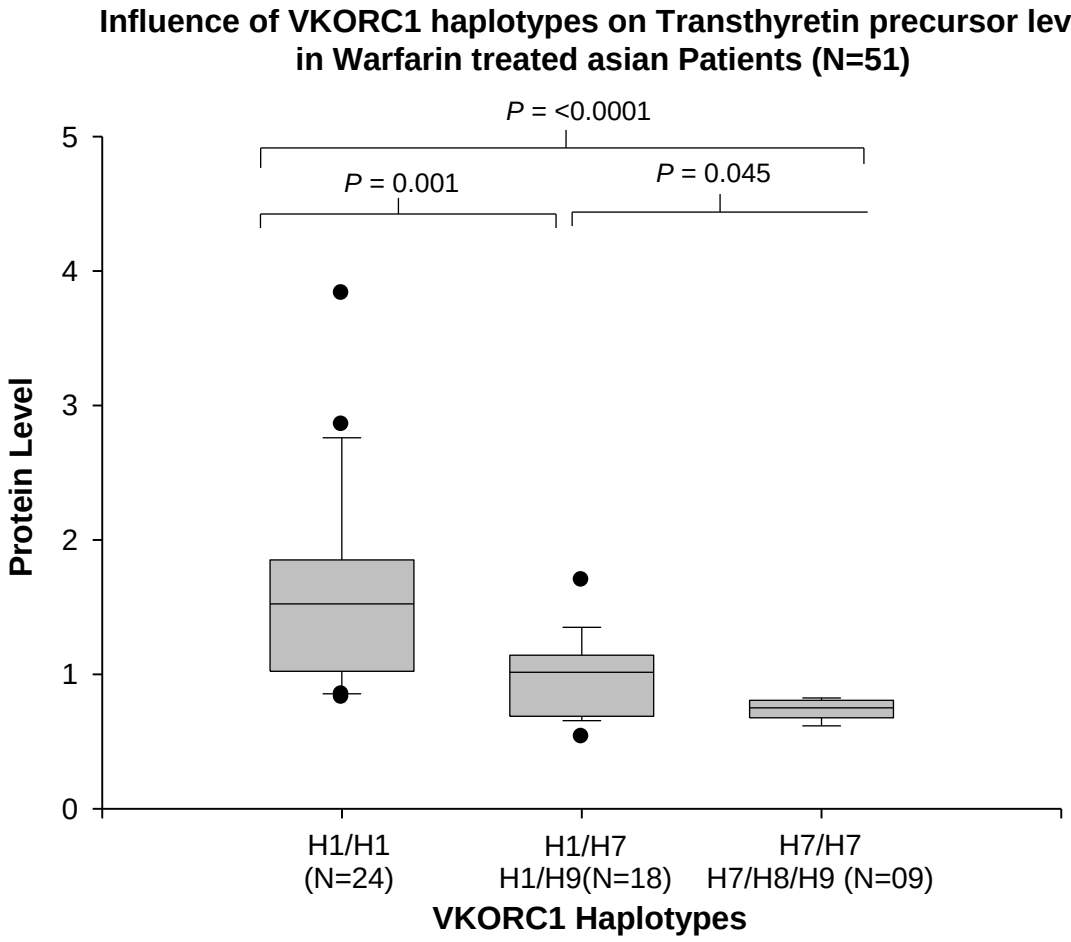

Figure 4.4 Influence of *VKORC1* Haplotypes on TTR Precursor Level in Warfarin Treated Asian Patients (This work is done in collaboration with my co-supervisor's group)

(Detailed description in page 63)

A

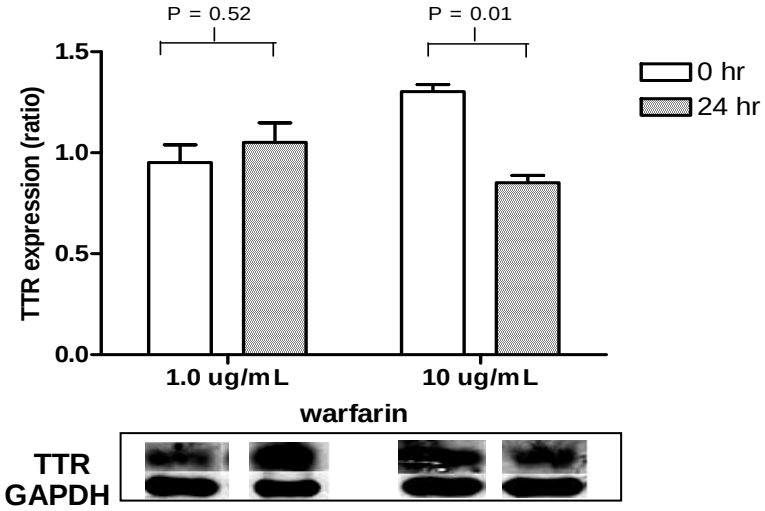

B

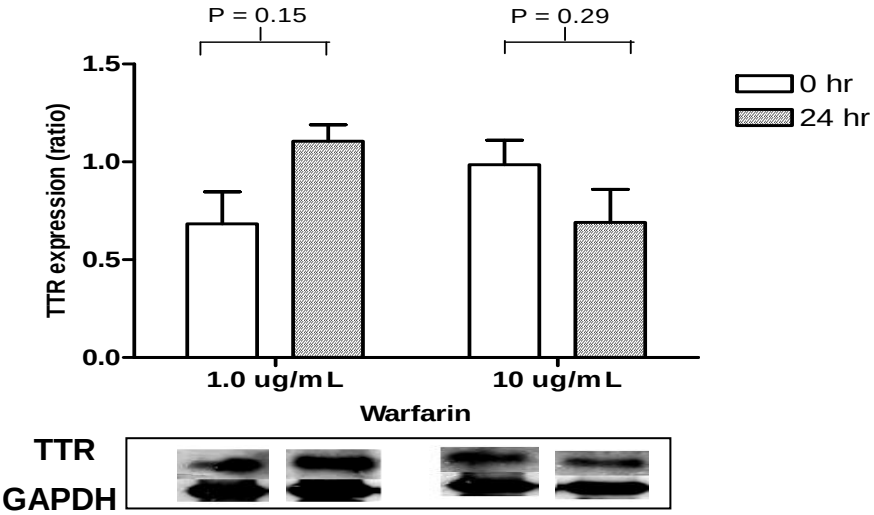

Figure 4.5 Western blot results of transthyretin expression levels in HepG2 cells exposed to low and high concentrations of warfarin (Detailed description in page 65)
.
A. TTR expression levels in HepG2 cells under serum free conditions.
B. TTR expression in levels HepG2 cells under non-serum free conditions.
(This work is done in collaboration with my co-supervisor's group)

4.4 Discussion

Pharmacoproteomics is fast expanding and proving to be a useful companion for pharmacogenetics and pharmacogenomics in drug development, diagnostics and toxicology studies. Pharmacoproteomic profiling in patients have several associated advantages with regards to personalized therapy: Firstly, it is directly associated with the observed phenotypic changes following drug treatment and secondly, it provides a better representation of individual variations observed between patients. The objective of the study was to investigate for warfarin-specific biomarkers by performing collective genetic and proteomic profiling in patients received low- and high-dose warfarin.

This study on plasma protein profiling showed that *TTR* (Transthyretin) precursor (54,980 Da.) was differentially expressed between patients receiving low- and high-dose warfarin. The results were shown that patients received low-dose of warfarin expressed higher *TTR* protein in plasma than the high-dose received patients. *TTR* is known to be produced in liver and released into the blood circulation as a functional homotetrameric protein. In clinical settings, *TTR* level is used as a biomarker for nutritional and/or inflammatory status, and also as an etiological agent to assess amyloidosis[123]. The functional *TTR* transports hormone thyroxine (T3 & T4) and retinoids by interacting with retinol binding protein (RBP)[124-125]. A recent estimate revealed that most of the circulating *TTR* (0.15 – 0.3 mg/ml; 3-6 μM) remains free ligand, which may be associated with multiple biological functions undiscovered [126]. The results from our proteomic profiling suggested that *TTR* can also serve as a

biomarker to identify patients for their warfarin metabolizing efficiency. The focus of our study is to compare patients receiving high dose of warfarin with those on low dose. Thus the control samples from healthy individuals take a less prominent role in this study. However, more healthy samples will be included in future investigations to make new findings even more significant.

Warfarin has been used as an oral anticoagulant for a long time to treat conditions like thrombotic complications. *VKORC1* gene has recently been referred to be a major target of warfarin, polymorphisms in this gene affects the warfarin drug sensitivity. Haplotype-based analysis of *VKORC1* has a potential to identify patients who require low- or high-dose of warfarin, as these haplotypes influence the *VKORC1* gene expression [127]. Notably, H1H1 diplotype group who receives low dosage of warfarin showed higher expression of *TTR* precursor level, whereas H1H7/H1H9 diplotype receives higher dosage showed lower *TTR* precursor level. The results indicate that *TTR* expression is inversely proportionate to *VKORC1* gene expression in warfarin treated Asian population.

The gene product is found in cellular component (extracellular), but gene product expressed in tissue. Further to investigate on the influence of *VKORC1* diplotypes in *TTR* gene expression, real-time PCR and protein immunoblot study have been performed in healthy hepatic tissues. Both analyses revealed absence of any significant difference in TTR mRNA and protein levels between the different *VKORC1* genotypic groups. (data not shown).

Therefore, we next investigated in an *in vitro* model if the differential expression levels of TTR were due to warfarin treatment effect. To ensure that the observed effects were due to free warfarin concentrations, HepG2 cells cultured under serum-minus as well as serum-plus conditions and exposed to low (1.0 µg/ml) and high (10 µg/ml) warfarin concentrations for 24 hrs showed the TTR expression patterns were inversely proportional to warfarin dosage. Western Blot analysis results also indicated higher levels of TTR expression in cell culture system exposed to low concentrations of warfarin compared with those exposed to high concentrations of warfarin. In a parallel study(with and without serum), warfarin showed negligible binding to TTR when studied using RP-HPLC as opposed to its being almost 100% bound with human albumin (Figure 4.5). These findings suggest that warfarin may induce TTR expression in a dose-dependent manner. Further studies are required to validate these findings.

Previous report showed that increased IL-6 decreases the transcription and translation of TTR in HepG2 cells [128-129]. Also, low-dose warfarin has previously been reported to exert an anti-inflammatory effect through the suppression of IL-6 activity, while high-dose warfarin tends to activate pro-inflammatory signaling via increased IL-6 production [130-132]. In our study, consistently with earlier findings, patients receiving high dose warfarin showed significantly increased levels of IL-6 in comparison with those receiving low-dose warfarin(data not shown). The exact mechanism for this observation is not known. Kater et al [130] had previously reported similar findings and suggested that warfarin exerts its anti-inflammatory actions by affecting the phosphorylation of I-κB. Further studies are required to elucidate the mechanism underlying these observations. There are possibly other experiments could

be done, for example, different enantiomers of warfarin clearance vs. VKORC1 haplotypes and dosage to see if there are any correlations. Taken together, a possible mechanism of Transthyretin expression pathway during low- and high-dose warfarin treatment could be proposed.

4.5 Section Conclusions

In summary, this study showed that variations in TTR levels were associated with specific dosing regimens of warfarin. Our data suggested that while genotyping alone has been able to identify genetic polymorphisms in the target genes for warfarin therapy, the iTRAQ-coupled LC-MS/MS analysis was able to identify specific protein in patients on low-dose warfarin. Taken together, this combined pharmacogenomics and pharmacoproteomics approach may be applied for other target-based therapies, in matching a particular biomarker in a group of patients, in complementary to the profile of genetic polymorphism. Based on clinical findings and from the Western blot analysis of expression of transthyretin precursor on a dosage dependent manner in HepG2 cells, we would like to identify specific proteins which might interact with transthyretin precursor and be involved in drug action mechanism. iTRAQ-coupled 2D LC-MS/MS was used to investigate on intracellular protein profile in HepG2 cells incubated with S(-) and R(+) warfarin in the next part.

5. Comparative Intracellular Proteomic Analysis of HepG2 cells Incubated by S(-) and R(+) Enantiomers of Chiral Drug Warfarin

(This section was from our paper published in Proteomics, 2010, 10(7): p. 1463-73. Permissions from this reference was obtained from publisher to use all the figures and tables)

5.1 Introduction

Apart from clinical study, investigation on chiral form of warfarin effects in a more homogenous system provides more information. Clinical form of warfarin is a racemic mixture with two enantiomers, name S(-) and R(+). Each of them displays unique properties and therapeutic effects, with S(-) form being more effective in vitro [12-13]. It decreases blood coagulation indirectly by inhibiting vitamin K cycle through interfering with VKOR activity by binding to the enzyme's disulfide motif, thus prevents the formation of free sulfhydryls leading to the inactivation of the enzyme[24-25] It has been shown that warfarin binds to the oxidized form of VKOR and prevents the formation of the free sulfhydryls requisite for vitamin K cycle activity[18, 26-27]. However, either from vitamin K epoxide form to vitamin K, or from vitamin K to hydroquinone, the overall cellular redox system for this enzyme is still unknown. It remains possible that one or more unknown physiological reductant could associate with VKOR to form enzyme complex[28].

In this study, we used iTRAQ 4-plex strategy (with reporter group m/z 114-117) to semi-quantify the differences in protein levels between untreated human liver cells and those incubated by S(-) and R(+) warfarin, respectively. To better reflect the in vivo condition, similar analysis was also carried out in cells incubated with warfarin in the presence of vitamin K. Several proteins including multi-task protein Protein SET, Protein Disulfide Isomerase A3(PDIA3), Protein DJ-1 and 14-3-3 Protein σ were either up or down-regulated. The results were also verified by Western blot analysis and ROS assay.

5.2 Experiment Procedures

First of all, the toxicity for warfarin S(-) and R(+) enantiomers in HepG2 cells was tested by MTT assay (Section 3.3). HepG2 cells were cultured and drug incubated, as described in Part 3 Materials and Methods (3.1 Cell Cultures). Two sets of experiments (without and with vitamin K) were designed. Then the cells were lysed and protein quantified and digested, labeled with iTRAQ reagents and subjected to 2D LC-MS/MS analysis. The procedures were described in Section 3.4-3.6. In addition, western blot analysis (Section 3.7) and cellular ROS assay (Section 3.9) were applied for the results validation.

5.3 Results

5.3.1 MTT Assay

MTT assay, which is a standard colorimetric assay, has been used to test cytotoxicity of reagents and cell viability. Most of drugs incubated in cell lines will generate unexpected cellular responses at certain concentration and at a certain incubation time. Assessing the drug treated cells and determining a proper drug concentration is one of the main purposes of our study. In addition, to build cellular protein profile in response to non-anticancer drug, warfarin, requires minimizing the toxicity effects which might lead to apoptosis or activate other drug-effect-unrelated signal pathways. To determine the appropriate concentration of warfarin used in our study, the human liver cell line HepG2 cells were incubated with increasing concentrations of individual enantiomers of warfarin, and cell viability was examined by the MTT assay. Cell viability in the presence of vitamin K was also determined separately. Figure 5.1 showed the results of MTT assay.

Panel A

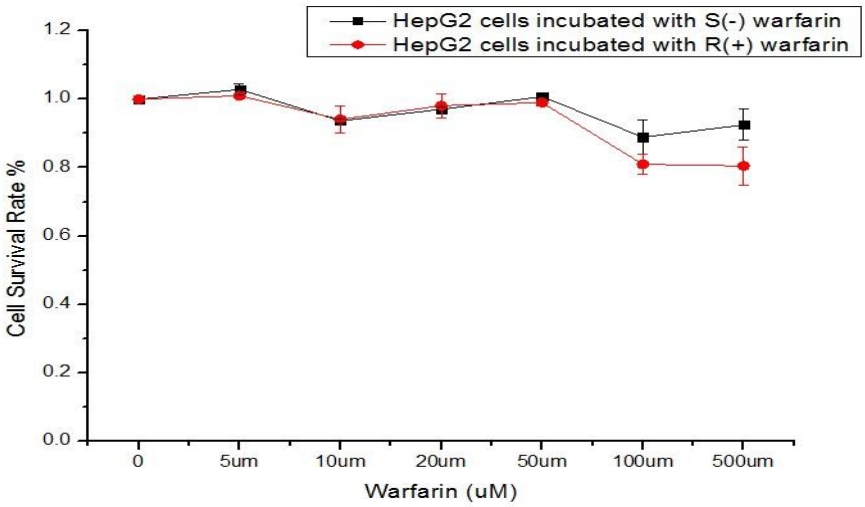

Panel B

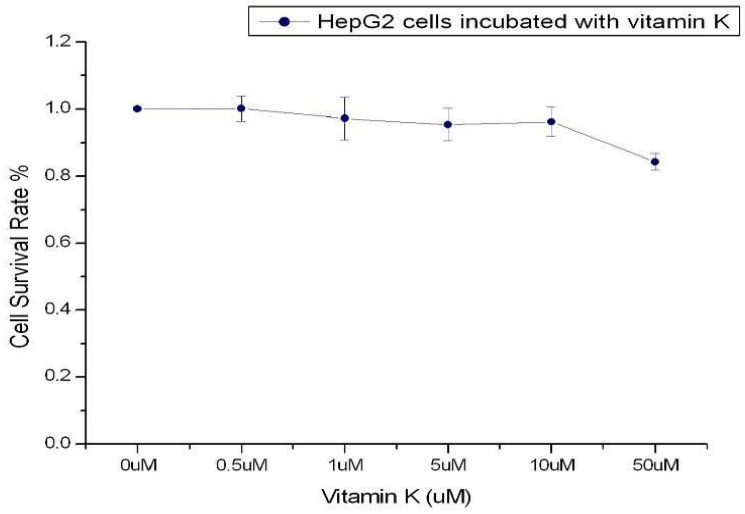

Figure 5.1 MTT Results for HepG2 Cells Incubated with (Panel A): S(-) and R(+) Warfarin; Panel B: vitamin K[133].

Our data indicated that no significant cytotoxicity for both S(-) and R(+) warfarin was observed at the concentrations below 50µM. For concentration above 100µM, R(+) appeared to be more toxic than S(-) warfarin. The concentration of 20μM was therefore chosen in all subsequent experiments in this study. In addition, our results also indicated that the cytotoxic effect of vitamin K was not significant when concentration was below 10µM. In our experiment, 0.5µM vitamin K was used to our study.

5.3.2 Protein Identification and Quantification

To establish a comprehensive cellular protein profile in response to incubation to warfarin, total protein was extracted from cells incubated with individual enantiomers of warfarin and subject to 2D LC-MS/MS analysis. The experiment was performed with three times. A total of 597 (set 1, cells incubated with warfarin) and 565 (set 2, cells incubated with vitamin K then warfarin) (Figure 5.2, page 77) unique proteins

were identified. The list of proteins identified can be found in Appendix. These proteins were separated into 7 categories based on their molecular functions. These included metabolism, structure, biosynthesis, stress and defense, signal transduction and transport.

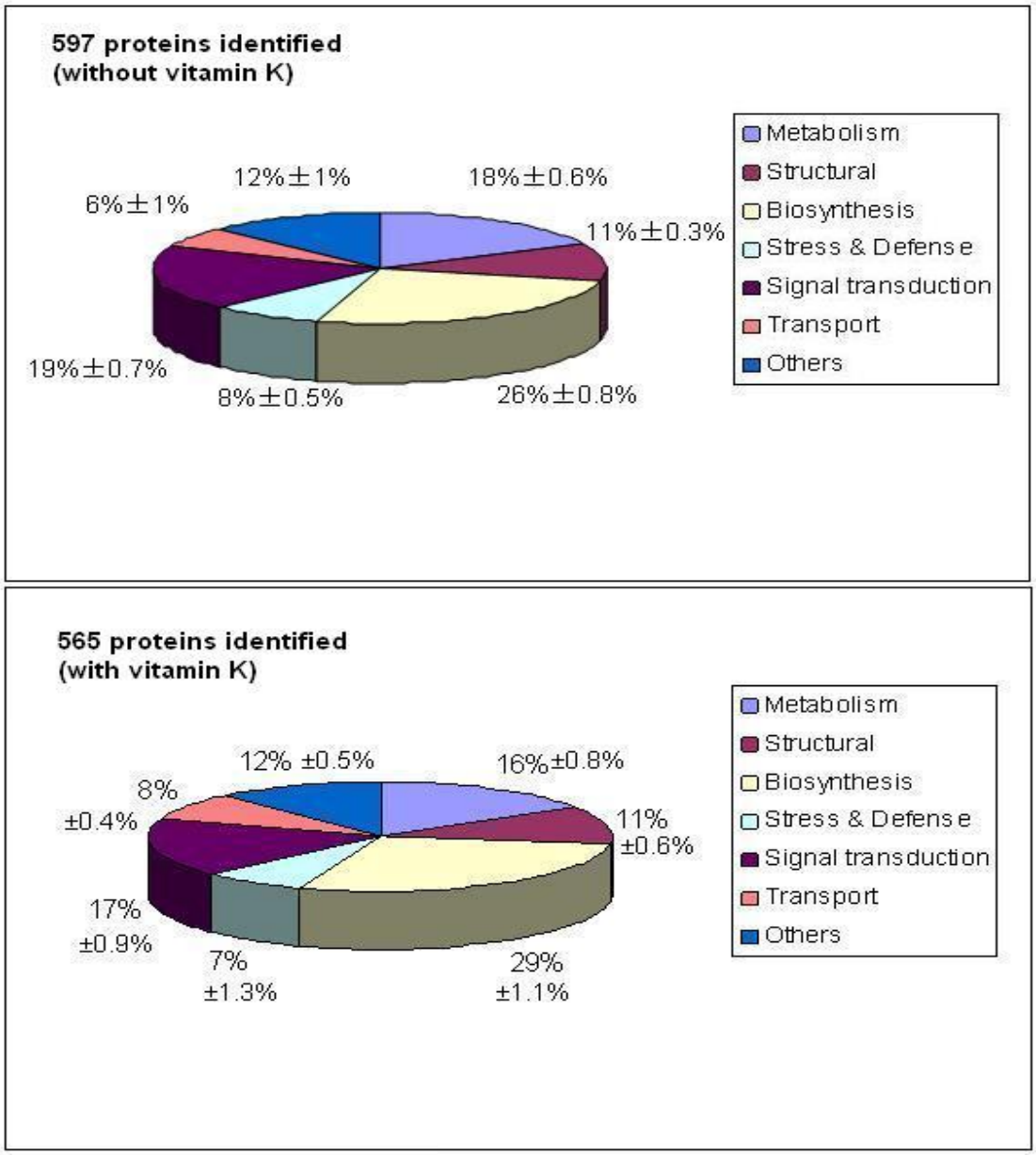

Figure 5.2 Proteins Identification and Categorization[133] (Detailed description in page 76)

Our results indicated that proteins identified in the two sets displayed similar ratio. In addition, a large number of proteins detected in both sets were involved in biosynthesis and metabolism regulated proteins.

Quantification assessment was performed by ProteinPilot software. Protein profiles generated by this software were undergone a filtering, by statistical criteria described in the Material and Methods part. To determine the significance threshold, *p* value of statistical t-test was calculated for each protein and only those proteins with $p < 0.05$ were selected. Results from the selection were summarized in Table 5.1 for cells incubated with the individual enantiomers of warfarin, and in Table 5.2 for cells incubated with the individual enantiomers of warfarin in the presence of vitamin K.

A total of 12 proteins showed changes in their level in Table 5.1, while the number of proteins displaying changes in their level was 25 in Table 5.2. Our results suggested that more proteins were differentially expressed in the presence of vitamin K. List of 95% peptides, charged state and protein functions can be found in Appendix.

Table 5.1. **Proteins Identified at Least Twice and Have Expression Ratio Varied at Least 10% (*p*<0.05), in the 1st Set of experiment, without Vitamin K Pre-incubation[133]**. C= control group, S= S(-) warfarin incubated group, R=R(+) warfarin incubated group. *P* values were calculated from student-t test. In this table, the control group is the untreated sample. (Appendix provided the 95% peptide sequences, charged states, and functions)

Table 5.1

Accession No.& Name	% Coverage	Avg.S:C (S.D.)	*p*(S:C)	Avg.R:C (S.D.)	*p*(R:C)	No.of detection	No.of Peptides (95%)
Metabolism							
P00338 L-lactate dehydrogenase A chain	64.46%	1.16 ±0.06	0.03	1.13 ±0.04	0.023	3	4
P15121 Aldose reductase	51.58%	0.9 ±0.03	0.013	0.99 ±0.08	p>0.05	3	5
Q14697 Neutral alpha-glucosidase AB	11.76%	0.85 ±0.01	0.011	0.95 ±0.04	p>0.05	2	5
Biosynthesis							
P31327 Carbamoyl-phosphate synthase	42.67%	1.1 ±0.02	0.006	1.15 ±0.04	0.003	3	14
P09651 Heterogeneous nuclear ribonucleoprotein A1	31.72%	1.11 ±0.02	0.004	1.08 ±0.02	0.01	3	6
P62277 40S ribosomal protein S13	23.18%	0.88 ±0.08	0.042	0.9 ±0.03	p>0.05	3	2
P39023 60S ribosomal protein L3	13.65%	1.18 ±0.01	0.009	1.18 ±0.05	p>0.05	2	2
Stress & Defense							
Q99497 Protein DJ-1	20.63%	0.86 ±0.01	0.012	0.84 ±0.01	0.009	2	2
Signal Transduction							
P31947 14-3-3 protein σ	22.18%	0.79 ±0.03	0.003	0.78 ±0.06	0.021	3	3
Q01105 Protein SET	12.76%	1.3 ±0.08	0.016	1 ±0.02	p>0.05	3	2
P49773 Histidine triad nucleotide-binding protein 1	26.98%	0.9 ±0.10	p>0.05	0.84 ±0.02	0.032	2	2

P09382 Galectin-1	43.70%	0.92 ±0.03	p>0.05	0.86 ±0.02	0.038	2	2

Table 5.2

Accession No.& Name	% Coverage	Avg.S:V (S.D.)	*p*(S:V)	Avg.R:V (S.D.)	*p*(R:V)	No. of detection	No.of Peptides (95%)
Metabolism							
P15121 Aldose reductase	37.66%	1.1 ±0.03	0.018	1.01 ±0.06	p>0.05	3	5
P25705 ATP synthase subunit α	23.15%	1.15 ±0.07	0.039	1.1 ±0.05	0.049	3	2
P06744 Glucose-6-phosphate isomerase	28.67%	1.1 ±0.01	0.029	0.97 ±0.01	0.045	2	2
P14618 Pyruvate kinase isozymes M1/M2	44.26%	1 ±0.01	p>0.05	0.9 ±0.02	0.05	2	7
P29401 Transketolase	20.70%	1.01 ±0.06	p>0.05	0.85 ±0.02	0.035	2	4
P04075 Fructose-bisphosphate aldolase A	31.32%	0.93 ±0.04	p>0.05	0.9 ±0.02	0.012	3	2
Structural							
O75369 Filamin-B	12.76%	0.76 ±0.04	0.031	0.97 ±0.01	p>0.05	3	2
P23528 Cofilin-1	28.31%	1.01 ±0.05	0.04	1.13 ±0.11	p>0.05	2	4
P57053 Histone H2B	49.21%	1.01 ±0.04	p>0.05	1.12 ±0.04	0.015	3	5
O43707 Alpha-actinin-4	22.28%	0.88 ±0.05	0.019	1.19 ±0.06	p>0.05	2	2
Biosynthesis							
P30101 Protein disulfide-isomerase A3	16.44%	0.84 ±0.03	0.039	0.91 ±0.01	0.039	3	2
P15559 NAD(P)H dehydrogenase[Quinone]	16.79%	0.86 ±0.04	0.017	0.98 ±0.03	p>0.05	3	2

P22087 rRNA 2'-O-methyltransferase fibrillarin	36.14%	0.85 ±0.10	p>0.05	1.19 ±0.07	0.049	3	2
P05387 60S acidic ribosomal protein P2	39.13%	0.94 ±0.11	p>0.05	0.87 ±0.04	0.05	2	3
Stress & Defense							
P01857 Ig gamma-1 chain C region	6.06%	1.28 ±0.13	0.039	1.16 ±0.08	p>0.05	3	2
P50454 Serpin H1	15.8%	0.69 ±0.03	0.02	0.82 ±0.17	p>0.05	2	3
Q99497 Protein DJ-1	46.59%	0.83 ±0.04	0.011	0.85 ±0.03	0.01	3	2
Signal Transduction							
P31947 14-3-3 Protein σ	31.05%	0.86 ±0.01	0.024	0.87 ±0.01	0.026	2	5
Q01105 Protein SET	19.30%	0.88 ±0.03	0.045	1.02 ±0.03	p>0.05	2	2
P23246 Splicing factor, proline- and glutamine-rich	28.71%	0.83 ±0.04	0.05	0.87 ±0.04	p>0.05	2	3
P27797 Calreticulin	20.09%	0.88 ±0.04	p>0.05	0.87 ±0.01	0.013	2	2
P10599 Thioredoxin	32.38%	0.89 ±0.02	0.038	1.16 ±0.08	p>0.05	2	2
P26599 Polypyrimidine tract-binding protein 1	29.79%	0.81 ±0.17	p>0.05	1.12 ±0.02	0.035	2	6
Transport							
P99999 Cytochrome c	11.43%	1.02 ±0.01	p>0.05	0.89 ±0.02	0.009	3	2
P14625 Endoplasmin	11.30%	1.13 ±0.01	0.026	1.01 ±0.04	p>0.05	2	3

Table 5.2 Proteins Identified at Least Twice and Have Expression Ratio Varied at Least 10% ($p<0.05$), in the 2nd Set of Experiment, with Vitamin K Pre- incubation[133]. V= Vitamin K treated group, S= Vitamin K incubated then S(-) warfarin incubated group, R= Vitamin K incubated then R(+) warfarin incubated group. *P* values were calculated from student-t test. In this table, the control group is the vitamin K treated sample. (Appendix provided the 95% peptide sequences, charged states, and functions)

Results showed that most proteins displayed similar changes in cells incubated with either S(-) or R(+) warfarin. A number of proteins showed changes to one but not all enantiomers of warfarin.

For example, Protein SET, a multi-tasking protein, involved in apoptosis, transcription, nucleosome assembly and histone binding, was up-regulated in S(-) warfarin incubated cells but not in those incubated with R(+) warfarin. Interestingly, this protein showed a decreased level in cells incubated with S(-) warfarin in the presence of vitamin K.

In Table 5.2, Protein disulfide isomerase A3(PDIA3), the S(-) warfarin incubated sample was down-regulated for 15% while R(+) warfarin 10%. This protein may play a role in vitamin K cycle regulation. In our results also showed NAD(P)H quinone oxidoreductase (NQO1) was

Dow-regulated for 15% in the S(-) warfarin incubated sample.

There were also two proteins Protein DJ-1 and 14-3-3 σ down-regulated without any differences in the cells incubated with S(-) and R(+) warfarin, regardless of the presence of vitamin K. For DJ-1, this protein was up-regulated for 20% in only vitamin K treated sample(p= 0.011), compared with control cells (without warfarin and vitamin K). After the incubation with either S(-) or R(+) warfarin, samples displayed the similar down-regulation ratio, around 15%. A peptide fragment information from DJ-1(set 2) was shown (Figure 5.3, page 79).

For 14-3-3 σ, in Table 5.1, the down-regulation ratio were around 20% for both S(-) and R(+) warfarin incubated groups, and in Table 5.2, the expression ratio were around 15% for both S(-) and R(+) warfarin incubated groups.

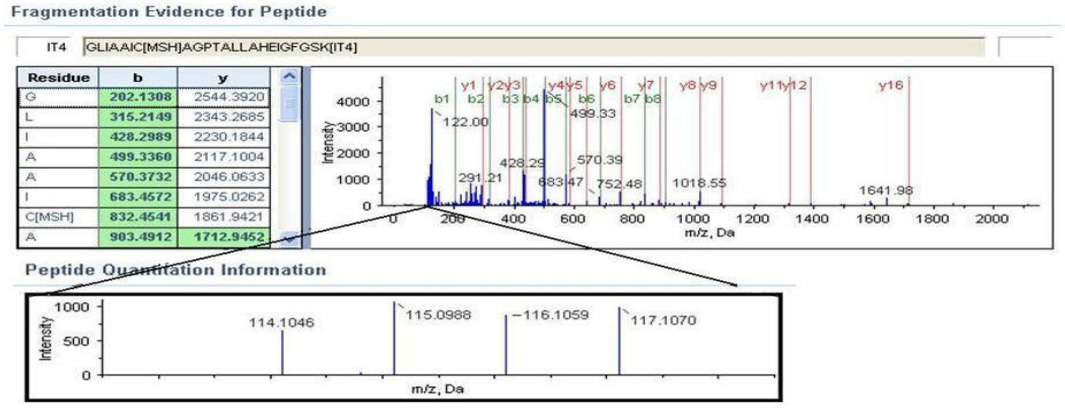

Figure 5.3 A Representative MS/MS Spectrum of a Peptide, GLIAAICAGPTALLAHEIGFGSK[133]. It was identified in set 2 experiment, of Protein DJ-1. The m/z 114 represents untreated sample, m/z 115 represents Vk incubated sample, m/z 116 represents S(-) warfarin incubated sample after Vk exposure, m/z 117 represents R(+) warfarin incubated sample after Vk exposure.

5.3.3 Western Blot Analysis

As shown in Table 5.1 and Table 5.2, most proteins displayed changes in their level varying from 15-30%. To examine if the changes were significant, Western blot analysis was carried out for three proteins, PDIA3, Protein DJ-1 and 14-3-3 σ. Results were obtained from cells incubated with individual enantiomers of warfarin (Figure 5.4, page 81, panel A) and those incubated with individual enantiomers of warfarin in the presence of vitamin K (Figure 5.4, panel B). The quantitative information calculated were shown in Figure 5.4, panel C and Figure 5.4, panel D, respectively.

Consistently with the LC-MS/MS analysis, all the three proteins showed reduced level in cells incubated with warfarin alone, compared with the control cells. The level of PDIA3, S(-) warfarin incubated group was down-regulated more in cells incubated with S(-) warfarin compared to those incubated with R(+) warfarin. Our results therefore suggested a differential effect of warfarin enantiomers on PDIA3. For Protein DJ-1, the levels of down-regulation for both S(-) and R(+) warfarin incubated groups appeared to be similar. The same results can also be observed on 14-3-3 σ. In vitamin K pre-incubated cells, all three proteins in the S(-) and R(+) warfarin incubation groups, were down-regulated compared to only vitamin K incubated sample. Taken together, the change identified in LC-MS/MS analysis was supported by our Western blot analysis.

Figure 5.4. Western Blot Analysis of Protein Expression for the Three Proteins, ERp57, 14-3-3 σ, protein DJ-1(page 85). ***Panel A***, three protein expression in the 1st set of experiment (without Vitamin K pre-incubation). ***Panel B***, three protein expression in the 2nd set of experiment (with Vitamin K pre-incubation). ***Panel C***, 1st set quantification data calculated by Bio-Rad QualityOne software, (a) data chart, (b) data values. ***Panel D***, 2nd set quantification data calculated by Bio-Rad QualityOne software, (a) data chart, (b) data values. Ctrl = the sample without any treatment, S-warf = the sample incubated by S(-) warfarin, R-warf = the sample incubated by R(+) warfarin; Vk = the sample only incubated by vitamin K, Vk+S-warf = the sample incubated by vitamin K then S(-) warfarin, Vk+R-warf = the sample incubated by vitamin K then R(+) warfarin. P values were calculated by T-test.

Panel A

1st set, without vitamin K pre-incubation

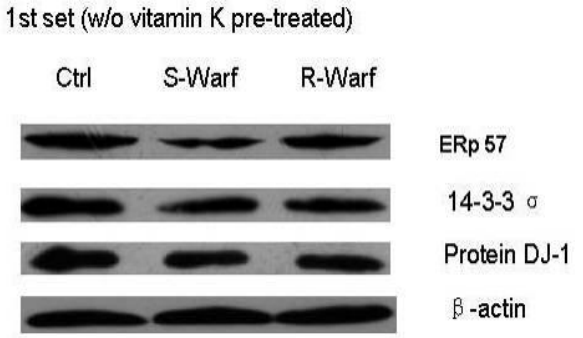

Panel B

2nd set, with vitamin K pre-incubation

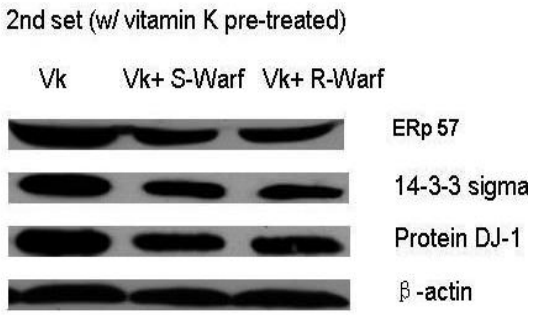

Panel C

(a)

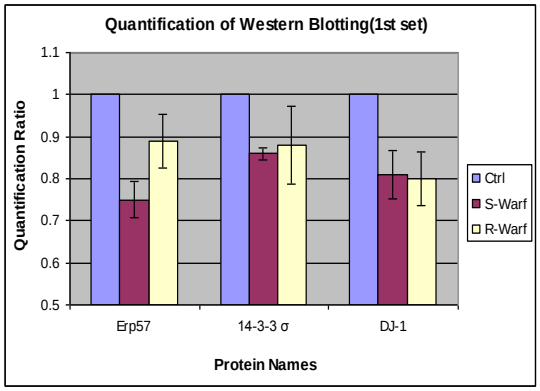

(b)

	ERp57	14-3-3 σ	DJ-1
Ctrl	1	1	1
S-Warf	0.75±0.04 (p <0.05)	0.86±0.06 (p <0.05)	0.81±0.01 (p <0.05)
R-Warf	0.89±0.06 (p <0.05)	0.88±0.11 (p <0.05)	0.8±0.03 (p <0.05)

Panel D

(a)

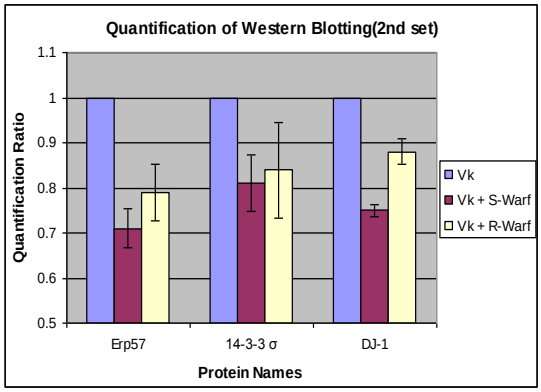

(b)

	ERp57	14-3-3 σ	DJ-1
Vk	1	1	1
Vk+ S-Warf	0.71±0.04 (p <0.05)	0.81±0.01 (p <0.05)	0.75±0.06 (p <0.05)
Vk+ R-Warf	0.79±0.06 (p <0.05)	0.84±0.09 (p <0.05)	0.88±0.06 (p <0.05)

Figure 5.4. Western Blot Analysis of ERp57, 14-3-3 Protein σ, protein DJ-1[133](Detailed description in page 83)

5.3.4 ROS Assay

Protein DJ-1, which was involved in cellular sensing of redox stress, was shown to be decreased in cells incubated with either enantiomer of warfarin (Table 5.1). The decrease was also observed in the presence of vitamin K (Table 5.2). To investigate the effects of S(-) and R(+) warfarin's biological influence on cellular reactive oxygen species level. ROS level was measured and results were shown (Figure 5.5, page 83, panel A and panel B), while panel A are the results for samples incubated with warfarin alone and panel B are the results for samples incubated with warfarin in the presence of vitamin K. In the first set, ROS level showed decreased in the S(-) and R(+) warfarin incubated samples, while samples incubated with S(-) and R(+) warfarin between each other did not vary significantly. In the second set, the ROS level was enhanced weakly in the vitamin K treated group, after S(-) and R(+) warfarin incubation(the 4^{th} and 5^{th} pictures in panel B), the ROS level reduced again. The results indicated that warfarin enantiomers have effects on reducing the ROS levels intracellularly. ROS assay has also elucidated that the ROS level for samples incubated with S(-) and R(+) warfarin themselves did not vary significantly.

Figure 5.5. ROS level of HepG2 Cells Incubated with Drugs. ROS of cells incubated with carboxy-H2DCFDA causes the green fluorescence. P-Ctrl indicates positive control which cells were incubated with TBHP, a fluorescence enhancer. N-Ctrl indicated negative control which cells were without any treatment. ***Panel A***, ROS level of 1^{st} set of experiment (without vitamin K pre- incubation). The left group was fluorescent view and the right group was fluorescent view with corresponding light view. ***Panel B***, ROS level of 2^{nd} set of experiment (with vitamin K pre incubation). The left group was fluorescent view and the right group was fluorescent view with corresponding light view.

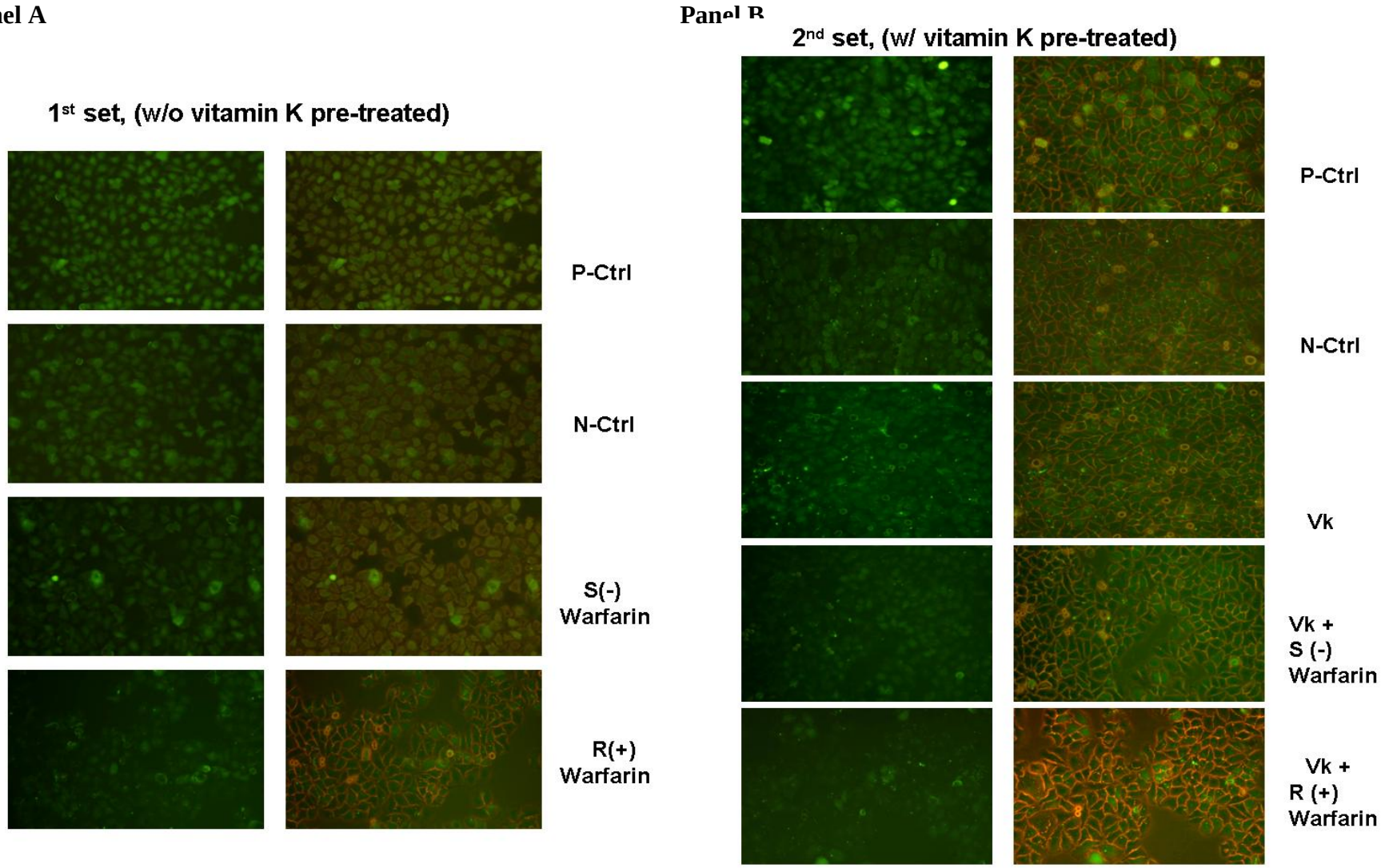

Figure 5.5. ROS level of HepG2 Cells Incubated with Drugs[133].(Detailed description in page 86)

5.4 Discussion

Comparing the protein profiles induced by drug enantiomers is an essential aim on study pharmacoproteomics, which may shed new light on drug development and clinical application. The goal of this study was to broaden our knowledge on the quantitative changes on proteins, stimulated by warfarin administration, and to compare them between S(-) and R(+) enantiomers. It may also to identify specific warfarin-targeted proteins that may be involved in vitamin K cycle and drug action. In our study, we chose cell-based system to investigate on the roles of warfarin S(-) and R(+) enantiomers in cellular response.

Down regulation of Protein disulfide-isomerase A3 in cells incubated with S(-) and R(+) warfarin.

Protein disulfide isomerases, located on endoplasmic reticulum, have several isoforms[134]. To date, there are 17 putative protein disulfide isomerases in humans[135]. These isomerases regulate the S-S bond and have highly conserved catalytic domains[136]. Warfarin targeted enzyme VKOR, which reduces vitamin K epoxide form to the active vitamin K hydroquinone form, has been proved to harbor a thioredoxin-like CXXC active center[24]. However, the cellular system which provides electrons to the active center is unknown. It has been shown that more than one protein component is needed for expression of VKOR enzyme activity[25]. VKOR activity is linked to dithiol redox exchange reactions catalyzed by proteins from protein disulfide isomerase (PDI) family, and PDI may be an electron donor to VKOR active center [25, 137]. Our LC-MS/MS analysis showed that PDIA3 was down-regulated in cells

incubated with S(-) warfarin. The down-regulation of this enzyme may be related to the reduced activity of VKOR enzyme targeted by warfarin, thus subsequently influenced the expression of PDIA3. The ratio variances between S(-) and R(+) warfarin incubated samples might be due to the different inhibition capabilities to VKOR enzyme of the two enantiomers, as S(-) warfarin is more effective than R(+) warfarin in VKOR inhibition[12]. Based on this information, we proposed that PDIA3 plays a role in regulating vitamin K cycle's activity.

Down regulation of Protein DJ-1 in cells incubated with both S(-) and R(+) warfarin. Protein DJ-1 firstly identified as a novel oncogene[41], is a multi-functional protein. And It functions as a redox-sensitive molecular chaperone and as a sensor for oxidative stress[138-139]. It is activated in an oxidative cytoplasmic environment. Interestingly, vitamin K is a redox cycling reaction, with vitamin K hydroquinone form being a cofactor for catalyzing gamma-carboxylation of glutamic acids into Gla residues on coagulating factors. In the process, oxygen is reduced to generate reactive oxygen species (ROS) that causes oxidative stress[23, 140-142]. Our ROS assay suggested that the elevated ROS level from vitamin K treatment was reduced by warfarin. Consistently, LC-MS/MS analysis showed that Protein DJ-1 was up-regulated in only vitamin K incubated cells while down-regulated in both S(-) and R(+) warfarin incubated samples. This result thus indicated that the down-regulation of this protein in S(-) and R(+) warfarin incubated samples might be a result of reduced activity of vitamin K cycle.

Interestingly, protein DJ-1is also a protease with transthyretin as one of the substrate[1]. It is possible that protein DJ-1 plays a role in individual's warfarin sensitivity. This protein protein DJ-1 may be associated with specific dosing regimens of warfarin and reflect the intracellular interaction of transthyretin precursor, thus provide more information on the discovery of unknown warfarin dosage dependent signaling pathway. And protein DJ-1 may also be a target in understanding the warfarin dosage variation. The different activities of vitamin K cycle then influence the intracellular ROS generation thus result in the fold changes of protein DJ-1. The subsequent extracellular release of transthyretin will be affected and can be detected in serum as a potential dosage marker.

In addition, it has been reported that loss of DJ-1 leads to deficits in NAD(P)H quinone oxidoreductase(NQO1, NAD(P)H quinone dehydrogenase)[143], which metabolizes vitamin K to it hydroquinone form. In our LC-MS/MS result, this protein was down-regulated in cells incubated by S(-) warfarin. Although NQO1 is not a direct target for warfarin incubation[142], it may have indirect influence on warfarin incubation to the reduced expression of NQO1, through the expression of DJ-1. This may then lead to the lower level of vitamin K hydroquinone formation and reduced vitamin K cycle activity.

Down-regulation of 14-3-3 protein σ on cells incubated with both S(-) and R(+) warfarin.

The 14-3-3 family of proteins contain seven isotypes in mammalian cells, and they play diverse roles in intracellular signaling, metabolism regulating, cell cycle,

apoptosis, transcription, stress responses, and malignant transformations[144]. It is also up-regulated by high level of cellular ROS [145]. Our results indicated that 14-3-3 protein σ was down-regulated in cells incubated with warfarin. It is possible that this protein may be sensitive to the intracellular reactive oxygen species. Interestingly, other proteins in 14-3-3 protein family interact with coagulation factors and influence the coagulation process[2].

Coagulating factor IX, like most gamma-carboxylation regulated coagulating factors, with the serine residue at position 158 phosphorylated[146]. 14-3-3 protein σ binds to a large number of partners, usually by recognition of a phosphoserine or phosphothreonine motif[147]. Binding modulates the activities of its binding partner. These suggest a possible role of 14-3-3 protein σ in post-translational modification of coagulating factor IX.

There are other eight metabolic related proteins shown expression ratio variation, the enzymes involved in cellular metabolism probably play roles on drug metabolism, detoxification and degradation. S(-) and R(+) are differentially metabolized by human cytochrome P450, S(-) warfarin is metabolized primarily by CYP2C9 and R(+) warfarin is metabolized by CYP1A2 and CYP3A4[16, 148]. During metabolic process, different drug enzymes lead to activate varies signal pathways, thus result in the differential expression of different proteins. There were also 3 structural proteins and 8 biosynthesis proteins, whose functions include cytoskeleton control, transcription and translation regulation, ribosome complex interactions. However, these common regulators are not specific for particular drug stimulation, thus it was difficult to

speculate through our experiment on whether a certain ribosomal component or a histone play roles at specific molecular level. Similar for the protein Ig gamma-1 chain C, the variation of this protein expression ratio may be the result on activation of a common toxicological response pathway, especially in the liver cells. There were also 8 proteins related to signal pathway regulation. The activation and inhibition of those proteins may be the contribution of drug induced general stress response, which affect the DNA synthesis and cell cycle.

5.5 Section Conclusions

We reported the intracellular protein profile in HepG2 cells incubated with S(-) and R(+) warfarin, using iTRAQ-coupled 2D LC-MS/MS and verified our results by Western blot analysis. The multi-task protein Protein SET showed significant elevation in cells incubated with S(-) warfarin but not in those incubated with R(+) warfarin. In the presence of vitamin K, PDIA3 which catalyzes the synthesis and rearrangement of –S–S– bonds in proteins may regulate VKOR activity. It was found to be down-regulated in cells incubated with S(-) warfarin compared with those incubated with R(+) warfarin. In addition, Protein DJ-1 and 14-3-3 Proteins were down-regulated in cells incubated with either S(-) or R(+) warfarin regardless of the presence of vitamin K. Taken together, our findings provided molecular evidence on a comprehensive protein profile on warfarin-cell interaction which may shed new lights on future improvement of warfarin therapy.

6. Comparative Extracellular Proteomic Analysis of HepG2 cells Incubated by S(-) and R(+) Enantiomers of Chiral Drug Warfarin

6.1 Introduction

In this study, we used iTRAQ 4-plex strategy (with reporter group m/z 114-117) to semi-quantify the differences in secreted protein levels between untreated human liver cells and those incubated by S(-) and R(+) warfarin, respectively. To better reflect the in vivo condition, similar analysis was also carried out in cells incubated with warfarin in the presence of vitamin K. Protein expression was verified by Western blot analysis. In addition, we treated 30 patients with racemic warfarin and the proteins from their serum samples were analyzed with the same method. This batch of experiment was designed as a clinical verification of protein secreted on warfarin treatment. We focus on understanding the biological differences between S(-) and R(+) warfarin by analyzing the secreted proteins from cell line incubated with individual enantiomers of warfarin, and to identify the drug targeted markers. In complementary, clinical data gave more evidences and support on the tendency of protein changes.

6.2 Experiment Procedures

HepG2 cells were cultured and drug incubated, as described in Section 2 Materials and Methods (3.1 Cell Cultures). Two sets of experiments (without and with vitamin K) were designed. Culture media was obtained and centrifuged at 3,000g for 10 minutes to

remove dead cells and debris. Culture media was transferred into 5kD ultra-filter concentrators (Sartorius, Germany) and centrifuged for 30 min at 4°C in swing bucket rotor. For analysis of clinical serum samples, Patient selection was described in Section 3.2. Protein concentrating by concentrator was not necessary. Briefly, blood samples were centrifuged, supernatant stored at -80ºC until use. Proteins from both cell line and clinical samples were quantified using 2-D Quant Kit. For each patient sample, 100µg proteins were separated, precipitated and digested, labeled with iTRAQ reagents and subjected to 2D LC-MS/MS analysis. The procedures were described in Section 3.4-3.6. All samples were analyzed in three independent analyses. In addition, Western blot analysis (Section 3.7) was applied on protein Apolipoprotein A-I for the validation of results.

6.3 Results and Discussion

To better understand the warfarin-induced anti-coagulating effects, the secretome of warfarin incubated hepatocytes was analyzed as most liver-originated coagulation related proteins are secreted. To this end, secreted proteins were isolated from cells incubated with individual enantiomers of warfarin and subject to 2D LC-MS/MS analysis. A total of 76 unique proteins in which 49 were secreted proteins, were obtained together for both sets with and without the presence of vitamin K. The list of proteins identified can be found in Appendix. A total of 5 proteins showed changes in their level. The low number of detected proteins in the culture medium was consistent with the nature of our analysis, namely the culture medium which contains far less

proteins compared with the intracellular cell environment, which was around 600 unique proteins in our previous intracellular study[133].

Results showed that most proteins displayed similar changes in cells incubated with either S(-) or R(+) warfarin. Some of proteins showed changes to one but not both enantiomers of warfarin. Results from the selection were summarized in Table 6.1(page 92)for cells incubated with the individual enantiomers of warfarin, and cells incubated with the individual enantiomers of warfarin in the presence of vitamin K. Most proteins displayed changes in their level varying from 15-25%. A peptide fragment information from α-2-HS glycoprotein (in the set with the presence of vitamin K) was shown in Figure 6.1(page 93).

Table 6.1 Proteins Identified in Cell-line Based Experiments(page 94). ***Left, warfarin,*** Proteins identified at least twice and have expression ratio varied at least 10% (p<0.05), in the set of experiment without Vitamin K pre- incubation. C= control group, S= S(-) warfarin incubated group, R= R(+) warfarin incubated group. In this table, the control group is the untreated sample***. Right, Warfarin + vitamin K,*** Proteins identified at least twice and have expression ratio varied at least 10% (p<0.05), in the set of experiment with Vitamin K pre- incubation. V= Vitamin K treated group, S= Vitamin K incubated then S(-) warfarin incubated group, R= Vitamin K incubated then R(+) warfarin incubated group. In this table, the control group is the vitamin K treated sample.

Table 6.1 Proteins Identified in Cell-line Based Experiments (Detailed description in page 94)

	Warfarin							Warfarin + vitamin K						
Accession Num. & Name	% Cov.	Avg.S:C (S.D.)	*p* (S:C)	Avg.R:C (S.D.)	*p* (R:C)	Num. of detect -ion	Num. of 95% peptides	% Cov.	Avg.S:V (S.D.)	*p* (S:V)	Avg.R:V (S.D.)	*p* (R:V)	Num. of detect -ion	Num. of 95% peptides
P01023 α-2-macroglobulin	48%	1.16±0.15	0.08	1.19±0.02	0.05	2	6	29.5%	1.1±0.08	0.04	1.09±0.05	0.03	2	6
P02765 α-2-HS-glycoprotein	52%	0.86±0.01	0.02	0.92±0.03	0.01	3	4	43.1%	0.79±0.04	0.01	0.93±0.05	0.07	2	4
P02647 Apolipoprotein A-I	63.7%	0.8±0.08	0.06	0.73±0.02	0.02	2	3	40.5%	0.82±0.01	0.02	0.76±0.03	0.01	2	3
P02679 Fibrinogen gamma chain	14.8%	0.88±0.07	0.05	0.86±0.05	0.06	2	2	-	-		-		1	2
Q14624 Inter-α-trypsin inhibitor heavy chain H4	43.6%	1.11±0.04	0.04	1.04±0.04	0.04	2	2	-	-		-		1	2

% cov = percentage of coverage

Avg.S:C = Average S:C; Avg.R:C = Average R:C

Avg.S:V = Average S:V; Avg.R:V = Average R:V

Num. of detection = Number of detection

Num. of 95% peptides = Number of 95% peptides detected in a particular protein

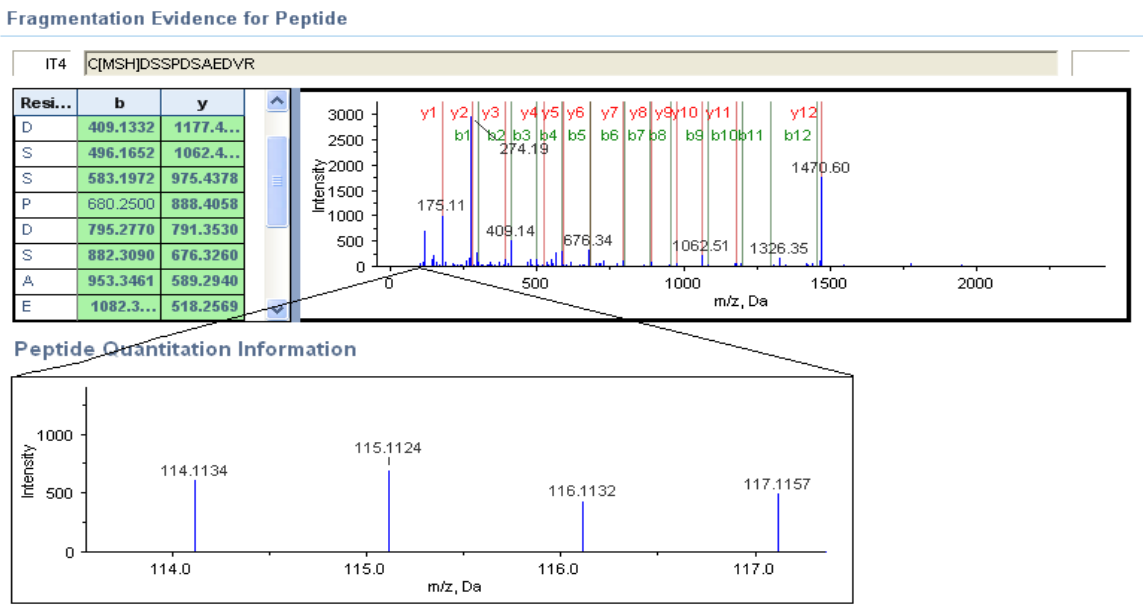

Figure 6.1, A Representative MS/MS Spectrum of a Peptide, CDSSPDSAEDVR. (Detailed description in page 91). It was identified in the cell-line batch, with the presence of vitamin K. The m/z 114 represents untreated sample, m/z 115 represents Vk incubated sample, m/z 116 represents S(-) warfarin incubated sample after Vk exposure, m/z 117 represents R(+) warfarin incubated sample after Vk exposure.

The secretome analysis in our cell-based system provided us with information on proteins which were secreted at the early stage of warfarin incubation. Conversely, similar analysis from patients receiving warfarin therapy would provide valuable validation on the significance of the early secretome in long-term warfarin therapy. To this end, we extracted serum proteins from patients who have been treated with warfarin for more than one month. The warfarin used in the therapy was of racemic nature, as no warfarin in individual enantiomers was available for clinical use. It was nevertheless useful for verification of our cell-based secretome analysis.

A total of 163 unique proteins were identified in the clinical samples. Interestingly, the 5 proteins which were detected in the cell line batch were also detected in the clinical

batch (Figure 6.2, page 99). Table 6.2(page 100-101) was the original data for the 5 proteins expression in 30 patients. List of 95% peptides, charged state and protein functions can be found in Appendix. A Box and Whisker Plot was drawn to explain the clinical data distribution. The fact that the tendency of either up- or down-regulated for a particular protein was the same in both settings indicated that changes in these 5 proteins were related to warfarin treatment instead of random stimulations. However, the exact ratio of protein expressions in cell line and clinical batch was different probably as a result of the intrinsic differences between cell lines and patients or the racemic warfarin in clinical samples. Quantification assessment was performed by ProteinPilot software. Protein profiles generated by this software were undergone a filtering, by statistical criteria described in the Materials and Methods.

6.3.1 Up-regulation of Inter-α-trypsin inhibitor heavy chain H4 and α-2-macroglobulin

There were two proteins inter-α-trypsin inhibitor heavy chain H4 and α-2-macroglobulin up-regulated regardless of the presence of vitamin K. In cell line batch, inter-α-trypsin inhibitor heavy chain H4 was up-regulated slightly in cells incubated with S(-) warfarin (11%) compared to R(+) warfarin (4%). In clinical batch, the protein was also up-regulated in all patients. Inter-α-trypsin inhibitor is one of the plasma serine-protease inhibitor[149], with no reported link to the effect of warfarin. Recent evidence suggests that this protein may well play a role in the process of anticoagulation.

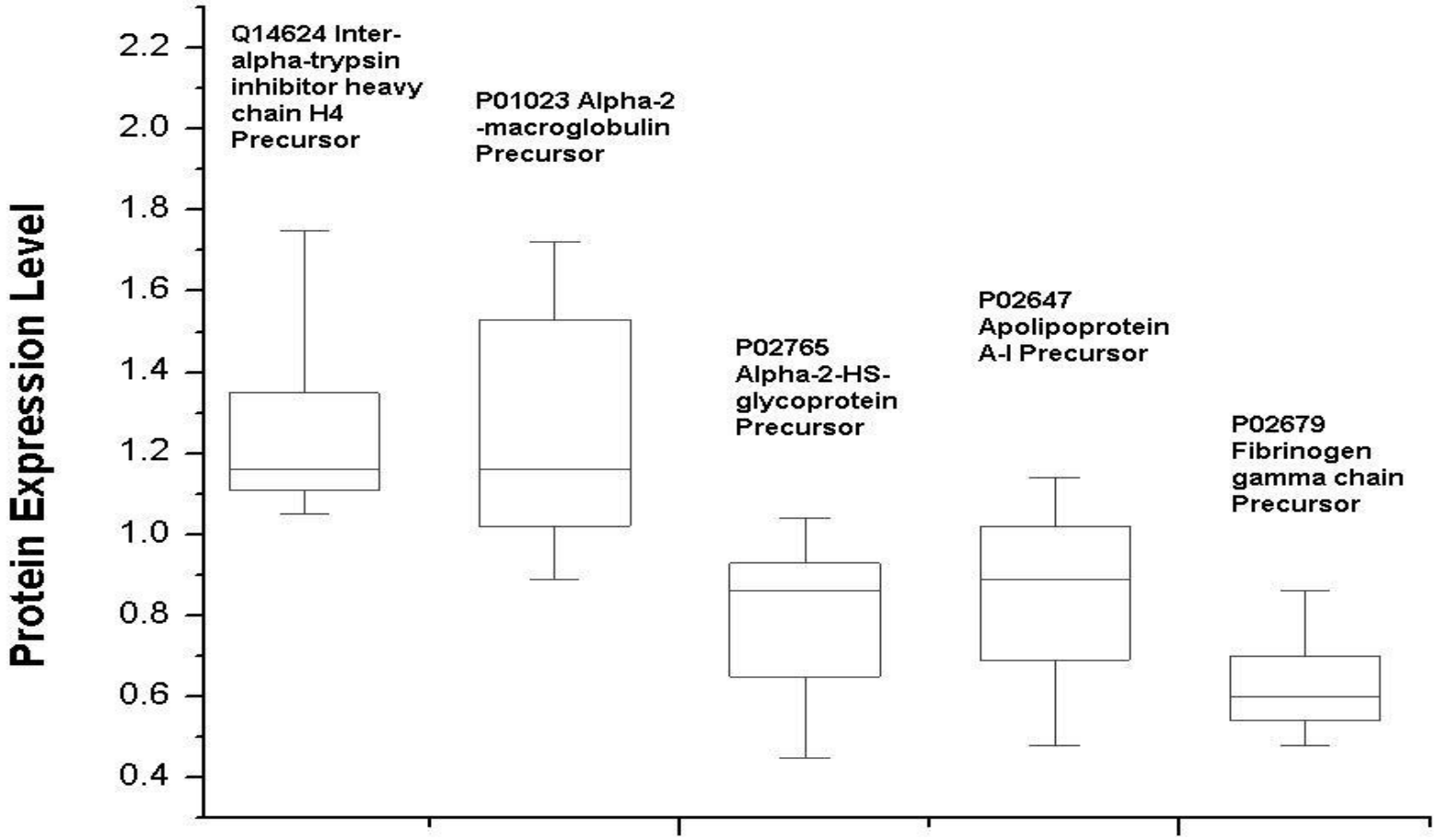

Figure 6.2 Pharmacoproteomics Analysis of Patients Receiving Warfarin. Five proteins identified in the cell line batch were verified by clinical data. Two of them were up-regulated while the rest were down-regulated. *(Detailed description in page 98)*

Table 6.2 Clinical Data of Serum Protein Expression from 30 Patients. ***(Detailed description in page 98)***

Patients' Number	**Protein Expression Ratio compared with Control**				
	Q14624 Inter-alpha-trypsin inhibitor heavy chain H4	P01023 Alpha-2-macroglobulin	P02765 Alpha-2-HS-glycoprotein	P02647 Apolipoprotein A-I	P02679 Fibrinogen gamma chain
1	1.75	1.02	0.45	1.06	0.86
2	1.35	1.63	0.79	0.68	0.55
3	1.34	1.58	0.65	0.56	0.71
4	1.3	1.52	0.58	0.88	0.59
5	1.23	1.25	0.56	0.95	0.6
6	1.16	1.44	0.93	0.94	0.67
7	1.14	1.47	0.9	0.9	0.63
8	1.12	1.15	0.89	0.86	0.6
9	1.1	1.06	0.86	1.01	0.7
10	1.09	1.04	0.94	1.02	0.57
11	1.08	0.95	0.98	0.69	0.55
12	1.07	0.94	1.01	1.06	0.73
13	1.05	0.89	1.02	0.63	0.53
14	1.06	1.6	0.54	1.1	0.52
15	1.07	0.92	0.57	1.14	0.48
16	1.09	0.95	0.61	0.48	0.51
17	1.11	1.72	0.64	0.66	0.53
18	1.13	1.05	0.73	0.68	0.56
19	1.15	1.1	0.8	1.06	0.62
20	1.17	1.14	0.81	0.81	0.55
21	1.18	1.15	0.86	0.89	0.75
22	1.23	1.16	0.87	0.44	0.54
23	1.24	1.46	0.96	0.87	0.85

24	1.27	1.39	0.92	0.92	0.59
25	1.33	1.36	0.9	0.88	0.61
26	1.32	1.53	0.91	0.99	0.56
27	1.31	1.56	0.89	1.01	0.68
28	1.27	1.58	0.97	0.78	0.73
29	1.35	1.6	0.99	1.09	0.55
30	1.69	0.9	0.87	1.11	0.58
Maximum	**1.75**	**1.72**	**1.02**	**1.14**	**0.86**
Minimum	**1.05**	**0.89**	**0.45**	**0.48**	**0.48**
Median	**1.16**	**1.16**	**0.87**	**0.89**	**0.6**
Quartile 1(Q1)	**1.11**	**1.04**	**0.68**	**0.69**	**0.55**
Quartile 3(Q3)	**1.32**	**1.53**	**0.93**	**1.02**	**0.68**

Firstly, the coagulation factors are generally serine proteases. As an inhibitor, inter-α-trypsin inhibitor may interact with coagulating factors thus inhibit their normal functions. Secondly, the substrate of plasma kallikrein, a serine protease which generates plasmin from plasminogen to enhance blood coagulation, has a significant sequence identity to heavy chains (HCs) of the inter-α-trypsin inhibitor superfamily[150]. Thirdly, it has been known that this protein acts as a probable component pertaining to disseminated intravascular coagulation(DIC), which is a disease leading to the forming of small blood clots in the blood vessels throughout the body. The DIC patients have lower level of this protein expression compared with normal group[151]. Warfarin has been used to treat patients with DIC to prevent further formation of blood clotting[152]. In our study, the elevated protein expression level may associate with warfarin treatment. We thus proposed that the expression level of inter-α-trypsin inhibitor may be related to warfarin therapy.

The other up-regulated protein detected in our analysis was α-2-macroglobulin. The up-regulation was observed in cells incubated with either S(-) or R(+) warfarin compared with control cells (absence of warfarin), but no significant changes between cells incubated with S(-) warfarin and those incubated with R(+) warfarin. Clinical data gave more support on the tendency of the protein changes. This protein is synthesized in the liver and secreted into plasma. It plays an important role in blood coagulation. Although this protein is not a vitamin K-dependent protein, it acts as an inhibitor of coagulation by inhibiting thrombin formation[3]. Prothrombin, the precursor of thrombin, is a vitamin K dependent coagulating factor, whose expression is inhibited

by warfarin. Thus the elevation of this protein may reflect the thrombin regulation by warfarin. It has also been reported that elevation of this protein level may in part provide protection from thrombosis[153].

6.3.2 Down-regulation of α-2-HS-glycoprotein, Apolipoprotein A-I and Fibrinogen γ chain

There were three down-regulated proteins in both cell line and clinical samples. For α-2-HS-glycoprotein, it was down-regulated in cells incubated with S(-) warfarin and to a greater extent compared with those incubated with R(+) warfarin. Our results therefore suggested a differential effect of warfarin enantiomers on α-2-HS-glycoprotein. Clinically, this protein also showed down-regulated for 15% in average.

This protein is secreted by hepatocytes. It forms a complex with Matrix Gla protein(MGP) and acts as a carrier for this insoluble protein in serum[154-155]. MGP has been shown to be an inhibitor of vascular calcification[156]. It is a protein which requires vitamin K dependent-γ-carboxylation for its activation. This activation is inhibited by warfarin. It has been reported in animal model that warfarin induces vascular calcification by inhibiting MGP expression[157] [158-159]. In our study, the down-regulation of α-2-HS-glycoprotein upon warfarin incubation may associate with reduced MGP expression. As detection of this insoluble MGP in proteomics is difficult, identification of its carrier instead would be an alternative way to monitor the side-effect of warfarin. Our study also provided evidences that S(-) and R(+) warfarin may contribute differently in warfarin's side-effect on vascular calcification.

Another down-regulated protein, apolipoprotein A-I, was down-regulated in cells incubated with S(-) warfarin to a lesser extent compared with those incubated with R(+) warfarin. To examine if the differences in the changes were significant, Western blot analysis was carried out for this protein (Figure 6.4, page 105). Results were obtained from cells incubated with individual enantiomers of warfarin and those incubated with individual enantiomers of warfarin in the presence of vitamin K. Consistently with the LC-MS/MS analysis, apolipoprotein A-I showed a reduced level in cells incubated with warfarin, compared with the control cells. Our Western blot analysis therefore confirmed that the level of this protein was down-regulated more in cells incubated with R(+) warfarin compared to those incubated with S(-) warfarin. In addition, commassie blue staining gave more evidences on controlling of total protein quantification (Figure 6.3).

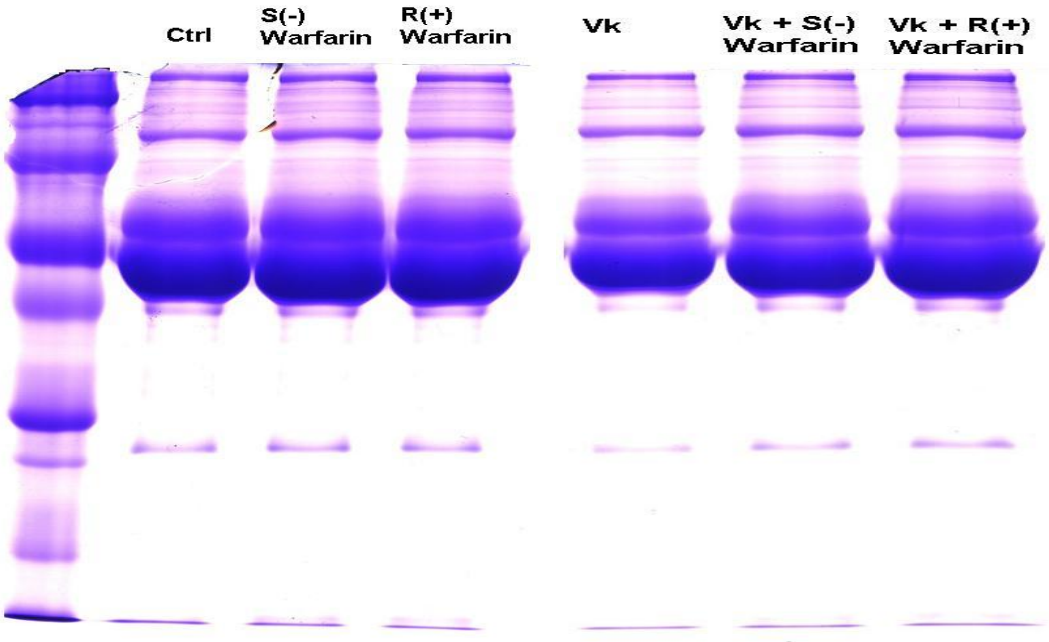

Figure 6.3 Total Protein Secreted Commasian Blue Staining on Warfarin Treatment

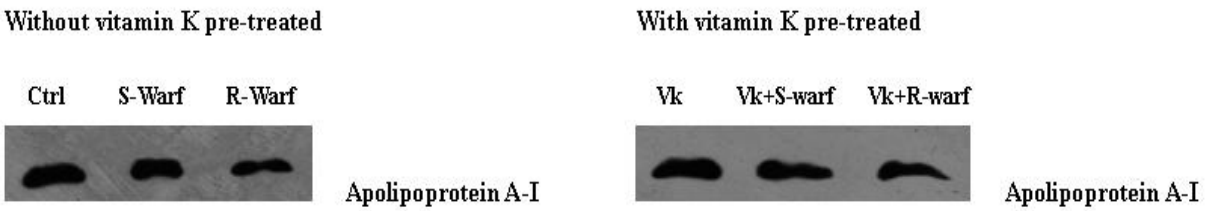

Protein	S:C	R:C
Apolipoprotein A-I	0. 75±0. 07	0. 61±0. 05
	P<0.05	P<0.05

Protein	S:V	R:V
Apolipoprotein A-I	0. 86±0. 04	0. 65±0. 11
	P<0.05	P<0.05

Figure 6.4, Western Blot Analysis of Protein Expression for Apolipoprotein A-I. ***Left***, protein expression in the experiment without Vitamin K pre-incubation. ***Right***, protein expression in the experiment with Vitamin K pre-incubation. Ctrl = sample without any treatment, S-warf = the sample incubated by S(-) warfarin, R-warf = the sample incubated by R(+) warfarin; Vk = the sample only incubated by vitamin K, Vk+S-warf = the sample incubated by vitamin K then S(-) warfarin, Vk+R-warf = the sample incubated by vitamin K then R(+) warfarin. ***Table,*** Quantification data calculated by Bio-Rad QualityOne software each. S:C = ratio of the sample incubated by S(-) warfarin and control cells, R:C = ratio of the sample incubated by R(+) warfarin and control cells, S:V= ratio of the sample incubated by vitamin K then S(-) warfarin and the sample only incubated by vitamin K; R:V= ratio of the sample incubated by vitamin K then R(+) warfarin and the sample only incubated by vitamin K. P values were calculated by T-test.**(Detailed description in page 104)**

In the results, the change identified in LC-MS/MS analysis was supported by our Western blot analysis. Quantitative information calculated was shown in Figure 6.4. Our results therefore suggested a differential effect of warfarin enantiomers on apolipoprotein A-I. In clinical batch, this protein was also down-regulated, but less significant.

Apolipoprotein A-I, is a well-known major component of high density lipoprotein (HDL) in the plasma and involved in the transportation of plasma lipids[160]. It has been reported that elevated plasma lipids appear to be procoagulant and may be

associated with either clinically significant thrombosis or elevated haemostatic markers of hypercoagulability[161]. Thus, the down-regulation of apolipoprotein A-I may indicate that the enhancement of anticoagulation effects by warfarin.

Our results also showed that fibrinogen gamma chain was down-regulated without any differences in cells incubated with either S(-) or R(+) warfarin, regardless of the presence of vitamin K. In clinical study, this protein was also down-regulated with a slightly larger ratio (40%). Fibrinogen which is synthesized in the liver is a major component in blood coagulation involving in formation of blood clots. The down-regulation of this protein indicated an enhanced level of anticoagulation by warfarin.

Extracellular proteomics by iTRAQ-coupled 2D LC-MS/MS was carried out as complementary to the identification in clinical sera. The findings indicated that in S(-) and R(+) warfarin incubated HepG2 cells, transthyretin precursor slightly varied compared to HepG2 without incubation, but no differences was observed in between the enantiomer drugs.

6.4 Section Conclusions

We reported the extracellular protein profile in HepG2 cells incubated with S(-) and R(+) warfarin, using iTRAQ-coupled 2D LC-MS/MS and followed by validation with Western blot analysis. In addition, the observed warfarin-associated protein changes were analyzed in serum samples of patients receiving warfarin therapy. Our results

indicated that inter-α-trypsin inhibitor heavy chain H4, apolipoprotein A-I and α-2-HS-glycoprotein showed changes in cells incubated with either S(-) or R(+) warfarin. For other proteins like α-2-macroglobulin and fibrinogen gamma chain, the changes were observed in cells incubated with either S(-) or R(+) warfarin compared with control cells (absence of warfarin), but no significant changes between cells incubated with S(-) warfarin and those incubated with R(+) warfarin. Our results indicated that those proteins may interfere with blood coagulation process, and possibly contribute to the warfarin's side-effect on vascular calcification. Clinical findings for the 5 proteins showed the same trends of changes, which indicated that the cell-line based systems can also be validated by clinical data.

7. Metabolic Profiling of HepG2 cells Incubated by S(-) and R(+) Enantiomers of Chiral Drug Warfarin

7.1 Introduction

Metabolomics is the systematic study of small-molecule metabolite profiles in specific cellular processes[162]. Small molecules, which belong to diverse categories such as organic acids, amino acids, fatty acids, carbohydrates, nucleosides and the conjugates, ketones and aldehydes, are involved in biochemical processes and provide a great deal of information on the status and functioning of a living system. They might work together with certain enzymes, or interact with other proteins or metabolites to influence cellular pathways and form metabolites networking. Study of metabolite profile directly reflects the phenotypic alterations in response to genetic or environmental changes, such as drug stimulations.

Globally study of cellular metabolic profile reveals the differences in biological responses between the enantiomer drugs. We reported the intracellular metabolic profile in HepG2 cells incubated with S(-) and R(+) warfarin by GCMS. Chemometric method PCA was applied to analyze the individual samples. A total of 80 metabolites belong to different categories were identified. Two batches of experiments (with and without the presence of vitamin K) were designed for results validation. In samples incubated with S(-) and R(+) warfarin, glucuronic acid showed significant decreased in cells incubated with R(+) warfarin but not in those incubated with S(-) warfarin. It may

partially explained the lower bio-activity of R(+) warfarin. And arachidonic acid showed increase in cells incubated with S(-) warfarin but not in those incubated with R(+) warfarin. In addition, a number of small molecules involved in γ-glutamyl cycle displayed ratio variations. Intracellular glutathione detection was further validated the results.

7.2 Experiment Procedures

In this study, cells were cultured and drug incubated, followed by cell lysis, metabolite extraction and derivatization, then GC-MS analysis. The metabolites were identified and quantified, with chemometric analysis for the metabolite profiles. In addition, cellular glutathione assay was carried out. The exact procedures can be found in Materials and Methods part in section 3 (3.10-3.13).

7.3 Results

To establish a comprehensive cellular metabolite profile in response to incubation of warfarin, metabolites were extracted from cells incubated with individual enantiomers of warfarin and subject to GC-MS analysis. The experiment was performed with three independent times. Figure 7.1 (page 111) was a representative for the overlay of chromatography of HepG2 incubated without and with S(-) or R(+) Warfarin. A total of 80 metabolites were identified. List of Metabolites detected, with the RT (retention time), Name and Class was showed in Appendix.

These metabolites were separated into 10 categories based on their chemical compositions. These included amino acids, hydroxyl acids, carbohydrates, nucleosides and nucleoside conjugates, fatty acids, alcohols, carboxylic acids, ketones, aldehydes and other organic acids which do not belong to any categories above. Figure 7.2 (page 112) was the distribution and categorization of all metabolites detected. The results indicated that a large number of metabolites detected in both sets (with and without vitamin K) were amino acids, hydroxyl acids, carbohydrates. It was shown that amino acids eluted first, then followed by carbohydrates (mainly monosaccharides), with the fatty acids came last.

For those peaks detected, the peak area was calculated and normalized using internal standard ribitol. Relative quantification assessment was performed by comparing the peak areas of individual samples. Results from the selection were summarized in Table 7.1 (page 110) for cells incubated with the individual enantiomers of warfarin, and for cells incubated with the individual enantiomers of warfarin in the presence of vitamin K.

A total of 10 metabolites showed changes in their level in Table 7.1(page 114). Most metabolites displayed similar changes in cells incubated with either S(-) or R(+) warfarin, however there are some of them showed changes to one but not all enantiomers of warfarin.

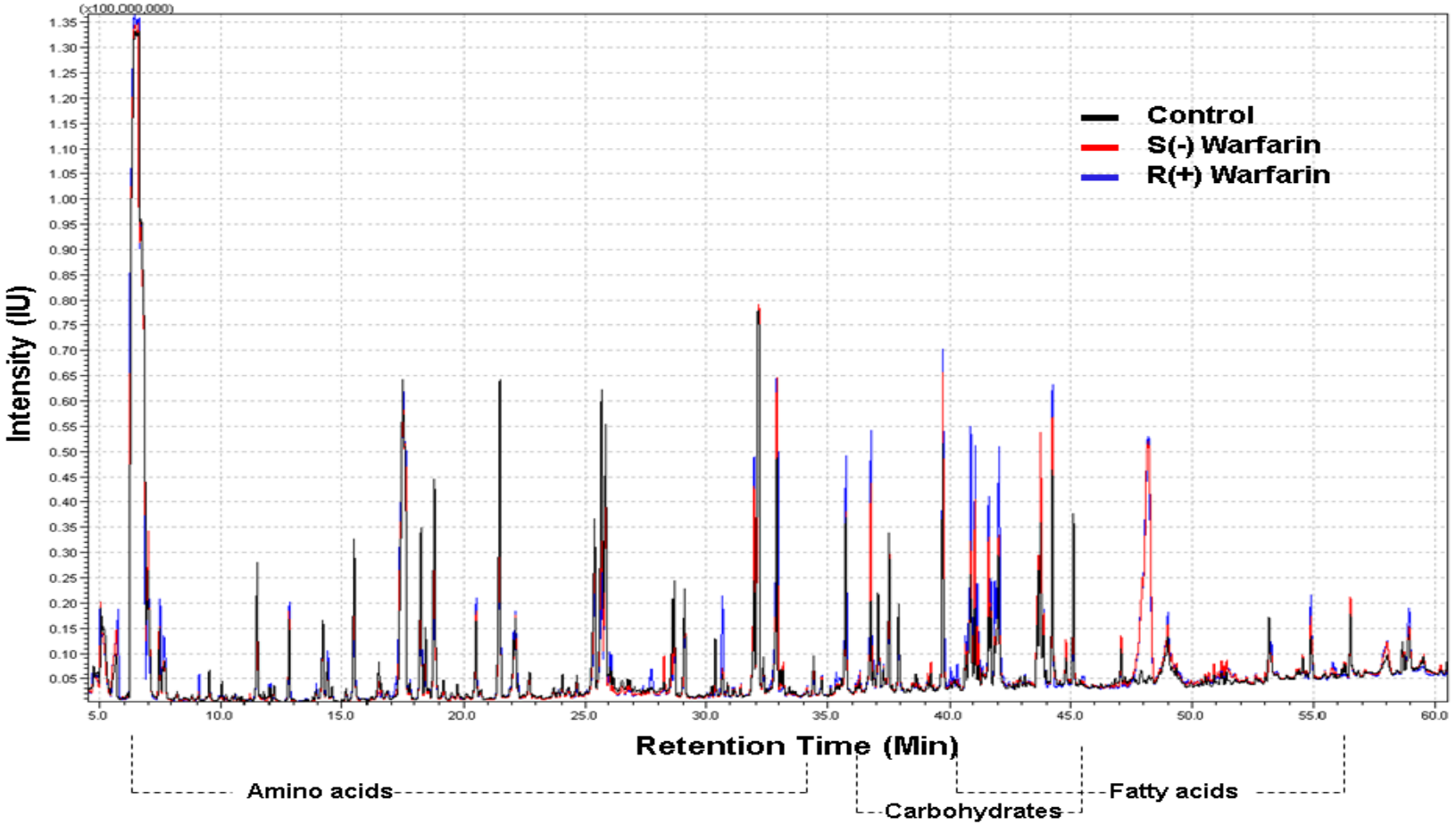

Figure 7.1 Overlay of Representative GC/MS Chromatography of HepG2 Cells Incubated by Warfarin S(-) and R(+) Enantiomers(Detailed description in page 109)

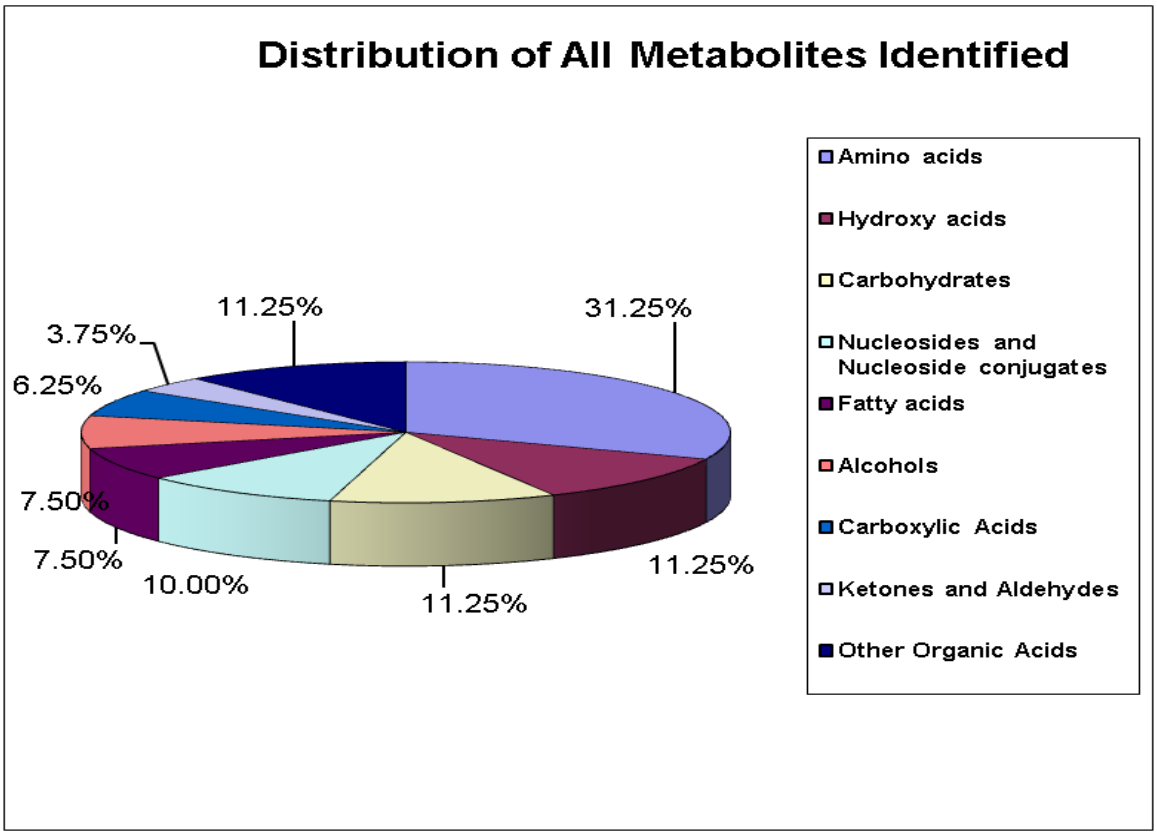

Figure 7.2 Categorization and Distribution of All 80 Metabolites Identified. (Detailed description in page 110)

For example, arachidonic acid, whose functions is involved coagulation process, was up-regulated in S(-) warfarin incubated cells for around 40% but not in those incubated with R(+) warfarin, while glucuronic acid showed down-regulated in R(+) warfarin but not in S(-) warfarin. In addition, glycine, 5-oxoproline, L-glutamine, L-valine and L-threonine showed up-regulation in both enantiomers with similar ratio; while L-serine, L-glutamate and L-lactic acid showed down-regulation. In the other batch, vitamin K enhanced batch showed the same results.

Subsequently, PCA results provided more information on multi-variables. PCA showed separations according to the principle components values on untreated, S(-)

warfarin and R(+) warfarin incubated samples. Each of the Control, S(-) warfarin and R(+) warfarin treated samples in the three independent experiments was analyzed. The results could be found in Figure 7.3 (page 115-116). In the score plot (Figure 7.3, panel A, p115), different groups had been clearly separated according to the scores. The further the distance in the plot, the more different the samples were. It can be concluded that S(-) warfarin has greater variance than R(+) warfarin from the untreated group (Control). In the loading plot (Figure 7.3, panel B, p115), different metabolites contributed to the loading values and separated according to the metabolic profiles. Those metabolites which had the larger variation between drug-treated and untreated samples were dispensed further from the origin. In addition, the results from vitamin K enhanced groups (Figure 7.3, panel CD, p116), provided further validation.

Table 7.1(page 114). **Metabolites Identified Whose Expression Ratio Varied at Least 10% in All Three Independent Experiments, in the Results without and with Vitamin K Pre- incubation.** In the left, C= control group, S= S(-) warfarin incubated group, R=R(+) warfarin incubated group. In the right, V= Vitamin K treated group, S= Vitamin K incubated then S(-) warfarin incubated group, R= Vitamin K incubated then R(+) warfarin incubated group. *P* values were calculated from student-t test.

Figure 7.3 (page 115-116). PCA Results for Relative Peak Intensities between Different Samples. *AB.* Score plot and loading plot for HepG2 cells incubated by warfarin enantiomers only. In the score plot, C1-C3 were cells without any treatment; S1-S3 were cells incubated by S(-) enantiomer of warfarin; R1-R3 were cells incubated by R(+) enantiomer of warfarin. In the loading plot, three PCs were selected to represent a spatial distribution of different metabolites. ***CD.*** Score plot and loading plot for HepG2 cells incubated by warfarin enantiomers, in the presence of vitamin K. In the score plot, V1-V3 were cells incubated by vitamin K only; S1-S3 were cells incubated by vitamin K then S(-) enantiomer of warfarin; R1-R3 were cells incubated by vitamin K then R(+) enantiomer of warfarin. In the loading plot, three PCs were selected to represent a spatial distribution of different metabolites.

Table 7.1(Detailed description in page 110)

		Warfarin						Warfarin + Vitamin K					
Name	Retention Time(min)	Ave S:C	(±)SD	p(S:C)	Ave R:C	(±)SD	p(R:C)	Ave S:V	(±)SD	p(S:V)	Ave R:V	(±)SD	p(R:V)
L-lactic acid	10.04	0.76	0.07	0.013	0.68	0.18	0.045	0.67	0.08	0.009	0.75	0.07	0.0112
Glycine	14.38	1.56	0.16	0.013	1.67	0.03	0.0003	1.49	0.09	0.005	1.51	0.07	0.0029
L-valine	15.52	1.44	0.05	0.002	1.31	0.13	0.049	1.43	0.04	0.001	1.3	0.05	0.0043
L-serine	20.59	0.78	0.03	0.002	0.86	0.03	0.009	0.67	0.07	0.006	0.75	0.07	0.0131
L-threonine	21.47	1.15	0.05	0.018	1.11	0.07	0.055	1.19	0.06	0.018	1.16	0.1	0.0575
5-oxoproline	25.88	1.61	0.1	0.005	1.32	0.04	0.003	1.46	0.06	0.003	1.45	0.11	0.0093
L-glutamate	28.66	0.77	0.06	0.011	0.74	0.11	0.027	0.76	0.04	0.004	0.75	0.06	0.0092
L-glutamine	33.14	1.84	0.06	0.0009	1.75	0.08	0.002	1.73	0.14	0.006	1.69	0.17	0.013
Glucuronic lactone	34.34	0.91	0.14	0.07	0.73	0.02	0.032	0.87	0.03	0.009	0.59	0.08	0.0058
Arachidonic acid	47.12	1.4	0.05	0.003	1.18	0.07	0.025	1.41	0.07	0.025	1.1	0.07	0.1289

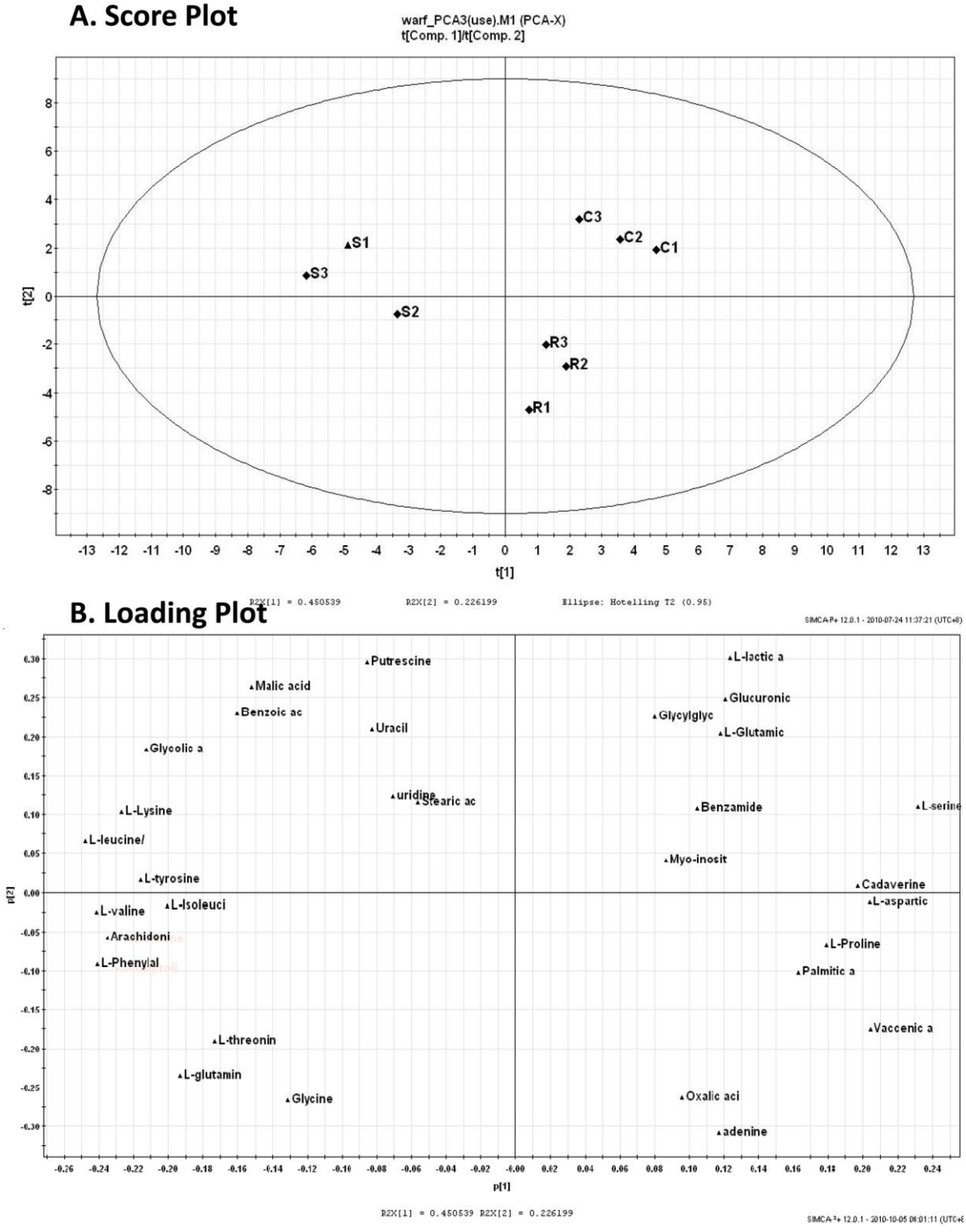

Figure 7.3 PCA Results for Relative Peak Intensities between Different Samples.

AB(Detailed description in page 113)

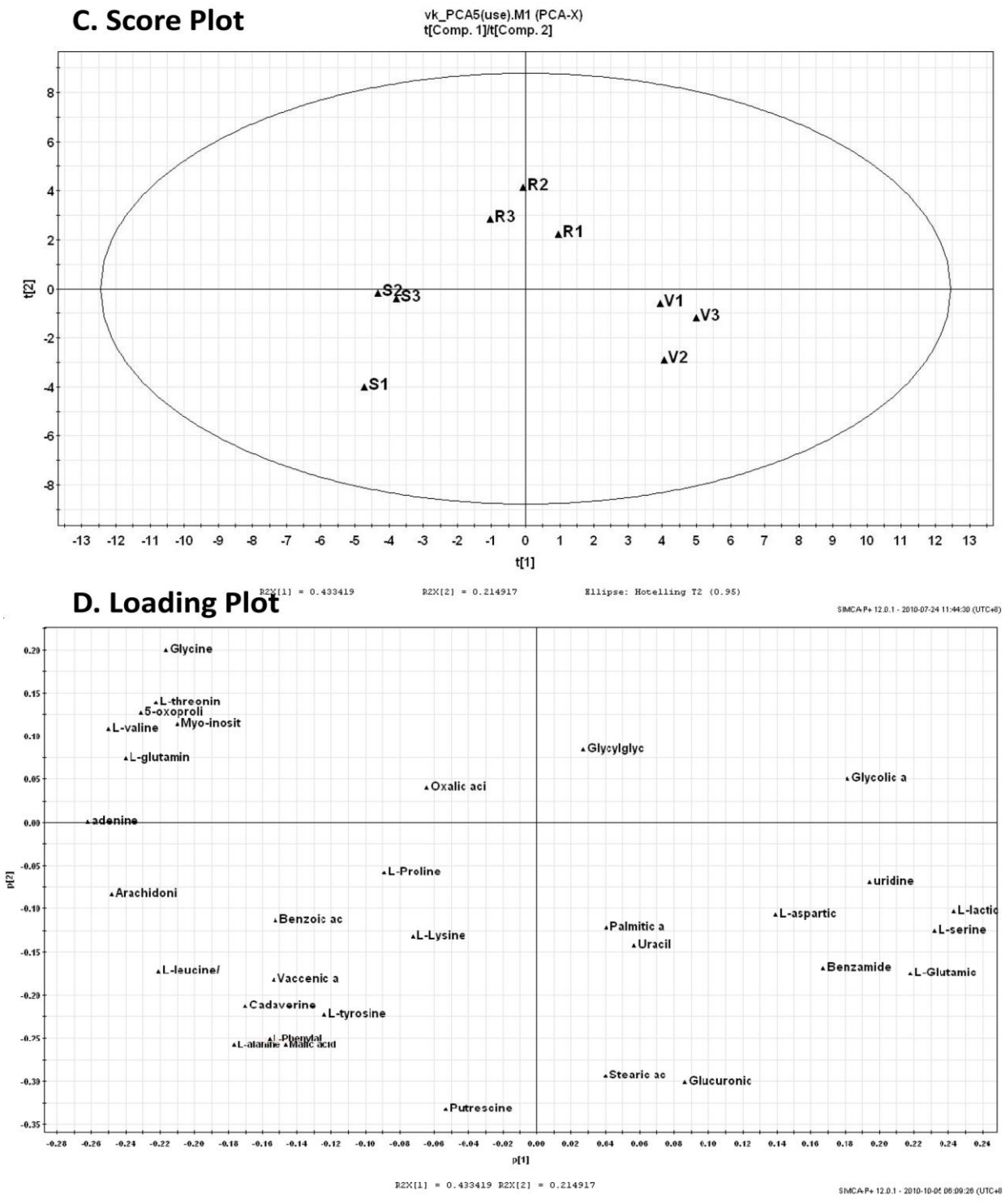

Figure 7.3 PCA Results for Relative Peak Intensities between Different Samples, CD.(Detailed description in page 113)

Several amino acids, including glycine, 5-oxoproline, L-glutamate were involved in glutathione (GSH) generation. To detected the intracellular glutathione level for validation of the changes of above amino acids on S(-) and R(+) warfarin, glutathione level was measured and results were shown in Figure 7.4 (page 118), while panel A were the results for samples incubated with warfarin alone and panel B are the results for samples incubated with warfarin in the presence of vitamin K. In the first set, glutathione level showed increased in the S(-) and R(+) warfarin incubated samples, while samples incubated with S(-) warfarin increased a bit more than R(+) warfarin. In the second set, the glutathione level was enhanced in the S(-) and R(+) warfarin, which was consistent with the 1st set results. It indicated that warfarin enantiomers have effects on enhancing the glutathione levels intracellularly.

Figure 7.4 Intracellular Glutathione Level of HepG2 Cells Incubated with Drugs *A*, glutathione level of 1st set of experiment (without vitamin K pre- incubation). The left group was fluorescent view and the right group was fluorescent view with corresponding light view. ***B***, glutathione level of 2nd set of experiment (with vitamin K pre- incubation). The left group was fluorescent view and the right group was fluorescent view with corresponding light view.

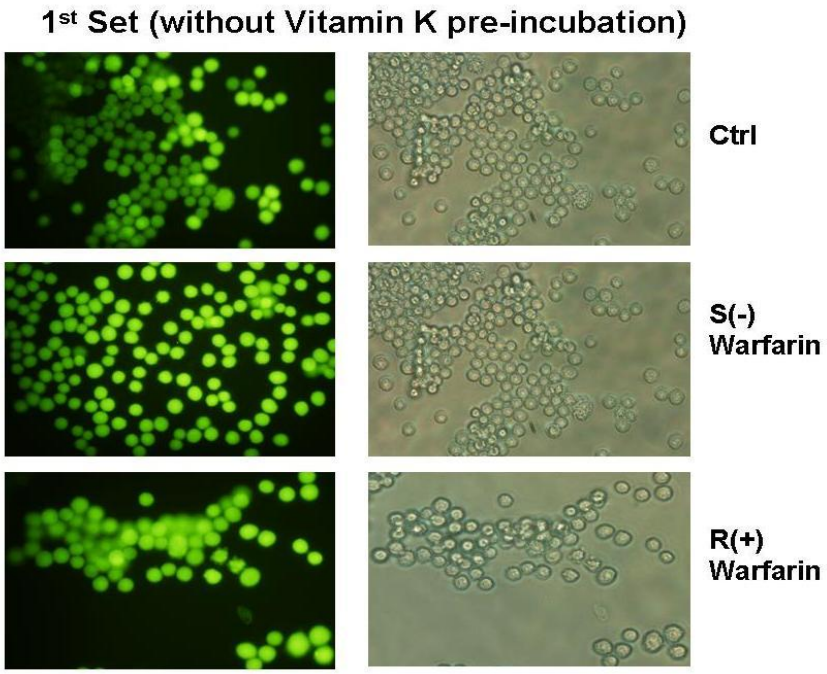

Figure 7.4 Intracellular Glutathione Level of HepG2 Cells Incubated with Drugs. A

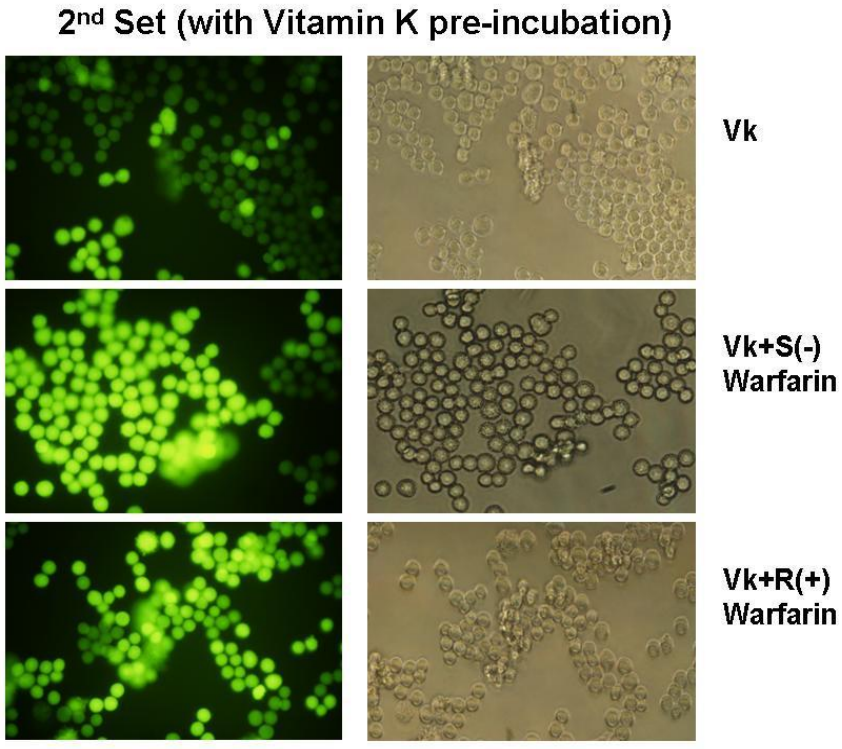

Figure 7.4 Intracellular Glutathione Level of HepG2 Cells Incubated with Drugs. B

(Detailed description in page 117)

7.4 Discussion

Influence on γ-glutamyl cycle and glutathione level by warfarin

In our results, it has been shown that several amino acids have their expression ratio varied. The elevated level of glycine, L-glutamine, 5-oxoproline and decreased level of L-glutamate may associate with warfarin induced glutathione production thus subsequently influenced γ-glutamyl cycle and hepatic γ-glutamyltransferase. An overall change in the cellular metabolic process by warfarin was depicted in Figure 7.5(page 117).

It has been reported that warfarin administration increased both serum and hepatic γ-glutamyltransferase activity in rats[163]. This protein γ-glutamyltransferase is a critical enzyme on γ-glutamyl cycle, which is a transport system for amino acids and generation of glutathione[164-165].

In γ-glutamyl cycle, glutathione is broken down to glycine, cysteine and glutamate. Four enzymes catalyze the reaction. γ-glutamyl transferase transfers γ-glutamyl moiety of glutathione to one amino acid, generation γ-glutamyl amino acid and cysteinylglycine. The cysteinylglycine is split to glycine and cysteine. γ-glutamyl cyclotransferase converts γ-glutamyl amino acid to 5-oxoproline and corresponding amino acid. Thus the process has transported the amino acid across the membrane. After that, 5-oxoproline is converted to glutamate by 5-oxoprolinase. The generated glutamate is combined with cysteine and glycine coming from previous cysteinylglycine and the glutathione synthetase to re-synthesize glutathione. Then the cycle repeats.

Figure 7.5 Overall Changes in the Cellular Metabolic Process by Warfarin(Page 121) The expression of GST, which is associated with Vitamin K Epoxide Reductase(VKOR) may be affected by warfarin incubation. The less oxidative environment created by ROS reduction in warfarin incubation (described in Part 5). Thus the ROS level may influence the expression of glutathione thus influence γ-glutamyl cycle with relative metabolites such as glycine, 5-oxoproline and glutamate. This cycle is a transport system for amino acids. Its regulation by warfarin may lead to increase of hepatic γ-glutamyl transferase activity. In addition, warfarin metabolism is stereo-selective. Arachidonic acid and glucuronic acid are affected by S(-) and R(+) warfarin, respectively. Expression ratio elevated molecules were highlighted in red while reduced highlighted in blue. An increased GSH-to-GSSG ratio is considered indicative of reduced ROS.

Combined with proteomics results, Protein Disulfide Isomerase A3 (PDIA3) with GST was proposed to be associated with VKOR to form enzyme complex. In addition, 14-3-3 Protein sigma, whose expression is down-regulated by warfarin, may interact with coagulation factors and influence their maturation.

GGCX: γ-glutamyl carboxylase; VKOR: vitamin K 2,3 epoxide reductase; NQO1: NAD(P)H quinone oxidoreductase 1. GST: Glutathione-S-transferase; AA: amino acid.

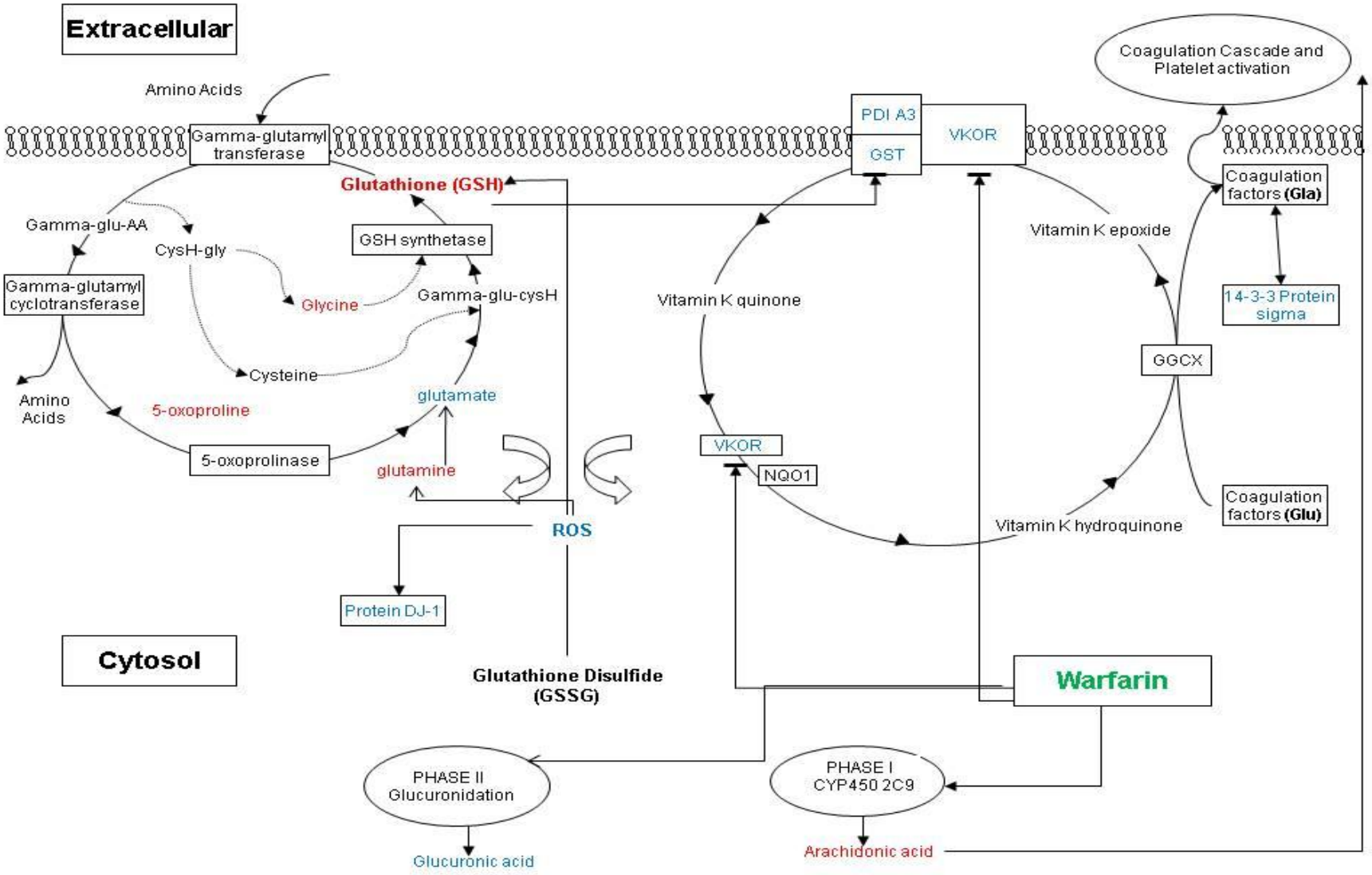

Figure 7.5 Overall Changes in the Cellular Metabolic Process by Warfarin (Detailed description in page 120)

Glutathione is an antioxidant which can help protect cells from reactive oxygen species (ROS). It exists in reduced form (GSH) and oxidized disulfide form (GSSG), and a decreased GSH-to-GSSG ratio is considered indicative of oxidative stress generated by ROS. Warfarin increases the hepatic total glutathione level that the increase is primarily due to elevated GSH levels with very little effect on GSSG level[163]. The results may indicate a decreased level of ROS generation on warfarin administration. In our previous study on intracellular protein profiles generated by HepG2 cells incubated with warfarin enantiomers, we have reported that protein DJ-1, which is a protein marker for intracellular ROS, was down-regulated in the cells incubated by warfarin[133]. This suggested a reduced level of intracellular ROS by warfarin, which was consistent with our metabolic profiles finding herein.

Glutathione is the substrate of Glutathione-S-transferase(GST). As it has been proposed that GST superfamily contained a group of warfarin-sensitive GST, which was associated with Vitamin K Epoxide Reductase (VKOR) and was a part of the transmembrane enzyme[166]. The outcome is: the elevation of glutathione may also be due to the deduced VKOR complex activity by warfarin. Thus affects γ-glutamyl cycle with several metabolites and hepatic γ-glutamyl transferase.

In addition, as γ-glutamyl cycle transports amino acids across the membrane, the elevation or decrease of other intracellular L-amino acid content, such as L-valine, L-serine or L-threonine may be attributed to the change of amino acid transportation of amino acid by γ-glutamyl cycle.

Influence on uptake of vitamin K by warfarin

Another possible reason for elevated level of intracellular glycine is: one function of glycine is to combine with cholic acid to form bile acid [167]. The binding will enhance the hepatic uptake of fat-soluble vitamin K[168]. In that case, increase of unbounded intracellular glycine may reflect the reduced uptake of vitamin K.

Influence on glucuronidation by warfarin stereo-selectivity

The next metabolite down-regulated is glucuronic lactone. It is the stable form of glucuronic acid, as glucuronic acid normally does not exist in free acid. Glucuronidation is a process of glucuronic acid conjugating with xenobiotic metabolism of substances such as drugs, to facility the transport and elimination of those substances[169-170]. The conjugation involves glycosidic bonds. It mainly occurs in the liver and is a part of phase II metabolism of drugs. Until very recently, it has been reported that glucuronidation could abolish the binding between warfarin and its targeting enzyme, VKOR, due to introduction of a bulky acidic sugar. [171]. In our results, R(+) warfarin incubated sample showed a more decreased level of this metabolite, compared to S(-) warfarin. It consists with the previous finding that R(+) warfarin may be more tended to be glucuronidated. The tendency of R(+) warfarin may contribute to the lower biological activity of this enantiomer.

Influence on arachidonic acid metabolism by warfarin stereo-selectivity

Another elevated metabolite is arachidonic acid. It is a polyunsaturated omega-6 fatty acid and presents in the phospholipids of cell membranes, in addition, involved in

cellular signaling[172]. Warfarin undergoes stereo-selective metabolism and S(-) enantiomer are mainly metabolized by Cytochrome P450 2C9 (CYP2C9) and R(+) warfarin by CYP1A2 and CYP3A4. In previous study, it has been addressed that CYP2C9 enzymes metabolize warfarin and arachidonic acid[173]. Possibly, the presence of S(-) warfarin enantiomer may affect the metabolism of arachidonic acid. Arachidonic acid is the precursor for synthesis thromboxane A2, which has prothrombotic properties[174]. This thromboxane A2 enhances the liver-generated fibrinogen binding to platelet for its activation[175]. Thus it does not exclude the possibility that the presence of warfarin, by regulating arachidonic metabolism, indirectly affected the coagulating process.

7.5 Section Conclusions

We reported the intracellular metabolic profile in HepG2 cells incubated with S(-) and R(+) warfarin, using GC-MS. Glucuronic acid, arachidonic acid showed variations in cells incubated with S(-) warfarin and R(+) warfarin. For other metabolites like glycine, 5-oxoproline and glutamate, the expressions each were found to be the same in cells incubated with either S(-) or R(+) warfarin. Our results indicated that the expression of those metabolites may partially explain the different bio-activities between the two enantiomers and addressed that the cycle for generation of glutathione may be interfered by warfarin. Taken together, our findings provided molecular evidence on a comprehensive metabolic profile on warfarin-cell interaction which may shed new lights on future improvement of warfarin therapy.

8. Conclusions and Future Direction

1) Background and Motivation

Warfarin is a commonly prescribed oral anticoagulant. Clinical studies of warfarin therapy have indicated that patients display different dosing requirement for warfarin, mainly to minimize the side-effects. Asian patients have been categorized in low- and high-dose groups. In addition to the recently established association between warfarin dosing and the patients' genetic polymorphism, it is expected that other changes including differentially expressed proteins also exist in these patients. Identification of a serum protein marker should complement the pharmacogenetic analysis toward a better prognosis of the drug dosing requirement.

Such identification can be carried out by pharmacoproteomics analysis, which is the proteomics analysis applied to clinical samples. The pharmacoproteomics also has the potential for the development of personalized medicine and provides helpful information in matching a particular target-based therapy to a particular biomarker in a subgroup of patient.

Notwithstanding the advantage offered by pharmacoproteomics, the identification of such markers in patients' serum samples has been limited by the intrinsic differences amongst patients. These differences directly impact on the accuracy of data obtained, thus requires large number of clinical samples to be analysed. This limitation can however be overcome by cell-based drug-cell interaction systems which offer a

homogenous environment and high reproducibility of results generated in the drug intrinsic mechanism study.

2) Clinical analysis and cell-based validation

In this project, the iTRAQ based quantitative proteomic method was applied to analyze a group of Asian patients to identify potential warfarin dosage protein markers in their sera. Concurrently, the same method was applied to establish the protein profiles in liver HepG2 cells incubated by warfarin. We found that significantly up-regulated level of transthyretin precursor in patients receiving low dose of warfarin but not in those on high dose of warfarin. Cell-based system was further used to confirm that this protein was associated with dosage variations. In fact, the Western blotting analysis has shown that, transthyretin precursor was expresses differentially in HepG2 cells incubated with low- and high- dose of warfarin.

3) *Toward a better understanding of mechanism of action of warfarin*

Based on our clinical findings, the cell-based proteomics analysis was further explored to identify specific proteins which might interact with transthyretin precursor and be involved in drug action mechanism. iTRAQ-coupled 2D LC-MS/MS was used to investigate intracellular protein profile in HepG2 cells incubated with S(-) and R(+) warfarin. Protein disulfide isomerase A3 was identified in the formation of warfarin-targeted enzyme complex and another protein, protein DJ-1 on both S(-) and R(+) warfarin treated samples was down-regulated. Transthyretin precursor was identified as a substrate for DJ-1 protease. This protein DJ-1 may be associated with specific dosing

regimens of warfarin and reflect the intracellular interaction of transthyretin precursor, thus provide more information on the discovery of unknown warfarin dosage dependent signaling pathway. And protein DJ-1 may also be a target in understanding the warfarin dosage variation. In addition, intracellular metabolic profile from HepG2 cells incubated with warfarin was analyzed using a GC-MS platform. A number of small molecules involved in γ-glutamyl cycle displayed variations to the ratio while other metabolites may explain the differences on bio-activities between warfarin enantiomers. A schematic diagram depicting the possible cellular changes induced by warfarin can be found in Figure 8.1. The combined proteomics and metabolomics information on the status of drug treatment and drug functions should provide a comprehensive understanding on overall warfarin-cell interaction and the dynamics of cellular responses.

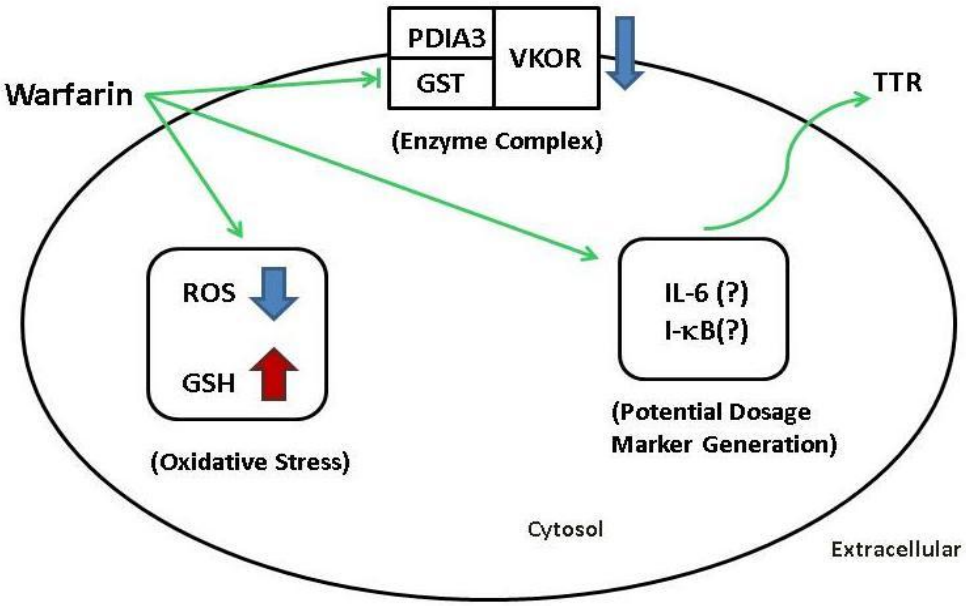

Figure 8.1. A schematic diagram depicted the possible cellular changes induced by warfarin. In this diagram, VKOR, together with a group of inter-membrane GST and PDIA3, formed warfarin-sensitive enzyme complex. Warfarin may also decrease the cellular ROS level, with GSH concentration increasing. In another aspect, potential warfarin dosage marker, transthyretin precursor's expression may be associated with IL-6 pathway with unknown mechanism on warfarin treatment.

VKOR: Vitamin K 2,3 epoxide reductase; GST: Glutathione-S-transferase; PDIA3: Protein Disulfide Isomerase A3; GSH: Glutathione; ROS: Reactive Oxygen Species.

4) ***New biomarkers discovery from cell-based systems***

Extracellular proteomics by iTRAQ-coupled 2D LC-MS/MS was carried out to complement our clinical data on transthyretin precursor, as well as to identify new potential biomarkers. The findings indicated that in S(-) and R(+) warfarin incubated HepG2 cells, transthyretin precursor slightly varied compared to HepG2 without incubation. There were no differences in the level of transthyretin precursor in the culture medium incubated with individual enantiomers of warfarin. Similarly to our intracellular proteomics platform, the iTRAQ-coupled 2D LC-MS/MS can be established to investigate the transthyretin precursor secretion from cells incubated with various doses of warfarin, hereby providing a validation tool for our clinical analysis.

For other biomarkers related to warfarin action mechanism, inter-α-trypsin inhibitor heavy chain H4, apolipoprotein A-I and α-2-HS-glycoprotein showed changes in cells incubated with either S(-) or R(+) warfarin. For α-2-macroglobulin and fibrinogen gamma chain, the changes were observed in cells incubated with either S(-) or R(+) warfarin compared to the control group. However, no significant changes were found between cells incubated with S(-) warfarin and those incubated with R(+) warfarin. Significantly, α-2-HS-glycoprotein may contribute to drug side effects. Clinical findings for the 5 proteins showed the same trends of changes, which indicated that the cell-line based systems can also be validated by clinical data.

Our Metabolomics findings revealed clearly complementary information to the proteomics data. In the future, to further analyze the cellular metabolic influences by warfarin enantiomers, secreted metabolites will be analyzed by GC-MS. In this study, we will semi-quantify the differences in secreted metabolite levels between un-incubated human liver cells and those incubated by S(-) and R(+) warfarin, respectively. This study expanded into secreted metabolomics analysis is to identify specific complementary metabolic biomarkers to protein markers. The extracellular results were then validated by clinical data.

5) Future Direction

This study has established a comprehensive cell-based platform for proteomic and metabolomics analysis for drug-cell interactions. Intracellular protein and metabolite profiles reveal the mechanism of drug actions, while extracellular protein and metabolite profiles give more evidence on the discovery of potential biomarker. It is hoped that this platform can be used to analyze drug toxicity, drug safety and side-effect. Such cell-based drug toxicity analysis is expected to bridge the gap between candidate drugs and their clinical application.

In the context of indentifying specific serum proteins in relation to warfarin dosing, our findings suggested that clinical analysis can be coupled to cell-based platform. By using proteomics and metabolomics technologies, clinical findings can be validated in cell-based systems, because of heterogeneity of clinical samples. Thus cell-based system can provide homogenous background and reproducible data, which gives more statistical

significance and exclusion of patients' genetic variations. And specific proteins or metabolites markers identified in cell-based system can also be validated by clinical data. Those clinical data can give more tendencies on the changes for a particular biomarker which is stimulated on drug or pathological alteration.

This interactive cell-based method coupled with clinical analysis platform both proteomics and metabolomics can be expanded to investigation on other drugs. An increasing number of drugs have been found to display dose dependency based on patients' genetic make-up. A pharmacogenetic study can be established for patients on drug therapy. In addition, pharmacoproteomics can be applied to reveal potential biomarkers in patients' samples. The potential biomarkers can be validated in a homogenous cell-line based system. Furthermore, this coupled platform can also be applied to membrane-anchored protein profile since many drug binding receptors are located on the plasma membrane.

We anticipate that our interactive platform can not only be applied to existing drugs for a better understanding of their biological impact, but can also be useful for pre-clinical toxicity testing of newly developed drugs. This can be coupled with the currently established drug testing in animal model to provide extensive information on drug toxicity and accelerate industrial drug development.

References

1. Koide-Yoshida, S., et al., *DJ-1 degrades transthyretin and an inactive form of DJ-1 is secreted in familial amyloidotic polyneuropathy.* International Journal of Molecular Medicine, 2007. **19**(6): p. 885-893.
2. Mu, F.T., et al., *A functional 14-3-3 zeta-independent association of PI3-kinase with glycoprotein Ib alpha, the major ligand-binding subunit of the platelet glycoprotein Ib-IX-V complex.* Blood, 2008. **111**(9): p. 4580-4587.
3. Deboer, J.P., et al., *Alpha-2-Macroglobulin Functions as an Inhibitor of Fibrinolytic, Clotting, and Neutrophilic Proteinases in Sepsis - Studies Using a Baboon Model.* Infection and Immunity, 1993. **61**(12): p. 5035-5043.
4. Bruice, P.Y., *Organic Chemistry*. 4th ed. 2004: Prentice Hall
5. MJ., M.J.O., *Stereochemistry in Drug Action.* Primary Care Companion Journal of Clinical Psychiatry, 2003. **5**(2): p. 70-73.
6. Wsol, V., L. Skalova, and B. Szotakova, *Chiral inversion of drugs: Coincidence or principle?* Current Drug Metabolism, 2004. **5**(6): p. 517-533.
7. Agranat, I., H. Caner, and J. Caldwell, *Putting chirality to work: The strategy of chiral switches.* Nature Reviews Drug Discovery, 2002. **1**(10): p. 753-768.
8. Tucker, G.T., *Chiral switches.* Lancet, 2000. **355**(9209): p. 1085-1087.
9. Drayer, D.E., *Pharmacodynamic and pharmacokinetic differences between drug enantiomers in humans: An overview.* Clinical Pharmacology and Therapeutics, 1986. **40**(2): p. 125-133.
10. Suttie, J.W., *Vitamin K in Health and Disease*. 2009: Taylor&Francis Group.
11. Hirsh, J., et al., *Oral anticoagulants: Mechanism of action, clinical effectiveness, and optimal therapeutic range.* Chest, 2001. **119**(1): p. 8S-21S.
12. Fasco, M.J. and L.M. Principe, *R-Warfarin and S-Warfarin Inhibition of Vitamin-K and Vitamin-K-2,3-Epoxide Reductase Activities in the Rat.* Journal of Biological Chemistry, 1982. **257**(9): p. 4894-4901.
13. Takahashi, H. and H. Echizen, *Pharmacogenetics of warfarin elimination and its clinical implications.* Clinical Pharmacokinetics, 2001. **40**(8): p. 587-603.
14. Oreilly, R.A., *STUDIES ON OPTICAL ENANTIOMORPHS OF WARFARIN IN MAN.* Clinical Pharmacology & Therapeutics, 1974. **16**(2): p. 348-354.
15. Rentsch, K.M., *The importance of stereoselective determination of drugs in the clinical laboratory.* Journal of Biochemical and Biophysical Methods, 2002. **54**(1-3): p. 1-9.
16. Kaminsky, L.S. and Z.Y. Zhang, *Human P450 metabolism of warfarin.* Pharmacology & Therapeutics, 1997. **73**(1): p. 67-74.
17. Wingard, L.B., R.A. Oreilly, and G. Levy, *Comparative pharmacokinetics of coumarin anticoagulants .34. pharmacokinetics of warfarin enantiomers - search for intrasubject correlations.* Clinical Pharmacology & Therapeutics, 1978. **23**(2): p. 212-217.
18. Oldenburg, J., *The Vitamin K Cycle.* Vitamins and Hormones, 2008. **78**: p. 35-62.
19. Wu, S.M., et al., *Cloning and Expression of the Cdna for Human Gamma-Glutamyl Carboxylase.* Science, 1991. **254**(5038): p. 1634-1636.
20. Gong, X., R. Gutala, and A.K. Jaiswal, *Quinone Oxidoreductases and Vitamin K Metabolism*, in *Vitamins and Hormones*. 2008. p. 85-101.

21. Stafford, D.W., *The vitamin K cycle.* Journal of Thrombosis and Haemostasis, 2005. **3**(8): p. 1873-1878.
22. Jin, D.Y., J.K. Tie, and D.W. Stafford, *The conversion of vitamin K epoxide to vitamin K quinone and vitamin K quinone to vitamin K hydroquinone uses the same active site cysteines.* Biochemistry, 2007. **46**(24): p. 7279-7283.
23. Berkner, K.L., *The vitamin K-dependent carboxylase.* Annual Review of Nutrition, 2005. **25**: p. 127-149.
24. Tie, J.K. and D.W. Stafford, *Structure and function of vitamin K epoxide reductase,* in *Vitamin K*. 2008, Elsevier Academic Press Inc: San Diego. p. 103-130.
25. Wajih, N., S.M. Hutson, and R. Wallin, *Disulfide-dependent protein folding is linked to operation of the vitamin K cycle in the endoplasmic reticulum - A protein disulfide isomerase-VKORC1 redox enzyme complex appears to be responsible for vitamin K-1 2,3-epoxide reduction.* Journal of Biological Chemistry, 2007. **282**(4): p. 2626-2635.
26. Farzaneh-Far, A., et al., *A polymorphism of the human matrix gamma-carboxyglutamic acid protein promoter alters binding of an activating protein-1 complex and is associated with altered transcription and serum levels.* Journal of Biological Chemistry, 2001. **276**(35): p. 32466-32473.
27. Rost, S., et al., *Compound heterozygous mutations in the gamma-glutamyl carboxylase gene cause combined deficiency of all vitamin K-dependent blood coagulation factors.* British Journal of Haematology, 2004. **126**(4): p. 546-549.
28. Ph Chu, *et al*. *Purified vitamin K epoxide reductase alone is sufficient for conversion of vitamin K epoxide to vitamin K and vitamin K to vitamin KH2.* Proceedings of the National Academy of Sciences of the United States of America, 2006. **103**(51): p. 19308-19313.
29. Wadelius, M. and M. Pirmohamed, *Pharmacogenetics of warfarin: current status and future challenges.* Pharmacogenomics Journal, 2007. **7**(2): p. 99-111.
30. Yin, T. and T. Miyata, *Warfarin dose and the pharmacogenomics of CYP2C9 and VKORC1 - Rationale and perspectives.* Thrombosis Research, 2007. **120**(1): p. 1-10.
31. Lal, S., et al., *Influence of APOE genotypes and VKORC1 haplotypes on warfarin dose requirements in Asian patients.* British Journal of Clinical Pharmacology, 2008. **65**(2): p. 260-264.
32. Rieder, M.J., et al., *Effect of VKORC1 haplotypes on transcriptional regulation and warfarin dose.* New England Journal of Medicine, 2005. **352**(22): p. 2285-2293.
33. L. Cancela et.al. *Molecular-Structure, Chromosome Assignment, and Promoter Organization of the Human Matrix Gla Protein Gene.* Journal of Biological Chemistry, 1990. **265**(25): p. 15040-15048.
34. Price, P.A., A.S. Otsuka, and J.W. Poser, *Characterization of a Î³ carboxyglutamic acid containing protein from bone.* Proceedings of the National Academy of Sciences of the United States of America, 1976. **73**(5): p. 1447-1451.
35. Price, P.A. and M.K. Williamson, *Primary structure of bovine matrix Gla protein, a new vitamin K-dependent bone protein.* Journal of Biological Chemistry, 1985. **260**(28): p. 14971-14975.

36. Lillicrap,et.al., *Practical Hemostasis and Thrombosis*. 2nd ed. 2009: Wiley.
37. Furie, B. and B.C. Furie, *Thrombus formation in vivo.* Journal of Clinical Investigation, 2005. **115**(12): p. 3355-3362.
38. Davie, E.W., K. Fujikawa, and W. Kisiel, *The coagulation cascade: Initiation, maintenance, and regulation.* Biochemistry, 1991. **30**(43): p. 10363-10370.
39. Sunnerhagen, M., et al., *Structure of the Ca2+-free GLA domain sheds light on membrane binding of blood coagulation proteins.* Nature Structural Biology, 1995. **2**(6): p. 504-509.
40. Dahlback, B. and B.O. Villoutreix, *The anticoagulant protein C pathway.* FEBS Letters, 2005. **579**(15): p. 3310-3316.
41. Hackeng, T.M. and J. Rosing, *Protein s as cofactor for TFPI.* Arteriosclerosis, Thrombosis, and Vascular Biology, 2009. **29**(12): p. 2015-2020.
42. Peng, J. and S.P. Gygi, *Proteomics: The move to mixtures.* Journal of Mass Spectrometry, 2001. **36**(10): p. 1083-1091.
43. Anderson, N.L. and N.G. Anderson, *Proteome and proteomics: New technologies, new concepts, and new words.* Electrophoresis, 1998. **19**(11): p. 1853-1861.
44. Cordwell, S.J., et al., *Subproteomics based upon protein cellular location and relative solubilities in conjunction with composite two-dimensional electrophoresis gels.* Electrophoresis, 2000. **21**(6): p. 1094-1103.
45. Shevchenko, A., et al., *Linking genome and proteome by mass spectrometry: Large-scale identification of yeast proteins from two dimensional gels.* Proceedings of the National Academy of Sciences of the United States of America, 1996. **93**(25): p. 14440-14445.
46. Mann, M., R.C. Hendrickson, and A. Pandey, *Analysis of proteins and proteomes by mass spectrometry*, in *Annual Review of Biochemistry*. 2001. p. 437-473.
47. Dettmer, K., P.A. Aronov, and B.D. Hammock, *Mass spectrometry-based metabolomics.* Mass Spectrometry Reviews, 2007. **26**(1): p. 51-78.
48. Cravatt, B.F., G.M. Simon, and J.R. Yates, *The biological impact of mass-spectrometry-based proteomics.* Nature, 2007. **450**(7172): p. 991-1000.
49. Frohlich, T. and G.J. Arnold, *Proteome research based on modern liquid chromatography - tandem mass spectrometry: separation, identification and quantification.* Journal of Neural Transmission, 2006. **113**(8): p. 973-994.
50. Simpson, R.J., *Proteins and Proteomics: A Laboratory Manual*. 1 ed. 2003, New York: Cold Spring Harbor Laboratory Press. 926.
51. Koomen, J., D. Hawke, and R. Kobayashi, *Developing an understanding of proteomics: An introduction to biological mass spectrometry.* Cancer Investigation, 2005. **23**(1): p. 47-59.
52. Jackson, P.J., et al., *Use of Electrospray-Ionization and Neutral Loss Liquid-Chromatography Tandem Mass-Spectrometry in Drug-Metabolism Studies.* Journal of Mass Spectrometry, 1995. **30**(3): p. 446-451.
53. McAlister, G.C., et al., *Implementation of electron-transfer dissociation on a hybrid linear ion trap-orbitrap mass spectrometer.* Analytical Chemistry, 2007. **79**(10): p. 3525-3534.
54. McMaster, M.C., *LC/MS : A Practical User's Guide*. 2005: Wiley.

55. Anderson, J.S., V.H. Vartanian, and D.A. Laude, *Evolution of Trapped Ion Cells in Fourier-Transform Ion-Cyclotron Resonance Mass-Spectrometry.* Trac-Trends in Analytical Chemistry, 1994. **13**(6): p. 234-239.
56. Dunn, W.B. and D.I. Ellis, *Metabolomics: Current analytical platforms and methodologies.* Trac-Trends in Analytical Chemistry, 2005. **24**(4): p. 285-294.
57. Blackstock, W.P. and M.P. Weir, *Proteomics: Quantitative and physical mapping of cellular proteins.* Trends in Biotechnology, 1999. **17**(3): p. 121-127.
58. Blagoev, B., et al., *A proteomics strategy to elucidate functional protein-protein interactions applied to EGF signaling.* Nature Biotechnology, 2003. **21**(3): p. 315-318.
59. Everley, P.A., et al., *Quantitative cancer proteomics: Stable isotope labeling with amino acids in cell culture (SILAC) as a tool for prostate cancer research.* Molecular and Cellular Proteomics, 2004. **3**(7): p. 729-735.
60. Ong, S.E., et al., *Stable isotope labeling by amino acids in cell culture, SILAC, as a simple and accurate approach to expression proteomics.* Molecular & cellular proteomics : MCP, 2002. **1**(5): p. 376-386.
61. Romijn, E.P., et al., *Expression clustering reveals detailed co-expression patterns of functionally related proteins during B cell differentiation: A proteomic study using a combination of one-dimensional gel electrophoresis, LC-MS/MS, and stable isotope labeling by amino acids in cell culture (SILAC).* Molecular and Cellular Proteomics, 2005. **4**(9): p. 1297-1310.
62. Gygi, S.P., et al., *Quantitative analysis of complex protein mixtures using isotope-coded affinity tags.* Nature Biotechnology, 1999. **17**(10): p. 994-999.
63. Yi, E.C., et al., *Increased quantitative proteome coverage with13C/ 12C-based, acid-cleavable isotope-coded affinity tag reagent and modified data acquisition scheme.* Proteomics, 2005. **5**(2): p. 380-387.
64. Schmidt, A., J. Kellermann, and F. Lottspeich, *A novel strategy for quantitative proteomics using isotope-coded protein labels.* Proteomics, 2005. **5**(1): p. 4-15.
65. Chakraborty, A. and F.E. Regnier, *Global internal standard technology for comparative proteomics.* Journal of Chromatography A, 2002. **949**(1-2): p. 173-184.
66. Hunt, T., et al., *Protein expression analysis and biomarker identification and quantification using multiplexed isobaric tagging technology - iTRAQ reagents.* Molecular & Cellular Proteomics, 2004. **3**(10): p. S286-S286.
67. Legrain, P. and L. Selig, *Genome-wide protein interaction maps using two-hybrid systems.* FEBS Letters, 2000. **480**(1): p. 32-36.
68. Schwikowski, B., P. Uetz, and S. Fields, *A network of protein-protein interactions in yeast.* Nature Biotechnology, 2000. **18**(12): p. 1257-1261.
69. Uetz, P., et al., *A comprehensive analysis of protein-protein interactions in Saccharomyces cerevisiae.* Nature, 2000. **403**(6770): p. 623-627.
70. Gavin, A.C., et al., *Functional organization of the yeast proteome by systematic analysis of protein complexes.* Nature, 2002. **415**(6868): p. 141-147.
71. Ho, Y., et al., *Systematic identification of protein complexes in Saccharomyces cerevisiae by mass spectrometry.* Nature, 2002. **415**(6868): p. 180-183.

72. Ashman, K., et al., *Cell signalling - the proteomics of it all.* Science"s STKE [electronic resource] : signal transduction knowledge environment, 2001. **2001**(103).
73. Com, E., et al., *Nerve growth factor receptor TrkA signaling in breast cancer cells involves Ku70 to prevent apoptosis.* Molecular and Cellular Proteomics, 2007. **6**(11): p. 1842-1854.
74. Gerstein, M., N. Lan, and R. Jansen, *Integrating interactomes.* Science, 2002. **295**(5553): p. 284-287.
75. Xenarios, I. and D. Eisenberg, *Protein interaction databases.* Current Opinion in Biotechnology, 2001. **12**(4): p. 334-339.
76. Mann, M. and O.N. Jensen, *Proteomic analysis of post-translational modifications.* Nature Biotechnology, 2003. **21**(3): p. 255-261.
77. Soskic, V., et al., *Functional proteomics analysis of signal transduction pathways of the platelet-derived growth factor Î² receptor.* Biochemistry, 1999. **38**(6): p. 1757-1764.
78. Pandey, A., et al., *Analysis of receptor signaling pathways by mass spectrometry: Identification of Vav-2 as a substrate of the epidermal and platelet-derived growth factor receptors.* Proceedings of the National Academy of Sciences of the United States of America, 2000. **97**(1): p. 179-184.
79. Peng, J., et al., *A proteomics approach to understanding protein ubiquitination.* Nature Biotechnology, 2003. **21**(8): p. 921-926.
80. Tauber, R. and W. Reutter, *Protein degradation in the plasma membrane of regenerating liver and Morris hepatomas.* European Journal of Biochemistry, 1978. **83**(1): p. 37-45.
81. Lesko, L., et al., *A rapid method for the isolation of rat liver plasma membranes using an aqueous two phase polymer system.* Biochimica et Biophysica Acta, 1973. **311**(2): p. 173-179.
82. Johansson, G., R. Gysin, and S.D. Flanagan, *Affinity partitioning of membranes. Evidence for discrete membrane domains containing cholinergic receptor.* Journal of Biological Chemistry, 1981. **256**(17): p. 9126-9135.
83. Persson, A., et al., *Purification of rat liver plasma membranes by wheat-germ-agglutinin affinity partitioning.* Biochemical Journal, 1991. **273**(1): p. 173-177.
84. Barinaga-Rementeria RamÃ-rez, I., P. Abedinpour, and B. Jergil, *Purification of caveolae by affinity two-phase partitioning using biotinylated antibodies and NeutrAvidin-dextran.* Analytical Biochemistry, 2004. **331**(1): p. 17-26.
85. Schindler, J., et al., *Proteomic analysis of brain plasma membranes isolated by affinity two-phase partitioning.* Molecular and Cellular Proteomics, 2006. **5**(2): p. 390-400.
86. Dancik, V., et al., *De novo peptide sequencing via tandem mass spectrometry.* Journal of Computational Biology, 1999. **6**(3-4): p. 327-342.
87. Dunn, W.B., *Current trends and future requirements for the mass spectrometric investigation of microbial, mammalian and plant metabolomes.* Physical Biology, 2008. **5**(1).
88. Oliver, S.G., et al., *Systematic functional analysis of the yeast genome.* Trends Biotechnol, 1998. **16**(9): p. 373-8.

89. Gohlke, R.S. and L.S. Wakeman, *Exploding-Film Sample Introduction for Mass-Spectrometry of Involatile or Thermally Labile Substances.* Analytical Chemistry, 1982. **54**(12): p. 2114-2115.
90. McFadden, W.H., *Liquid Chromatography-Mass Spectrometry Systems and Applications.* Journal of Chromatographic Science, 1980. **18**(3): p. 97-115.
91. Hu, Q.Z., et al., *The Orbitrap: a new mass spectrometer*. Journal of Mass Spectrometry, 2005. **40**(4): p. 430-443.
92. Vandergreef, J. and W.M.A. Niessen, *Hyphenated Methods in Mass-Spectrometry.* International Journal of Mass Spectrometry and Ion Processes, 1992. **118**: p. 857-873.
93. Nicholson, J.K., J.C. Lindon, and E. Holmes, *'Metabonomics': Understanding the metabolic responses of living systems to pathophysiological stimuli via multivariate statistical analysis of biological NMR spectroscopic data.* Xenobiotica, 1999. **29**(11): p. 1181-1189.
94. Nicholson, J.K., et al., *Metabonomics: A platform for studying drug toxicity and gene function.* Nature Reviews Drug Discovery, 2002. **1**(2): p. 153-161.
95. Brindle, J.T., et al., *Rapid and noninvasive diagnosis of the presence and severity of coronary heart disease using ¹H-NMR-based metabonomics.* Nature Medicine, 2002. **8**(12): p. 1439-1444.
96. Wilson, I.D., et al., *High resolution "ultra performance" liquid chromatography coupled to oa-TOF mass spectrometry as a tool for differential metabolic pathway profiling in functional genomic studies.* Journal of Proteome Research, 2005. **4**(2): p. 591-598.
97. Plumb, R., et al., *Metabonomic analysis of mouse urine by liquid-chromatography-time of flight mass spectrometry (LC-TOFMS): Detection of strain, diurnal and gender differences.* Analyst, 2003. **128**(7): p. 819-823.
98. Halket, J.M., et al., *Chemical derivatization and mass spectral libraries in metabolic profiling by GC/MS and LC/MS/MS.* Journal of Experimental Botany, 2005. **56**(410): p. 219-243.
99. Wang, F., *Biomarker methods in Drug Discovery and Development*. 2008: Springer.
100. Grob, R., *Modern Practice of Gas Chromatography*. Fourth ed. 2004, New York: Wiley.
101. Roessner, G.S.U., *Matabolome Analysis: An Introduction*. 2007: Wiley.
102. Halket, J.M. and V.G. Zaikin, *Derivatization in mass spectrometry - 1. Silylation.* European Journal of Mass Spectrometry, 2003. **9**(1): p. 1-21.
103. Wold, S., K. Esbensen, and P. Geladi, *Principal component analysis.* Chemometrics and Intelligent Laboratory Systems, 1987. **2**(1-3): p. 37-52.
104. Trygg, J. and S. Wold, *Orthogonal projections to latent structures (O-PLS).* Journal of Chemometrics, 2002. **16**(3): p. 119-128.
105. Trygg, J., E. Holmes, and T. Lundstedt, *Chemometrics in metabonomics.* Journal of Proteome Research, 2007. **6**(2): p. 469-479.
106. Lafaye, A., et al., *Profiling of sulfoconjugates in urine by using precursor ion and neutral loss scans in tandem mass spectrometry. Application to the investigation of heavy metal toxicity in rats.* Journal of Mass Spectrometry, 2004. **39**(6): p. 655-664.

107. Jemal, M., et al., *A strategy for metabolite identification using triple-quadrupole mass spectrometry with enhanced resolution and accurate mass capability.* Rapid Communications in Mass Spectrometry, 2003. **17**(24): p. 2732-2740.
108. Foltz, D.J., et al., *Narrow-bore sample trapping and chromatography combined with quadrupole/time-of-flight mass spectrometry for ultra-sensitive identification of in vivo and in vitro metabolites.* Journal of Chromatography B-Analytical Technologies in the Biomedical and Life Sciences, 2005. **825**(2): p. 144-151.
109. Mortishire-Smith, R.J., et al., *Use of Metabonomics to Identify Impaired Fatty Acid Metabolism as the Mechanism of a Drug-Induced Toxicity.* Chemical Research in Toxicology, 2004. **17**(2): p. 165-173.
110. Yang, C., et al., *Profiling of central metabolism in human cancer cells by two-dimensional NMR, GC-MS analysis, and isotopomer modeling.* Metabolomics, 2008. **4**(1): p. 13-29.
111. Vallejo, M., et al., *Plasma fingerprinting with GC-MS in acute coronary syndrome.* Analytical and Bioanalytical Chemistry, 2009. **394**(6): p. 1517-1524.
112. JK Nichlson, et. al. *The Handbook of Metabonomics and Metabolomics* 2007: Elsevier BV.
113. Widodo, et al., *Metabolic responses to salt stress of barley (Hordeum vulgare L.) cultivars, Sahara and Clipper, which differ in salinity tolerance.* Journal of Experimental Botany, 2009. **60**(14): p. 4089-4103.
114. Mullner, S., T. Neumann, and F. Lottspeich, *Proteomics - A new way for drug target discovery.* Arzneimittel-Forschung/Drug Research, 1998. **48**(1): p. 93-95.
115. Mosmann, T., *Rapid colorimetric assay for cellular growth and survival: application to proliferation and cytotoxicity assays.* J Immunol Methods, 1983. **65**(1-2): p. 55-63.
116. Sui, J.J., et al., *ITRAQ-coupled 2D LC-MS/MS analysis on protein profile in vascular smooth muscle cells incubated with S- and R-enantiomers of propranolol: Possible role of metabolic enzymes involved in cellular anabolism and antioxidant activity.* Journal of Proteome Research, 2007. **6**(5): p. 1643-1651.
117. Sui, J.J., et al., *Comparative proteomics analysis of vascular smooth muscle cells incubated with S- and R-enantiomers of Atenolol using iTRAQ-coupled two-dimensional LC-MS/MS.* Molecular & Cellular Proteomics, 2008. **7**(6): p. 1007-1018.
118. Maurer, B.J., et al., *Increase of ceramide and induction of mixed apoptosis necrosis by N-(4-hydroxyphenyl)-retinamide in neuroblastoma cell lines.* Journal of the National Cancer Institute, 1999. **91**(13): p. 1138-1146.
119. Zhang, J.H., et al., *Protein profile in neuroblastoma cells incubated with S- and R-enantiomers of ibuprofen by iTRAO-coupled 2-D LC-MS/MS analysis: Possible action of induced proteins on Alzheimer's disease.* Proteomics, 2008. **8**(8): p. 1595-1607.
120. Mainak, M., et al., *Development and validation of a gas chromatography/mass spectrometry method for the metabolic profiling of human colon tissue.* Rapid Communications in Mass Spectrometry, 2009. **23**(4): p. 487-494.
121. Atherton, H.J., et al., *A combined 1H-NMR spectroscopy- and mass spectrometry-based metabolomic study of the PPAR-alpha null mutant mouse defines profound*

systemic changes in metabolism linked to the metabolic syndrome. Physiological Genomics, 2006. **27**(2): p. 178-186.
122. Kimmel, S.E., *Warfarin therapy: in need of improvement after all these years.* Expert Opinion on Pharmacotherapy, 2008. **9**(5): p. 677-686.
123. Potter, M.A. and G. Luxton, *Transthyretin measurement as a screening tool for protein calorie malnutrition in emergency hospital admissions.* Clinical Chemistry and Laboratory Medicine, 2002. **40**(12): p. 1349-1354.
124. Purkey, H.E., M.I. Dorrell, and J.W. Kelly, *Evaluating the binding selectivity of transthyretin amyloid fibril inhibitors in blood plasma.* Proceedings of the National Academy of Sciences of the United States of America, 2001. **98**(10): p. 5566-5571.
125. Palha, J.A., *Transthyretin as a thyroid hormone carrier: Function revisited.* Clinical Chemistry and Laboratory Medicine, 2002. **40**(12): p. 1292-1300.
126. Buxbaum, J.N. and N. Reixach, *Transthyretin: the servant of many masters.* Cellular and Molecular Life Sciences, 2009. **66**(19): p. 3095-3101.
127. Sandanaraj, E., et al., *VKORC1 Diplotype-Derived Dosing Model to Explain Variability in Warfarin Dose Requirements in Asian Patients.* Drug Metabolism and Pharmacokinetics, 2009. **24**(4): p. 365-375.
128. Bartalena, L., et al., *Effects of interleukin-6 on the expression of thyroid hormone-binding protein genes in cultured human hepatoblastoma-derived (Hep G2) cells.* Molecular Endocrinology, 1992. **6**(6): p. 935-942.
129. Citarella, F., et al., *Interleukin-6 downregulates factor XII production by human hepatoma cell line (HepG2).* Blood, 1997. **90**(4): p. 1501-1507.
130. Kater, A.P., et al., *Dichotomal effect of the coumadin derivative warfarin on inflammatory signal transduction.* Clinical and Diagnostic Laboratory Immunology, 2002. **9**(6): p. 1396-1397.
131. Maclean, P.S., et al., *Anticoagulation with warfarin downregulates inflammation.* Journal of Thrombosis and Haemostasis, 2003. **1**(8): p. 1838-1839.
132. Kurohara, M.a.N., M, *Low-dose Warfarin Functions as an Immunomodulator to Prevent Cyclophosphamide-induced NOD Diabetes.* Kobe J. Med. Sci., 2008. **51**(1): p. E1-E13.
133. Bai, J., et al., *A comparative proteomic analysis of HepG2 cells incubated by S(-) and R(+) enantiomers of anti-coagulating drug warfarin.* Proteomics, 2010. **10**(7): p. 1463-1473.
134. Karala, A.R., et al., *Protein disulfide isomerases from C-elegans are equally efficient at thiol-disulfide exchange in simple peptide-based systems but show differences in reactivity towards protein substrates.* Antioxidants & Redox Signaling, 2007. **9**(11): p. 1815-1823.
135. Maattanen, P., et al., *ERp57 and PDI: multifunctional protein disulfide isomerases with similar domain architectures but differing substrate-partner associations.* Biochemistry and Cell Biology-Biochimie Et Biologie Cellulaire, 2006. **84**(6): p. 881-889.
136. Kozlov, G., et al., *Crystal structure of the bb ' domains of the protein disulfide isomerase ERp57.* Structure, 2006. **14**(8): p. 1331-1339.

137. Soute, B.A.M., et al., *Stimulation of the Dithiol-Dependent Reductases in the Vitamin-K Cycle by the Thioredoxin System - Strong Synergistic Effects with Protein Disulfide-Isomerase.* Biochemical Journal, 1992. **281**: p. 255-259.
138. Shendelman, S., et al., *DJ-1 is a redox-dependent molecular chaperone that inhibits alpha-synuclein aggregate formation.* Plos Biology, 2004. **2**(11): p. 1764-1773.
139. Lev, N., et al., *Oxidative insults induce DJ-1 upregulation and redistribution: Implications for neuroprotection.* Neurotoxicology, 2008. **29**(3): p. 397-405.
140. Margittai, E., et al., *Participation of Low Molecular Weight Electron Carriers in Oxidative Protein Folding.* International Journal of Molecular Sciences, 2009. **10**(3): p. 1346-1359.
141. Verrax, J., et al., *In Situ Modulation of Oxidative Stress: A Novel and Efficient Strategy to Kill Cancer Cells.* Current Medicinal Chemistry, 2009. **16**(15): p. 1821-1830.
142. Gong, X., *Quinone oxidoreductases and vitamin K metabolism.* Vitamins and Hormones, 2008. **78**: p. 85-101.
143. Clements, C.M., et al., *DJ-1, a cancer- and Parkinson's disease-associated protein, stabilizes the antioxidant transcriptional master regulator Nrf2.* Proceedings of the National Academy of Sciences of the United States of America, 2006. **103**(41): p. 15091-15096.
144. Medina, A., et al., *The role of stratifin in fibroblast-keratinocyte interaction.* Molecular and Cellular Biochemistry, 2007. **305**(1-2): p. 255-264.
145. Yan, Y., V.M. Weaver, and I.A. Blair, *Analysis of protein expression during oxidative stress in breast epithelial cells using a stable isotope labeled proteome internal standard.* Journal of Proteome Research, 2005. **4**(6): p. 2007-2014.
146. Atoda, H., E. Yokota, and T. Morita, *Characterization of a monoclonal antibody B1 that recognizes phosphorylated Ser-158 in the activation peptide region of human coagulation factor IX.* Journal of Biological Chemistry, 2006. **281**(14): p. 9314-9320.
147. Wilker, E.W., et al., *A structural basis for 14-3-3 sigma functional specificity.* Journal of Biological Chemistry, 2005. **280**(19): p. 18891-18898.
148. McAleer, S.D., et al., *Steady-state clearance rates of warfarin and its enantiomers in therapeutically dosed patients.* Chirality, 1997. **9**(1): p. 13-16.
149. Flahaut, C., et al., *Disulphide bonds assignment in the inter-alpha-inhibitor heavy chains - Structural and functional implications.* European Journal of Biochemistry, 1998. **255**(1): p. 107-115.
150. Nishimura, H., et al., *Cdna and Deduced Amino-Acid-Sequence of Human Pk-120, a Plasma Kallikrein-Sensitive Glycoprotein.* Febs Letters, 1995. **357**(2): p. 207-211.
151. Ishizaki, T., et al., *Inter-Alpha-Trypsin Inhibitor - as a Probable Component Pertaining to Disseminated Intravascular Coagulation (Dic).* Acta Haematologica Japonica, 1980. **43**(3): p. 587-592.
152. Chen, K.T., H.J. Lin, and W.J. Lee, *Severe disseminated intravascular coagulation caused by congestive heart failure and left ventricular thrombus.* European Journal of Emergency Medicine, 2007. **14**(2): p. 87-89.

153. Cvirn, G., S. Gallistl, and W. Muntean, *Effects of alpha(2)-macroglobulin and antithrombin on thrombin generation and inhibition in cord and adult plasma.* Thrombosis Research, 2001. **101**(3): p. 183-191.
154. Price, P.A., et al., *Discovery of a high molecular weight complex of calcium, phosphate, fetuin, and matrix gamma-carboxyglutamic acid protein in the serum of etidronate-treated rats.* Journal of Biological Chemistry, 2002. **277**(6): p. 3926-3934.
155. Wajih, N. and R. Wallin, *Identification of alpha 2-HS glycoprotein as a human serum carrier of matrix Gla protein (MGP) and evidence for vitamin K4 as a modulator of gene expression in proliferating vascular smooth muscle cells.* Faseb Journal, 2006. **20**(4): p. A134-A134.
156. Wajih, N., et al., *Processing and transport of matrix gamma-carboxyglutamic acid protein and bone morphogenetic protein-2 in cultured human vascular smooth muscle cells - Evidence for an uptake mechanism for serum fetuin.* Journal of Biological Chemistry, 2004. **279**(41): p. 43052-43060.
157. Price, P.A., S.A. Faus, and M.K. Williamson, *Warfarin-induced artery calcification is accelerated by growth and vitamin D.* Arteriosclerosis Thrombosis and Vascular Biology, 2000. **20**(2): p. 317-327.
158. Danziger, J., *Vitamin K-dependent proteins, warfarin, and vascular calcification.* Clinical Journal of the American Society of Nephrology, 2008. **3**(5): p. 1504-1510.
159. Price, P.A., S.A. Faus, and M.K. Williamson, *Warfarin causes rapid calcification of the elastic lamellae in rat arteries and heart valves.* Arteriosclerosis Thrombosis and Vascular Biology, 1998. **18**(9): p. 1400-1407.
160. Duriez, P. and J.C. Fruchart, *High-density lipoprotein subclasses and apolipoprotein A-I.* Clinica Chimica Acta, 1999. **286**(1-2): p. 97-114.
161. Miller, G., *Lipoproteins and thrombosis: effects of lipid lowering.* Current Opinion in Lipidology, 1995. **6**: p. 38-42.
162. Daviss, B., *Growing pains for metabolomics.* Scientist, 2005. **19**(8): p. 25-28.
163. Lake, B.G. and P. Grasso, *Comparison of the hepatotoxicity of coumarin in the rat, mouse, and Syrian hamster: A dose and time response study.* Fundamental and Applied Toxicology, 1996. **34**(1): p. 105-117.
164. Orlowski, M. and A. Meister, *The gamma-glutamyl cycle: a possible transport system for amino acids.* Proceedings of the National Academy of Sciences of the United States of America, 1970. **67**(3): p. 1248-1255.
165. Meister, A., *The Î³ glutamyl cycle. Diseases associated with specific enzyme deficiencies.* Annals of Internal Medicine, 1974. **81**(2): p. 247-253.
166. Cain, D., S.M. Hutson, and R. Wallin, *Assembly of the warfarin-sensitive vitamin K 2,3-epoxide reductase enzyme complex in the endoplasmic reticulum membrane.* Journal of Biological Chemistry, 1997. **272**(46): p. 29068-29075.
167. Kevresan, S., et al., *Biosynthesis of bile acids in mammalian liver.* European Journal of Drug Metabolism and Pharmacokinetics, 2006. **31**(3): p. 145-156.
168. Hollander, D. and E. Rim, *Vitamin K2 absorption by rat everted small intestinal sacs.* American Journal of Physiology, 1976. **231**(2): p. 415-419.
169. Ritter, J.K., *Roles of glucuronidation and UDP-glucuronosyltransferases in xenobiotic bioactivation reactions.* Chemico-Biological Interactions, 2000. **129**(1-2): p. 171-193.

170. Jansing, R.L., E.S. Chao, and L.S. Kaminsky, *Phase II metabolism of warfarin in primary culture of adult rat hepatocytes.* Molecular Pharmacology, 1992. **41**(1): p. 209-215.
171. Miller, G.P., et al., *Assessing cytochrome P450 and UDP-glucuronosyltransferase contributions to warfarin metabolism in humans.* Chemical Research in Toxicology, 2009. **22**(7): p. 1239-1245.
172. Baynes, J.W.M.H.D., *Medical Biochemistry* 2nd ed. 2005: Elsevier.
173. Kaur-Knudsen, D., S.E. Bojesen, and B.G. Nordestgaard, *Common polymorphisms in CYP2C9, subclinical atherosclerosis and risk of ischemic vascular disease in 52000 individuals.* Pharmacogenomics Journal, 2009. **9**(5): p. 327-332.
174. Catella, F., et al., *11-Dehydrothromboxane B2: A quantitative index of thromboxane A2 formation in the human circulation.* Proceedings of the National Academy of Sciences of the United States of America, 1986. **83**(16): p. 5861-5865.
175. Al Mondhiry, H., J.O. Ballard, and V. McGarvey, *Fibrinogen interaction with human platelets: Effect of other coagulation factors, prostaglandins and platelet inhibitors.* Thrombosis Research, 1983. **31**(3): p. 415-426.

Appendix

Part 5

List of 95% peptides, charged state and protein functions

Table 1(without vitamin K)

Accession No.& Name	Seq. of 95% peptides	Peptide Charged State	Functions
Metabolism			
P00338 L-lactate dehydrogenase A chain	LKGEMMDLQHGSLFLR	4	Catalyzes (S)-lactate + NAD+ =
	LVIITAGAR	2	pyruvate + NADH.
	TLHPDLGTDKDKEQWK	5	
	VIGSGCNLDSAR	2	
P15121 Aldose reductase	VAIDVGYR	3	Catalyzes the NADPH-dependent reduction of a wide variety of
	NLVVIPK	3	carbonyl-containing compounds.
	MPILGLGTWK	3	
	REELFIVSK	3	
	VCALLSCTSHK	3	
Q14697 Neutral alpha-glucosidase AB	GLLEFEHQR	3	Cleaves sequentially the 2 innermost alpha-1,3-linked glucose
	WLLGAGKPAAVVLQTK	2	residues from the Glc2Man9GlcNAc2 oligosaccharide precursor
	HHGPQTLYLPVTLSSIPVFQR	4	of immature glycoprotein.

	LSFQHDPETSVLVLR	3	
	LVAIVDPHIK	3	
Biosynthesis			
P31327 Carbamoyl-phosphate synthase	AFAISGPFNVQFLVK	3	Involved in the urea cycle of ureotelic animals where the enzyme plays an important role in removing excess ammonia from the cell
	FLGVAEQLHNEGFK	4	
	AQTAHIVLEDGTK	3	
	FVHDNYVIR	3	
	GAEVHLVPWNHDFTK	4	
	GILIGIQQSFRPR	3	
	HLPTLDHPIIPADYVAIK	5	
	IALGIPLPEIK	3	
	KEPLFGISTGNLITGLAAGAK	4	
	MCHPSIEGFTPR	3	
	SIFSAVLDELK	3	
	TLGVDFIDVATK	3	
	VSGLLVLDYSK	3	
	VSQEHPVVLTK	3	
P09651 Heterogeneous nuclear ribonucleoprotein A1	GFGFVTYATUEEVDAAMNAR	3	Involved in the packaging of pre-mRNA into hnRNP particles.
	YHTVNGHNCEVR	4	
	SSGPYGGGGQYFAKPR	4	
	KIFVGGIK	3	
	KIFVGGIKEDTEEHHLR	5	
	IFVGGIKEDTEEHHLR	5	

P62277 40S ribosomal protein S13	GLAPDLPEDLYHLIK	4	Translational elongation
	KGLTPSQIGVILR	4	
P39023 60S ribosomal protein L3	VACIGAWHPAR	3	Translational elongation
	IGQGYLIK	2	
Stress & Defense			
Q99497 Protein DJ-1	GLIAAICAGPTALLAHEIGFGSK	4	Function as a redox-sensitive chaperone and as a sensor for oxidative stress.
	VTVAGLAGK	2	
Signal Transduction			
P31947 14-3-3 protein σ	EKVETELQGVCDTVLGLLDSHLIK	5	Adapter protein implicated in the regulation of a large spectrum of signaling pathway.
	VLSSIEQK	3	
	NLLSVAYK	2	
Q01105 Protein SET	EFHLNESGDDSSKIDNFWVTTFVNHPQVSALLG EED	4	Multitasking protein, involved in apoptosis, transcription, nucleosome assembly
	EEALHYLTR	2	and histone binding.
P49773 Histidine triad nucleotide-binding protein 1	AQVARPGGDTIFGK	3	Hydrolyzes adenosine 5'- mono-phosphoramidate substrates.
	CLAFHDISPQAPTHFLVIPK	4	
P09382 Galectin-1	DSNNLCLHFNPR	3	May regulate apoptosis, cell proliferation and cell differentiation.
	AADGDFK	2	

Table 2 (with vitamin K)

Accession No.& Name	Seq. of 95% peptides	Peptide Charged State	Functions
Metabolism			
P15121 Aldose reductase	VAIDUGYR	2	Catalyzes the NADPH-dependent reduction of a wide variety of carbonyl
	NLVVIPK	2	-containing compounds
	LWCTYHEK	3	
	MPILGLGTWK	3	
	REELFIVSK	3	
P25705 ATP synthase subunit α	FENAFLSHVVSQHQALLGTIR	4	Mitochondrial membrane ATP synthase.
	VLSIGDGJAR	2	
P06744 Glucose-6-phosphate isomerase	NLVTEDVMR	2	Glycolytic enzyme.
	VDHQTGPIVWGEPGTNGQHAFYQLIHQGTK	5	
P14618 Pyruvate kinase isozymes M1/M2	AGKPVICATQMLESMIK	4	Glycolytic enzyme that catalyzes the transfer of phosphoryl group from
	GDLGIEIPAEK	2	phosphoenolpyruvate (PEP) to ADP, generating ATP.
	GADFLVTEVENGGSLGSK	3	
	GVNLPGAAVDLPAVSEK	3	
	LDIDSPDITAR	2	
	PVAVALDTK	2	
	TATESFASDPILYR	3	
P29401 Transketolase	IIALDGDTK	2	Sedoheptulose7phosphate +D-glyceraldehyde3-phosphate = D-ribose

	ILATPPQEDAPSVDIANIR	3	5-phosphate+D-xylulose 5-phosphate.
	ISSDLDGHPVPK	3	
	SVPTSTVFYPSDGVATEK	3	
P04075 Fructose-bisphosphate aldolase A	ADDGRPFPQVIK	3	D-fructose1,6 bisphosphate = glycerone phosphate+D glyceraldehyde
	GILAADESTGSIAK	3	3 phosphate.
Structural			
O75369 Filamin-B	LKPGAPLKPK	4	Connects cell membrane constituents to the actin cytoskeleton.
	HIPGSPFTAK	3	
P23528 Cofilin-1	KEDLVFIFWAPESAPLK	4	Controls reversibly actin polymerization and depolymerization in a pH-
	MLPDKDCR	2	sensitive manner.
	EILVGDVGQTVDDPYATFVK	4	
	NIILEEGK	2	
P57053 Histone H2B	AMGIMNSFVNDIFER	3	Core nucleosome component.
	ESYSVYVYK	2	
	KESYSVYVYK	4	
	LLLPGELAK	2	
	PHYNKRSTITSR	3	
O43707 Alpha-actinin-4	DGLAFNALIHR	3	F-actin cross - linking protein which is thought to anchor actin to a variety
	EAILAIHK	3	of intracellular structures.
Biosynthesis			
P30101 Protein disulfide-isomerase A3	EATNPPVIQEEKPK	4	Catalyzes the synthesis and rearrangement of -S-S- bonds in proteins.
	TADGIVSHLK	3	
P15559 NAD(P)H dehydrogenase[Quinone]	ALIVLAHSER	3	A quinone reductase in connection with conjugation reactions of

	VLAHSER	2	hydroquinones involved in biosynthetic processes.
P22087 rRNA 2'-O-methyltransferase fibrillarin	DHAVVVGVYRPPPK	4	Involved in pre-rRNA processing.
	AWNPFR	2	
P05387 60S acidic ribosomal protein P2	NIEDVIAQGIGK	3	Plays an important role in the elongation step of protein synthesis.
	LASVPAGGAVAVSAAPGSAAPAAGSAPAAAEEK	4	
	ILDSVGIEADDDR	3	
Stress & Defense			
P01857 Ig gamma-1 chain C region	GPSVFPLAPSSK	3	Immune response
	ALPAPIEK	2	
P50454 Serpin H1	HLAGLGLTEAIDK	3	Stress Response.Involved as a chaperone in the biosynthetic pathway
	LSSLIILMPHHVEPLER	4	of collagen.
	LFYADHPFIFLVR	3	
Q99497 Protein DJ-1	GLIAAICAGPTALLAHEIGFGSK	4	Function as a redox-sensitive chaperone and as a sensor for oxidative stress.
_	VTVAGLAGK	2	
Signal Transduction			
P31947 14-3-3 Protein σ	EKVETELQGVCDTVLGLLDSHLIK	5	Adapter protein implicated in the regulation of a large spectrum of
_	VLSSIEQK	2	signaling pathway.
_	SAYQEAMDISK	3	
_	DSTLIMQLLR	2	
_	NLLSVAYK	2	
Q01105 Protein SET	EFHLNESGDDSSKIDNFWVTTFVNHPQVSALLGEED	4	Involved in apoptosis, transcription,nucleosome assembly and
	EEALHYLTR	2	histone binding.

P23246 Splicing factor, proline- and glutamine-rich	FATHAAALSVR	3	DNA- and RNA binding protein, involved in several nuclear processes.
	EQVEKNMK	2	
	LFVGNLPADITEDEFK	3	
P27797 Calreticulin	CKDDEFTHLYTLIVRPDNTYEVK	5	Molecular calcium binding, chaperone promoting folding, oligomeric
	FYGDEEKDK	3	assembly in the ER via calreticulin/ calnexin cycle.
P10599 Thioredoxin	MIKPFFHSLSEK	4	Catalyzes dithiol-disulfide exchange reactions.
	TAFQEALDAAGDK	3	
P26599 Polypyrimidine tract-binding protein 1	IIVENLFYPVTLDVLHQIFSK	4	Promote the binding of U2 snRNP to pre-mRNA.
	VKILFNK	2	
	KLPIDVTEGEVISLGLPFGK	4	
	NNQFQALLQYADPVSAQHAK	4	
	GQPIYIQFSNHK	4	
	SVPNVHGALAPLAIPSAAAAAAAAGR	4	
Transport			
P99999 Cytochrome c	TGPNLHGLFGR	3	Electron carrier protein.
	GDVEK	2	
P14625 Endoplasmin	GVVDSDDLPLNVSR	2	Molecular chaperone that functions in the processing and transport of
	NLLHVTDTGVGMTR	3	secreted proteins.
	ELISNASDALDK	3	

List of 597 proteins identified in the set without vitamin K

	Accession #	Name
1	sp|P08238|HS90B_HUMAN	Heat shock protein HSP 90-beta
2	sp|P14618|KPYM_HUMAN	Pyruvate kinase isozymes M1/M2
3	sp|P31327|CPSM_HUMAN	Carbamoyl-phosphate synthase [ammonia], mitochondrial
4	sp|P02768|ALBU_HUMAN	Serum albumin
5	sp|P07437|TBB5_HUMAN	Tubulin beta chain
6	sp|P10809|CH60_HUMAN	60 kDa heat shock protein, mitochondrial
7	sp|O43707|ACTN4_HUMAN	Alpha-actinin-4
8	sp|P63261|ACTG_HUMAN	Actin, cytoplasmic 2
9	sp|O75369|FLNB_HUMAN	Filamin-B
10	sp|P06733|ENOA_HUMAN	Alpha-enolase
11	sp|P11142|HSP7C_HUMAN	Heat shock cognate 71 kDa protein
12	sp|P04406|G3P_HUMAN	Glyceraldehyde-3-phosphate dehydrogenase
13	sp|P68363|TBA1B_HUMAN	Tubulin alpha-1B chain
14	sp|P00338|LDHA_HUMAN	L-lactate dehydrogenase A chain
15	sp|P49327|FAS_HUMAN	Fatty acid synthase
16	sp|P68104|EF1A1_HUMAN	Elongation factor 1-alpha 1
17	sp|P00558|PGK1_HUMAN	Phosphoglycerate kinase 1
18	sp|P13639|EF2_HUMAN	Elongation factor 2
19	sp|P08107|HSP71_HUMAN	Heat shock 70 kDa protein 1
20	sp|Q00610|CLH1_HUMAN	Clathrin heavy chain 1
21	sp|P04075|ALDOA_HUMAN	Fructose-bisphosphate aldolase A
22	sp|P05787|K2C8_HUMAN	Keratin, type II cytoskeletal 8
23	sp|P05783|K1C18_HUMAN	Keratin, type I cytoskeletal 18
24	sp|P60174|TPIS_HUMAN	Triosephosphate isomerase
25	sp|P21333|FLNA_HUMAN	Filamin-A
26	sp|P06744|G6PI_HUMAN	Glucose-6-phosphate isomerase
27	sp|P07237|PDIA1_HUMAN	Protein disulfide-isomerase

List of 565 proteins identified in the set with vitamin K

	Accession #	Name
1	sp|P02768|ALBU_HUMAN	Serum albumin
2	sp|P08238|HS90B_HUMAN	Heat shock protein HSP 90-beta
3	sp|P10809|CH60_HUMAN	60 kDa heat shock protein, mitochondrial
4	sp|P14618|KPYM_HUMAN	Pyruvate kinase isozymes M1/M2
5	sp|P06733|ENOA_HUMAN	Alpha-enolase
6	sp|P31327|CPSM_HUMAN	Carbamoyl-phosphate synthase [ammonia], mitochondrial
7	sp|P07437|TBB5_HUMAN	Tubulin beta chain
8	sp|P13639|EF2_HUMAN	Elongation factor 2
9	sp|O75369|FLNB_HUMAN	Filamin-B
10	sp|P11142|HSP7C_HUMAN	Heat shock cognate 71 kDa protein
11	sp|O43707|ACTN4_HUMAN	Alpha-actinin-4
12	sp|P04406|G3P_HUMAN	Glyceraldehyde-3-phosphate dehydrogenase
13	sp|P68363|TBA1B_HUMAN	Tubulin alpha-1B chain
14	sp|P63261|ACTG_HUMAN	Actin, cytoplasmic 2
15	sp|P00558|PGK1_HUMAN	Phosphoglycerate kinase 1
16	sp|P68104|EF1A1_HUMAN	Elongation factor 1-alpha 1
17	sp|P00338|LDHA_HUMAN	L-lactate dehydrogenase A chain
18	sp|P05787|K2C8_HUMAN	Keratin, type II cytoskeletal 8
19	sp|P05783|K1C18_HUMAN	Keratin, type I cytoskeletal 18
20	sp|P60174|TPIS_HUMAN	Triosephosphate isomerase
21	sp|P08107|HSP71_HUMAN	Heat shock 70 kDa protein 1
22	sp|P04075|ALDOA_HUMAN	Fructose-bisphosphate aldolase A
23	sp|P15121|ALDR_HUMAN	Aldose reductase
24	sp|P26641|EF1G_HUMAN	Elongation factor 1-gamma
25	sp|P07900|HS90A_HUMAN	Heat shock protein HSP 90-alpha
26	sp|P08670|VIME_HUMAN	Vimentin
27	sp|P49327|FAS_HUMAN	Fatty acid synthase

28	sp|P29401|TKT_HUMAN	Transketolase
29	sp|P61978|HNRPK_HUMAN	Heterogeneous nuclear ribonucleoprotein K
30	sp|P08670|VIME_HUMAN	Vimentin
31	sp|P23921|RIR1_HUMAN	Ribonucleoside-diphosphate reductase large subunit
32	sp|P55072|TERA_HUMAN	Transitional endoplasmic reticulum ATPase
33	sp|P07900|HS90A_HUMAN	Heat shock protein HSP 90-alpha
34	sp|P02545|LMNA_HUMAN	Lamin-A/C
35	sp|P06576|ATPB_HUMAN	ATP synthase subunit beta, mitochondrial
36	sp|P15121|ALDR_HUMAN	Aldose reductase
37	sp|P36578|RL4_HUMAN	60S ribosomal protein L4
38	sp|P30041|PRDX6_HUMAN	Peroxiredoxin-6
39	sp|P53396|ACLY_HUMAN	ATP-citrate synthase
40	sp|P35579|MYH9_HUMAN	Myosin-9
41	sp|Q09666|AHNK_HUMAN	Neuroblast differentiation-associated protein AHNAK
42	sp|P22392|NDKB_HUMAN	Nucleoside diphosphate kinase B
43	sp|P26641|EF1G_HUMAN	Elongation factor 1-gamma
44	sp|P07195|LDHB_HUMAN	L-lactate dehydrogenase B chain
45	sp|P09651|ROA1_HUMAN	Heterogeneous nuclear ribonucleoprotein A1
46	sp|P07355|ANXA2_HUMAN	Annexin A2
47	sp|Q08211|DHX9_HUMAN	ATP-dependent RNA helicase A
48	sp|Q13813|SPTA2_HUMAN	Spectrin alpha chain, brain
49	sp|P13797|PLST_HUMAN	Plastin-3
50	sp|P11021|GRP78_HUMAN	78 kDa glucose-regulated protein
51	sp|Q9BTM1|H2AJ_HUMAN	Histone H2A.J
52	sp|Q12906|ILF3_HUMAN	Interleukin enhancer-binding factor 3
53	sp|P27797|CALR_HUMAN	Calreticulin
54	sp|Q06830|PRDX1_HUMAN	Peroxiredoxin-1
55	sp|P38646|GRP75_HUMAN	Stress-70 protein, mitochondrial

28	sp|Q00610|CLH1_HUMAN	Clathrin heavy chain 1
29	sp|P23921|RIR1_HUMAN	Ribonucleoside-diphosphate reductase large subunit
30	sp|P07237|PDIA1_HUMAN	Protein disulfide-isomerase
31	sp|P08729|K2C7_HUMAN	Keratin, type II cytoskeletal 7
32	sp|Q13813|SPTA2_HUMAN	Spectrin alpha chain, brain
33	sp|P30041|PRDX6_HUMAN	Peroxiredoxin-6
34	sp|P29401|TKT_HUMAN	Transketolase
35	sp|Q09666|AHNK_HUMAN	Neuroblast differentiation-associated protein AHNAK
36	sp|P35579|MYH9_HUMAN	Myosin-9
37	sp|P31947|1433S_HUMAN	14-3-3 protein sigma
38	sp|P21333|FLNA_HUMAN	Filamin-A
39	sp|P07355|ANXA2_HUMAN	Annexin A2
40	sp|P07195|LDHB_HUMAN	L-lactate dehydrogenase B chain
41	sp|Q06830|PRDX1_HUMAN	Peroxiredoxin-1
42	sp|P62937|PPIA_HUMAN	Peptidyl-prolyl cis-trans isomerase A
43	sp|P61978|HNRPK_HUMAN	Heterogeneous nuclear ribonucleoprotein K
44	sp|P06744|G6PI_HUMAN	Glucose-6-phosphate isomerase
45	sp|Q08211|DHX9_HUMAN	ATP-dependent RNA helicase A
46	sp|P13797|PLST_HUMAN	Plastin-3
47	sp|P09651|ROA1_HUMAN	Heterogeneous nuclear ribonucleoprotein A1
48	sp|Q13200|PSMD2_HUMAN	26S proteasome non-ATPase regulatory subunit 2
49	sp|P27797|CALR_HUMAN	Calreticulin
50	sp|P27824|CALX_HUMAN	Calnexin
51	sp|P02545|LMNA_HUMAN	Lamin-A/C
52	sp|P30101|PDIA3_HUMAN	Protein disulfide-isomerase A3
53	sp|P07737|PROF1_HUMAN	Profilin-1
54	sp|P36578|RL4_HUMAN	60S ribosomal protein L4
55	sp|P63241|IF5A1_HUMAN	Eukaryotic translation initiation factor 5A-1

56	sp|Q01105|SET_HUMAN	Protein SET
57	sp|P07737|PROF1_HUMAN	Profilin-1
58	sp|P22314|UBA1_HUMAN	Ubiquitin-like modifier-activating enzyme 1
59	sp|P62937|PPIA_HUMAN	Peptidyl-prolyl cis-trans isomerase A
60	sp|P27824|CALX_HUMAN	Calnexin
61	sp|P50454|SERPH_HUMAN	Serpin H1
62	sp|P48643|TCPE_HUMAN	T-complex protein 1 subunit epsilon
63	sp|P07954|FUMH_HUMAN	Fumarate hydratase, mitochondrial
64	sp|P26599|PTBP1_HUMAN	Polypyrimidine tract-binding protein 1
65	sp|Q15149|PLEC1_HUMAN	Plectin-1
66	sp|P14625|ENPL_HUMAN	Endoplasmin
67	sp|P08729|K2C7_HUMAN	Keratin, type II cytoskeletal 7
68	sp|Q13200|PSMD2_HUMAN	26S proteasome non-ATPase regulatory subunit 2
69	sp|Q99880|H2B1L_HUMAN	Histone H2B type 1-L
70	sp|P15880|RS2_HUMAN	40S ribosomal protein S2
71	sp|P08195|4F2_HUMAN	4F2 cell-surface antigen heavy chain
72	sp|P06748|NPM_HUMAN	Nucleophosmin
73	sp|P31947|1433S_HUMAN	14-3-3 protein sigma
74	sp|P63241|IF5A1_HUMAN	Eukaryotic translation initiation factor 5A-1
75	sp|P23528|COF1_HUMAN	Cofilin-1
76	sp|P62988|UBIQ_HUMAN	Ubiquitin
77	sp|P50395|GDIB_HUMAN	Rab GDP dissociation inhibitor beta
78	sp|Q9UQ80|PA2G4_HUMAN	Proliferation-associated protein 2G4
79	sp|P60842|IF4A1_HUMAN	Eukaryotic initiation factor 4A-I
80	sp|Q00839|HNRPU_HUMAN	Heterogeneous nuclear ribonucleoprotein U
81	sp|P22626|ROA2_HUMAN	Heterogeneous nuclear ribonucleoproteins A2/B1
82	sp|P18669|PGAM1_HUMAN	Phosphoglycerate mutase 1
83	sp|P39023|RL3_HUMAN	60S ribosomal protein L3

56	sp|P60842|IF4A1_HUMAN	Eukaryotic initiation factor 4A-I
57	sp|P06576|ATPB_HUMAN	ATP synthase subunit beta, mitochondrial
58	sp|P12814|ACTN1_HUMAN	Alpha-actinin-1
59	sp|P53396|ACLY_HUMAN	ATP-citrate synthase
60	sp|P50395|GDIB_HUMAN	Rab GDP dissociation inhibitor beta
61	sp|P16104|H2AX_HUMAN	Histone H2A
62	sp|Q01105|SET_HUMAN	Protein SET
63	sp|P37802|TAGL2_HUMAN	Transgelin-2
64	sp|P14625|ENPL_HUMAN	Endoplasmin
65	sp|P15531|NDKA_HUMAN	Nucleoside diphosphate kinase A
66	sp|Q9UQ80|PA2G4_HUMAN	Proliferation-associated protein 2G4
67	sp|P50454|SERPH_HUMAN	Serpin H1
68	sp|P23528|COF1_HUMAN	Cofilin-1
69	sp|O00299|CLIC1_HUMAN	Chloride intracellular channel protein 1
70	sp|P08195|4F2_HUMAN	4F2 cell-surface antigen heavy chain
71	sp|P06748|NPM_HUMAN	Nucleophosmin
72	sp|P78371|TCPB_HUMAN	T-complex protein 1 subunit beta
73	sp|P00505|AATM_HUMAN	Aspartate aminotransferase, mitochondrial
74	sp|P46940|IQGA1_HUMAN	Ras GTPase-activating-like protein IQGAP1
75	sp|Q14974|IMB1_HUMAN	Importin subunit beta-1
76	sp|P48643|TCPE_HUMAN	T-complex protein 1 subunit epsilon
77	sp|Q12906|ILF3_HUMAN	Interleukin enhancer-binding factor 3
78	sp|Q16719|KYNU_HUMAN	Kynureninase
79	sp|P55072|TERA_HUMAN	Transitional endoplasmic reticulum ATPase
80	sp|P04083|ANXA1_HUMAN	Annexin A1
81	sp|P57053|H2BFS_HUMAN	Histone H2B type F-S
82	sp|Q16576|RBBP7_HUMAN	Histone-binding protein RBBP7
83	sp|P22626|ROA2_HUMAN	Heterogeneous nuclear ribonucleoproteins A2/B1

84	sp|P62826|RAN_HUMAN	GTP-binding nuclear protein Ran
85	sp|P46940|IQGA1_HUMAN	Ras GTPase-activating-like protein IQGAP1
86	sp|P05187|PPB1_HUMAN	Alkaline phosphatase, placental type
87	sp|Q14697|GANAB_HUMAN	Neutral alpha-glucosidase AB
88	sp|P42224|STAT1_HUMAN	Signal transducer and activator of transcription 1-alpha/beta
89	sp|P49588|SYAC_HUMAN	Alanyl-tRNA synthetase, cytoplasmic
90	sp|O60664|M6PBP_HUMAN	Mannose-6-phosphate receptor-binding protein 1
91	sp|P37802|TAGL2_HUMAN	Transgelin-2
92	sp|Q02878|RL6_HUMAN	60S ribosomal protein L6
93	sp|P02786|TFR1_HUMAN	Transferrin receptor protein 1
94	sp|Q04695|K1C17_HUMAN	Keratin, type I cytoskeletal 17
95	sp|Q13283|G3BP1_HUMAN	Ras GTPase-activating protein-binding protein 1
96	sp|P05141|ADT2_HUMAN	ADP/ATP translocase 2
97	sp|P08865|RSSA_HUMAN	40S ribosomal protein SA
98	sp|P62158|CALM_HUMAN	Calmodulin
99	sp|P63244|GBLP_HUMAN	Guanine nucleotide-binding protein subunit beta-2-like 1
100	sp|Q15181|IPYR_HUMAN	Inorganic pyrophosphatase
101	sp|P55209|NP1L1_HUMAN	Nucleosome assembly protein 1-like 1
102	sp|P30101|PDIA3_HUMAN	Protein disulfide-isomerase A3
103	sp|P12814|ACTN1_HUMAN	Alpha-actinin-1
104	sp|P30153|2AAA_HUMAN	Serine/threonine-protein phosphatase 2A 65 kDa regulatory subunit A alpha isoform
105	sp|Q13501|SQSTM_HUMAN	Sequestosome-1
106	sp|P23246|SFPQ_HUMAN	Splicing factor, proline- and glutamine-rich
107	sp|Q16576|RBBP7_HUMAN	Histone-binding protein RBBP7
108	sp|Q15365|PCBP1_HUMAN	Poly(rC)-binding protein 1
109	sp|P62701|RS4X_HUMAN	40S ribosomal protein S4, X isoform

84	sp|Q9Y490|TLN1_HUMAN	Talin-1
85	sp|P61313|RL15_HUMAN	60S ribosomal protein L15
86	sp|P62826|RAN_HUMAN	GTP-binding nuclear protein Ran
87	sp|P14324|FPPS_HUMAN	Farnesyl pyrophosphate synthetase
88	sp|P05141|ADT2_HUMAN	ADP/ATP translocase 2
89	sp|P49588|SYAC_HUMAN	Alanyl-tRNA synthetase, cytoplasmic
90	sp|P15880|RS2_HUMAN	40S ribosomal protein S2
91	sp|Q13283|G3BP1_HUMAN	Ras GTPase-activating protein-binding protein 1
92	sp|P39023|RL3_HUMAN	60S ribosomal protein L3
93	sp|P19338|NUCL_HUMAN	Nucleolin
94	sp|P25705|ATPA_HUMAN	ATP synthase subunit alpha, mitochondrial
95	sp|P22314|UBA1_HUMAN	Ubiquitin-like modifier-activating enzyme 1
96	sp|P02647|APOA1_HUMAN	Apolipoprotein A-I
97	sp|Q13838|UAP56_HUMAN	Spliceosome RNA helicase BAT1
98	sp|P62701|RS4X_HUMAN	40S ribosomal protein S4, X isoform
99	sp|P12268|IMDH2_HUMAN	Inosine-5'-monophosphate dehydrogenase 2
100	sp|P80723|BASP_HUMAN	Brain acid soluble protein 1
101	sp|P00441|SODC_HUMAN	Superoxide dismutase [Cu-Zn]
102	sp|P35241|RADI_HUMAN	Radixin
103	sp|P07954|FUMH_HUMAN	Fumarate hydratase, mitochondrial
104	sp|Q14697|GANAB_HUMAN	Neutral alpha-glucosidase AB
105	sp|P38646|GRP75_HUMAN	Stress-70 protein, mitochondrial
106	sp|Q9Y266|NUDC_HUMAN	Nuclear migration protein nudC
107	sp|P11021|GRP78_HUMAN	78 kDa glucose-regulated protein
108	sp|Q00839|HNRPU_HUMAN	Heterogeneous nuclear ribonucleoprotein U
109	sp|P02786|TFR1_HUMAN	Transferrin receptor protein 1

110	sp|Q29718|1B82_HUMAN	HLA class I histocompatibility antigen, B-82 alpha chain	110	sp|P07910|HNRPC_HUMAN	Heterogeneous nuclear ribonucleoproteins C1/C2
111	sp|Q15366|PCBP2_HUMAN	Poly(rC)-binding protein 2	111	sp|P05187|PPB1_HUMAN	Alkaline phosphatase, placental type
112	sp|Q14566|MCM6_HUMAN	DNA replication licensing factor MCM6	112	sp|O00410|IPO5_HUMAN	Importin-5
113	sp|P07910|HNRPC_HUMAN	Heterogeneous nuclear ribonucleoproteins C1/C2	113	sp|P43243|MATR3_HUMAN	Matrin-3
114	sp|Q16719|KYNU_HUMAN	Kynureninase	114	sp|P62988|UBIQ_HUMAN	Ubiquitin
115	sp|P80723|BASP_HUMAN	Brain acid soluble protein 1	115	sp|Q15181|IPYR_HUMAN	Inorganic pyrophosphatase
116	sp|P34897|GLYM_HUMAN	Serine hydroxymethyltransferase, mitochondrial	116	sp|P13010|KU86_HUMAN	ATP-dependent DNA helicase 2 subunit 2
117	sp|P17931|LEG3_HUMAN	Galectin-3	117	sp|P52272|HNRPM_HUMAN	Heterogeneous nuclear ribonucleoprotein M
118	sp|P04792|HSPB1_HUMAN	Heat shock protein beta-1	118	sp|P32969|RL9_HUMAN	60S ribosomal protein L9
119	sp|P30048|PRDX3_HUMAN	Thioredoxin-dependent peroxide reductase, mitochondrial	119	sp|P67809|YBOX1_HUMAN	Nuclease-sensitive element-binding protein 1
120	sp|P55060|XPO2_HUMAN	Exportin-2	120	sp|P62906|RL10A_HUMAN	60S ribosomal protein L10a
121	sp|O00299|CLIC1_HUMAN	Chloride intracellular channel protein 1	121	sp|P12004|PCNA_HUMAN	Proliferating cell nuclear antigen
122	sp|P10599|THIO_HUMAN	Thioredoxin	122	sp|Q04695|K1C17_HUMAN	Keratin, type I cytoskeletal 17
123	sp|P78371|TCPB_HUMAN	T-complex protein 1 subunit beta	123	sp|P62081|RS7_HUMAN	40S ribosomal protein S7
124	sp|P07477|TRY1_HUMAN	Trypsin-1	124	sp|P61604|CH10_HUMAN	10 kDa heat shock protein, mitochondrial
125	sp|P23396|RS3_HUMAN	40S ribosomal protein S3	125	sp|P62258|1433E_HUMAN	14-3-3 protein epsilon
126	sp|P31689|DNJA1_HUMAN	DnaJ homolog subfamily A member 1	126	sp|P32119|PRDX2_HUMAN	Peroxiredoxin-2
127	sp|P15559|NQO1_HUMAN	NAD(P)H dehydrogenase [quinone] 1	127	sp|Q16658|FSCN1_HUMAN	Fascin
128	sp|P49411|EFTU_HUMAN	Elongation factor Tu, mitochondrial	128	sp|P62841|RS15_HUMAN	40S ribosomal protein S15
129	sp|P62258|1433E_HUMAN	14-3-3 protein epsilon	129	sp|P40926|MDHM_HUMAN	Malate dehydrogenase, mitochondrial
130	sp|Q15233|NONO_HUMAN	Non-POU domain-containing octamer-binding protein	130	sp|P28066|PSA5_HUMAN	Proteasome subunit alpha type-5
131	sp|P00441|SODC_HUMAN	Superoxide dismutase [Cu-Zn]	131	sp|Q99497|PARK7_HUMAN	Protein DJ-1
132	sp|P61313|RL15_HUMAN	60S ribosomal protein L15	132	sp|P31689|DNJA1_HUMAN	DnaJ homolog subfamily A member 1
133	sp|P35241|RADI_HUMAN	Radixin	133	sp|P30153|2AAA_HUMAN	Serine/threonine-protein phosphatase 2A 65 kDa regulatory subunit A alpha isoform
134	sp|Q16881|TRXR1_HUMAN	Thioredoxin reductase 1, cytoplasmic	134	sp|P18669|PGAM1_HUMAN	Phosphoglycerate mutase 1
135	sp|P35232|PHB_HUMAN	Prohibitin OS=Homo sapiens GN=PHB PE=1 SV=1	135	sp|P09429|HMGB1_HUMAN	High mobility group protein B1
136	sp|P01857|IGHG1_HUMAN	Ig gamma-1 chain C region	136	sp|O95373|IPO7_HUMAN	Importin-7

137	sp|P46777|RL5_HUMAN	60S ribosomal protein L5	137	sp|P99999|CYC_HUMAN	Cytochrome c
138	sp|P42704|LPPRC_HUMAN	Leucine-rich PPR motif-containing protein, mitochondrial	138	sp|P62249|RS16_HUMAN	40S ribosomal protein S16
139	sp|P22102|PUR2_HUMAN	Trifunctional purine biosynthetic protein adenosine-3	139	sp|P25786|PSA1_HUMAN	Proteasome subunit alpha type-1
140	sp|O95817|BAG3_HUMAN	BAG family molecular chaperone regulator 3	140	sp|P17931|LEG3_HUMAN	Galectin-3
141	sp|P04080|CYTB_HUMAN	Cystatin-B	141	sp|P09960|LKHA4_HUMAN	Leukotriene A-4 hydrolase 2
142	sp|P19338|NUCL_HUMAN	Nucleolin	142	sp|P05387|RLA2_HUMAN	60S acidic ribosomal protein P2
143	sp|P08758|ANXA5_HUMAN	Annexin A5	143	sp|P01834|IGKC_HUMAN	Ig kappa chain C region
144	sp|Q92973|TNPO1_HUMAN	Transportin-1	144	sp|P08758|ANXA5_HUMAN	Annexin A5
145	sp|P00505|AATM_HUMAN	Aspartate aminotransferase, mitochondrial	145	sp|P49411|EFTU_HUMAN	Elongation factor Tu, mitochondrial
146	sp|P43243|MATR3_HUMAN	Matrin-3	146	sp|P55060|XPO2_HUMAN	Exportin-2
147	sp|P40926|MDHM_HUMAN	Malate dehydrogenase, mitochondrial	147	sp|Q9H361|PABP3_HUMAN	Polyadenylate-binding protein 3
148	sp|P46783|RS10_HUMAN	40S ribosomal protein S10	148	sp|P15559|NQO1_HUMAN	NAD(P)H dehydrogenase [quinone] 1
149	sp|P25705|ATPA_HUMAN	ATP synthase subunit alpha, mitochondrial	149	sp|P31943|HNRH1_HUMAN	Heterogeneous nuclear ribonucleoprotein H
150	sp|P14324|FPPS_HUMAN	Farnesyl pyrophosphate synthetase	150	sp|P46782|RS5_HUMAN	40S ribosomal protein S5
151	sp|P99999|CYC_HUMAN	Cytochrome c	151	sp|Q15084|PDIA6_HUMAN	Protein disulfide-isomerase A6
152	sp|P49915|GUAA_HUMAN	GMP synthase [glutamine-hydrolyzing]	152	sp|Q15366|PCBP2_HUMAN	Poly(rC)-binding protein 2
153	sp|P58107|EPIPL_HUMAN	Epiplakin	153	sp|Q15149|PLEC1_HUMAN	Plectin-1
154	sp|P62081|RS7_HUMAN	40S ribosomal protein S7	154	sp|P04792|HSPB1_HUMAN	Heat shock protein beta-1
155	sp|Q9H4A4|AMPB_HUMAN	Aminopeptidase B	155	sp|P55209|NP1L1_HUMAN	Nucleosome assembly protein 1-like 1
156	sp|Q7KZF4|SND1_HUMAN	Staphylococcal nuclease domain-containing protein 1	156	sp|P01857|IGHG1_HUMAN	Ig gamma-1 chain C region
157	sp|P09382|LEG1_HUMAN	Galectin-1	157	sp|P32322|P5CR1_HUMAN	Pyrroline-5-carboxylate reductase 1, mitochondrial
158	sp|P35637|FUS_HUMAN	RNA-binding protein FUS	158	sp|P68036|UB2L3_HUMAN	Ubiquitin-conjugating enzyme E2 L3
159	sp|P49321|NASP_HUMAN	Nuclear autoantigenic sperm protein	159	sp|P63244|GBLP_HUMAN	Guanine nucleotide-binding protein subunit beta-2-like 1
160	sp|Q9BWD1|THIC_HUMAN	Acetyl-CoA acetyltransferase, cytosolic	160	sp|Q16881|TRXR1_HUMAN	Thioredoxin reductase 1, cytoplasmic
161	sp|P60891|PRPS1_HUMAN	Ribose-phosphate pyrophosphokinase 1	161	sp|P30085|KCY_HUMAN	UMP-CMP kinase
162	sp|P32322|P5CR1_HUMAN	Pyrroline-5-carboxylate reductase 1, mitochondrial	162	sp|P26639|SYTC_HUMAN	Threonyl-tRNA synthetase, cytoplasmic
163	sp|P00491|PNPH_HUMAN	Purine nucleoside phosphorylase	163	sp|P62241|RS8_HUMAN	40S ribosomal protein S8

164	sp|Q9Y617|SERC_HUMAN	Phosphoserine aminotransferase
165	sp|P49773|HINT1_HUMAN	Histidine triad nucleotide-binding protein 1
166	sp|P29966|MARCS_HUMAN	Myristoylated alanine-rich C-kinase substrate
167	sp|P16989|DBPA_HUMAN	DNA-binding protein A
168	sp|P12268|IMDH2_HUMAN	Inosine-5'-monophosphate dehydrogenase 2
169	sp|P09429|HMGB1_HUMAN	High mobility group protein B1
170	sp|P04843|RPN1_HUMAN	Dolichyl-diphosphooligosaccharide--protein glycosyltransferase subunit 1
171	sp|P04083|ANXA1_HUMAN	Annexin A1
172	sp|Q9UBQ0|VPS29_HUMAN	Vacuolar protein sorting-associated protein 29
173	sp|P62906|RL10A_HUMAN	60S ribosomal protein L10a
174	sp|P27635|RL10_HUMAN	60S ribosomal protein L10
175	sp|P05387|RLA2_HUMAN	60S acidic ribosomal protein P2
176	sp|P68036|UB2L3_HUMAN	Ubiquitin-conjugating enzyme E2 L3
177	sp|P62841|RS15_HUMAN	40S ribosomal protein S15
178	sp|P01834|IGKC_HUMAN	Ig kappa chain C region
179	sp|P18124|RL7_HUMAN	60S ribosomal protein L7
180	sp|O00410|IPO5_HUMAN	Importin-5
181	sp|P23381|SYWC_HUMAN	Tryptophanyl-tRNA synthetase, cytoplasmic
182	sp|Q08945|SSRP1_HUMAN	FACT complex subunit SSRP1
183	sp|P62277|RS13_HUMAN	40S ribosomal protein S13
184	sp|Q1KMD3|HNRL2_HUMAN	Heterogeneous nuclear ribonucleoprotein U-like protein 2
185	sp|Q01518|CAP1_HUMAN	Adenylyl cyclase-associated protein 1
186	sp|P35613|BASI_HUMAN	Basigin
187	sp|P25786|PSA1_HUMAN	Proteasome subunit alpha type-1
188	sp|P02647|APOA1_HUMAN	Apolipoprotein A-I
189	sp|Q14847|LASP1_HUMAN	LIM and SH3 domain protein 1
164	sp|P61204|ARF3_HUMAN	ADP-ribosylation factor 3
165	sp|P60903|S10AA_HUMAN	Protein S100-A10
166	sp|P22102|PUR2_HUMAN	Trifunctional purine biosynthetic protein adenosine-3
167	sp|O60664|M6PBP_HUMAN	Mannose-6-phosphate receptor-binding protein 1
168	sp|P46783|RS10_HUMAN	40S ribosomal protein S10
169	sp|Q15185|TEBP_HUMAN	Prostaglandin E synthase 3
170	sp|P68032|ACTC_HUMAN	Actin, alpha cardiac muscle 1
171	sp|P60660|MYL6_HUMAN	Myosin light polypeptide 6
172	sp|P10599|THIO_HUMAN	Thioredoxin
173	sp|P35637|FUS_HUMAN	RNA-binding protein FUS
174	sp|P22234|PUR6_HUMAN	Multifunctional protein ADE2
175	sp|Q92688|AN32B_HUMAN	Acidic leucine-rich nuclear phosphoprotein 32 family member B
176	sp|P05161|UCRP_HUMAN	Interferon-induced 17 kDa protein
177	sp|Q9Y617|SERC_HUMAN	Phosphoserine aminotransferase
178	sp|Q02878|RL6_HUMAN	60S ribosomal protein L6
179	sp|P26599|PTBP1_HUMAN	Polypyrimidine tract-binding protein 1
180	sp|P18621|RL17_HUMAN	60S ribosomal protein L17
181	sp|P31949|S10AB_HUMAN	Protein S100-A11
182	sp|P08865|RSSA_HUMAN	40S ribosomal protein SA
183	sp|Q7KZF4|SND1_HUMAN	Staphylococcal nuclease domain-containing protein 1
184	sp|P62424|RL7A_HUMAN	60S ribosomal protein L7a
185	sp|P51991|ROA3_HUMAN	Heterogeneous nuclear ribonucleoprotein A3
186	sp|Q6P2Q9|PRP8_HUMAN	Pre-mRNA-processing-splicing factor 8
187	sp|P50990|TCPQ_HUMAN	T-complex protein 1 subunit theta
188	sp|O76021|RL1D1_HUMAN	Ribosomal L1 domain-containing protein 1
189	sp|P60866|RS20_HUMAN	40S ribosomal protein S20

190	sp|Q9Y266|NUDC_HUMAN	Nuclear migration protein nudC	190	sp|Q07020|RL18_HUMAN	60S ribosomal protein L18
191	sp|P12004|PCNA_HUMAN	Proliferating cell nuclear antigen	191	sp|P09622|DLDH_HUMAN	Dihydrolipoyl dehydrogenase, mitochondrial
192	sp|P32969|RL9_HUMAN	60S ribosomal protein L9	192	sp|P68371|TBB2C_HUMAN	Tubulin beta-2C chain
193	sp|P28066|PSA5_HUMAN	Proteasome subunit alpha type-5	193	sp|P22392|NDKB_HUMAN	Nucleoside diphosphate kinase B
194	sp|Q9Y490|TLN1_HUMAN	Talin-1	194	sp|P31946|1433B_HUMAN	14-3-3 protein beta/alpha
195	sp|P34932|HSP74_HUMAN	Heat shock 70 kDa protein 4	195	sp|P22087|FBRL_HUMAN	rRNA 2'-O-methyltransferase fibrillarin
196	sp|O43175|SERA_HUMAN	D-3-phosphoglycerate dehydrogenase	196	sp|Q86VP6|CAND1_HUMAN	Cullin-associated NEDD8-dissociated protein 1
197	sp|P38606|VATA_HUMAN	V-type proton ATPase catalytic subunit A	197	sp|Q15233|NONO_HUMAN	Non-POU domain-containing octamer-binding protein
198	sp|P26639|SYTC_HUMAN	Threonyl-tRNA synthetase, cytoplasmic	198	sp|Q99832|TCPH_HUMAN	T-complex protein 1 subunit eta
199	sp|Q02790|FKBP4_HUMAN	FK506-binding protein 4	199	sp|Q8NC51|PAIRB_HUMAN	Plasminogen activator inhibitor 1 RNA-binding protein
200	sp|P01842|LAC_HUMAN	Ig lambda chain C regions	200	sp|Q14978|NOLC1_HUMAN	Nucleolar phosphoprotein p130
201	sp|Q14103|HNRPD_HUMAN	Heterogeneous nuclear ribonucleoprotein D0	201	sp|Q14566|MCM6_HUMAN	DNA replication licensing factor MCM6
202	sp|P52272|HNRPM_HUMAN	Heterogeneous nuclear ribonucleoprotein M	202	sp|P60891|PRPS1_HUMAN	Ribose-phosphate pyrophosphokinase 1
203	sp|P14866|HNRPL_HUMAN	Heterogeneous nuclear ribonucleoprotein L	203	sp|P55265|DSRAD_HUMAN	Double-stranded RNA-specific adenosine deaminase
204	sp|Q14974|IMB1_HUMAN	Importin subunit beta-1	204	sp|Q9Y265|RUVB1_HUMAN	RuvB-like 1
205	sp|P07602|SAP_HUMAN	Proactivator polypeptide	205	sp|Q9UL46|PSME2_HUMAN	Proteasome activator complex subunit 2
206	sp|P32119|PRDX2_HUMAN	Peroxiredoxin-2	206	sp|Q99714|HCD2_HUMAN	3-hydroxyacyl-CoA dehydrogenase type-2
207	sp|Q06323|PSME1_HUMAN	Proteasome activator complex subunit 1	207	sp|P53618|COPB_HUMAN	Coatomer subunit beta
208	sp|P43487|RANG_HUMAN	Ran-specific GTPase-activating protein	208	sp|P31948|STIP1_HUMAN	Stress-induced-phosphoprotein 1
209	sp|P05455|LA_HUMAN	Lupus La protein	209	sp|P29692|EF1D_HUMAN	Elongation factor 1-delta
210	sp|P18621|RL17_HUMAN	60S ribosomal protein L17	210	sp|P23284|PPIB_HUMAN	Peptidyl-prolyl cis-trans isomerase B
211	sp|Q13838|UAP56_HUMAN	Spliceosome RNA helicase BAT1	211	sp|P17987|TCPA_HUMAN	T-complex protein 1 subunit alpha
212	sp|O14980|XPO1_HUMAN	Exportin-1	212	sp|P14866|HNRPL_HUMAN	Heterogeneous nuclear ribonucleoprotein L
213	sp|Q15029|U5S1_HUMAN	116 kDa U5 small nuclear ribonucleoprotein component	213	sp|P07099|HYEP_HUMAN	Epoxide hydrolase 1
214	sp|P51858|HDGF_HUMAN	Hepatoma-derived growth factor	214	sp|O75340|PDCD6_HUMAN	Programmed cell death protein 6
215	sp|Q9Y3I0|CV028_HUMAN	UPF0027 protein C22orf28	215	sp|Q9Y2W1|TR150_HUMAN	Thyroid hormone receptor-associated protein 3
216	sp|O43852|CALU_HUMAN	Calumenin	216	sp|Q9UGI8|TES_HUMAN	Testin
217	sp|P50991|TCPD_HUMAN	T-complex protein 1 subunit delta	217	sp|Q9BWD1|THIC_HUMAN	Acetyl-CoA acetyltransferase, cytosolic

218	sp|P61604|CH10_HUMAN	10 kDa heat shock protein, mitochondrial	218	sp|Q12905|ILF2_HUMAN	Interleukin enhancer-binding factor 2
219	sp|P25815|S100P_HUMAN	Protein S100-P	219	sp|P62158|CALM_HUMAN	Calmodulin
220	sp|P08708|RS17_HUMAN	40S ribosomal protein S17	220	sp|P35613|BASI_HUMAN	Basigin
221	sp|Q9BUF5|TBB6_HUMAN	Tubulin beta-6 chain	221	sp|P20618|PSB1_HUMAN	Proteasome subunit beta type-1
222	sp|P05161|UCRP_HUMAN	Interferon-induced 17 kDa protein	222	sp|O75494|FUSIP_HUMAN	FUS-interacting serine-arginine-rich protein 1
223	sp|P55795|HNRH2_HUMAN	Heterogeneous nuclear ribonucleoprotein H2	223	sp|Q9Y3F4|STRAP_HUMAN	Serine-threonine kinase receptor-associated protein
224	sp|Q13435|SF3B2_HUMAN	Splicing factor 3B subunit 2	224	sp|Q92841|DDX17_HUMAN	Probable ATP-dependent RNA helicase DDX17
225	sp|O95373|IPO7_HUMAN	Importin-7	225	sp|Q8IZP2|F10A4_HUMAN	Protein FAM10A4
226	sp|P42765|THIM_HUMAN	3-ketoacyl-CoA thiolase, mitochondrial	226	sp|Q15365|PCBP1_HUMAN	Poly(rC)-binding protein 1
227	sp|P27348|1433T_HUMAN	14-3-3 protein theta	227	sp|P62899|RL31_HUMAN	60S ribosomal protein L31
228	sp|O00231|PSD11_HUMAN	26S proteasome non-ATPase regulatory subunit 11	228	sp|P62847|RS24_HUMAN	40S ribosomal protein S24
229	sp|P51991|ROA3_HUMAN	Heterogeneous nuclear ribonucleoprotein A3	229	sp|P46777|RL5_HUMAN	60S ribosomal protein L5
230	sp|P31948|STIP1_HUMAN	Stress-induced-phosphoprotein 1	230	sp|P30050|RL12_HUMAN	60S ribosomal protein L12
231	sp|P37837|TALDO_HUMAN	Transaldolase	231	sp|P29966|MARCS_HUMAN	Myristoylated alanine-rich C-kinase substrate
232	sp|P23284|PPIB_HUMAN	Peptidyl-prolyl cis-trans isomerase B	232	sp|P27635|RL10_HUMAN	60S ribosomal protein L10
233	sp|Q9UMS4|PRP19_HUMAN	Pre-mRNA-processing factor 19	233	sp|P26447|S10A4_HUMAN	Protein S100-A4
234	sp|P62917|RL8_HUMAN	60S ribosomal protein L8	234	sp|P23396|RS3_HUMAN	40S ribosomal protein S3
235	sp|P62241|RS8_HUMAN	40S ribosomal protein S8	235	sp|P21291|CSRP1_HUMAN	Cysteine and glycine-rich protein 1
236	sp|P24534|EF1B_HUMAN	Elongation factor 1-beta	236	sp|P08708|RS17_HUMAN	40S ribosomal protein S17
237	sp|P26640|SYVC_HUMAN	Valyl-tRNA synthetase	237	sp|P07108|ACBP_HUMAN	Acyl-CoA-binding protein
238	sp|P06753|TPM3_HUMAN	Tropomyosin alpha-3 chain	238	sp|P05455|LA_HUMAN	Lupus La protein
239	sp|Q15185|TEBP_HUMAN	Prostaglandin E synthase 3	239	sp|P05386|RLA1_HUMAN	60S acidic ribosomal protein P1
240	sp|Q14978|NOLC1_HUMAN	Nucleolar phosphoprotein p130	240	sp|P01842|LAC_HUMAN	Ig lambda chain C regions
241	sp|O00425|IF2B3_HUMAN	Insulin-like growth factor 2 mRNA-binding protein 3	241	sp|P00966|ASSY_HUMAN	Argininosuccinate synthase
242	sp|P11940|PABP1_HUMAN	Polyadenylate-binding protein 1	242	sp|P00491|PNPH_HUMAN	Purine nucleoside phosphorylase
243	sp|Q15637|SF01_HUMAN	Splicing factor 1	243	sp|P54577|SYYC_HUMAN	Tyrosyl-tRNA synthetase, cytoplasmic
244	sp|P35268|RL22_HUMAN	60S ribosomal protein L22	244	sp|P62750|RL23A_HUMAN	60S ribosomal protein L23a
245	sp|P68371|TBB2C_HUMAN	Tubulin beta-2C chain	245	sp|P27348|1433T_HUMAN	14-3-3 protein theta

246	sp|P15531|NDKA_HUMAN	Nucleoside diphosphate kinase A	246	sp|P38919|IF4A3_HUMAN	Eukaryotic initiation factor 4A-III
247	sp|P31946|1433B_HUMAN	14-3-3 protein beta/alpha	247	sp|P49915|GUAA_HUMAN	GMP synthase [glutamine-hydrolyzing]
248	sp|P63104|1433Z_HUMAN	14-3-3 protein zeta/delta	248	sp|Q08945|SSRP1_HUMAN	FACT complex subunit SSRP1
249	sp|P67809|YBOX1_HUMAN	Nuclease-sensitive element-binding protein 1	249	sp|Q06323|PSME1_HUMAN	Proteasome activator complex subunit 1
250	sp|Q9UL46|PSME2_HUMAN	Proteasome activator complex subunit 2	250	sp|Q15637|SF01_HUMAN	Splicing factor 1
251	sp|P55265|DSRAD_HUMAN	Double-stranded RNA-specific adenosine deaminase	251	sp|Q15029|U5S1_HUMAN	116 kDa U5 small nuclear ribonucleoprotein component
252	sp|Q9Y383|LC7L2_HUMAN	Putative RNA-binding protein Luc7-like 2	252	sp|O94925|GLSK_HUMAN	Glutaminase kidney isoform, mitochondrial
253	sp|P22087|FBRL_HUMAN	rRNA 2'-O-methyltransferase fibrillarin	253	sp|P38606|VATA_HUMAN	V-type proton ATPase catalytic subunit A
254	sp|Q99623|PHB2_HUMAN	Prohibitin-2	254	sp|Q92973|TNPO1_HUMAN	Transportin-1
255	sp|P61247|RS3A_HUMAN	40S ribosomal protein S3a	255	sp|Q04637|IF4G1_HUMAN	Eukaryotic translation initiation factor 4 gamma 1
256	sp|O60701|UGDH_HUMAN	UDP-glucose 6-dehydrogenase	256	sp|Q99623|PHB2_HUMAN	Prohibitin-2
257	sp|Q9NQC3|RTN4_HUMAN	Reticulon-4	257	sp|P21266|GSTM3_HUMAN	Glutathione S-transferase Mu 3
258	sp|Q92928|RAB1C_HUMAN	Putative Ras-related protein Rab-1C	258	sp|P11166|GTR1_HUMAN	Solute carrier family 2, facilitated glucose transporter member 1
259	sp|Q16658|FSCN1_HUMAN	Fascin	259	sp|P51858|HDGF_HUMAN	Hepatoma-derived growth factor
260	sp|Q07666|KHDR1_HUMAN	KH domain-containing, RNA-binding, signal transduction-associated protein 1	260	sp|P35232|PHB_HUMAN	Prohibitin
261	sp|P62847|RS24_HUMAN	40S ribosomal protein S24	261	sp|P18124|RL7_HUMAN	60S ribosomal protein L7
262	sp|P29692|EF1D_HUMAN	Elongation factor 1-delta	262	sp|Q02543|RL18A_HUMAN	60S ribosomal protein L18a
263	sp|P04844|RPN2_HUMAN	Dolichyl-diphosphooligosaccharide--protein glycosyltransferase subunit 2	263	sp|P63104|1433Z_HUMAN	14-3-3 protein zeta/delta
264	sp|Q9Y265|RUVB1_HUMAN	RuvB-like 1	264	sp|Q01650|LAT1_HUMAN	Large neutral amino acids transporter small subunit 1
265	sp|Q9UGI8|TES_HUMAN	Testin	265	sp|P60981|DEST_HUMAN	Destrin
266	sp|Q92841|DDX17_HUMAN	Probable ATP-dependent RNA helicase DDX17	266	sp|Q14498|RBM39_HUMAN	RNA-binding protein 39
267	sp|Q8IZP2|F10A4_HUMAN	Protein FAM10A4	267	sp|O60832|DKC1_HUMAN	H/ACA ribonucleoprotein complex subunit 4
268	sp|Q15084|PDIA6_HUMAN	Protein disulfide-isomerase A6	268	sp|P62269|RS18_HUMAN	40S ribosomal protein S18
269	sp|Q13765|NACA_HUMAN	Nascent polypeptide-associated complex subunit alpha	269	sp|O95340|PAPS2_HUMAN	Bifunctional 3'-phosphoadenosine 5'-phosphosulfate synthetase 2
270	sp|P62314|SMD1_HUMAN	Small nuclear ribonucleoprotein Sm D1	270	sp|Q9P2E9|RRBP1_HUMAN	Ribosome-binding protein 1
271	sp|P46778|RL21_HUMAN	60S ribosomal protein L21	271	sp|Q9Y3A5|SBDS_HUMAN	Ribosome maturation protein SBDS
272	sp|P31939|PUR9_HUMAN	Bifunctional purine biosynthesis protein	272	sp|O15372|EIF3H_HUMAN	Eukaryotic translation initiation factor 3 subunit H

		PURH			
273	sp|P31153|METK2_HUMAN	S-adenosylmethionine synthetase isoform type-2	273	sp|Q96KP4|CNDP2_HUMAN	Cytosolic non-specific dipeptidase
274	sp|P30085|KCY_HUMAN	UMP-CMP kinase	274	sp|P60900|PSA6_HUMAN	Proteasome subunit alpha type-6
275	sp|P20618|PSB1_HUMAN	Proteasome subunit beta type-1	275	sp|P62316|SMD2_HUMAN	Small nuclear ribonucleoprotein Sm D2
276	sp|P16435|NCPR_HUMAN	NADPH--cytochrome P450 reductase	276	sp|Q8IYD1|ERF3B_HUMAN	Eukaryotic peptide chain release factor GTP-binding subunit ERF3B
277	sp|P09960|LKHA4_HUMAN	Leukotriene A-4 hydrolase	277	sp|Q9Y383|LC7L2_HUMAN	Putative RNA-binding protein Luc7-like 2
278	sp|P07099|HYEP_HUMAN	Epoxide hydrolase 1	278	sp|Q96C19|EFHD2_HUMAN	EF-hand domain-containing protein D2
279	sp|P05388|RLA0_HUMAN	60S acidic ribosomal protein P0	279	sp|P27816|MAP4_HUMAN	Microtubule-associated protein 4
280	sp|O15427|MOT4_HUMAN	Monocarboxylate transporter 4	280	sp|Q9BTT0|AN32E_HUMAN	Acidic leucine-rich nuclear phosphoprotein 32 family member E
281	sp|Q92597|NDRG1_HUMAN	Protein NDRG1	281	sp|P46778|RL21_HUMAN	60S ribosomal protein L21
282	sp|Q8NC51|PAIRB_HUMAN	Plasminogen activator inhibitor 1 RNA-binding protein	282	sp|P30048|PRDX3_HUMAN	Thioredoxin-dependent peroxide reductase, mitochondrial
283	sp|Q15631|TSN_HUMAN	Translin	283	sp|P23526|SAHH_HUMAN	Adenosylhomocysteinase
284	sp|Q00796|DHSO_HUMAN	Sorbitol dehydrogenase	284	sp|Q9NYF8|BCLF1_HUMAN	Bcl-2-associated transcription factor 1
285	sp|P62249|RS16_HUMAN	40S ribosomal protein S16	285	sp|P62277|RS13_HUMAN	40S ribosomal protein S13
286	sp|P60660|MYL6_HUMAN	Myosin light polypeptide 6	286	sp|P78417|GSTO1_HUMAN	Glutathione S-transferase omega-1
287	sp|P51665|PSD7_HUMAN	26S proteasome non-ATPase regulatory subunit 7	287	sp|P04843|RPN1_HUMAN	Dolichyl-diphosphooligosaccharide--protein glycosyltransferase subunit 1
288	sp|P35237|SPB6_HUMAN	Serpin B6	288	sp|O43175|SERA_HUMAN	D-3-phosphoglycerate dehydrogenase
289	sp|P30050|RL12_HUMAN	60S ribosomal protein L12	289	sp|P34897|GLYM_HUMAN	Serine hydroxymethyltransferase, mitochondrial
290	sp|P28799|GRN_HUMAN	Granulins	290	sp|P34932|HSP74_HUMAN	Heat shock 70 kDa protein 4
291	sp|P26447|S10A4_HUMAN	Protein S100-A4	291	sp|Q9H4A4|AMPB_HUMAN	Aminopeptidase B
292	sp|P09622|DLDH_HUMAN	Dihydrolipoyl dehydrogenase, mitochondrial	292	sp|P01859|IGHG2_HUMAN	Ig gamma-2 chain C region
293	sp|O75340|PDCD6_HUMAN	Programmed cell death protein 6	293	sp|P04080|CYTB_HUMAN	Cystatin-B
294	sp|Q99497|PARK7_HUMAN	Protein DJ-1	294	sp|P17812|PYRG1_HUMAN	CTP synthase 1
295	sp|Q14019|COTL1_HUMAN	Coactosin-like protein	295	sp|O14561|ACPM_HUMAN	Acyl carrier protein, mitochondrial
296	sp|P62899|RL31_HUMAN	60S ribosomal protein L31	296	sp|P61353|RL27_HUMAN	60S ribosomal protein L27
297	sp|P60866|RS20_HUMAN	40S ribosomal protein S20	297	sp|P37837|TALDO_HUMAN	Transaldolase
298	sp|P22234|PUR6_HUMAN	Multifunctional protein ADE2	298	sp|Q9BTE3|CJ119_HUMAN	UPF0557 protein C10orf119

299	sp|P14314|GLU2B_HUMAN	Glucosidase 2 subunit beta
300	sp|P07108|ACBP_HUMAN	Acyl-CoA-binding protein
301	sp|P00387|NB5R3_HUMAN	NADH-cytochrome b5 reductase 3
302	sp|O76003|GLRX3_HUMAN	Glutaredoxin-3
303	sp|O75347|TBCA_HUMAN	Tubulin-specific chaperone A
304	sp|P53618|COPB_HUMAN	Coatomer subunit beta
305	sp|P05386|RLA1_HUMAN	60S acidic ribosomal protein P1
306	sp|P41250|SYG_HUMAN	Glycyl-tRNA synthetase
307	sp|Q14061|COX17_HUMAN	Cytochrome c oxidase copper chaperone
308	sp|Q01082|SPTB2_HUMAN	Spectrin beta chain, brain 1
309	sp|P62424|RL7A_HUMAN	60S ribosomal protein L7a
310	sp|Q9NZ01|GPSN2_HUMAN	Synaptic glycoprotein SC2
311	sp|Q96AG4|LRC59_HUMAN	Leucine-rich repeat-containing protein 59
312	sp|Q8NBS9|TXND5_HUMAN	Thioredoxin domain-containing protein 5
313	sp|P62316|SMD2_HUMAN	Small nuclear ribonucleoprotein Sm D2
314	sp|P40227|TCPZ_HUMAN	T-complex protein 1 subunit zeta
315	sp|P11586|C1TC_HUMAN	C-1-tetrahydrofolate synthase, cytoplasmic
316	sp|Q93045|STMN2_HUMAN	Stathmin-2
317	sp|Q9BTT0|AN32E_HUMAN	Acidic leucine-rich nuclear phosphoprotein 32 family member E
318	sp|P54577|SYYC_HUMAN	Tyrosyl-tRNA synthetase, cytoplasmic
319	sp|P21266|GSTM3_HUMAN	Glutathione S-transferase Mu 3
320	sp|P00966|ASSY_HUMAN	Argininosuccinate synthase
321	sp|P25398|RS12_HUMAN	40S ribosomal protein S12
322	sp|Q15459|SF3A1_HUMAN	Splicing factor 3 subunit 1
323	sp|P62750|RL23A_HUMAN	60S ribosomal protein L23a
324	sp|P62318|SMD3_HUMAN	Small nuclear ribonucleoprotein Sm D3
325	sp|P13010|KU86_HUMAN	ATP-dependent DNA helicase 2 subunit 2
326	sp|Q562R1|ACTBL_HUMAN	Beta-actin-like protein 2

299	sp|P62263|RS14_HUMAN	40S ribosomal protein S14
300	sp|P62318|SMD3_HUMAN	Small nuclear ribonucleoprotein Sm D3
301	sp|P39019|RS19_HUMAN	40S ribosomal protein S19
302	sp|P42704|LPPRC_HUMAN	Leucine-rich PPR motif-containing protein, mitochondrial
303	sp|Q1KMD3|HNRL2_HUMAN	Heterogeneous nuclear ribonucleoprotein U-like protein 2
304	sp|P43487|RANG_HUMAN	Ran-specific GTPase-activating protein
305	sp|P25788|PSA3_HUMAN	Proteasome subunit alpha type-3
306	sp|Q13347|EIF3I_HUMAN	Eukaryotic translation initiation factor 3 subunit I
307	sp|O43852|CALU_HUMAN	Calumenin
308	sp|P32320|CDD_HUMAN	Cytidine deaminase
309	sp|Q9NQC3|RTN4_HUMAN	Reticulon-4
310	sp|Q96HC4|PDLI5_HUMAN	PDZ and LIM domain protein 5
311	sp|P62917|RL8_HUMAN	60S ribosomal protein L8
312	sp|Q9UQ35|SRRM2_HUMAN	Serine/arginine repetitive matrix protein 2
313	sp|P05388|RLA0_HUMAN	60S acidic ribosomal protein P0
314	sp|Q14103|HNRPD_HUMAN	Heterogeneous nuclear ribonucleoprotein D0
315	sp|Q9Y224|CN166_HUMAN	UPF0568 protein C14orf166
316	sp|Q9ULJ7|ANR50_HUMAN	Ankyrin repeat domain-containing protein 50
317	sp|Q86V81|THOC4_HUMAN	THO complex subunit 4
318	sp|Q96PK6|RBM14_HUMAN	RNA-binding protein 14
319	sp|Q6NZI2|PTRF_HUMAN	Polymerase I and transcript release factor
320	sp|P11310|ACADM_HUMAN	Medium-chain specific acyl-CoA dehydrogenase, mitochondrial
321	sp|Q7Z6Z7|HUWE1_HUMAN	E3 ubiquitin-protein ligase HUWE1
322	sp|Q9BQG0|MBB1A_HUMAN	Myb-binding protein 1A
323	sp|Q9NTK5|OLA1_HUMAN	Obg-like ATPase 1
324	sp|Q15393|SF3B3_HUMAN	Splicing factor 3B subunit 3
325	sp|Q15042|RB3GP_HUMAN	Rab3 GTPase-activating protein catalytic subunit
326	sp|O00232|PSD12_HUMAN	26S proteasome non-ATPase regulatory subunit 12

327	sp|P35610|SOAT1_HUMAN	Sterol O-acyltransferase 1
328	sp|P38919|IF4A3_HUMAN	Eukaryotic initiation factor 4A-III
329	sp|P31949|S10AB_HUMAN	Protein S100-A11
330	sp|P61353|RL27_HUMAN	60S ribosomal protein L27
331	sp|Q99714|HCD2_HUMAN	3-hydroxyacyl-CoA dehydrogenase type-2
332	sp|P61769|B2MG_HUMAN	Beta-2-microglobulin
333	sp|P60903|S10AA_HUMAN	Protein S100-A10
334	sp|Q9H2U2|IPYR2_HUMAN	Inorganic pyrophosphatase 2, mitochondrial
335	sp|Q8NFJ5|RAI3_HUMAN	Retinoic acid-induced protein 3
336	sp|O14561|ACPM_HUMAN	Acyl carrier protein, mitochondrial
337	sp|O15523|DDX3Y_HUMAN	ATP-dependent RNA helicase DDX3Y
338	sp|P68133|ACTS_HUMAN	Actin, alpha skeletal muscle
339	sp|P62263|RS14_HUMAN	40S ribosomal protein S14
340	sp|P00492|HPRT_HUMAN	Hypoxanthine-guanine phosphoribosyltransferase
341	sp|Q16531|DDB1_HUMAN	DNA damage-binding protein 1
342	sp|P42771|CD2A1_HUMAN	Cyclin-dependent kinase inhibitor 2A, isoforms 1/2/3
343	sp|P27695|APEX1_HUMAN	DNA-(apurinic or apyrimidinic site) lyase
344	sp|Q96AE4|FUBP1_HUMAN	Far upstream element-binding protein 1
345	sp|Q92688|AN32B_HUMAN	Acidic leucine-rich nuclear phosphoprotein 32 family member B
346	sp|P39019|RS19_HUMAN	40S ribosomal protein S19
347	sp|P13489|RINI_HUMAN	Ribonuclease inhibitor
348	sp|P05023|AT1A1_HUMAN	Sodium/potassium-transporting ATPase subunit alpha-1
349	sp|Q6GMV3|CB079_HUMAN	Uncharacterized protein C2orf79
350	sp|Q01844|EWS_HUMAN	RNA-binding protein EWS
351	sp|Q92598|HS105_HUMAN	Heat shock protein 105 kDa
352	sp|Q02543|RL18A_HUMAN	60S ribosomal protein L18a
353	sp|P49448|DHE4_HUMAN	Glutamate dehydrogenase 2, mitochondrial

327	sp|Q96K21|ZFY19_HUMAN	Zinc finger FYVE domain-containing protein 19
328	sp|Q13310|PABP4_HUMAN	Polyadenylate-binding protein 4
329	sp|Q9UMS4|PRP19_HUMAN	Pre-mRNA-processing factor 19
330	sp|Q96AE4|FUBP1_HUMAN	Far upstream element-binding protein 1
331	sp|Q05932|FOLC_HUMAN	Folylpolyglutamate synthase, mitochondrial
332	sp|P63173|RL38_HUMAN	60S ribosomal protein L38
333	sp|P51665|PSD7_HUMAN	26S proteasome non-ATPase regulatory subunit 7
334	sp|Q9BQE3|TBA1C_HUMAN	Tubulin alpha-1C chain
335	sp|Q9BUF5|TBB6_HUMAN	Tubulin beta-6 chain
336	sp|P61981|1433G_HUMAN	14-3-3 protein gamma
337	sp|Q6FI13|H2A2A_HUMAN	Histone H2A type 2-A
338	sp|Q562R1|ACTBL_HUMAN	Beta-actin-like protein 2
339	sp|O00148|DDX39_HUMAN	ATP-dependent RNA helicase DDX39
340	sp|Q71UI9|H2AV_HUMAN	Histone H2A.V
341	sp|P08727|K1C19_HUMAN	Keratin, type I cytoskeletal 19
342	sp|P16989|DBPA_HUMAN	DNA-binding protein A
343	sp|Q13162|PRDX4_HUMAN	Peroxiredoxin-4
344	sp|P39687|AN32A_HUMAN	Acidic leucine-rich nuclear phosphoprotein 32 family member A
345	sp|P52597|HNRPF_HUMAN	Heterogeneous nuclear ribonucleoprotein F
346	sp|Q92598|HS105_HUMAN	Heat shock protein 105 kDa
347	sp|Q01844|EWS_HUMAN	RNA-binding protein EWS
348	sp|Q9H2G2|SLK_HUMAN	STE20-like serine/threonine-protein kinase
349	sp|P47914|RL29_HUMAN	60S ribosomal protein L29
350	sp|Q14204|DYHC1_HUMAN	Cytoplasmic dynein 1 heavy chain 1
351	sp|Q14839|CHD4_HUMAN	Chromodomain-helicase-DNA-binding protein 4
352	sp|Q13428|TCOF_HUMAN	Treacle protein
353	sp|Q8WUM0|NU133_HUMAN	Nuclear pore complex protein Nup133

354	sp|O15479|MAGB2_HUMAN	Melanoma-associated antigen B2	354	sp|Q9UHD8|SEPT9_HUMAN	Septin-9
355	sp|Q13347|EIF3I_HUMAN	Eukaryotic translation initiation factor 3 subunit I	355	sp|Q92621|NU205_HUMAN	Nuclear pore complex protein Nup205
356	sp|Q13907|IDI1_HUMAN	Isopentenyl-diphosphate Delta-isomerase 1	356	sp|P35658|NU214_HUMAN	Nuclear pore complex protein Nup214
357	sp|P23526|SAHH_HUMAN	Adenosylhomocysteinase	357	sp|P05023|AT1A1_HUMAN	Sodium/potassium-transporting ATPase subunit alpha-1
358	sp|P49368|TCPG_HUMAN	T-complex protein 1 subunit gamma	358	sp|P01023|A2MG_HUMAN	Alpha-2-macroglobulin
359	sp|Q96HC4|PDLI5_HUMAN	PDZ and LIM domain protein 5	359	sp|Q07157|ZO1_HUMAN	Tight junction protein ZO-1
360	sp|Q96KP4|CNDP2_HUMAN	Cytosolic non-specific dipeptidase	360	sp|P49448|DHE4_HUMAN	Glutamate dehydrogenase 2, mitochondrial
361	sp|O60506|HNRPQ_HUMAN	Heterogeneous nuclear ribonucleoprotein Q	361	sp|P23246|SFPQ_HUMAN	Splicing factor, proline- and glutamine-rich
362	sp|P46782|RS5_HUMAN	40S ribosomal protein S5	362	sp|P17844|DDX5_HUMAN	Probable ATP-dependent RNA helicase DDX5
363	sp|Q15645|TRP13_HUMAN	Thyroid receptor-interacting protein 13	363	sp|Q9Y262|IF3EI_HUMAN	Eukaryotic translation initiation factor 3 subunit E-interacting protein
364	sp|P50579|AMPM2_HUMAN	Methionine aminopeptidase 2	364	sp|P50570|DYN2_HUMAN	Dynamin-2
365	sp|Q99729|ROAA_HUMAN	Heterogeneous nuclear ribonucleoprotein A/B	365	sp|P49756|RBM25_HUMAN	Probable RNA-binding protein 25
366	sp|O00264|PGRC1_HUMAN	Membrane-associated progesterone receptor component 1	366	sp|O95197|RTN3_HUMAN	Reticulon-3
367	sp|P51572|BAP31_HUMAN	B-cell receptor-associated protein 31	367	sp|O14980|XPO1_HUMAN	Exportin-1
368	sp|Q04760|LGUL_HUMAN	Lactoylglutathione lyase	368	sp|Q9UNZ2|NSF1C_HUMAN	NSFL1 cofactor p47
369	sp|O75947|ATP5H_HUMAN	ATP synthase subunit d, mitochondrial	369	sp|Q9UL25|RAB21_HUMAN	Ras-related protein Rab-21
370	sp|O43776|SYNC_HUMAN	Asparaginyl-tRNA synthetase, cytoplasmic	370	sp|Q9NZB2|F120A_HUMAN	Constitutive coactivator of PPAR-gamma-like protein 1
371	sp|Q9P2E9|RRBP1_HUMAN	Ribosome-binding protein 1	371	sp|Q9NSE4|SYIM_HUMAN	Isoleucyl-tRNA synthetase, mitochondrial
372	sp|Q13011|ECH1_HUMAN	Delta(3,5)-Delta(2,4)-dienoyl-CoA isomerase, mitochondrial	372	sp|Q96CV9|OPTN_HUMAN	Optineurin
373	sp|P30043|BLVRB_HUMAN	Flavin reductase	373	sp|Q93008|USP9X_HUMAN	Probable ubiquitin carboxyl-terminal hydrolase FAF-X
374	sp|Q13185|CBX3_HUMAN	Chromobox protein homolog 3	374	sp|Q86TG7|PEG10_HUMAN	Retrotransposon-derived protein PEG10
375	sp|P60900|PSA6_HUMAN	Proteasome subunit alpha type-6	375	sp|P62191|PRS4_HUMAN	26S protease regulatory subunit 4
376	sp|O76070|SYUG_HUMAN	Gamma-synuclein	376	sp|P51572|BAP31_HUMAN	B-cell receptor-associated protein 31
377	sp|P32320|CDD_HUMAN	Cytidine deaminase	377	sp|P35237|SPB6_HUMAN	Serpin B6
378	sp|Q8TEM1|PO210_HUMAN	Nuclear pore membrane glycoprotein 210	378	sp|P26640|SYVC_HUMAN	Valyl-tRNA synthetase
379	sp|P40429|RL13A_HUMAN	60S ribosomal protein L13a	379	sp|P10155|RO60_HUMAN	60 kDa SS-A/Ro ribonucleoprotein

380	sp|P37235|HPCL1_HUMAN	Hippocalcin-like protein 1	380	sp|P06737|PYGL_HUMAN	Glycogen phosphorylase, liver form
381	sp|Q00341|VIGLN_HUMAN	Vigilin	381	sp|O15479|MAGB2_HUMAN	Melanoma-associated antigen B2
382	sp|P30084|ECHM_HUMAN	Enoyl-CoA hydratase, mitochondrial	382	sp|Q9Y4L1|HYOU1_HUMAN	Hypoxia up-regulated protein 1
383	sp|P20700|LMNB1_HUMAN	Lamin-B1	383	sp|Q9UNM6|PSD13_HUMAN	26S proteasome non-ATPase regulatory subunit 13
384	sp|P62136|PP1A_HUMAN	Serine/threonine-protein phosphatase PP1-alpha catalytic subunit	384	sp|Q9NVP1|DDX18_HUMAN	ATP-dependent RNA helicase DDX18
385	sp|Q05639|EF1A2_HUMAN	Elongation factor 1-alpha 2	385	sp|Q9HA77|SYCM_HUMAN	Probable cysteinyl-tRNA synthetase, mitochondrial
386	sp|P63010|AP2B1_HUMAN	AP-2 complex subunit beta-1	386	sp|Q96HN2|SAHH3_HUMAN	Putative adenosylhomocysteinase 3
387	sp|Q15691|MARE1_HUMAN	Microtubule-associated protein RP/EB family member 1	387	sp|Q96AY3|FKB10_HUMAN	FK506-binding protein 10
388	sp|Q9NZ45|CISD1_HUMAN	CDGSH iron sulfur domain-containing protein 1	388	sp|Q92979|NEP1_HUMAN	Probable ribosome biogenesis protein NEP1
389	sp|Q6P2Q9|PRP8_HUMAN	Pre-mRNA-processing-splicing factor 8	389	sp|Q92499|DDX1_HUMAN	ATP-dependent RNA helicase DDX1
390	sp|Q9UQ35|SRRM2_HUMAN	Serine/arginine repetitive matrix protein 2	390	sp|Q8WVC0|LEO1_HUMAN	RNA polymerase-associated protein LEO1
391	sp|Q92616|GCN1L_HUMAN	Translational activator GCN1	391	sp|Q7L2H7|EIF3M_HUMAN	Eukaryotic translation initiation factor 3 subunit M
392	sp|Q12965|MYO1E_HUMAN	Myosin-Ie	392	sp|Q2NL82|TSR1_HUMAN	Pre-rRNA-processing protein TSR1 homolog
393	sp|P07814|SYEP_HUMAN	Bifunctional aminoacyl-tRNA synthetase	393	sp|Q16555|DPYL2_HUMAN	Dihydropyrimidinase-related protein 2
394	sp|Q86VP6|CAND1_HUMAN	Cullin-associated NEDD8-dissociated protein 1	394	sp|Q08J23|NSUN2_HUMAN	tRNA (cytosine-5-)-methyltransferase NSUN2
395	sp|O00541|PESC_HUMAN	Pescadillo homolog 1	395	sp|Q07021|C1QBP_HUMAN	Complement component 1 Q subcomponent-binding protein, mitochondrial
396	sp|P17844|DDX5_HUMAN	Probable ATP-dependent RNA helicase DDX5	396	sp|P63010|AP2B1_HUMAN	AP-2 complex subunit beta-1
397	sp|P11310|ACADM_HUMAN	Medium-chain specific acyl-CoA dehydrogenase, mitochondrial	397	sp|P55084|ECHB_HUMAN	Trifunctional enzyme subunit beta, mitochondrial
398	sp|P16152|CBR1_HUMAN	Carbonyl reductase [NADPH] 1	398	sp|P54727|RD23B_HUMAN	UV excision repair protein RAD23 homolog B
399	sp|Q96HE7|ERO1A_HUMAN	ERO1-like protein alpha	399	sp|P53985|MOT1_HUMAN	Monocarboxylate transporter 1
400	sp|Q9BQE3|TBA1C_HUMAN	Tubulin alpha-1C chain	400	sp|P49773|HINT1_HUMAN	Histidine triad nucleotide-binding protein 1
401	sp|Q6FI13|H2A2A_HUMAN	Histone H2A type 2-A	401	sp|P49189|AL9A1_HUMAN	4-trimethylaminobutyraldehyde dehydrogenase
402	sp|Q04917|1433F_HUMAN	14-3-3 protein eta	402	sp|P38159|HNRPG_HUMAN	Heterogeneous nuclear ribonucleoprotein G
403	sp|P61981|1433G_HUMAN	14-3-3 protein gamma	403	sp|P36542|ATPG_HUMAN	ATP synthase subunit gamma, mitochondrial
404	sp|Q8NHM4|TRY6_HUMAN	Putative trypsin-6	404	sp|P23381|SYWC_HUMAN	Tryptophanyl-tRNA synthetase, cytoplasmic
405	sp|Q71UI9|H2AV_HUMAN	Histone H2A.V	405	sp|P13489|RINI_HUMAN	Ribonuclease inhibitor
406	sp|O00148|DDX39_HUMAN	ATP-dependent RNA helicase DDX39	406	sp|P09525|ANXA4_HUMAN	Annexin A4

407	sp|P07951|TPM2_HUMAN	Tropomyosin beta chain
408	sp|Q13162|PRDX4_HUMAN	Peroxiredoxin-4
409	sp|P52597|HNRPF_HUMAN	Heterogeneous nuclear ribonucleoprotein F
410	sp|P39687|AN32A_HUMAN	Acidic leucine-rich nuclear phosphoprotein 32 family member A
411	sp|P05556|ITB1_HUMAN	Integrin beta-1
412	sp|Q7L2J0|MEPCE_HUMAN	7SK snRNA methylphosphate capping enzyme
413	sp|Q9BZQ8|NIBAN_HUMAN	Protein Niban
414	sp|O75390|CISY_HUMAN	Citrate synthase, mitochondrial
415	sp|Q9NSE4|SYIM_HUMAN	Isoleucyl-tRNA synthetase, mitochondrial
416	sp|O60256|KPRB_HUMAN	Phosphoribosyl pyrophosphate synthetase-associated protein 2
417	sp|Q96HN2|SAHH3_HUMAN	Putative adenosylhomocysteinase 3
418	sp|P30566|PUR8_HUMAN	Adenylosuccinate lyase
419	sp|Q15257|PTPA_HUMAN	Serine/threonine-protein phosphatase 2A regulatory subunit B'
420	sp|P45974|UBP5_HUMAN	Ubiquitin carboxyl-terminal hydrolase 5
421	sp|O60610|DIAP1_HUMAN	Protein diaphanous homolog 1
422	sp|Q9Y2W1|TR150_HUMAN	Thyroid hormone receptor-associated protein 3
423	sp|Q99805|TM9S2_HUMAN	Transmembrane 9 superfamily member 2
424	sp|Q6NZI2|PTRF_HUMAN	Polymerase I and transcript release factor
425	sp|Q99613|EIF3C_HUMAN	Eukaryotic translation initiation factor 3 subunit C
426	sp|Q86V81|THOC4_HUMAN	THO complex subunit 4
427	sp|P01023|A2MG_HUMAN	Alpha-2-macroglobulin
428	sp|O95340|PAPS2_HUMAN	Bifunctional 3'-phosphoadenosine 5'-phosphosulfate synthetase 2
429	sp|O95197|RTN3_HUMAN	Reticulon-3
430	sp|Q9NVP1|DDX18_HUMAN	ATP-dependent RNA helicase DDX18
431	sp|Q99832|TCPH_HUMAN	T-complex protein 1 subunit eta
407	sp|P00492|HPRT_HUMAN	Hypoxanthine-guanine phosphoribosyltransferase
408	sp|O95433|AHSA1_HUMAN	Activator of 90 kDa heat shock protein ATPase homolog 1
409	sp|O76070|SYUG_HUMAN	Gamma-synuclein
410	sp|O75955|FLOT1_HUMAN	Flotillin-1
411	sp|O75531|BAF_HUMAN	Barrier-to-autointegration factor
412	sp|O75390|CISY_HUMAN	Citrate synthase, mitochondrial
413	sp|O15427|MOT4_HUMAN	Monocarboxylate transporter 4
414	sp|O00571|DDX3X_HUMAN	ATP-dependent RNA helicase DDX3X
415	sp|Q9UM00|TMCO1_HUMAN	Transmembrane and coiled-coil domain-containing protein 1
416	sp|Q9UK76|HN1_HUMAN	Hematological and neurological expressed 1 protein
417	sp|Q9UHD9|UBQL2_HUMAN	Ubiquilin-2
418	sp|Q9NZ01|GPSN2_HUMAN	Synaptic glycoprotein SC2
419	sp|Q9NR31|SAR1A_HUMAN	GTP-binding protein SAR1a
420	sp|Q9H910|HN1L_HUMAN	Hematological and neurological expressed 1-like protein
421	sp|Q9BY44|EIF2A_HUMAN	Eukaryotic translation initiation factor 2A
422	sp|Q9BQA1|MEP50_HUMAN	Methylosome protein 50
423	sp|Q99417|MYCBP_HUMAN	C-Myc-binding protein
424	sp|Q92928|RAB1C_HUMAN	Putative Ras-related protein Rab-1C
425	sp|Q92734|TFG_HUMAN	Protein TFG
426	sp|Q8NHM4|TRY6_HUMAN	Putative trypsin-6
427	sp|Q8ND56|LS14A_HUMAN	Protein LSM14 homolog A
428	sp|Q7L2J0|MEPCE_HUMAN	7SK snRNA methylphosphate capping enzyme
429	sp|Q6ZQN7|SO4C1_HUMAN	Solute carrier organic anion transporter family member 4C1
430	sp|Q5JNZ5|RS26L_HUMAN	Putative 40S ribosomal protein S26-like 1
431	sp|Q59GN2|R39L5_HUMAN	Putative 60S ribosomal protein L39-like 5

432	sp|Q92621|NU205_HUMAN	Nuclear pore complex protein Nup205
433	sp|Q86TG7|PEG10_HUMAN	Retrotransposon-derived protein PEG10
434	sp|Q04637|IF4G1_HUMAN	Eukaryotic translation initiation factor 4 gamma 1
435	sp|P62191|PRS4_HUMAN	26S protease regulatory subunit 4
436	sp|P49748|ACADV_HUMAN	Very long-chain specific acyl-CoA dehydrogenase, mitochondrial
437	sp|P16615|AT2A2_HUMAN	Sarcoplasmic/endoplasmic reticulum calcium ATPase 2
438	sp|P01009|A1AT_HUMAN	Alpha-1-antitrypsin
439	sp|Q9NTZ6|RBM12_HUMAN	RNA-binding protein 12
440	sp|Q9NSD9|SYFB_HUMAN	Phenylalanyl-tRNA synthetase beta chain
441	sp|Q16555|DPYL2_HUMAN	Dihydropyrimidinase-related protein 2
442	sp|Q13243|SFRS5_HUMAN	Splicing factor, arginine/serine-rich 5
443	sp|P47712|PA24A_HUMAN	Cytosolic phospholipase A2
444	sp|P46379|BAT3_HUMAN	Large proline-rich protein BAT3
445	sp|P04181|OAT_HUMAN	Ornithine aminotransferase, mitochondrial
446	sp|O75533|SF3B1_HUMAN	Splicing factor 3B subunit 1
447	sp|Q9Y3F4|STRAP_HUMAN	Serine-threonine kinase receptor-associated protein
448	sp|Q9ULV4|COR1C_HUMAN	Coronin-1C
449	sp|Q9NZB2|F120A_HUMAN	Constitutive coactivator of PPAR-gamma-like protein 1
450	sp|Q9NW13|RBM28_HUMAN	RNA-binding protein 28
451	sp|Q9BW27|NUP85_HUMAN	Nucleoporin NUP85
452	sp|Q92499|DDX1_HUMAN	ATP-dependent RNA helicase DDX1
453	sp|Q8WVC0|LEO1_HUMAN	RNA polymerase-associated protein LEO1
454	sp|Q53EL6|PDCD4_HUMAN	Programmed cell death protein 4
455	sp|Q16836|HCDH_HUMAN	Hydroxyacyl-coenzyme A dehydrogenase, mitochondrial
456	sp|Q13492|PICAL_HUMAN	Phosphatidylinositol-binding clathrin assembly protein
457	sp|Q10713|MPPA_HUMAN	Mitochondrial-processing peptidase subunit alpha
432	sp|Q15691|MARE1_HUMAN	Microtubule-associated protein RP/EB family member 1
433	sp|Q15257|PTPA_HUMAN	Serine/threonine-protein phosphatase 2A regulatory subunit B'
434	sp|Q14694|UBP10_HUMAN	Ubiquitin carboxyl-terminal hydrolase 10
435	sp|Q13228|SBP1_HUMAN	Selenium-binding protein 1
436	sp|Q10713|MPPA_HUMAN	Mitochondrial-processing peptidase subunit alpha
437	sp|Q02790|FKBP4_HUMAN	FK506-binding protein 4
438	sp|P68400|CSK21_HUMAN	Casein kinase II subunit alpha
439	sp|P67936|TPM4_HUMAN	Tropomyosin alpha-4 chain
440	sp|P62834|RAP1A_HUMAN	Ras-related protein Rap-1A
441	sp|P62805|H4_HUMAN	Histone H4
442	sp|P55769|NH2L1_HUMAN	NHP2-like protein 1
443	sp|P50914|RL14_HUMAN	60S ribosomal protein L14
444	sp|P50579|AMPM2_HUMAN	Methionine aminopeptidase 2
445	sp|P49720|PSB3_HUMAN	Proteasome subunit beta type-3
446	sp|P48147|PPCE_HUMAN	Prolyl endopeptidase
447	sp|P47712|PA24A_HUMAN	Cytosolic phospholipase A2
448	sp|P43686|PRS6B_HUMAN	26S protease regulatory subunit 6B
449	sp|P42224|STAT1_HUMAN	Signal transducer and activator of transcription 1-alpha/beta
450	sp|P41743|KPCI_HUMAN	Protein kinase C iota type
451	sp|P41091|IF2G_HUMAN	Eukaryotic translation initiation factor 2 subunit 3
452	sp|P35268|RL22_HUMAN	60S ribosomal protein L22
453	sp|P32929|CGL_HUMAN	Cystathionine gamma-lyase
454	sp|P31939|PUR9_HUMAN	Bifunctional purine biosynthesis protein PURH
455	sp|P30084|ECHM_HUMAN	Enoyl-CoA hydratase, mitochondrial
456	sp|P27695|APEX1_HUMAN	DNA-(apurinic or apyrimidinic site) lyase
457	sp|P26373|RL13_HUMAN	60S ribosomal protein L13

458	sp|Q07065|CKAP4_HUMAN	Cytoskeleton-associated protein 4	458	sp|P21796|VDAC1_HUMAN	Voltage-dependent anion-selective channel protein 1
459	sp|P60228|EIF3E_HUMAN	Eukaryotic translation initiation factor 3 subunit E	459	sp|P13804|ETFA_HUMAN	Electron transfer flavoprotein subunit alpha, mitochondrial
460	sp|P47914|RL29_HUMAN	60S ribosomal protein L29	460	sp|P07602|SAP_HUMAN	Proactivator polypeptide
461	sp|P46060|RAGP1_HUMAN	Ran GTPase-activating protein 1	461	sp|O75828|CBR3_HUMAN	Carbonyl reductase [NADPH] 3
462	sp|P17987|TCPA_HUMAN	T-complex protein 1 subunit alpha	462	sp|O60610|DIAP1_HUMAN	Protein diaphanous homolog 1
463	sp|P17812|PYRG1_HUMAN	CTP synthase 1	463	sp|O43598|RCL_HUMAN	c-Myc-responsive protein Rcl
464	sp|O76031|CLPX_HUMAN	ATP-dependent Clp protease ATP-binding subunit clpX-like, mitochondrial	464	sp|O43396|TXNL1_HUMAN	Thioredoxin-like protein 1
465	sp|O43598|RCL_HUMAN	c-Myc-responsive protein Rcl	465	sp|O15347|HMGB3_HUMAN	High mobility group protein B3
466	sp|O15067|PUR4_HUMAN	Phosphoribosylformylglycinamidine synthase	466	sp|O00231|PSD11_HUMAN	26S proteasome non-ATPase regulatory subunit 11
467	sp|Q9Y4X5|ARI1_HUMAN	Protein ariadne-1 homolog	467	sp|Q9Y3E0|GOT1B_HUMAN	Vesicle transport protein GOT1B
468	sp|Q9UNM6|PSD13_HUMAN	26S proteasome non-ATPase regulatory subunit 13	468	sp|Q9Y2V2|CHSP1_HUMAN	Calcium-regulated heat stable protein 1
469	sp|Q9HAV0|GBB4_HUMAN	Guanine nucleotide-binding protein subunit beta-4	469	sp|Q9Y2Q3|GSTK1_HUMAN	Glutathione S-transferase kappa 1
470	sp|Q9BUP0|EFHD1_HUMAN	EF-hand domain-containing protein D1	470	sp|Q9UNX3|RL26L_HUMAN	60S ribosomal protein L26-like 1
471	sp|Q96P70|IPO9_HUMAN	Importin-9	471	sp|Q9H3K6|BOLA2_HUMAN	BolA-like protein 2
472	sp|Q96C36|P5CR2_HUMAN	Pyrroline-5-carboxylate reductase 2	472	sp|Q9BWJ5|SF3B5_HUMAN	Splicing factor 3B subunit 5
473	sp|Q5JNZ5|RS26L_HUMAN	Putative 40S ribosomal protein S26-like 1	473	sp|Q99536|VAT1_HUMAN	Synaptic vesicle membrane protein VAT-1 homolog
474	sp|Q16891|IMMT_HUMAN	Mitochondrial inner membrane protein	474	sp|Q99439|CNN2_HUMAN	Calponin-2
475	sp|Q14657|LAGE3_HUMAN	L antigen family member 3	475	sp|Q969Z0|TBRG4_HUMAN	Protein TBRG4
476	sp|Q13228|SBP1_HUMAN	Selenium-binding protein 1	476	sp|Q969M3|YIPF5_HUMAN	Protein YIPF5
477	sp|Q08257|QOR_HUMAN	Quinone oxidoreductase	477	sp|Q6YN16|HSDL2_HUMAN	Hydroxysteroid dehydrogenase-like protein 2
478	sp|P68400|CSK21_HUMAN	Casein kinase II subunit alpha	478	sp|Q6FI81|CPIN1_HUMAN	Anamorsin
479	sp|P62913|RL11_HUMAN	60S ribosomal protein L11	479	sp|Q6EEV6|SUMO4_HUMAN	Small ubiquitin-related modifier 4
480	sp|P55010|IF5_HUMAN	Eukaryotic translation initiation factor 5	480	sp|Q15843|NEDD8_HUMAN	NEDD8
481	sp|P54886|P5CS_HUMAN	Delta-1-pyrroline-5-carboxylate synthetase	481	sp|Q15631|TSN_HUMAN	Translin
482	sp|P49189|AL9A1_HUMAN	4-trimethylaminobutyraldehyde dehydrogenase	482	sp|Q14847|LASP1_HUMAN	LIM and SH3 domain protein 1
483	sp|P48444|COPD_HUMAN	Coatomer subunit delta	483	sp|Q14061|COX17_HUMAN	Cytochrome c oxidase copper chaperone
484	sp|P46736|BRCC3_HUMAN	BRCA1/BRCA2-containing complex	484	sp|Q14019|COTL1_HUMAN	Coactosin-like protein

		subunit 3			
485	sp|P45880|VDAC2_HUMAN	Voltage-dependent anion-selective channel protein 2	485	sp|Q13185|CBX3_HUMAN	Chromobox protein homolog 3
486	sp|P42766|RL35_HUMAN	60S ribosomal protein L35	486	sp|Q13011|ECH1_HUMAN	Delta(3,5)-Delta(2,4)-dienoyl-CoA isomerase, mitochondrial
487	sp|P40925|MDHC_HUMAN	Malate dehydrogenase, cytoplasmic	487	sp|Q12996|CSTF3_HUMAN	Cleavage stimulation factor 77 kDa subunit
488	sp|P40855|PEX19_HUMAN	Peroxisomal biogenesis factor 19	488	sp|Q01628|IFM3_HUMAN	Interferon-induced transmembrane protein 3
489	sp|P37198|NUP62_HUMAN	Nuclear pore glycoprotein p62	489	sp|Q00796|DHSO_HUMAN	Sorbitol dehydrogenase
490	sp|P26373|RL13_HUMAN	60S ribosomal protein L13	490	sp|P62829|RL23_HUMAN	60S ribosomal protein L23
491	sp|P22695|QCR2_HUMAN	Cytochrome b-c1 complex subunit 2, mitochondrial	491	sp|P62314|SMD1_HUMAN	Small nuclear ribonucleoprotein Sm D1
492	sp|P21291|CSRP1_HUMAN	Cysteine and glycine-rich protein 1	492	sp|P62244|RS15A_HUMAN	40S ribosomal protein S15a
493	sp|O94992|HEXI1_HUMAN	Protein HEXIM1	493	sp|P61769|B2MG_HUMAN	Beta-2-microglobulin
494	sp|O76021|RL1D1_HUMAN	Ribosomal L1 domain-containing protein 1	494	sp|P61586|RHOA_HUMAN	Transforming protein RhoA
495	sp|O43670|ZN207_HUMAN	Zinc finger protein 207	495	sp|P61247|RS3A_HUMAN	40S ribosomal protein S3a
496	sp|O15372|EIF3H_HUMAN	Eukaryotic translation initiation factor 3 subunit H	496	sp|P53999|TCP4_HUMAN	Activated RNA polymerase II transcriptional coactivator p15
497	sp|Q9Y6B6|SAR1B_HUMAN	GTP-binding protein SAR1b	497	sp|P52907|CAZA1_HUMAN	F-actin-capping protein subunit alpha-1
498	sp|Q9Y2Z4|SYYM_HUMAN	Tyrosyl-tRNA synthetase, mitochondrial	498	sp|P51580|TPMT_HUMAN	Thiopurine S-methyltransferase
499	sp|Q9Y2V2|CHSP1_HUMAN	Calcium-regulated heat stable protein 1	499	sp|P50897|PPT1_HUMAN	Palmitoyl-protein thioesterase 1
500	sp|Q9Y2Q3|GSTK1_HUMAN	Glutathione S-transferase kappa 1	500	sp|P50402|EMD_HUMAN	Emerin
501	sp|Q9UNX3|RL26L_HUMAN	60S ribosomal protein L26-like 1	501	sp|P50238|CRIP1_HUMAN	Cysteine-rich protein 1
502	sp|Q9UL25|RAB21_HUMAN	Ras-related protein Rab-21	502	sp|P46109|CRKL_HUMAN	Crk-like protein
503	sp|Q9H910|HN1L_HUMAN	Hematological and neurological expressed 1-like protein	503	sp|P42771|CD2A1_HUMAN	Cyclin-dependent kinase inhibitor 2A, isoforms 1/2/3
504	sp|Q9H2H8|PPIL3_HUMAN	Peptidyl-prolyl cis-trans isomerase-like 3	504	sp|P42765|THIM_HUMAN	3-ketoacyl-CoA thiolase, mitochondrial
505	sp|Q9C005|DPY30_HUMAN	Protein dpy-30 homolog	505	sp|P37235|HPCL1_HUMAN	Hippocalcin-like protein 1
506	sp|Q9BWF3|RBM4_HUMAN	RNA-binding protein 4	506	sp|P37108|SRP14_HUMAN	Signal recognition particle 14 kDa protein
507	sp|Q969M3|YIPF5_HUMAN	Protein YIPF5	507	sp|P35244|RFA3_HUMAN	Replication protein A 14 kDa subunit
508	sp|Q8IVT2|CS021_HUMAN	Uncharacterized protein C19orf21	508	sp|P31153|METK2_HUMAN	S-adenosylmethionine synthetase isoform type-2
509	sp|Q14694|UBP10_HUMAN	Ubiquitin carboxyl-terminal hydrolase 10	509	sp|P30046|DOPD_HUMAN	D-dopachrome decarboxylase
510	sp|Q07021|C1QBP_HUMAN	Complement component 1 Q subcomponent-binding protein,	510	sp|P25787|PSA2_HUMAN	Proteasome subunit alpha type-2

		mitochondrial			
511	sp|Q06210|GFPT1_HUMAN	Glucosamine--fructose-6-phosphate aminotransferase [isomerizing] 1	511	sp|P24844|MYL9_HUMAN	Myosin regulatory light polypeptide 9
512	sp|Q01628|IFM3_HUMAN	Interferon-induced transmembrane protein 3	512	sp|P24752|THIL_HUMAN	Acetyl-CoA acetyltransferase, mitochondrial
513	sp|P82930|RT34_HUMAN	28S ribosomal protein S34, mitochondrial	513	sp|P24534|EF1B_HUMAN	Elongation factor 1-beta
514	sp|P67775|PP2AA_HUMAN	Serine/threonine-protein phosphatase 2A catalytic subunit alpha isoform	514	sp|P20810|ICAL_HUMAN	Calpastatin
515	sp|P62834|RAP1A_HUMAN	Ras-related protein Rap-1A	515	sp|P17096|HMGA1_HUMAN	High mobility group protein HMG-I/HMG-Y
516	sp|P62805|H4_HUMAN	Histone H4	516	sp|P09211|GSTP1_HUMAN	Glutathione S-transferase P
517	sp|P62244|RS15A_HUMAN	40S ribosomal protein S15a	517	sp|P06493|CDC2_HUMAN	Cell division control protein 2 homolog
518	sp|P61964|WDR5_HUMAN	WD repeat-containing protein 5	518	sp|P00387|NB5R3_HUMAN	NADH-cytochrome b5 reductase 3
519	sp|P61088|UBE2N_HUMAN	Ubiquitin-conjugating enzyme E2 N	519	sp|O95674|CDS2_HUMAN	Phosphatidate cytidylyltransferase 2
520	sp|P60953|CDC42_HUMAN	Cell division control protein 42 homolog	520	sp|O76003|GLRX3_HUMAN	Glutaredoxin-3
521	sp|P55769|NH2L1_HUMAN	NHP2-like protein 1	521	sp|O75459|GAGB1_HUMAN	G antigen family B member 1
522	sp|P55084|ECHB_HUMAN	Trifunctional enzyme subunit beta, mitochondrial	522	sp|O75347|TBCA_HUMAN	Tubulin-specific chaperone A
523	sp|P46937|YAP1_HUMAN	65 kDa Yes-associated protein	523	sp|O75083|WDR1_HUMAN	WD repeat-containing protein 1
524	sp|P41743|KPCI_HUMAN	Protein kinase C iota type	524	sp|O43765|SGTA_HUMAN	Small glutamine-rich tetratricopeptide repeat-containing protein alpha PE=1 SV=1
525	sp|P35244|RFA3_HUMAN	Replication protein A 14 kDa subunit	525	sp|O43670|ZN207_HUMAN	Zinc finger protein 207
526	sp|P32929|CGL_HUMAN	Cystathionine gamma-lyase	526	sp|O00541|PESC_HUMAN	Pescadillo homolog 1
527	sp|P25787|PSA2_HUMAN	Proteasome subunit alpha type-2	527	sp|Q96P70|IPO9_HUMAN	Importin-9
528	sp|P16070|CD44_HUMAN	CD44 antigen	528	sp|P12111|CO6A3_HUMAN	Collagen alpha-3(VI) chain
529	sp|P13073|COX41_HUMAN	Cytochrome c oxidase subunit 4 isoform 1, mitochondrial	529	sp|P46459|NSF_HUMAN	Vesicle-fusing ATPase
530	sp|P12277|KCRB_HUMAN	Creatine kinase B-type	530	sp|Q16778|H2B2E_HUMAN	Histone H2B type 2-E
531	sp|P11166|GTR1_HUMAN	Solute carrier family 2, facilitated glucose transporter member 1	531	sp|P27708|PYR1_HUMAN	CAD protein
532	sp|P09211|GSTP1_HUMAN	Glutathione S-transferase P	532	sp|P49368|TCPG_HUMAN	T-complex protein 1 subunit gamma
533	sp|P06493|CDC2_HUMAN	Cell division control protein 2 homolog	533	sp|P18206|VINC_HUMAN	Vinculin
534	sp|O75955|FLOT1_HUMAN	Flotillin-1	534	sp|Q9BTV5|FSD1_HUMAN	Fibronectin type III and SPRY domain-containing protein 1
535	sp|O75934|SPF27_HUMAN	Pre-mRNA-splicing factor SPF27	535	sp|Q9BUJ2|HNRL1_HUMAN	Heterogeneous nuclear ribonucleoprotein U-like protein 1

536	sp|O75531|BAF_HUMAN	Barrier-to-autointegration factor	536	sp|O75694|NU155_HUMAN	Nuclear pore complex protein Nup155
537	sp|O75494|FUSIP_HUMAN	FUS-interacting serine-arginine-rich protein 1	537	sp|Q13907|IDI1_HUMAN	Isopentenyl-diphosphate Delta-isomerase 1
538	sp|O75083|WDR1_HUMAN	WD repeat-containing protein 1	538	sp|P53634|CATC_HUMAN	Dipeptidyl-peptidase 1
539	sp|O43765|SGTA_HUMAN	Small glutamine-rich tetratricopeptide repeat-containing protein alpha	539	sp|Q9Y5K5|UCHL5_HUMAN	Ubiquitin carboxyl-terminal hydrolase isozyme L5
540	sp|O00303|EIF3F_HUMAN	Eukaryotic translation initiation factor 3 subunit F	540	sp|Q13765|NACA_HUMAN	Nascent polypeptide-associated complex subunit alpha
541	sp|Q9Y6C9|MTCH2_HUMAN	Mitochondrial carrier homolog 2	541	sp|P36507|MP2K2_HUMAN	Dual specificity mitogen-activated protein kinase kinase 2
542	sp|Q9Y3E0|GOT1B_HUMAN	Vesicle transport protein GOT1B	542	sp|P14868|SYDC_HUMAN	Aspartyl-tRNA synthetase, cytoplasmic
543	sp|Q9Y3D9|RT23_HUMAN	28S ribosomal protein S23, mitochondrial	543	sp|O00487|PSDE_HUMAN	26S proteasome non-ATPase regulatory subunit 14
544	sp|Q9Y3B3|TMED7_HUMAN	Transmembrane emp24 domain-containing protein 7	544	sp|A6NM28|ZFP92_HUMAN	Zinc finger protein 92 homolog
545	sp|Q9UM00|TMCO1_HUMAN	Transmembrane and coiled-coil domain-containing protein 1	545	sp|P11586|C1TC_HUMAN	C-1-tetrahydrofolate synthase, cytoplasmic
546	sp|Q9ULC4|MCTS1_HUMAN	Malignant T cell amplified sequence 1	546	sp|Q9ULD0|OGDHL_HUMAN	2-oxoglutarate dehydrogenase E1 component-like, mitochondrial
547	sp|Q9UK76|HN1_HUMAN	Hematological and neurological expressed 1 protein	547	sp|Q9Y3D9|RT23_HUMAN	28S ribosomal protein S23, mitochondrial
548	sp|Q9P0S9|TM14C_HUMAN	Transmembrane protein 14C	548	sp|Q04837|SSB_HUMAN	Single-stranded DNA-binding protein, mitochondrial
549	sp|Q9BY44|EIF2A_HUMAN	Eukaryotic translation initiation factor 2A	549	sp|P60228|EIF3E_HUMAN	Eukaryotic translation initiation factor 3 subunit E
550	sp|Q6PJG6|CG027_HUMAN	HEAT repeat-containing protein C7orf27	550	sp|O60437|PEPL_HUMAN	Periplakin
551	sp|Q6EEV6|SUMO4_HUMAN	Small ubiquitin-related modifier 4	551	sp|Q16851|UGPA_HUMAN	UTP--glucose-1-phosphate uridylyltransferase
552	sp|Q59GN2|R39L5_HUMAN	Putative 60S ribosomal protein L39-like 5	552	sp|O60256|KPRB_HUMAN	Phosphoribosyl pyrophosphate synthetase-associated protein 2
553	sp|Q12905|ILF2_HUMAN	Interleukin enhancer-binding factor 2	553	sp|P49736|MCM2_HUMAN	DNA replication licensing factor MCM2
554	sp|P63173|RL38_HUMAN	60S ribosomal protein L38	554	sp|Q15459|SF3A1_HUMAN	Splicing factor 3 subunit 1
555	sp|P62829|RL23_HUMAN	60S ribosomal protein L23	555	sp|P00533|EGFR_HUMAN	Epidermal growth factor receptor
556	sp|P61586|RHOA_HUMAN	Transforming protein RhoA	556	sp|Q9NTZ6|RBM12_HUMAN	RNA-binding protein 12
557	sp|P54727|RD23B_HUMAN	UV excision repair protein RAD23 homolog B	557	sp|P84098|RL19_HUMAN	60S ribosomal protein L19
558	sp|P53999|TCP4_HUMAN	Activated RNA polymerase II transcriptional coactivator p15	558	sp|P40763|STAT3_HUMAN	Signal transducer and activator of transcription 3
559	sp|P53634|CATC_HUMAN	Dipeptidyl-peptidase 1	559	sp|Q13263|TIF1B_HUMAN	Transcription intermediary factor 1-beta
560	sp|P52565|GDIR1_HUMAN	Rho GDP-dissociation inhibitor 1	560	sp|P13667|PDIA4_HUMAN	Protein disulfide-isomerase A4

561	sp|P50914|RL14_HUMAN	60S ribosomal protein L14
562	sp|P50402|EMD_HUMAN	Emerin
563	sp|P48047|ATPO_HUMAN	ATP synthase subunit O, mitochondrial
564	sp|P21796|VDAC1_HUMAN	Voltage-dependent anion-selective channel protein 1
565	sp|P20962|PTMS_HUMAN	Parathymosin
566	sp|P17096|HMGA1_HUMAN	High mobility group protein HMG-I/HMG-Y
567	sp|O75459|GAGB1_HUMAN	G antigen family B member 1
568	sp|O43169|CYB5B_HUMAN	Cytochrome b5 type B
569	sp|O00170|AIP_HUMAN	AH receptor-interacting protein
570	sp|Q13126|MTAP_HUMAN	S-methyl-5'-thioadenosine phosphorylase
571	sp|P33778|H2B1B_HUMAN	Histone H2B type 1-B
572	sp|Q9H307|PININ_HUMAN	Pinin
573	sp|P06737|PYGL_HUMAN	Glycogen phosphorylase, liver form
574	sp|P33176|KINH_HUMAN	Kinesin-1 heavy chain
575	sp|P20042|IF2B_HUMAN	Eukaryotic translation initiation factor 2 subunit 2
576	sp|P14868|SYDC_HUMAN	Aspartyl-tRNA synthetase, cytoplasmic
577	sp|Q96CV9|OPTN_HUMAN	Optineurin
578	sp|Q08J23|NSUN2_HUMAN	tRNA (cytosine-5-)-methyltransferase NSUN2
579	sp|O95372|LYPA2_HUMAN	Acyl-protein thioesterase 2
580	sp|Q9Y5K5|UCHL5_HUMAN	Ubiquitin carboxyl-terminal hydrolase isozyme L5
581	sp|Q9BWJ5|SF3B5_HUMAN	Splicing factor 3B subunit 5
582	sp|P37108|SRP14_HUMAN	Signal recognition particle 14 kDa protein
583	sp|P61204|ARF3_HUMAN	ADP-ribosylation factor 3
584	sp|P78417|GSTO1_HUMAN	Glutathione S-transferase omega-1
585	sp|P49756|RBM25_HUMAN	Probable RNA-binding protein 25
586	sp|Q9NR56|MBNL1_HUMAN	Muscleblind-like protein 1
587	sp|Q7Z6Z7|HUWE1_HUMAN	E3 ubiquitin-protein ligase HUWE1
588	sp|Q12874|SF3A3_HUMAN	Splicing factor 3A subunit 3
561	sp|P40429|RL13A_HUMAN	60S ribosomal protein L13a
562	sp|P31150|GDIA_HUMAN	Rab GDP dissociation inhibitor alpha
563	sp|Q9Y3I0|CV028_HUMAN	UPF0027 protein C22orf28
564	sp|Q16531|DDB1_HUMAN	DNA damage-binding protein 1
565	sp|P42766|RL35_HUMAN	60S ribosomal protein L35

589	sp|P49736|MCM2_HUMAN	DNA replication licensing factor MCM2
590	sp|P38117|ETFB_HUMAN	Electron transfer flavoprotein subunit beta
591	sp|Q5JRM2|YX016_HUMAN	Uncharacterized protein LOC347487
592	sp|P84098|RL19_HUMAN	60S ribosomal protein L19
593	sp|Q9Y316|MEMO1_HUMAN	Protein MEMO1
594	sp|Q9BZZ5|API5_HUMAN	Apoptosis inhibitor 5
595	sp|P30046|DOPD_HUMAN	D-dopachrome decarboxylase
596	sp|P40261|NNMT_HUMAN	Nicotinamide N-methyltransferase
597	sp|Q9Y3A5|SBDS_HUMAN	Ribosome maturation protein SBDS

Part 6

List of 95% peptides, charged state and protein functions

Accession No.& Name	Seq. of 95% peptides	Peptide Charged State	Functions
P01023 α-2-macroglobulin	DLKPAIVK	3	Inhibit all four classes of proteinases
	DTVIKPLLVEPEGLEK	4	by a unique 'trapping' mechanism.
	MVSGFIPLKPTVK	4	Play a role in coagulation.
	QFSFPLSSEPFQGS	3	
	TEVSSNHVLIYLDK	3	
	TQTVQAHYILN	3	
P02765 α-2-HS-glycoprotein	CDSSPDSAEDVR	2	Promotes endocytosis, possesses opsonic
	CNLLAEK	2	properties and influences the mineral
	KCDSSPDSAEDVR	3	phase of bone.
	HTFMGVVSLGSPSGEVSHPRK	4	
P02647 Apolipoprotein A-I	ATEHLSTLSEK	3	Participates in the reverse transport of
	DLATVYVDVLK	2	cholesterol from tissues to the liver for
	DYVSQFEGSALGK	3	excretion.
P02679 Fibrinogen gamma chain	LTIGEGQQHHLGGAK	4	Yielding monomers that polymerize into fibrin,
	MLEEIMK	2	acting as a cofactor in platelet aggregation.
Q14624 Inter-α-trypsin inhibitor heavy chain H4	ETLFSVMPGLK	3	Multi-functional. May be involved in acute
	GSEMVVAGK	2	phase reactions.

List of 76 Culture Media Proteins Detected

	Accession #	Name
1	P01008	Antithrombin-III precursor
2	P01023	Alpha-2-macroglobulin precursor
3	P02765	Alpha-2-HS-glycoprotein precursor
4	P02788	Lactotransferrin precursor
5	P19823	Inter-alpha-trypsin inhibitor heavy chain H2 precursor
6	P07477	Trypsin-1 precursor
7	P63261	Actin, cytoplasmic 2
8	P60709	Actin, cytoplasmic 1
9	P01024	Complement C3 precursor
10	P00747	Plasminogen precursor
11	P02771	Alpha-fetoprotein precursor
12	P20742	Pregnancy zone protein precursor
13	P02787	Serotransferrin precursor
14	Q14624	Inter-alpha-trypsin inhibitor heavy chain H4 precursor
15	P02647	Apolipoprotein A-I precursor
16	P36955	Pigment epithelium-derived factor precursor
17	P02768	Serum albumin precursor
18	P16157	Ankyrin-1
19	P02766	Transthyretin precursor
20	Q16695	Histone H3.1t
21	P22314	Ubiquitin-activating enzyme E1
22	P28838	Cytosol aminopeptidase
23	P01042	Kininogen-1 precursor
24	O95497	Pantetheinase precursor
25	Q16777	Histone H2A type 2-C

List of 163 Clinic Serum Proteins Detected

	Accession	Name
1	P02763	Alpha-1-acid glycoprotein 1 precursor
2	P01024	Complement C3 precursor
3	P01023	Alpha-2-macroglobulin precursor
4	P04114	Apolipoprotein B-100 precursor
5	P0278	Serotransferrin precursor
6	P01009	Alpha-1-antitrypsin precursor
7	P0C0L4	Complement C4-A precursor
8	P0C0L5	Complement C4-B precursor
9	P02679	Fibrinogen gamma chain precursor
10	P01857	Ig gamma-1 chain C region
11	P02671	Fibrinogen alpha chain precursor
12	P02647	Apolipoprotein A-I precursor
13	P02675	Fibrinogen beta chain precursor
14	P00738	Haptoglobin precursor
15	P01876	Ig alpha-1 chain C region
16	P02751	Fibronectin precursor
17	P01871	Ig mu chain C region
18	P01842	Ig lambda chain C regions
19	P02790	Hemopexin precursor
20	P00450	Ceruloplasmin precursor
21	P01859	Ig gamma-2 chain C region
22	P01834	Ig kappa chain C region
23	P19823	Inter-alpha-trypsin inhibitor heavy chain H2 precursor
24	P02768	Serum albumin precursor
25	P02766	Transthyretin precursor

26	P23142	Fibulin-1 precursor	26	P02765	Alpha-2-HS-glycoprotein precursor
27	Q99878	Histone H2A type 1-J	27	P04217	Alpha-1B-glycoprotein precursor
28	P02042	Hemoglobin subunit delta	28	P68871	Hemoglobin subunit beta
29	Q00975	Voltage-dependent N-type calcium channel subunit alpha-1B	29	P06727	Apolipoprotein A-IV precursor
30	P51587	Breast cancer type 2 susceptibility protein	30	P02652	Apolipoprotein A-II precursor
31	P23921	Ribonucleoside-diphosphate reductase large subunit	31	P01011	Alpha-1-antichymotrypsin precursor
32	Q494V2	Coiled-coil domain-containing protein 37	32	P02656	Apolipoprotein C-III precursor
33	P05452	Tetranectin precursor	33	P19827	Inter-alpha-trypsin inhibitor heavy chain H1 precursor
34	P04004	Vitronectin precursor	34	P00751	Complement factor B precursor
35	P02774	Vitamin D-binding protein precursor	35	P01042	Kininogen-1 precursor light chain
36	P49720	Proteasome subunit beta type 3	36	P02774	Vitamin D-binding protein precursor
37	Q8WZ42	Titin	37	P01768	Ig heavy chain V-III region CAM
38	P35030	Trypsin-3 precursor	38	P08697	Alpha-2-antiplasmin precursor
39	P02679	Fibrinogen gamma chain precursor	39	P01861	Ig gamma-4 chain C region
40	P02675	Fibrinogen beta chain precursor	40	P69905	Hemoglobin subunit alpha
41	P02671	Fibrinogen alpha chain precursor	41	P01717	Ig lambda chain V-IV region Hil
42	P07478	Trypsin-2 precursor	42	Q14624	Inter-alpha-trypsin inhibitor heavy chain H4 precursor
43	Q96P50	Centaurin-beta-5	43	P01019	Angiotensinogen precursor
44	P68363	Tubulin alpha-1B chain	44	P04196	Histidine-rich glycoprotein precursor
45	Q9UNM6	26S proteasome non-ATPase regulatory subunit 13	45	P25311	Zinc-alpha-2-glycoprotein precursor
46	Q96H78	Solute carrier family 25 member 44	46	P27169	Serum paraoxonase/arylesterase 1
47	P01857	Ig gamma-1 chain C region	47	P05155	Plasma protease C1 inhibitor precursor
48	P01859	Ig gamma-2 chain C region	48	P04003	C4b-binding protein alpha chain
49	P01834	Ig kappa chain C region	49	P06313	Ig kappa chain V-IV region JI precursor
50	P61769	Beta-2-microglobulin precursor	50	P02654	Apolipoprotein C-I precursor
51	P02763	Alpha-1-acid glycoprotein 1precursor	51	P01031	Complement C5 precursor
52	P09429	High mobility group protein B1	52	P04004	Vitronectin precursor
53	Q9ULJ8	Neurabin-1	53	P00747	Plasminogen precursor
54	Q9nYQ6	Cadherin EGF LAG seven-pass G-type receptor 1precursor	54	P01610	Ig kappa chain V-I region WEA

55	P06748	Nucleophosmin
56	P68871	Hemoglobin subunit beta
57	P19827	Inter-alpha-trypsin inhibitor heavy chain H1precursor
58	P35670	Copper-transporting ATPase 2
59	Q9H8M2	Bromodomain-containing protein 9
60	P06733	Alpha-enolase
61	P08697	Alpha-2-antiplasmin precursor
62	Q9HCC0	Methylcrotonoyl-CoA carboxylase beta chain, mitochondrial
63	P02452	Collagen alpha-1(I) chain precursor
64	P01009	Alpha-1-antitrypsin precursor
65	P01842	Ig lambda chain C region
66	P13639	Elongation factor 2
67	P20848	Putative alpha-1-antitrypsin-related protein precursor
68	Q12882	Dihydropyrimidine dehydrogenase [NADP+] precursor
69	P04264	Keratin, type II cytoskeletal 1
70	Q96QK1	Vacuolar protein sorting-associated protein 35
71	Q9UKL3	CASP8-associated protein 2
72	Q9UEW8	STE20/SPS1-related proline-alanine-rich protein kinase
73	P02753	Retinol-binding protein 4
74	O96028	Probable histone-lysine N-methyltransferase NSD2
75	P14618	Pyruvate kinase isozymes M1/M2
76	P11277	Spectrin beta chain, erythrocyte

55	P08603	Complement factor H precursor
56	P00739	Haptoglobin-related protein precursor
57	P10909	Clusterin precursor
58	P35542	Serum amyloid A-4 protein precursor
59	P05546	Heparin cofactor 2 precursor
60	P23083	Ig heavy chain V-I region V35 precursor
61	P01008	Antithrombin-III precursor
62	P00736	Complement C1r subcomponent precursor
63	P01781	Ig heavy chain V-III region GAL
64	P02749	Beta-2-glycoprotein 1 precursor
65	P01621	Ig kappa chain V-III region NG9 precursor
66	P06396	Gelsolin precursor
67	P19652	Alpha-1-acid glycoprotein 2 precursor
68	P02649	Apolipoprotein E precursor
69	P06316	Ig lambda chain V-I region BL2 precursor
70	O14791	Apolipoprotein-L1 precursor
71	P02655	Apolipoprotein C-II precursor
72	P01860	Ig gamma-3 chain C region
73	P02746	Complement C1q subcomponent subunit B precursor
74	P01766	Ig heavy chain V-III region BRO
75	Q96PD5	N-acetylmuramoyl-L-alanine amidase precursor
76	P51884	Lumican precursor
77	P10643	Complement component C7 precursor
78	P05156	Complement factor I precursor (Human)
79	P06311	Ig kappa chain V-III region IARC/BL41 precursor
80	P01601	Ig kappa chain V-I region HK101 precursor
81	P05783	Keratin, type I cytoskeletal 18
82	P01611	Ig kappa chain V-I region Wes
83	P01617	Ig kappa chain V-II region TEW

84	P29401	Transketolase
85	P36955	Pigment epithelium-derived factor precursor
86	P68104	Elongation factor 1-alpha 1
87	P07355	Annexin A2
88	Q9UQ80	Proliferation-associated protein 2G4
89	Q8IUE6	Histone H2A type 2-B
90	P02747	Complement C1q subcomponent subunit C precursor
91	P01779	Ig heavy chain V-III region TUR
92	Q6FI13	Histone H2A type 2-A
93	Q13790	Apolipoprotein F precursor
94	P01591	Immunoglobulin J chain
95	P04433	Ig kappa chain V-III region VG precursor
96	P04211	Ig lambda chain V region 4A precursor
97	P02753	Plasma retinol-binding protein precursor
98	P11142	Heat shock cognate 71 kDa protein
99	P15814	Immunoglobulin lambda-like polypeptide 1 precursor
100	P13671	Complement component C6 precursor
101	P35858	Insulin-like growth factor-binding protein complex acid labile chain precursor
102	P02743	Serum amyloid P-component precursor
103	P04406	Glyceraldehyde-3-phosphate dehydrogenase
104	P80748	Ig lambda chain V-III region LOI
105	P06733	Alpha-enolase
106	Q13103	Secreted phosphoprotein 24
107	P08238	Heat shock protein HSP 90-beta
108	P13639	Elongation factor 2
109	P00558	Phosphoglycerate kinase 1
110	P06748	Nucleophosmin
111	P63261	Actin, cytoplasmic 2

112	P22792	Carboxypeptidase N subunit 2 precursor
113	Q08174	Protocadherin-1
114	P10809	60 kDa heat shock protein, mitochondrial precursor
115	P18136	Ig kappa chain V-III region HIC precursor
116	P26599	Polypyrimidine tract-binding protein 1
117	Q13796	Protein Shroom2
118	P60174	Triosephosphate isomerase
119	P02545	Lamin-A/C
120	P78371	T-complex protein 1 subunit beta
121	P14625	Endoplasmin precursor
122	Q04695	Keratin, type I cytoskeletal 17
123	O14980	Exportin-1
124	P01877	Ig alpha-2 chain C region
125	P06310	Ig kappa chain V-II region RPMI 6410 precursor
126	P01605	Ig kappa chain V-I region Lay
127	Q96ST3	Intraflagellar transport protein 140 homolog
128	P04075	Fructose-bisphosphate aldolase A
129	P29622	Kallistatin precursor
130	P63241	Eukaryotic translation initiation factor 5A-1
131	P61604	10 kDa heat shock protein, mitochondrial
132	O95445	Apolipoprotein M
133	P05787	Keratin, type II cytoskeletal 8
134	Q16850	Cytochrome P450 51A
135	P01743	Ig heavy chain V-I region HG3 precursor
136	P00734	Prothrombin precursor
137	P08107	Heat shock 70 kDa protein 1
138	P43652	Afamin precursor
139	Q8TDX9	Polycystic kidney disease protein 1-like 1
140	P59044	NACHT, LRR and PYD domains-containing protein 6

141	P02750	Leucine-rich alpha-2-glycoprotein
142	P08185	Corticosteroid-binding globulin
143	O75636	Ficolin-3
144	P02760	Protein AMBP precursor
145	O15264	Mitogen-activated protein kinase 13
146	Q9H8T0	AKT-interacting protein
147	Q96L93	Kinesin-like protein KIF16B
148	O95714	Probable E3 ubiquitin-protein ligase HERC2
149	P07358	Complement component C8 beta chain
150	P01762	Ig heavy chain V-III region TRO
151	Q15166	Serum paraoxonase/lactonase 3
152	Q9BWU0	Kanadaptin
153	Q8WYA	Intraflagellar transport protein 81 homolog
154	Q9Y493	Zonadhesin
155	P09110	3-ketoacyl-CoA thiolase, peroxisomal
156	Q92997	Segment polarity protein dishevelled homolog DVL-3
157	P35568	Insulin receptor substrate 1
158	Q9UIF8	Bromodomain adjacent to zinc finger domain protein 2B
159	Q15276	Rab GTPase-binding effector protein 1
160	Q9UQ35	Serine/arginine repetitive matrix protein 2
161	Q9P2R7	Succinyl-CoA ligase [ADP-forming] subunit beta, mitochondrial
162	Q8IUH4	Probable palmitoyltransferase ZDHHC13
163	P35244	Replication protein A 14 kDa subunit

Part 7

List of Metabolites detected, with the RT (retention time), Name and Class

	RT	Name	Class
1	7.48	Acetamide	Others
2	7.77	Boroic acid	Others
3	9.52	Benzamide	Ketones and Aldehydes
4	10.04	L-lactic acid	Hydroxy acid
5	10.48	Glycolic acid	Hydroxy acid
6	11.54	L-alanine	Amino acid
7	12.17	hydroxylamine	Alcohols
8	12.8	Oxalic acid	Carboxylic Acid
9	13.76	L-Alpha-aminobutyric acid	Amino acid
10	13.89	Pentonic acid	Others
11	14.38	Glycine	Amino acid
12	14.58	Malonic acid	Carboxylic Acid
13	15.52	L-valine	Amino acid
14	16.15	Urea	Ketones and Aldehydes
15	16.56	Acetoacetic acid	Others
16	16.58	Benzoic acid	Others
17	17.42	L-leucine	Amino acid
18	17.52	Phosphoric acid	Others
19	17.86	Glycerol	Alcohols
20	18.26	L-Isoleucine	Amino acid
21	18.46	L-Proline	Amino acid
22	18.48	Succinic acid	Carboxylic Acids
23	18.8	Glycylglycine	Amino acid
24	19.63	Glyceric acid	Hydroxy acid
25	19.85	Uracil	Nucleosides and Nucleoside conjugates
26	20.59	L-serine	Amino acid
27	21.47	L-threonine	Amino acid
28	21.99	Thymine	Nucleosides and Nucleoside conjugates
29	23.77	3-methyl-2-ketobutyric acid	Others
30	23.93	hydroxypyruvic	Hydroxy acid
31	24.11	carbamic acid	Amino acid
32	24.73	Malic acid	Carboxylic Acid
33	25.69	L-aspartic acid	Amino acid
34	25.79	L-methionine	Amino acid
35	25.88	5-oxoproline	Amino acid
36	26.06	cystathionine	Amino acid
37	28.25	Ribofuranoside	Nucleosides and Nucleoside conjugates
38	28.66	L-Glutamic acid	Amino acid
39	29.15	L-Phenylalanine	Amino acid
40	30.22	Asparagine	Amino acid

41	31.95	Aconitic acid	Carboxylic Acid
42	32.34	Putrescine	Others
43	33.14	L-glutamine	Amino acid
44	34.34	glucuronic acid	Ketones and Aldehydes
45	34.44	Citrulline	Amino acid
46	34.87	Ribonic acid	Hydroxy acid
47	34.89	Myristic acid	Fatty acid
48	35.75	adenine	Nucleosides and Nucleoside conjugates
49	36.72	D-glucose	Carbohydrates
50	36.9	D-mannose	Carbohydrates
51	37.08	L-Lysine	Amino acid
52	37.16	L-histidine	Amino acid
53	37.22	3-4-dihydroxy-mandelic	Hydroxy acid
54	37.31	D-glucitol	Alcohols
55	37.61	L-tyrosine	Amino acid
56	38.01	D-Galactose	Carbohydrates
57	38.11	Fructose	Carbohydrates
58	39.78	Palmitic acid	Fatty acid
59	40.69	Ribofuranose derivatives	Carbohydrates
60	40.91	D-ribose	Carbohydrates
61	41.1	Oleic acid	Fatty acid
62	41.36	Glucosamine	Carbohydrates
63	41.48	N-Acetyl-L-tyrosine	Amino acid
64	41.79	Myo-inositol	Alcohols
65	42.63	Stearic acid	Fatty acid
66	43.73	Vaccenic acid	Fatty acid
67	43.95	Glucose-6-phosphate	Carbohydrates
68	44.05	L-cysteine	Amino acid
69	45.21	Cadaverine	Others
70	46.31	alpha-ketoisovaleric acid	Others
71	47.12	Arachidonic acid	Fatty acid
72	48.45	Cholesterol	Steroids
73	48.99	Inositol-derivative	Alcohols
74	49.08	uridine	Nucleosides and Nucleoside conjugates
75	51.54	Inosine	Nucleosides and Nucleoside conjugates
76	51.69	3-hydroxyadipic acid	Hydroxy acid
77	52.19	Maltose	Carbohydrates
78	53.29	Gluconic acid	Hydroxy acid
79	54.95	Adenosine	Nucleosides and Nucleoside conjugates
80	56.52	Pyrimidinone derivative	Nucleosides and Nucleoside conjugates